FINAL REPORT

ELECTRON ACCELERATOR FOR AEROBEE 350 ROCKET - DESCRIPTION, DEVELOPMENT AND FLIGHT PERFORMANCE

by:

Ion Physics Corporation
Burlington, Massachusetts

Prepared for:

National Aeronautics and Space Administration
Goddard Space Flight Center
Greenbelt, Maryland

Contract No. NAS5-9326

30 November 1970

ION PHYSICS CORPORATION
A Subsidiary of High Voltage Engineering Corporation
BURLINGTON, MASSACHUSETTS

Requests for copies of this report should be referred to

National Aeronautics and Space Administration
Office of Scientific and Technical Information
Attention: AFSS-A
Washington, D.C. 20546

FINAL REPORT

ELECTRON ACCELERATOR FOR AEROBEE 350 ROCKET - DESCRIPTION, DEVELOPMENT AND FLIGHT PERFORMANCE

by

William C. Beggs

to

NASA-GSFC

Contract NAS 5-9326

ION PHYSICS CORPORATION
BURLINGTON, MASSACHUSETTS

TABLE OF CONTENTS

Section			Page
1	DESCRIPTION OF IPC SUPPLIED ROCKET PAYLOAD		1
	1.1 Design Philosophy		1
	1.2 Package Specifications		5
	1.2.1 Beam Output		5
	1.2.2 Monitor Outputs		6
	1.2.3 Inputs		7
	1.2.4 Operational Sequences (Flight Unit) 5-9326-1		8
	1.2.5 Operational Tolerances		8
	1.2.6 Battery Complement		10
	1.2.7 System Weight		10
	1.2.8 Environmental		10
	1.3 System Design		11
	1.3.1 Electron Guns		15
		1.3.1.1 Configuration	15
		1.3.1.2 Beam Characteristics	21
		1.3.1.3 Operational Requirements/ Characteristics	21
		1.3.1.4 Mounting and Techniques	29
		1.3.1.5 Description of Gun Opening Technique	33
		1.3.1.6 Electron Gun Disposition and Totaled Payload Characteristics	36
	1.3.2 At Volts Sub-Systems		40
		1.3.2.1 Filament Regulator	40
		1.3.2.2 Second Grid Supply	46
		1.3.2.3 Beam Current Controller	49
		1.3.2.4 At-Volts Batteries	53
	1.3.3 Experiment Programmer		56
		1.3.3.1 Mounting/Positioning	57
		1.3.3.2 Sequencing	57
		1.3.3.3 Description of Operation of the Programmer Circuits	61

TABLE OF CONTENTS (CONTINUED)

Section			Page
1	1.3.4	High Voltage - Beam Current Supply	68
		1.3.4.1 Subsystem General Characteristics	68
		1.3.4.2 Packaging Design	73
		1.3.4.3 Circuit Operation	73
	1.3.5	Main Batteries	76
		1.3.5.1 General Configuration	76
		1.3.5.2 Mounting	78
		1.3.5.3 Flight Preparations	78
		1.3.5.4 Regulation	78
		1.3.5.5 Lifetime - Rechargeability	78
	1.3.6	Gun-Opening (Break-Seal) Circuits	80
		1.3.6.1 Mounting - Placement	80
		1.3.6.2 Circuit Operation	82
	1.3.7	T/M and Ground Monitoring Circuits	83
		1.3.7.1 High Voltage Monitor	83
		1.3.7.2 Beam Current Monitor - Beam Current "Resistors"	85
		1.3.7.3 Housekeeping Monitors	85
	1.4	Systems Test Console	109
		1.4.1 Top Panel Controls and Indicators	113
2	DEVELOPMENT/TEST EFFORT		115
	2.1	Summary of the Development Effort	115
		2.1.1 Gun Development	115
		2.1.2 High Voltage Converter Development	117
	2.2	First Vacuum Integration Test	118
	2.3	Final Systems Testing Unit 1	122
		2.3.1 Final Vacuum Integration Test Unit 1	125
	2.4	Field Testing and Integration - Unit 1	136
3	17.03 ROCKET EXPERIMENT - OPERATION AND RESULTS		141
	3.1	Launch Data - Payload Performance, Aerobee 17 Aerobee 17.03	141

TABLE OF CONTENTS (CONTINUED)

Section		Page
3	3.1.1 Housekeeping Data Reduction	141
	3.1.2 Pulse Program Data Reduction	145
	3.2 Collector Current Monitor-Data Reduction and Associated Experiment Analysis	170
	REFERENCES	179
	APPENDIX	180

LIST OF TABLES

Table		Page
I	Experiment Pulse Program	9
II	Specification Sheet Electron Tube, EE-65	22, 23
III	Electron Gun EE-65	39
IV	Arc Voltage for Various Cathode Materials, (Taken from M. P. Reece, Proc. I.E.E., Vol. 110, No. 4, April 1963)	120
V	Reduced Data - Vacuum Integration Test - Unit 1 Run 5-14C-68, Total Collected Current	126
VI	Data Reduction - Vacuum Integration Test - Unit 1 Run 5-14C-68 - Beam Voltage Regulation	129
VIIa	Pre & Post Electrical Checkout Comparisons for Vibration Tests of 12-20-68, Unit 1	139
VIIb	Pre & Post Vibration Timing Comparisons for Vibration Tests of 12-20-68, Unit 1	140
VIII	17.03 Key Events	142
IX	Housekeeping During 17.03 Flight	146
X	Electron Pulse Data Analysis	147

LIST OF ILLUSTRATIONS

Figure		Page
1	Electron Accelerator for Aerobee 350 Rocket	2
2	Sketch of Package	3
3	Electron Accelerator Circuit Diagram	12
4	10 keV - 1/2 Ampere Electron Accelerator - Exploded View 1	13
5	10 keV - 1/2 Ampere Electron Accelerator - Exploded View 2	14
6a, b, c	System Interconnecting Diagram	16, 17, 18
7	Machlett EE-65 Electron Gun Configuration	17
8	EE-65 Electron Gun Internal Configuration	20
9	Beam Angular Distribution EE-65	24
10	Grid Transfer Characteristics Typical EE-65 Electron Gun	25
11	Effect of Filament Potential on Grid Transfer Characteristics	26
12	Plate Characteristics Typical EE-65 Electron Gun	27
13	Grid Transfer Characteristics as a Function of G2 Voltage	28
14	Grid Transfer Characteristics at Low V_{g2}	30
15	G2 Interception Current	31
16	Gun Deck	32
17	Close-up of Gun Mountings	34
18	Gun Mounts and Cabling - Pressurized Side	35
19	Electron Gun EE-65 - Before and After Opening	37
20	Break Seal Operational Reliability Test Program	38
21	17.03 Totalled Gun Characteristics	41
22	Totalled Gun Characteristics Unit 2	42
23	Insulated Plate Sub-Assembly - View 1	43
24	Insulated Plate Sub-Assembly - View 2	44
25	Filament Regulator Schematic	45

LIST OF ILLUSTRATIONS (CONTINUED)

Figure		Page
26	Pre-Accelerator 800 V Converter Schematic	47
27	Pre-Accelerator Supply	48
28	Basic at Volts Gun Circuit	50
29	Beam Current Controller Schematic	51
30	Low Voltage Section - Beam Current Controller Time Delay Board	54
31	16 Volt Battery	55
32	Top Section of Cannister	58
33	Experiment Programmer - Covers Removed	59
34	Experiment Programmer Schematic	62
35	Lower Section of Pressure Cannister - Covers Removed.	69
36	High Voltage Converter Control Logic/Amplifier - Schematic	70
37	10 kV - 500 mA High Voltage Converter Connection - Schematic	71
38	1.25 kV - 500 mA High Voltage Converter Module - Schematic	72
39	High Voltage Module Load Regulation	75
40	High Current Battery - Cover Removed	77
41	Load Regulation - Yardney XE71 Battery	79
42	Break Seal Circuit	81
43	High Voltage Monitor Schematic	84
44	Beam Current Monitor Schematic	86
45	Beam Current Monitor Calibration Unit #1	87
46	Beam Current Monitor Calibration Unit #2	88
47	Beam Current Monitor Temperature Sensitivity at 500 mA Input - Unit #1	89
48	Upper Deck T/M Conditioning Box	90
49	Upper Deck T/M Conditioning - Schematic	92
50	Temperature Sensor Conditioning Circuit	93

LIST OF ILLUSTRATIONS (CONTINUED)

Figure		Page
51	Package Pressure Monitor Unit #1.	95
52	Package Pressure Monitor Calibration Unit #2	96
53	High Voltage Converter Heat Sink Monitor Unit #1	97
54	Converter Heat Sink Temperature T/M Calibration Unit #2	98
55	Positive Battery (#1) Monitor Calibration Unit #1.	99
56	Negative Battery (#2) Monitor Calibration Unit #1	100
57	Positive Main Battery Monitor Calibration - Unit 2	101
58	Negative Main Battery Monitor Calibration - Unit 2	102
59	Break-Seal Monitor Calibration - Unit 1.	104
60	Break-Seal Monitor Calibration - Unit 2.	105
61	Secondary Electron Coefficient for Steel.	106
62	Cap Current to Return Current Ratio	107
63	Cap Current to Return Current Ratio	108
64a, b	Systems Checkout Console and Cable Interconnections	110, 111
65	Systems Checkout Console	112
66	IPC Large Vacuum Facility	124
67	Test Setup - Large Vacuum Facility	127
68	Typical Two Section Faraday Current Vacuum Integration Test	130
69	17.03 Flight-Gun Opening Sequence	143
70	Battery Pulse-Down During Gun Opening	144
71	17.03 Collector Current Monitor Calibration Comparison of Flight and Back-up Units	171
72	Collector Current Monitor S/N 1 17.03 Flight "BEST" Calibration Curve	172
73	1st Signature Pulse $9^h48^m55^s.306$ UT	174
74	2nd Signature Pulse-Collector Current $9^h49^m22^s.537$ UT . . .	175
75	3rd Signature Pulse 8.8 kV, 500 mA $9^h49^m52^s.586$ UT.	176
76	4th Signature Pulse $9^h49^m22^s.537$ UT Collector Current . . .	177

ACKNOWLEDGEMENTS

Major contributions to the program effort are listed below:

W. Beggs	Project Manager/Project Scientist and Electron Gun Development and Test
H. Bouwensch	Mechanical Engineering - Structure Packaging
R. Elcox	Filament Regulator, 800 V Converter, Programmer, Beam Current Controller Development and Test
R. Harrison	B. S. Circuitry; High Voltage Converter; Monitoring Circuits, Systems Integration and Test; Project Engineer, Field Operations
F. McCoy	Field Test Console, B. S. Test Program, Battery Test Program, Systems Test Program
C. Salisbury	Project Technician - System Wiring, Integration and Field Test - Launch Operations

INTRODUCTION

The report which follows describes the development and test of two electron accelerator systems for Aerobee 350 rocket use and the flight and flight performance of one of the systems. The system was successfully used to inject a beam of electrons into the upper atmosphere from an Aerobee 350 sounding rocket for the purpose of establishing whether a beam could be ejected from a vehicle into the upper atmosphere, could pass through the existing and beam generated background plasma without strongly and deleteriously interacting with it, and could produce adequate excitation and ionization for ground viewing by optical and radar viewing equipment. The flight (Aerobee 17.03) took place from Wallops Island, Virginia, January 26, 1969 at 9^h45^m UT.

The report is organized in three basic sections. The first describes the system and gives operational specifications and calibrations for both units. The second section, largely a summary section, deals with the key issues, problem areas and solutions of the design and development program. The details of this program have been well covered in the rather detailed Bi-Monthly progress reports generated under the contract, except for the later months of the effort devoted to field operations with the first unit and acceptance testing of the second unit. These months are covered in more detail in the section. The third section of the report covers the launch operation, the payload performance and a partial analysis of the results, particularly concerning the results of the collector current measurements.

The T/M reception on the flight was excellent and the payload performance without fault.

SECTION 1
DESCRIPTION OF IPC SUPPLIED ROCKET PAYLOAD

Each of the payloads supplied by IPC is designed to be attached at its aft most point to a GSFC supplied ring which forms part of the collector spool. The forward plate of the payload is in contact with a three fingered yoke assembly upon which the spring driven nose cone eject assembly, supplied by GSFC, is attached.

Physically, the payload consists of (a) a pressurized cylinder, penetrated by the electron guns and connectors and (b) a structure which mates the pressurized cannister to the GSFC ring below it and upon which is mounted the two pressurized main batteries. A view of the assembled package is given in Figure 1. Figure 2 gives an outline sketch of the system. The two connectors which connect the package electrically to telemetry, instrumentation power and umbilicals are located along a line through the center at the aft end of the pressurized cannister. The main batteries which are each in their own pressurized box are connected via a "Y" cable to a third connector along the same line, to the pressurized cannister. Small three pin connectors on each battery require cabling, not supplied, to the instrumentation section.

1.1 Design Philosophy

The basic design philosophy for the electron beam relates to the uncertainty of the launching conditions. Part of the purpose of the basic experiment was to determine acceptable launching conditions. It was feared that, in addition to the possibility that the beam might turn around due to charge buildup on the vehicle, it might turn around locally due to its own space charge. Simple theory indicates that significant axial potentials can build up in a space charge limited beam within a "small number" of beam radii. Accordingly, the design produced a beam of the largest possible radius. This was done by utilizing ten small guns arrayed around a circle of the maximum diameter possible, within the constraints of the packaging. The basic design ranges of beam current and beam voltage, in

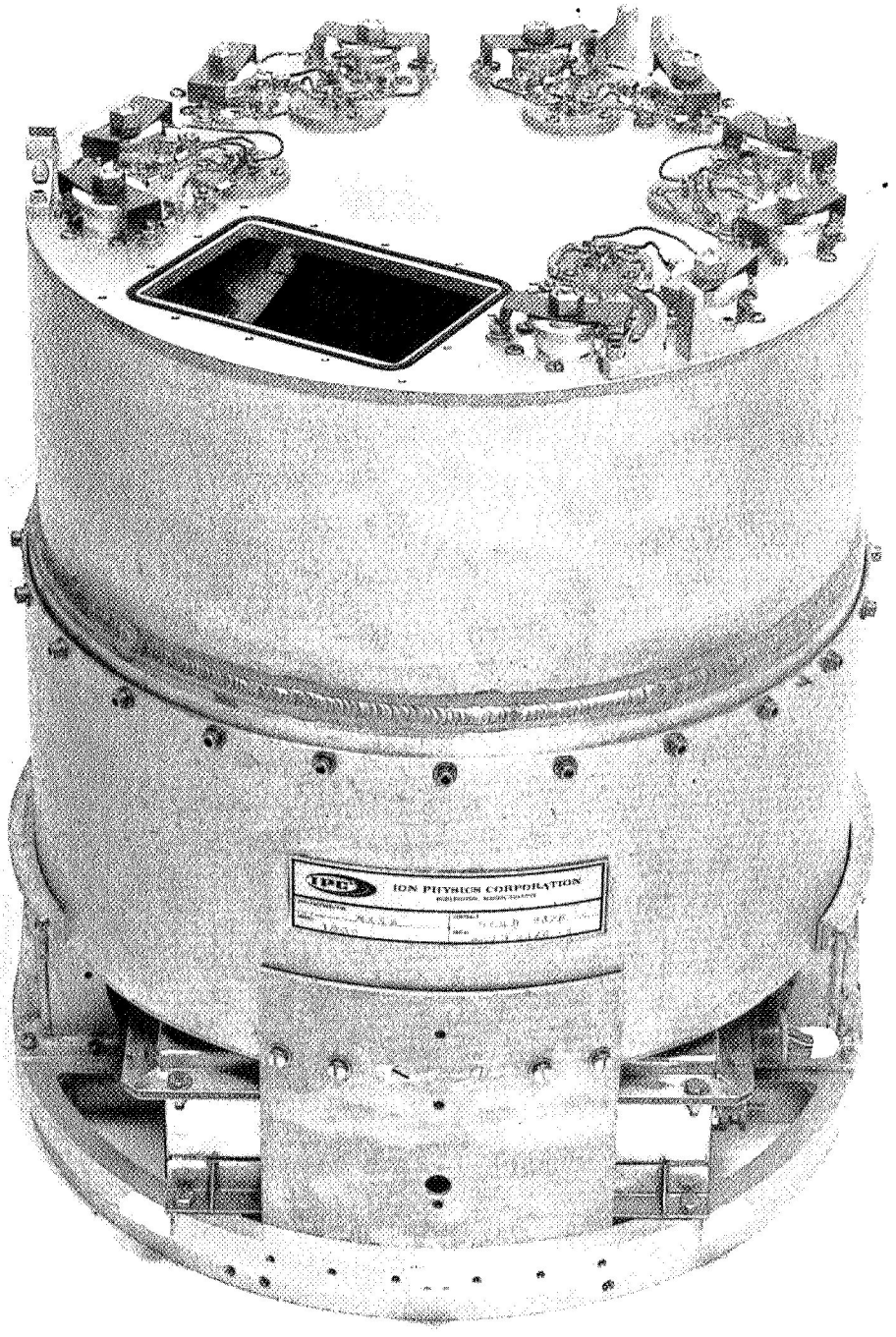

Figure 1. Electron Accelerator for Aerobee 350 Rocket.

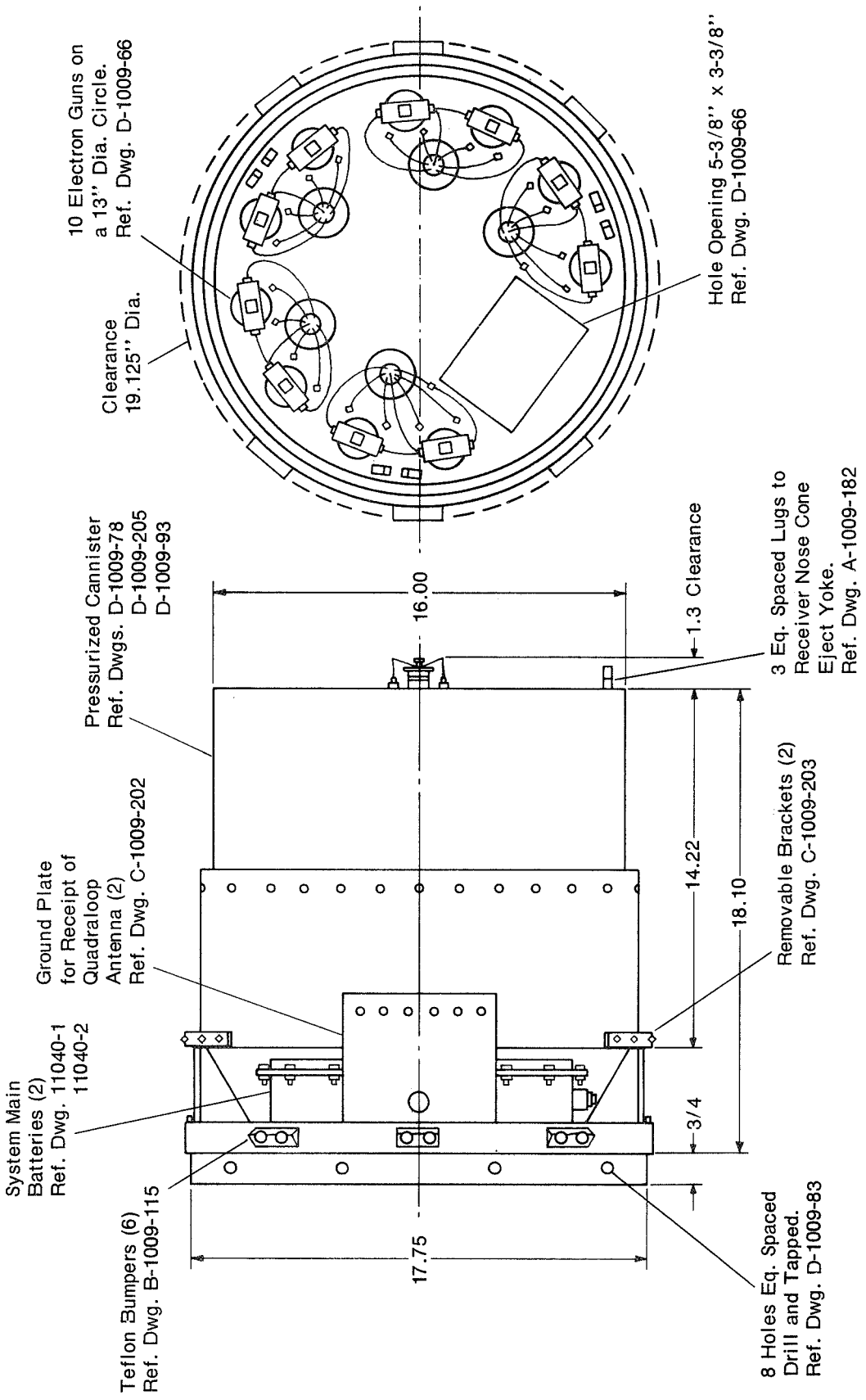

Figure 2. Sketch of Package.

1-6039

addition, precluded the use of a single gun to perform the operation. (This is discussed in more detail in the section on Electron Gun Development.)

The basic package design was constrained by the electron gun design. In order to utilize existing tube technology and come up with compact gun designs, the gun cathodes were required to be of low work function type. This type of cathode has the great advantage of operating at low temperatures and hence low filament power, and of being easily fabricated in large area configurations; however, the type is much more subject to poisoning by gases, particularly organic vapors, water vapor, and the type of gases used for h.v. insulation. Hence it was necessary to force upon the rocket integrator rather stringent outgassing constraints on their packages, and upon nose cone outgassing. The latter constraint along with a requirement from the aluminized mylar collector design eventually forced the entire IPC payload back thru payload and including the collector package, to be enclosed in a vacuum tight cannister which was pumped down before launch. Use of the cannister then allowed a lighter fiber-glass none-cone to be used.

For the IPC package the outgassing constraint forced the design to remove all possible external sources of outgassing from the gun area and from the rest of the package. Vacuum penetrations in the design are sealed with low outgassing rate Viton O-rings. Organic wire insulation and insulators were not allowed. Epoxies in the gun area were also forbidden. Important tests required were (a) ability to pump the pressurized section down to vacuum in a set period of time, (b) helium leak checking of the flight ready cannister to high vacuum specifications and, (c) leak checks on the battery cases.

A further important design consideration on the package relates to the acceptance testing. At some point in the process of development checkout at IPC, integration and checkout at GSFC-Sounding Rocket Branch, and testing at GSFC Greenbelt, Maryland it would be necessary to exercise the complete electron accelerator system for the entire expected flight time using the flight experiment program. This implied operating the guns in an open state with a beam into a vacuum chamber. It was determined fairly early in the program that this test would be performed in the IPC 6 ft. diameter x 10 ft. long high vacuum chamber.

The nature of the gun opening technique and the gun cathodes precluded the reuse of the opened guns for testing unless they remain in the vacuum. Additionally it would be expected that problems might arise during the test which might be capable of being redesigned and/or repaired in a short time. This strongly suggested that the package be designed so that the rear of the package be outside the vacuum system and capable of being serviced completely without access to the gun deck plate. To meet this criterion for the forwardmost section of the pressurized cannister, a second piece was made conforming in all dimensions to the flight section except with a vacuum flange externally which could be mated with the end of the vacuum system. Upon completing all testing, flight items were to be stripped from the test section and remounted together with new guns in the flight section.

An additional major design consideration was forced by the lifetime limitations of the main batteries. These batteries, as discussed in the section on battery system development, in order to meet the weight, current and voltage requirements were necessarily provided with very thin interplate separators which in turn caused the possibility of possible cell shorting after only two weeks subsequent to filling. Also interplate leakages were increased. It became obvious that the batteries had to be external to the pressurized cannister in an accessible location for quick replacement if launch holds would be long.

The design resulting has taken care of these problems.

1.2 Package Specifications

1.2.1 Beam Output

One second and one tenth second nominal electron beam pulses at energies ranging from 1.25 to 10.0 keV over a current range from 1.5 mA to 500 mA. The beam is made up of beamlets from ten individual guns arrayed on a 13 inch diameter circle. Beamlet axes are along the thrust axis. Beamlet divergence is such that 80% or greater current is inside of a 10 ° half angle.

1.2.2 Monitor Outputs

Function	Range	Type	Calibration Factor (Flight Unit)
Beam Voltage	-0.50 to 5.5 V	linear	-2.9 kV/volt
Beam Current	not clamped	approx. log	4.64 V at 500 mA
Positive Main Battery	-0.5 to 5.5 V	linear	11.31 volts/volt
Negative Main Battery	-0.5 to 5.5 V	linear	9.0 volts/volt
Break Seal Monitor	-0.5 to 5.5 V		Calib. curve 0.55 V for ten open guns
Package Pressure	-0.5 to 5.5 V	linear	4.86 psia/volt
High Voltage Converter Heat Sink Temperature	-0.5 to 5.5 V	semi-linear	Calib. curve 2.86 V at 100 °F
B.C.M. Block Temperature	-0.5 to 5.5 V	semi-linear	Calib. curve 2.84 V at 100 °F
Electron Guns - Total Cap. Current	(to gnd checkout)	linear	133 mA/volt
Beam Voltage	(to gnd checkout)	linear	-2.9 kV/volt
Positive Main Battery volts	(to gnd checkout)	linear	1V/volt
Positive Main Battery CT volts	(to gnd checkout)	linear	1V/volt
Negative Main Battery volts	(to gnd checkout)	linear	1V/volt
Negative Main Battery CT volts	(to gnd checkout)	linear	1V/volt
Programmer Battery volts	(to gnd checkout)	linear	1V/volt

Function	Range	Type	Calibration Factor (Flight Unit)
Beam Current Monitor "Resistor"	(to gnd checkout)	linear	0.97 amp/ volt
Package Pressure	(to gnd checkout)	linear	4.86 psia/ volt
Program turn-on Latching Relay Position	(to gnd checkout)	latch - unlatch position	---
Breakseal Ledex Home Position	(to gnd checkout)	on - off	---

1.2.3 Inputs

ROCKET

Function	Requirement
Break Seal Start	+28V for 3 < t < 12 sec. three alternate leads
Programmer Start	+28V for t > 15 ms. three alternate leads
Programmer Stop	+28V for t > 15 ms. three alternate leads
Instrument Power	+28V ~ 100 mA
Modify Beam Current (on gnd)	switch closure for flight

GROUND

Function	Requirement
Battery Heater Blankets Power	40 $\longrightarrow$ 100 v AC/DC - 1 amp
Programmer Start	+28V for t > 15 ms.
Programmer Stop	+28V for t > 15 ms.

1.2.4 Operational Sequences (Flight Unit) 5-9326-1

(Timing setting ranges are given in the description of the several units.)

BREAK SEAL INITIATE

Time From Start	Event
0.00	Uni-junction oscillator starts charging
3.71 sec.	Ledex to pos. 2, Current to open guns 5, 1, 9, 3
7.26 sec.	Ledex to pos. 3, Current to open guns 6, 2, 8, 4
10.81 sec.	Ledex to pos. 4, Current to open guns 7, 10
14.36 sec.	Ledex back to pos. 1

EXPERIMENT PROGRAM (See Table I)

Time From Start	Event
0.00	Relay latches, power to programmer filament relay on
12.00 sec.	Power to registers. Reset to 1st position
15.00 sec.	1st pulse-high voltage on. 2nd grid voltage on
15.10 sec.	1st pulse - current on
15.20 sec.	1st pulse ends - current off - h.v. off - G_2 voltage off
18.00 sec.	2nd pulse - h.v. on - G_2 volts on

1.2.5 Operational Tolerances

Beam Voltage	±15% of nominal
Beam Current Settings	±10% of nominal
Beam Current Variation	±10% of nominal
Pulse Length	±5% of nominal
Pulse Spacing	±15% of nominal

Table I. Experiment Pulse Program

Nominal pulse spacing between pulse starts 3.0 sec.

Pulse No.	Nominal Voltage (kV)	Nominal Current (mA)	Length of Current Pulse (sec.)
1	5.6	1.5	0.100
2	5.6	5.0	0.100
3	5.6	15	0.100
4	5.6	50	0.100
5	5.6	150	0.100
6	5.6	500	0.100
7	2.8	15	0.100
8	2.8	50	0.100
9	2.8	150	0.100
10	2.8	500	0.100
11	10	500	1.00
12	1.4	15	0.100
13	1.4	50	0.100
14	1.4	150	0.100
15	1.4	500	0.100
16	10	1.5	0.100
17	10	5.0	0.100
18	10	15	0.100
19	10	50	0.100
20	10	150	0.100
21	10	500	1.00

Program repeated automatically to shutdown.

1.2.6 Battery Complement

(1) Main batteries:

(a) Yardney E-11040 battery pack modified to IPC drawing C1009-242-1 comprised of 23 PMV-5-(7) AgO-Zn Cells.

(b) Yardney E-11040 battery pack modified to IPC drawing C1009-242-2 comprised of 23 PMV-5-(7) AgO-Zn Cells.

(2) Filament/800 v Converter battery - consisting of nine Yardney PMC-3-8 AgO-Zn Cells in a sealed battery case. IPC drawing C1009-22.

(3) Beam Current Controller battery - consisting of two Gulton Industries 17VO-180 ssc sealed button Ni-Cd batteries in series in a case IPC drawing C1009-21.

(4) Programmer Battery - consisting of two Gulton Industries 5VO-180 ssc sealed button Ni-Cd batteries in series in a case IPC drawing B1009-161.

1.2.7 System Weight

124.5 lb exclusive of the R. P. A. package.

1.2.8 Environmental

Vibration: Unit 1 was tested prior to flight to levels which generally subjected the payload to 1-1/2 times the levels called out in NASA-GSFC S-320-SR-1 for Aerobee payloads, both for sinusoidal sweep and random vibration. Unit 1 was subsequently tested twice to the levels given in S-320-SR-1 and survived the launch environment successfully.

Acceleration: Unit 1 was subjected to centrifuge along the thrust axis for 30 sec. at a level of 15g.

Altitude: During test operations at IPC Unit 1 was successfully subjected to 1 x 10^{-6} torr pressure. At GSFC a test at 8 x 10^{-3} torr was made successfully.

1.3 System Design

A summary of the overall subsystem relationships is given in Figure 3 and, as is evident there, the system consists of the electron guns, power supplies to operate the guns, an experiment programmer to set the pulses in length, energy, and current, circuitry for opening the guns and monitoring circuits to determine the operational status of the system through a T/M link in the air or hard lines through the umbilical while on the ground.

During high voltage pulsing a number of the subsystems rise to the high voltage on the cathode. These units, namely the filament supply, the second grid supply, part of the beam current controller and both the 15 V battery and the 44 V G1 Bias battery are all mounted upon a fiberglass plate which provides the required 15 kV insulation for the units. Each unit is turned on and off by means of specially isolated reed relays developed at IPC. These relays allow the energizing coils to be at ground potential while the reed switches are at the high voltage. The fiberglass plate is itself mounted into the forward half of the pressurized cannister as can be seen in the exploded views of the system, Figures 4 and 5. The rest of the forward cannister half, contains the electron guns, which are removable from the front face of the system, the T/M conditioning box, the programmer battery and the experiment programmer itself which is mounted in a hole in the fiberglass plate. The other half of the cannister contains mainly the high voltage beam current converter system which is housed in a completely rfi/emi shielded and filtered enclosure of its own. The rest of the section contains the gun opening circuits and some of the T/M conditioning circuits.

The two main batteries are mounted on a ring assembly which attaches to the GSFC supplied collector spool assembly. The pressurized cannister is attached to this ring assembly by means of two fixed brackets and two removable brackets. The fixed brackets are designed to accept quadraloop antennas and act as acceptable ground planes. The removable brackets are designed so that

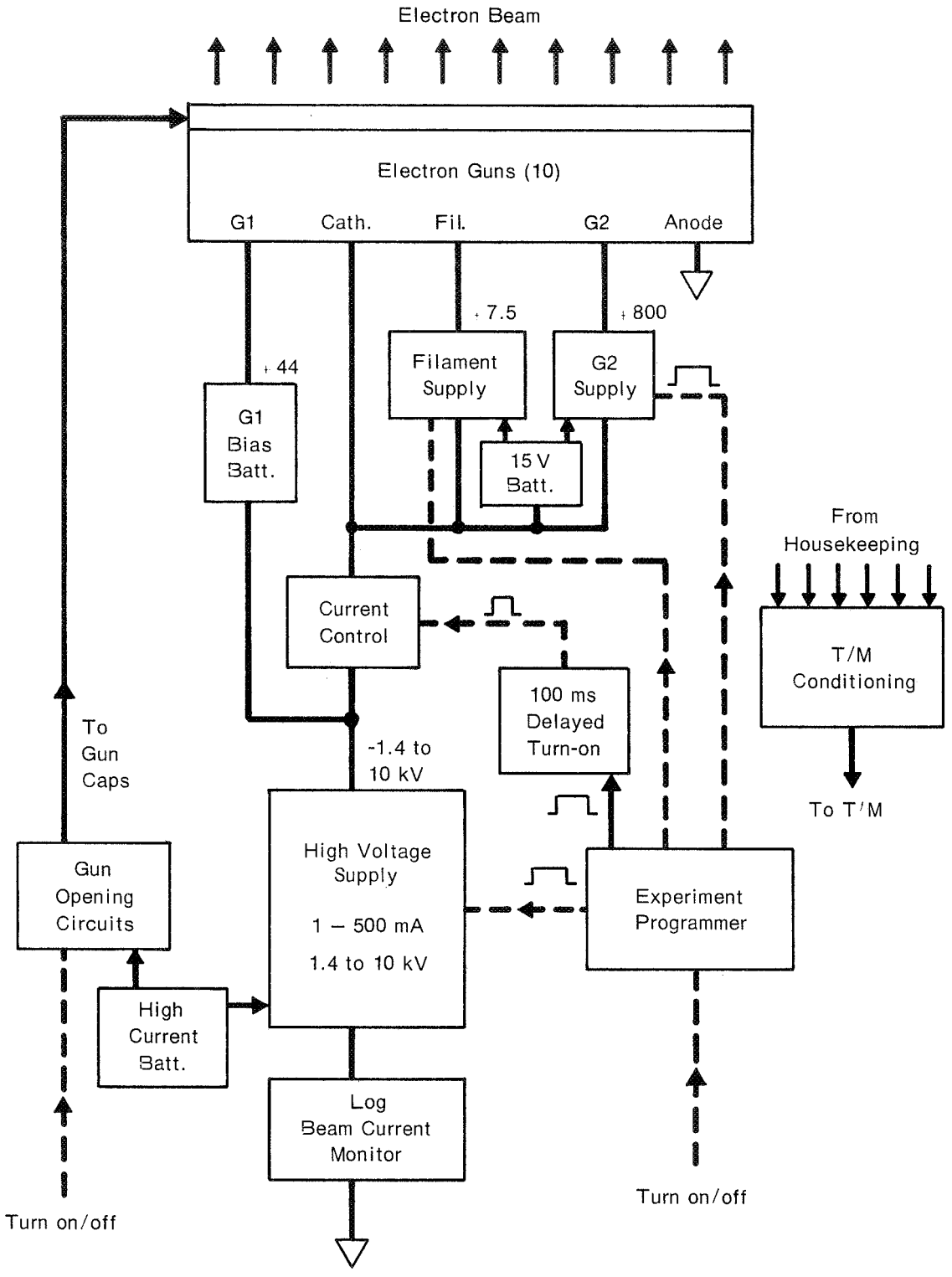

Figure 3. Electron Accelerator Circuit Diagram.

1-6040

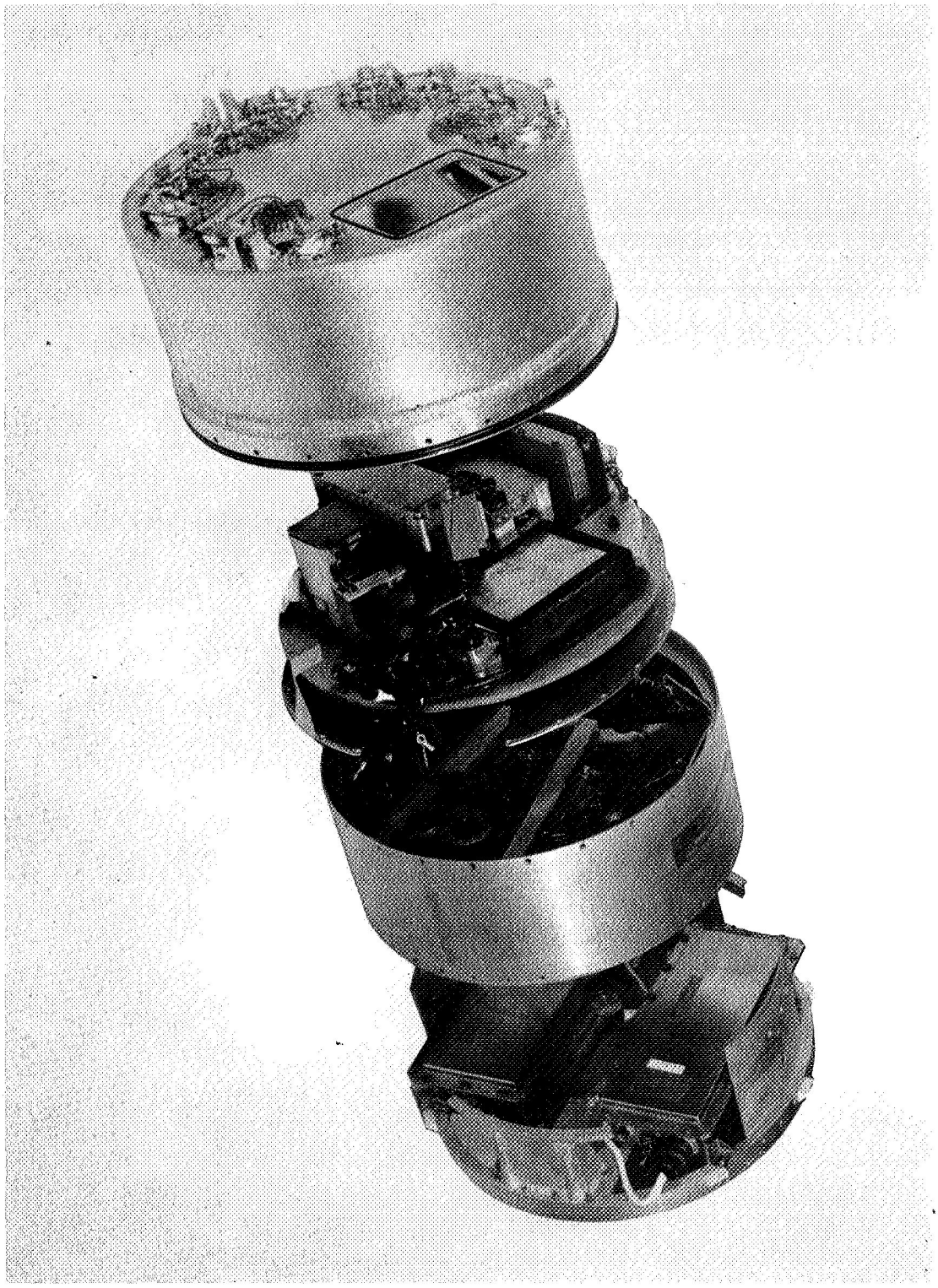

Figure 4. 10 keV - 1/2 Ampere Electron Accelerator - Exploded View 1.

2-1553

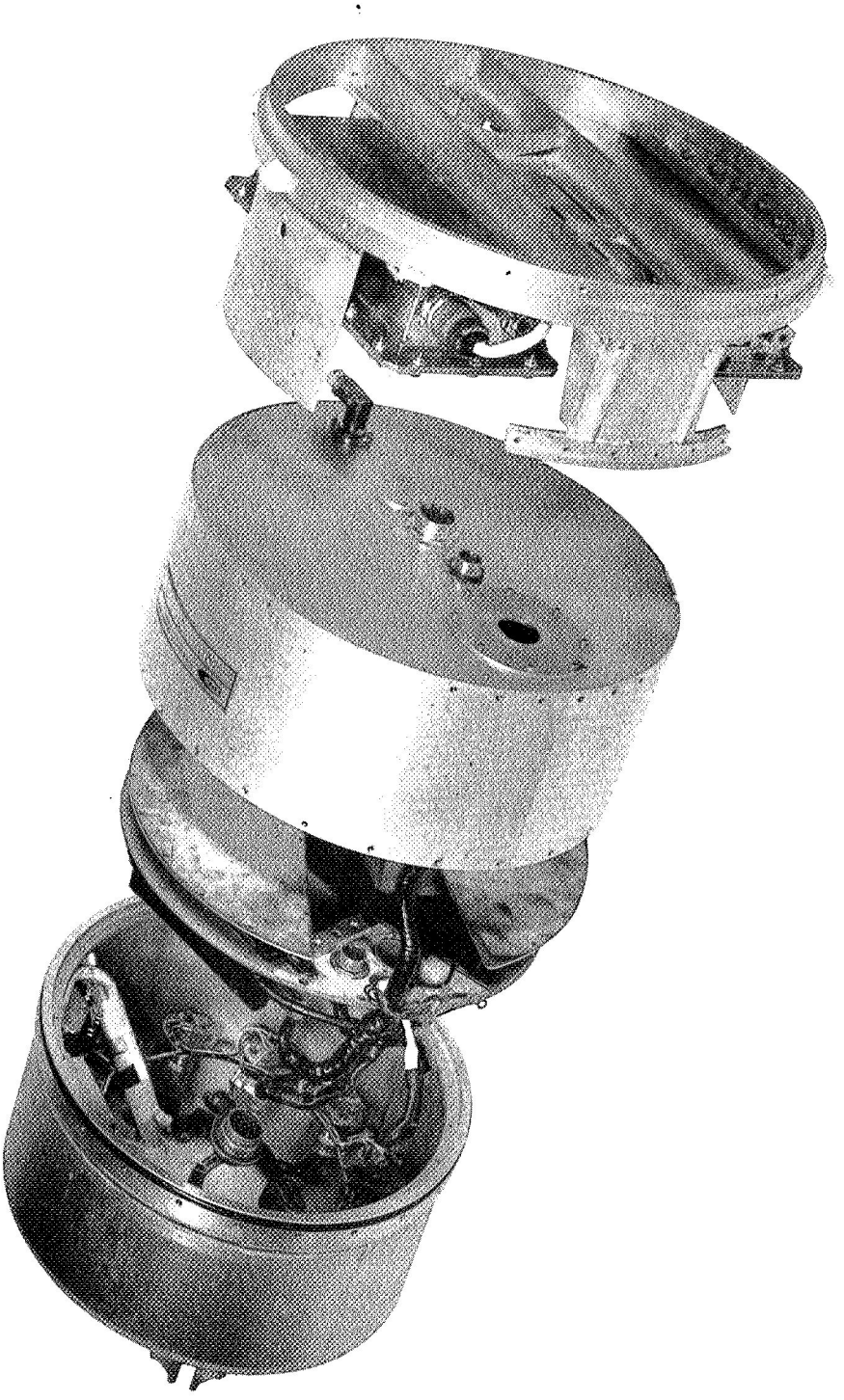

Figure 5. 10 keV - 1/2 Ampere Electron Accelerator - Exploded View 2.

2-1554

the batteries can be removed for replacement and for access to the package electrical connectors mounted along a central line in the aft most plate of the pressurized cannister. Also mounted in this plate is the evacuate-fill valve for pressurizing the cannister.

The system is connected electrically through a number of cables - Figure 6 - a, b, and c gives these interconnections and the schematic numbers associated with each subassembly.

1.3.1 Electron Guns

The electron guns used in the system were developed partly at Ion Physics and partly at Machlett Laboratories, a division of Raytheon Company. Ion Physics performed the optical system development while Machlett developed the gun opening technique and production configurations. The design is based rather heavily upon the U.H.F. planar triode technology developed to high production capability at Machlett. The result is an extremely compact and rugged gun which can be operated at reduced duty cycle in the closed condition, is opened cleanly and reliably, and can produce electron beams from 0 to 75 mA at beam energies from 1.2 to 10 keV. To produce the required beams up to 500 mA, ten of these guns are arrayed around part of a 13 inch circle pointing up the vehicle axis.

1.3.1.1 Configuration

The external configuration of the gun is given in Figure 7. All dimensions in the figure are in inches. The shield ring is added at Ion Physics Corporation using a soft solder ring to the Machlett supplied ring. The addition of the IPC part improves the high voltage hold-off capability for the insulator between anode and second grid as well as providing a surface for finger attachment.

The internal configuration is given in Figure 8. Materials used are high strength alumina insulators, copper end cap, kovar flanges and electrodes, tungsten mesh 2nd grid, gold plated tungsten first grid and quick warm-up oxide cathode.

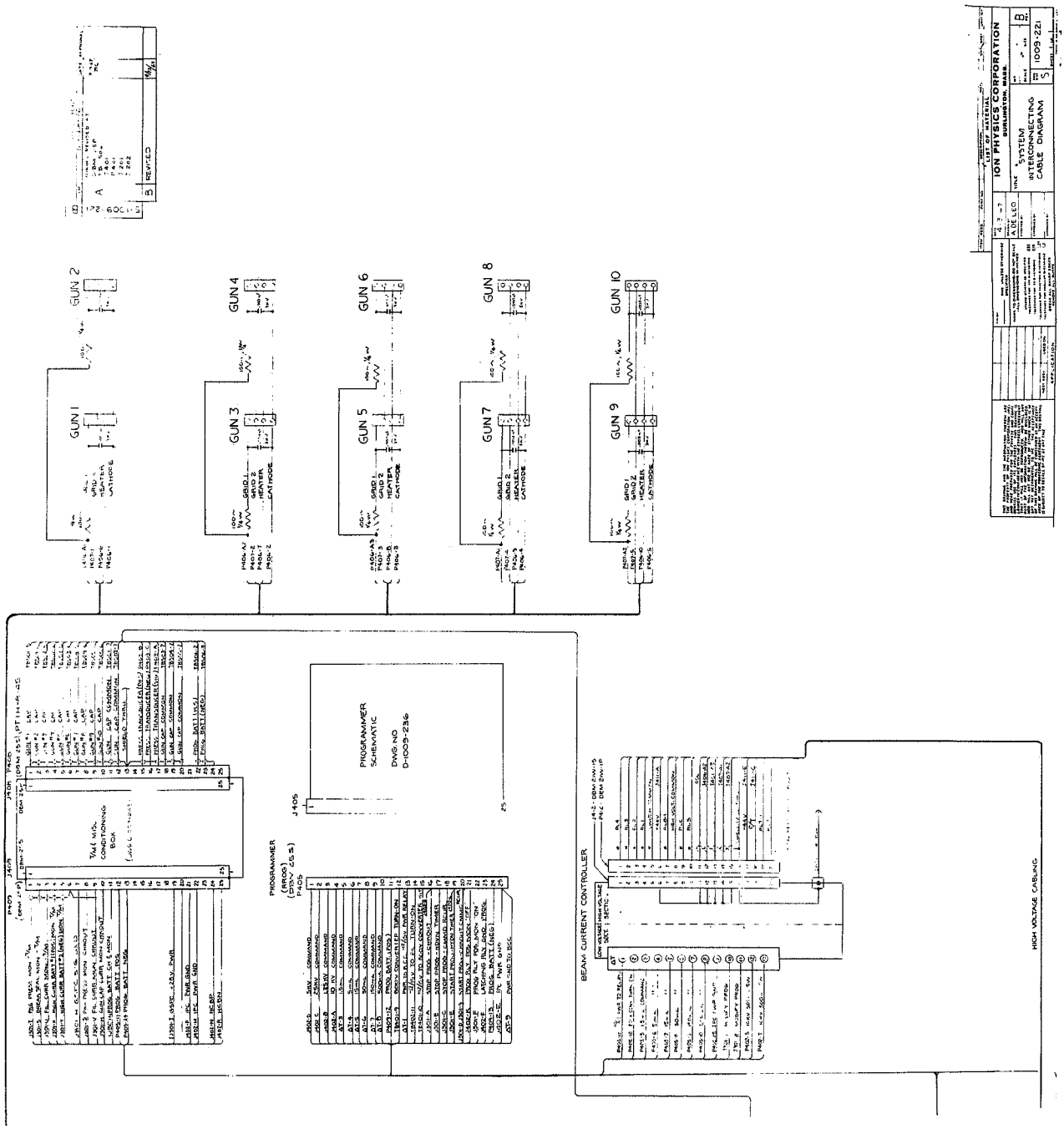

Figure 6a. System Interconnecting Diagram.

1-6041a

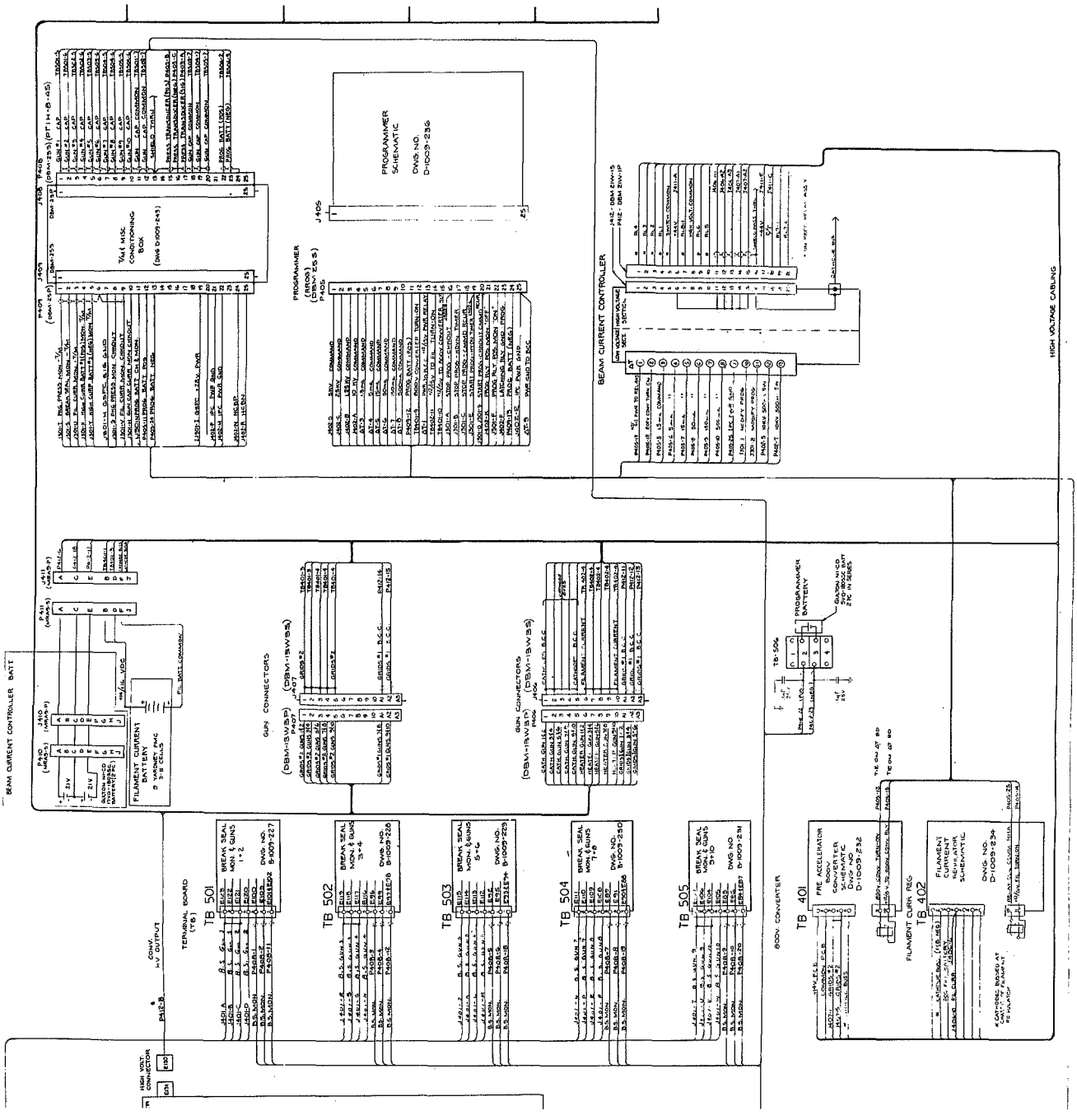

Figure 6b. System Interconnecting Diagram.

1-6041b

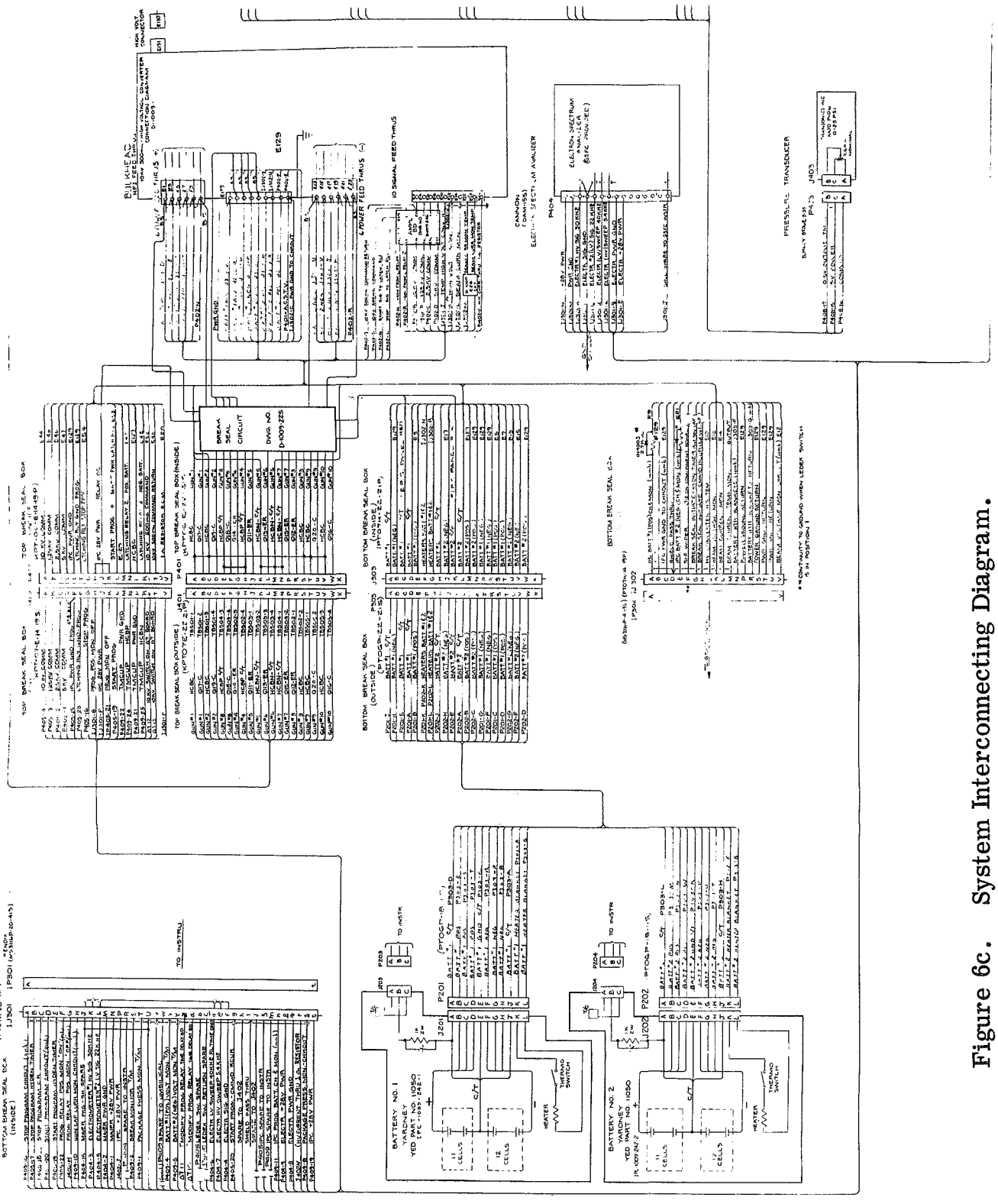

Figure 6c. System Interconnecting Diagram.

1-6041c

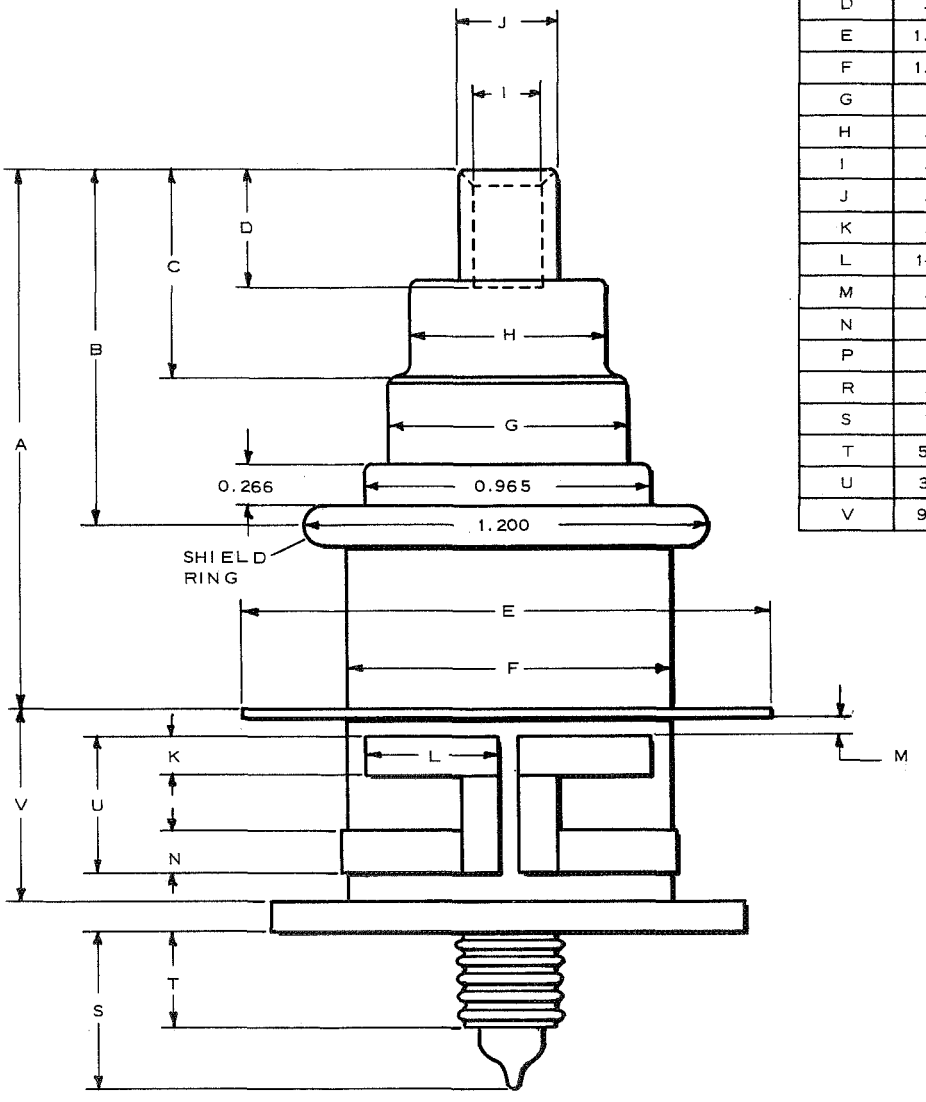

DIMENSIONAL SPECS.		
DIM.	MIN.	MAX.
A	1.652	1.695
B	1.082	1.139
C	.632	–
D	.328	–
E	1.660	1.668
F	1.015	1.035
G	–	.795
H	.655	.665
I	.210	.220
J	.310	.325
K	.125	.140
L	1-1/8	–
M	.065	.075
N	.125	.140
P	.67	.69
R	.060	.075
S	1/2	–
T	5/16	–
U	3/8	–
V	9/16	–

Figure 7. Machlett EE-65 Electron Gun Configuration.

1-6042

70 mA - 12 kV Electron Gun

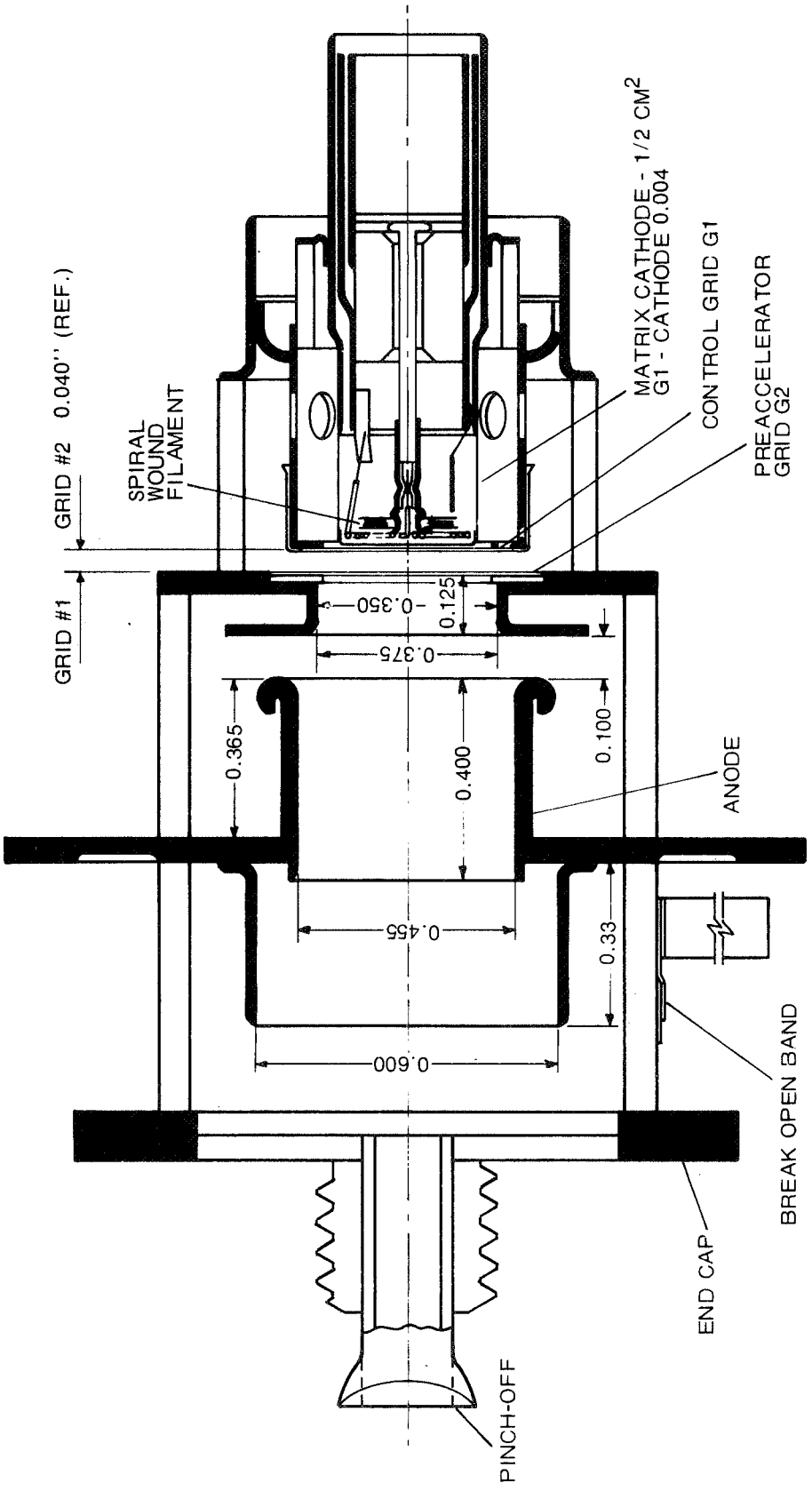

Figure 8. EE-65 Electron Gun Internal Configuration.

1-6043

1.3.1.2 Beam Characteristics

During the course of the development program the beam from a gun was exited into a vacuum chamber and into a multi section cylinderical Faraday cage. Each section of the cage was biased several different ways and the currents to each measured to obtain a self consistent picture free of secondary electron intertransfers. Beam divergence was calculated and the results are displayed in Figure 9. It was expected that some of the beam percentage displayed at large angles is due to uncertainties in the technique particularly with regard to secondaries impinging on the closest cylinderical section to the anode. The curve shows a hard core within about 10 ° half angle which contains, except for the 1.2 keV case, at least 80% of the beam.

1.3.1.3 Operational Requirements/Characteristics

The operational characteristics of the closed gun are given by Machlett in their final report to IPC on contract GH-10722 appearing in Table II.

The guns, upon receipt at IPC were required to pass additional tests before being accepted for flight use. A hi-pot test with cap end in vacuum and the other end in one atmosphere of SF_6 was performed to 15 kV potential difference between anode and G2, with the cathode and filament tied to G2. Major breakdowns or leakage currents into the microampere range were cause for rejection. In addition, an operational check was made on each gun to determine grid transfer characteristics at the operating filament potential of 7 to 7.5 V.

A typical grid transfer characteristic is given in Figure 10. Generally speaking, at the operating filament potential of 7.0 volts the curve is somewhat steeper. This is demonstrated in Figure 11 which presents grid transfer curves for gun #208 at 6.3 V and 8.0 V filament potential.

Plate characteristics of a typical gun are given in Figure 12. As a tube, the gun appears to act very much like a beam power pentode.

Grid transfer characteristics at varying G2 potential are given in Figure 13. At very low second grid potentials the current to the anode is limited by the perveance of the cathode, G1, G2-triode structure as is clearly

Table II. Specification Sheet Electron Tube, EE-65.

Description: Electron Gun

Absolute Maximum Ratings:

Parameter	E_f	E_b	e_b	E_{c2}	E_{c1}	i_b	i_{c1}
Unit	V	kVdc	kV	Vdc	Vdc	mA	mA
	6.3 ± 5%	10	10	1000	-150	100	50
Parameter	$\dagger_{c2}$	$\dagger_p$	Du	P_{g1}	P_{g2}	P_p	TE
Unit	mA	ms		W	W	W	°C
	10	100	.04	1	3	500 Note 1	250

NOTES:

1. If maximum plate dissipation is desired, adequate cooling must be provided to keep the seal and envelope temperatures of the anode and anode end cap within the maximum permissible level.

2. During this test the droop of the plate current should be recorded and be smaller than ik = 25 mA.

3. The design approval tests are only required at the beginning of an order or contract to verify the mechanical structure. Perform test on three tubes selected from the first lot. If more than one tube fails, the test shall become a part of the production test with an AQL of 6.5 inspection level S3. After three consecutive successful submissions, the test shall revert to a three tube once per order test. This is not a destructive test.

4. With the tube cold and the voltages applied as indicated, the tube should be tested for external arc-overs. There shall be no evidence of failure as indicated by external arc-over.

Table II. Continued.

PRODUCTION TEST	Conditions	Symbol	Limits Min.	Max.	Units
Beater Current	E_f = 6.3	if	.75	.95	A
Insulation of Electrodes	E_f = 6.3; E_b = E_k = E_{c2} = 0; E_{ci} = -500 Vdc	R	50	-	Meg.
Cut-off Voltage	E_f = 6.3; E_{bb} = 10 kVdc; E_{c2} = 800 Vdc $E_{ci/ib}$ = 5 μAdc	$-E_c$	-5	-11	Vdc
Pulse Test	E_f = 6.3; E_{bb} 10 kVdc; E_{c2} = 800 Vdc	ec	2	8	V
	E_{ci} = -10 Vdc to -30 Vdc; ec/ib = 75 mA	ic	-	20	-
	†p = 5 ms ± .5 ms; Du = .04 ± .005 (See Note 2)				
Dimensions	As per outline drawing				
DESIGN TEST	See Note 3				
Voltage Arc-over Test (1)	E_k = E_{c1} = E_{c2} = 0; E_b = 5 kVdc E_f = 0 V; See Note 4				
Voltage Arc-over Test (2)	E_k = E_{c1} = 0; E_{c2} = E_b = 1.5 kVdc E_f = 0 V; See Note 4				
Vibration (1) Sinusoidal	10 - 50 cps 3.0 G 50 - 100 cps 6.0 G 160 - 2000 cps 10.0 G — In all three planes				
Vibration (2) Random Noise	20 - 2000 cps .05 G^2/cps for 10 seconds In all three planes				
Post Vibration	Pulse Test				

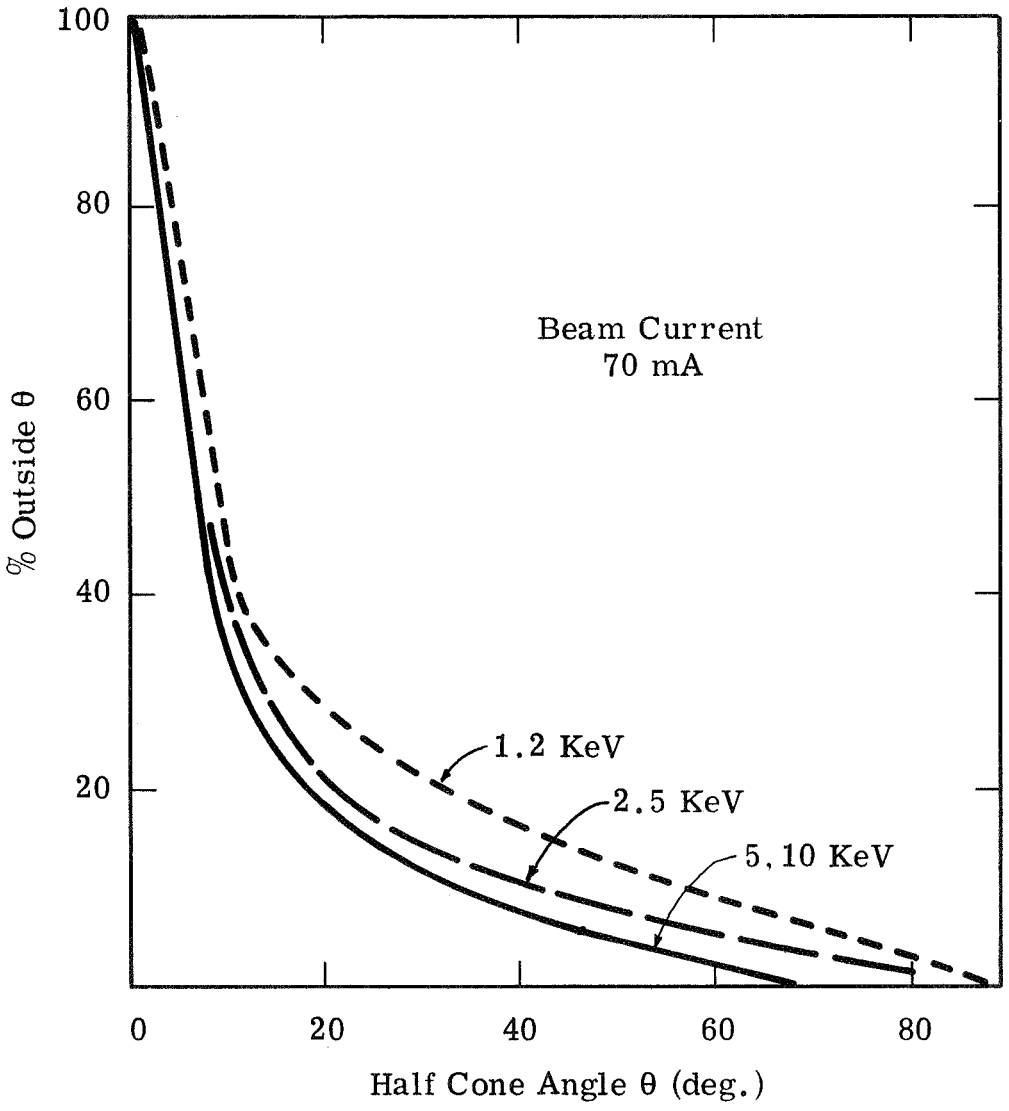

Figure 9. Beam Angular Distribution EE-65.

1-6041

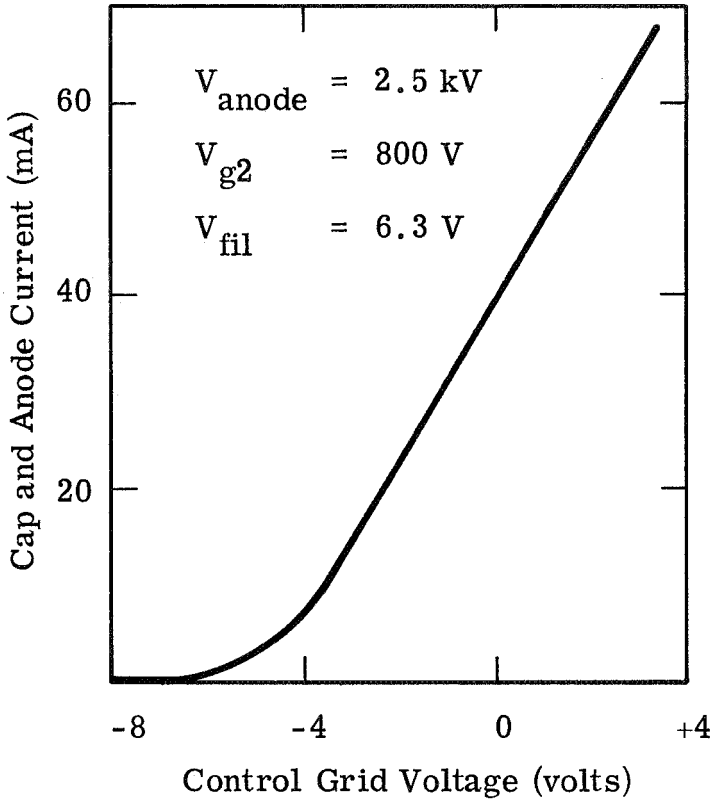

Figure 10. Grid Transfer Characteristics Typical EE-65 Electron Gun.

1-6046

EE-65 #208

$V_{anode\text{-}cathode}$ = 2.5 kV

$V_{g2\text{-}cathode}$ = 800 V

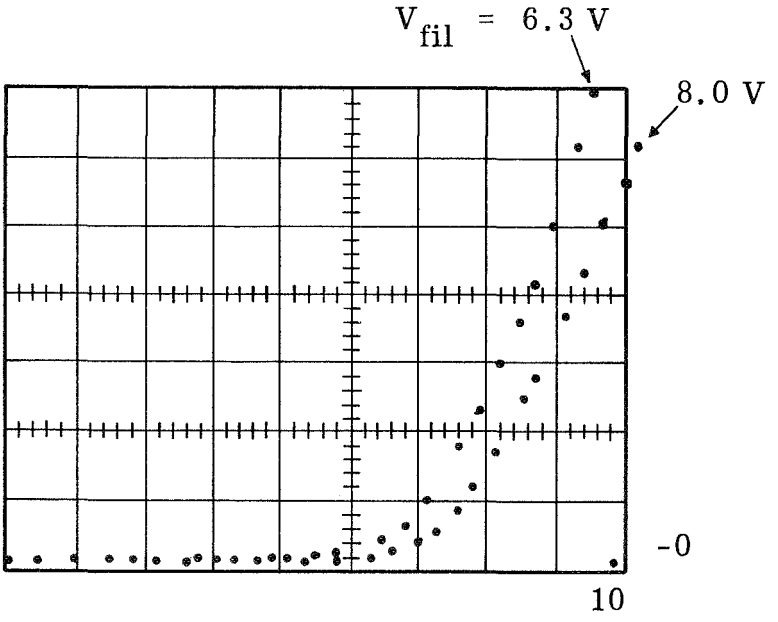

VERTICAL - Anode Current
10 mA/div.

HORIZONTAL - G, volts 2 V/DIV

Figure 11. Effect of Filament Potential on Grid Transfer Characteristics.

1-6047

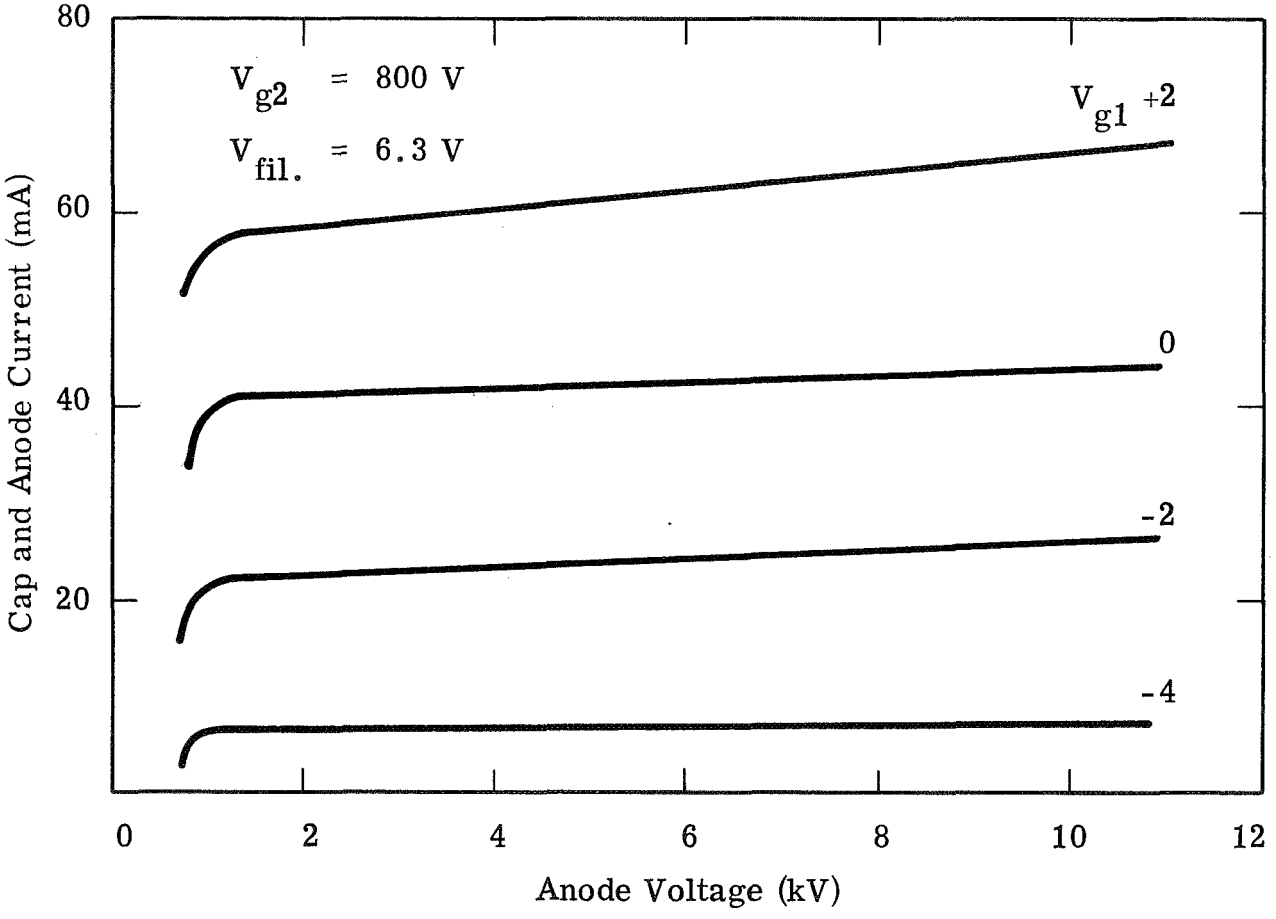

Figure 12. Plate Characteristics Typical EE-65 Electron Gun.

1-6048

EE-65 #208

V_{anode} = 2.5 kV

$V_{fil.}$ = 8.0 V

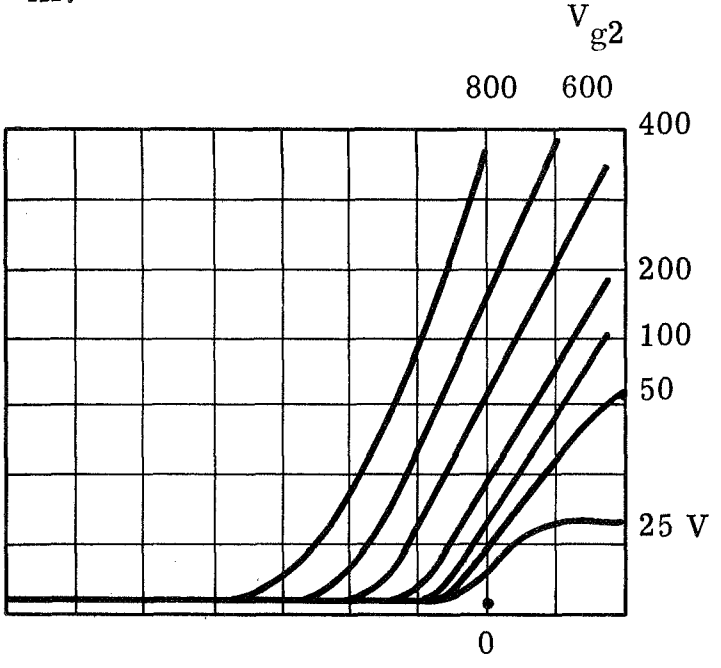

HORIZ. - V_{g1} 2 V/div.

VERT. - $I_{anode + cap}$ 10 mA/div.

Figure 13. Grid Transfer Characteristics as a Function of G2 Voltage.

1-6049

demonstrated in Figure 14. The figure also demonstrates the extent of the anode-G2 field penetration into the G1 - G2 interelectrode space.

Electrical interception on the second grid is given in Figure 15. There is little variation in the percentage over a large range of G2 voltages and anode voltages. At the lowest beam current and highest beam voltage it amounts to 3%. At the highest beam currents and lowest beam voltages it amounts to 6.4%. The grid itself is made up of 0.001 inch knitted tungsten mesh with about a 90% geometrical transmission so it is obvious that some focusing is occurring at the grid openings. The power dissipated on this grid at the higher currents settings is sufficient to cause it to reach a yellow white incandescence corresponding roughly to a temperature of 1500 °C. The emission current density is still less than 0.1 μ amp/cm^2 at this temperature - so that no secondary emission of consequence should occur. However, for pulses longer than 100 ms there appears to be a temporary (50 - 100 ms) increase in transconductance probably caused by differential heat up of the control grid with respect to the cathode. The amount of this increase appears to be somewhat dependent upon the time the gun filaments have been on. (No increase if just turned on, 15% increase if on for 15 minutes or more.)

The ratings given by the Machlett Division of Raytheon Corporation with regard to pulse on time have been tested at up to 2.5 seconds with guns opened into a vacuum at beam currents up to 85 mA without deleterious effect on the gun operation. As tested over the course of the contract and in flight there is no performance degradation for one second, 50 mA pulses.

1.3.1.4 Mounting and Techniques

The guns are plugged into gun mounts from the forward part of the payload as in Figure 16. The vacuum pressure seal is made with 1/16 inch Viton O-rings. A beryllium-copper flat spring is screwed down upon two ceramic standoffs and the nickel tabs for gun opening are lugged down to two more standoffs. Bare copper wires from the four standoffs lead to a glass-metal header where they are high-temperature brazed. A closeup of the area

EE-65 #208

V_{g2} = 25 V

V_{fil} = 8.0 V

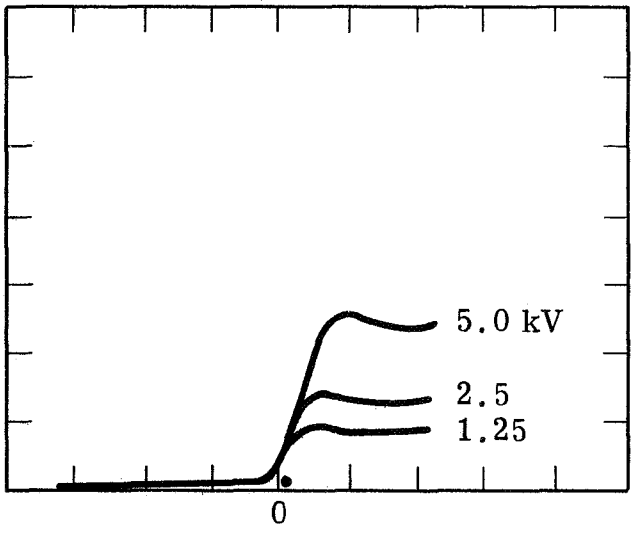

HORIZ. - V_{g1} 5 V/div.

VERT. - $I_{anode + cap}$ 10 mA/div.

Figure 14. Grid Transfer Characteristics at Low V_{g2}.

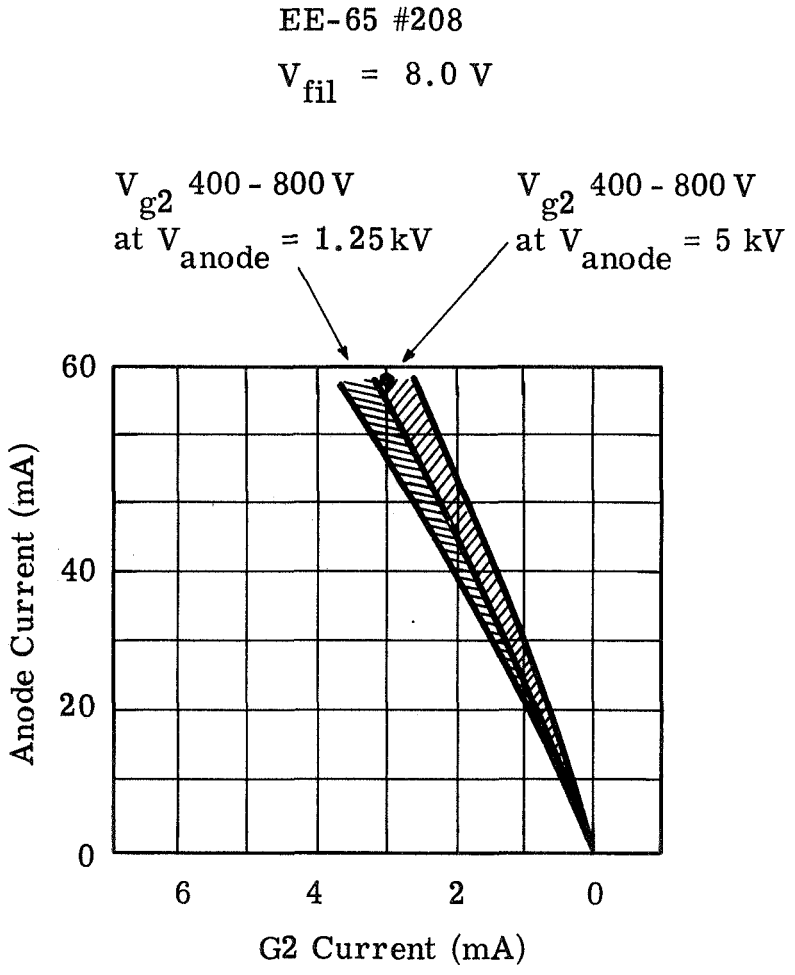

Figure 15. G2 Interception Current.

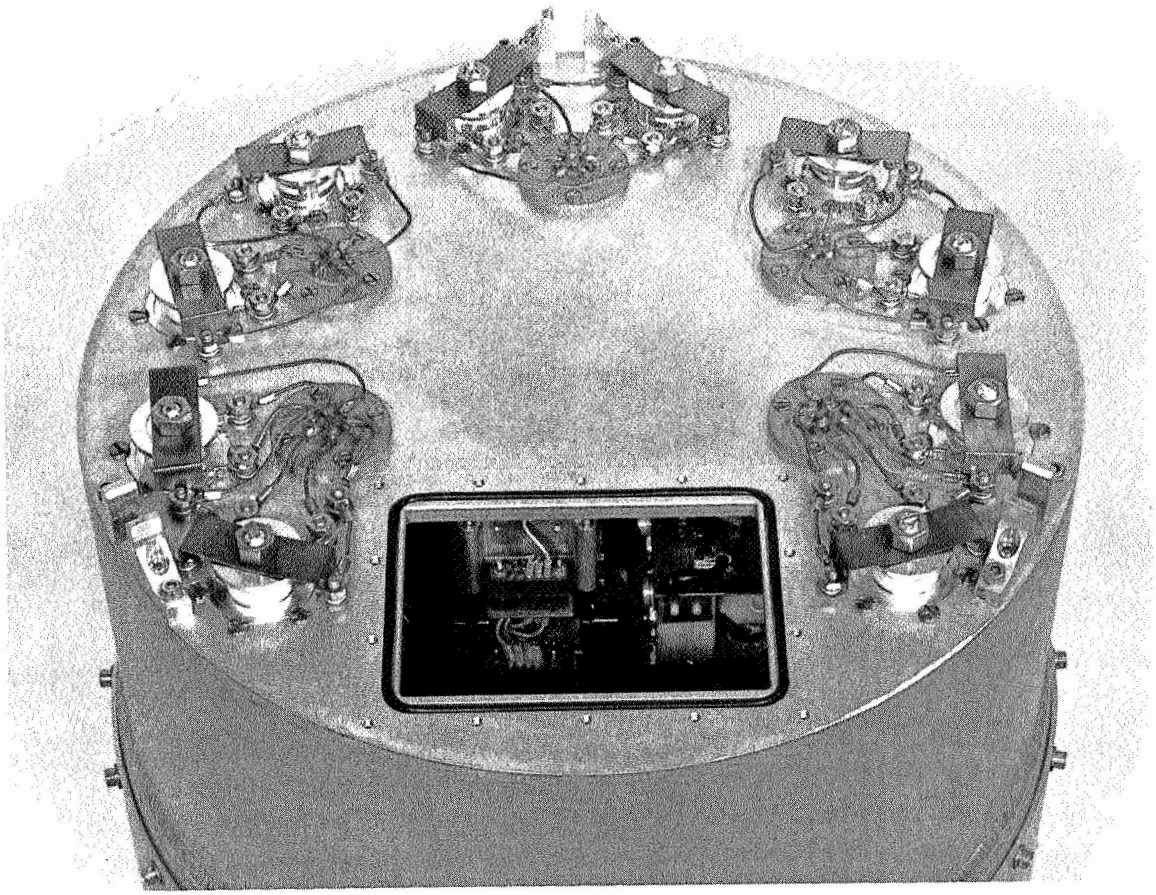

Figure 16. Gun Deck.

is given in Figure 17. It can be seen that the feedthrough is itself brazed to a stainless steel ring which is itself sealed to the top plate using a Viton O-ring.

The mounting and cabling arrangement inside the pressurized cannister can be seen in Figure 18. Basically the gun socket structure is made up of three plastic insulators topped by an aluminum plate at cathode potential. Three smaller insulators mounted on this plate hold the G1 cylinderical finger stock plate and the G2 contact. The filament - cathode connector, also of beryllium-copper finger stock, is force fit into the cathode plate. As can be seen from the figure, connections are made at the cathode plate and cabling is built up on the cathode plates themselves. The two "D" connectors visible carry the filament, cathode, G1 and G2 connections to the insulated plate below. Cabling from the feedthroughs which provides power to open the guns and signals to indicate open-closed condition is also shown in the Figure. Separation from the high voltage cabling is obtained by passing this cable along the structural brace to a D hole in the edge of the insulating plate where the connector is attached. When the insulating plate and its mounted supplies is attached to the cannister these three connections (the two D connections and the pygmy) must be mated.

1.3.1.5 Description of Gun Opening Technique

The gun opening technique was first proposed by Machlett and then developed during the course of their CPFF subcontract with IPC. It involves firing a 1/8 inch Moly-Manganese band onto the breakseal insulator leaving only a short break in the band (refer to Figure 7). A short perpendicular strip of the same material is fired onto the two ends at the same time. After firing, a strip of nickel is then spot welded to the perpendicular end and then brazed with a high temperature silver-gold braze. When the guns are mounted in their sockets, stainless steel lugs are mechanically crimped to the nickel wire ends allowing some slack for vibration and temperature isolation. When a heavy current (nominally 15 V - 50 amp) is passed through the band it thermally stresses the insulator across its thickness, and in about 2-3 seconds causes it to crack cleanly around the periphery. The crack, except in the area of attachment almost

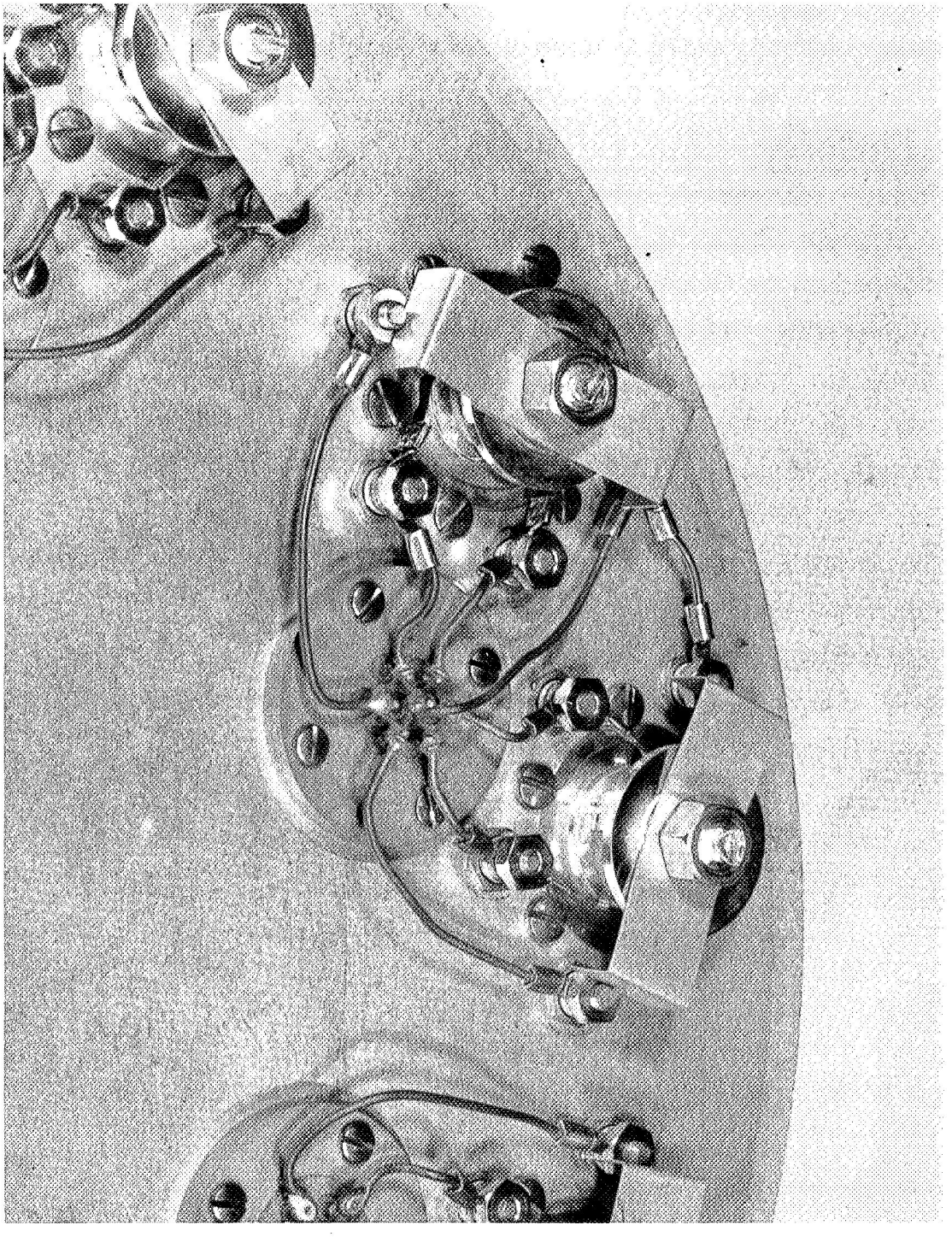

Figure 17. Close-up of Gun Mountings.

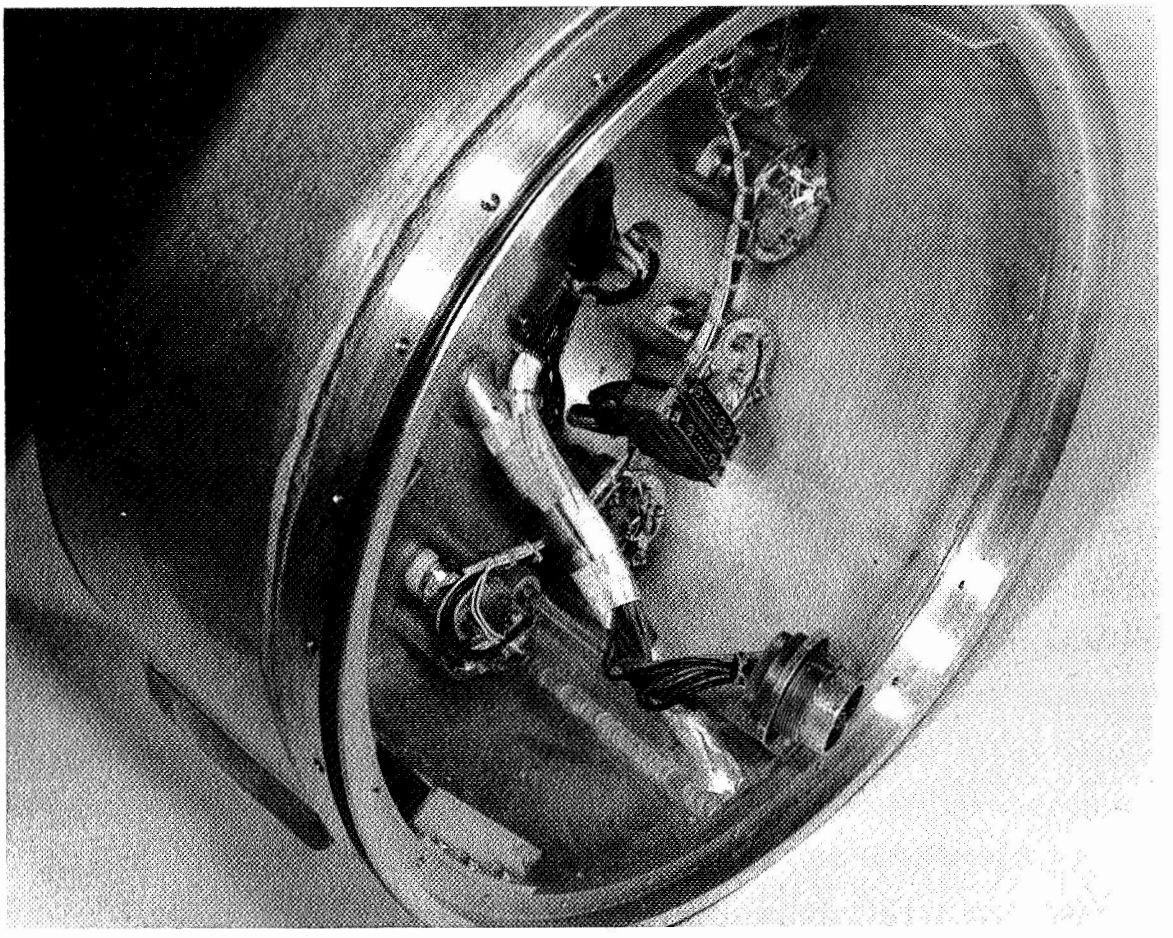

Figure 18. Gun Mounts and Cabling - Pressurized Side.

exactly splits the band in half. An actual break can be seen in Figure 18. The crack, it can be seen, dips in the attachment area towards the attachment. The dip generally occurs in such a way that in the immediate area the band cross-section is quite small, leading in about 50% of the cases to band burnout at these places with some molten metal release to the environment as well as some gas evolution. This has never caused a problem of cathode poisoning.

Because of the large number of guns required for the experiment (10) and the fact that the experiment fails if the guns do not open, a program of reliability testing was initiated during the contract to establish the reliable range of firing conditions. This test program which included the test of over seventy modules, is described in the development section of the report. Figure 20 reproduces the least squares analysis on the time to fire of the bands. At much reduced voltage, the insulator does not break but sits and cooks. At much increased voltage, i.e., greater than about 19 volts the band itself and/or nickel tabs melt or vaporize, again without cracking the insulator. The data in Figure 20 were taken using identical transistor switching circuits to those to be used in the payload. In addition, the identical mechanical mountings, including vacuum interface and spring system were used. This analysis was used to set the number of battery cells used to power the circuits and the sequencing time for breaking open groups of guns. Typically, for a supply voltage of 15 V with a switching circuit drop of three volts, the current at start of the operation is 65 amp, tailing off to 43 amp at the time of break. Since the batteries were rated to only 130 amp. and it was determined during the course of the development program that bands must operate as close to skin potential as possible, it became necessary to switch only two gun bands into each battery at a time; hence requiring the guns to be opened sequentially.

1.3.1.6 Electron Gun Disposition and Totaled Payload Characteristics

Table III presents the disposition of EE-65 electron guns for the flight, those mounted in the 2nd unit payload, and backup guns. Characteristics of these guns and the other guns used in the program, as tested at Machlett, are given in the Appendix.

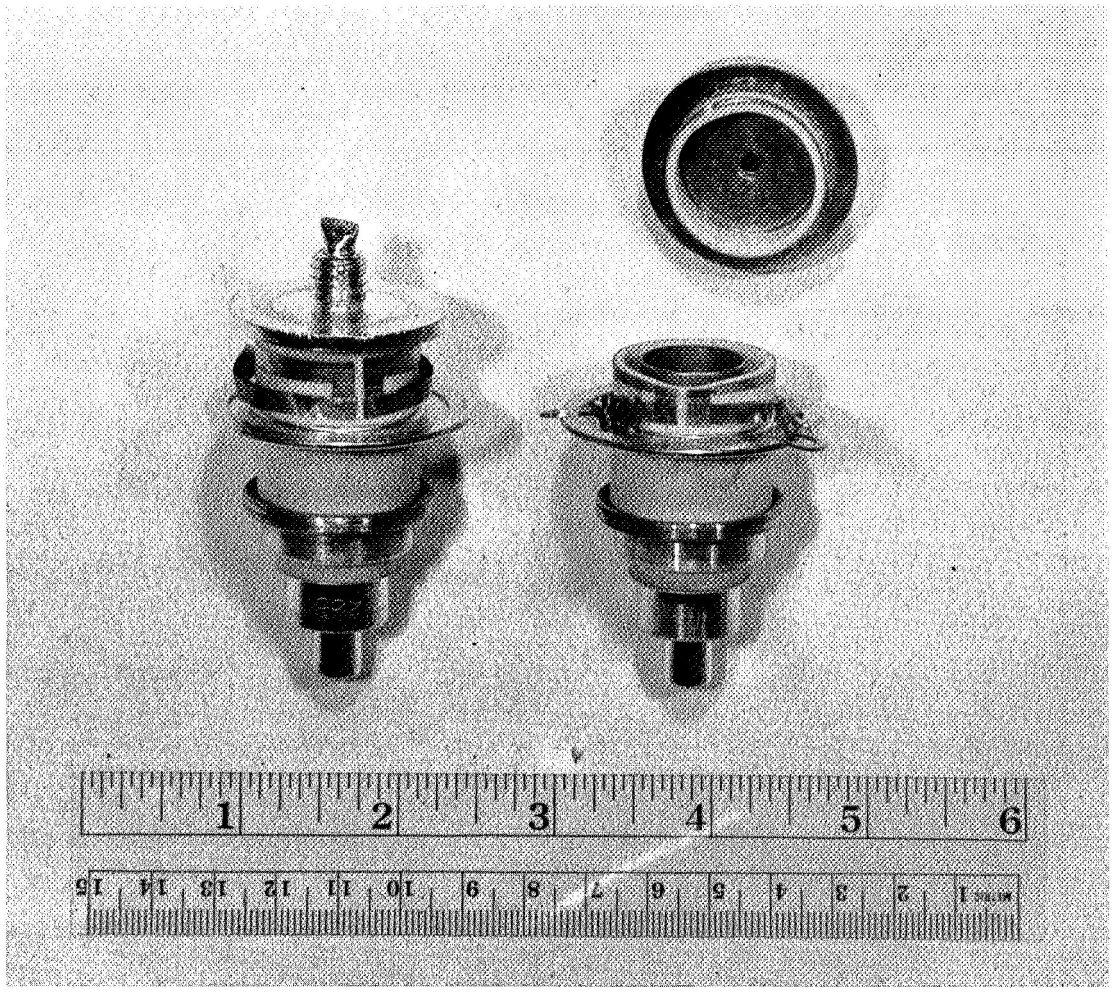

Figure 19. Electron Gun EE-65 - Before and After Opening.

2-1558

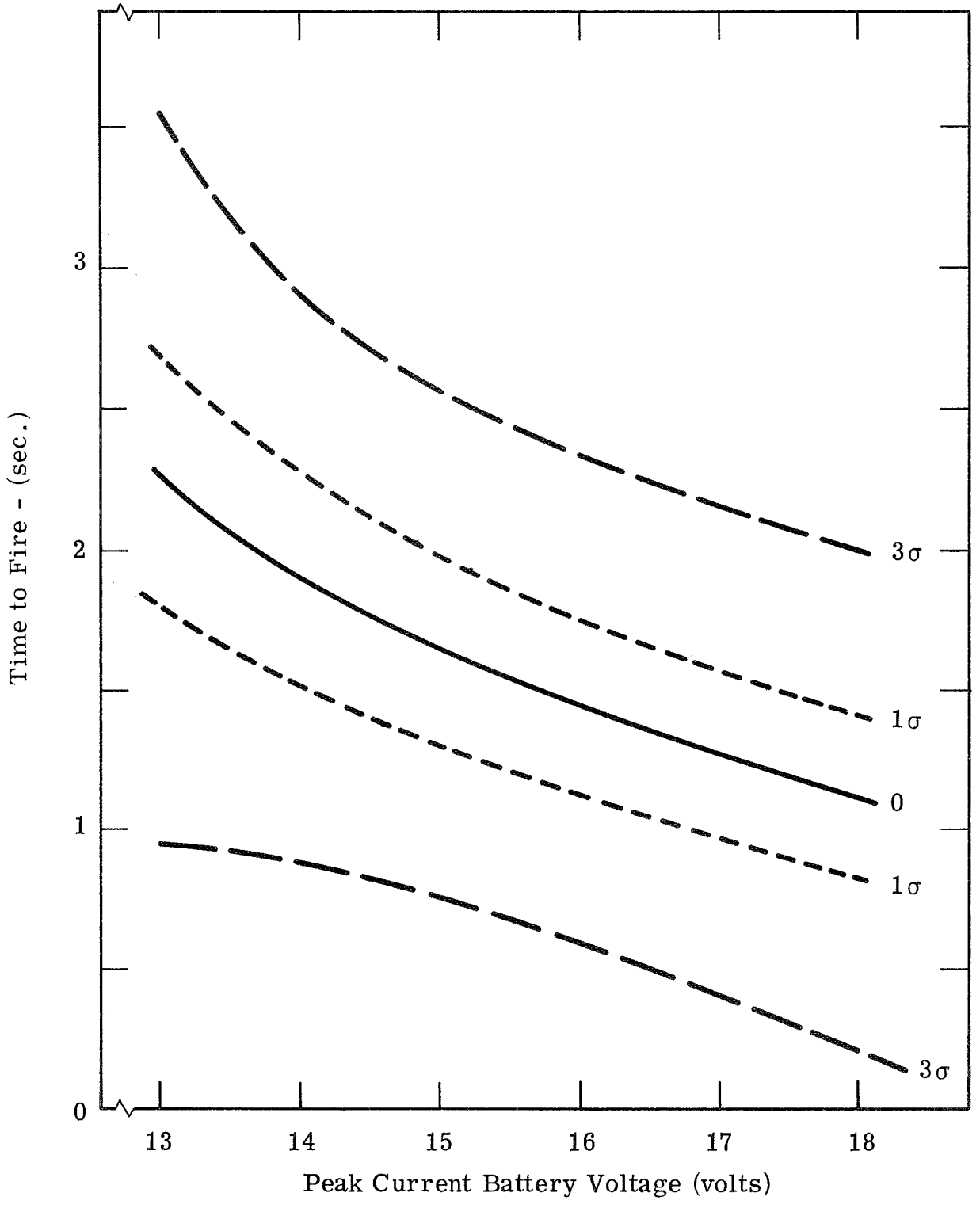

Figure 20. Break Seal Operational Reliability Test Program.

1-6052

Table III. Electron Gun EE-65

Position in pkg.*	Disposition: Flown in 17.03 GE Unit 1	Disposition: Mounted in Unit 2	Disposition: Backup, Unmounted
1	247	270	209
2	252	245	210
3	257	249	218
4	258	250	219
5	261	251	221
6	262	256	222
7	211	259	223
8	269	273	231
9	276	274	
10	216	275	

*Counting clockwise around the circle from the Maier pkg., looking from above the system.

As mentioned before, complete grid bias curves were taken of each gun upon receipt at IPC. Since all gun elements were paralleled a composite grid bias curve could be constructed for each set of 10 guns used. Together with the known G1 battery voltage of 44V this curve was used to determine the cathode resistors for the desired currents. The curves for the 17.03 GE flight guns and for the guns presently mounted in the 2nd unit are given in Figures 21 and 22 respectively.

1.3.2 At Volts Sub-Systems

As mentioned before, the filament supply, second grid supply, beam current controller and batteries to supply these subsystems are all operated with respect to the gun cathode, i.e., they ride the high voltage up when it is turned on. These units are isolated from the vehicle skin by mounting them on a 1/8 inch fiberglass plate. Two views of the sub-assembly are given in Figures 23 and 24. Also mounted on the plate but separated from the at-volts units is the experiment programmer which is mounted from below (Figure 23) through a hole in the plate, and the time delay board which contains circuitry for delaying beam current turn-on. Both of these units are referenced to the vehicle skin potentials. The isolated reed relays, which set the beam current levels are prominent in Figure 24. The coils for these relays are operated through the time delay board and hence are referenced to vehicle ground. The reed switches inside each coil are referenced to the beam current controller and hence are at volts. Similar reed relays are mounted on the filament regulator and the grid two supply to turn them on and off appropriately.

1.3.2.1 Filament Regulator

The filament regulator takes 16 V DC power from the at volts silver-zinc battery and passes it through a series voltage regulator to drop the voltage to the required 7 - 7.5V at the gun filaments. The unit schematic is given in Figure 25. Reference voltage is supplied by the two IN751 zener diodes in series with resistor R1 across the battery. Resistor R2 allows the output voltage to be

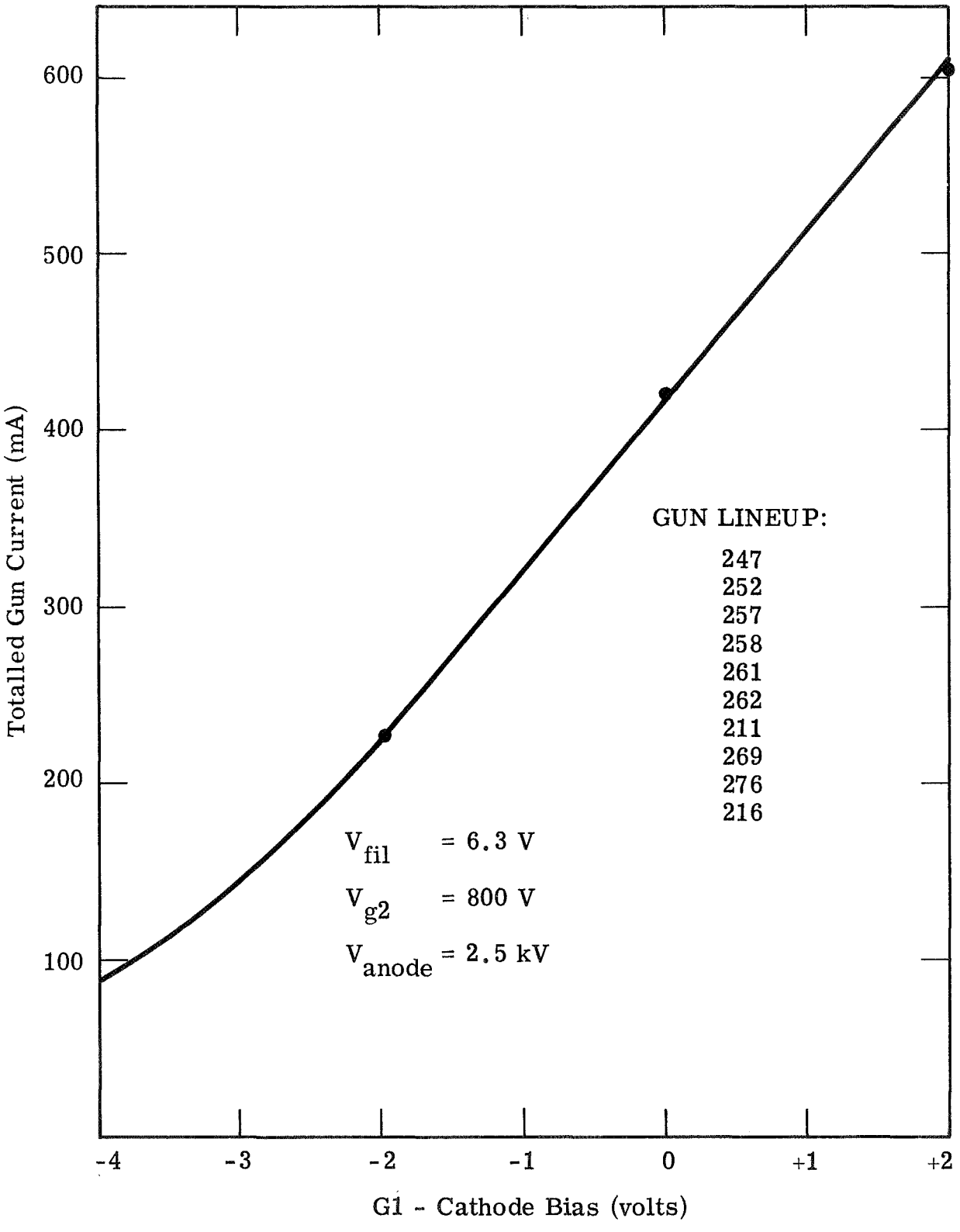

Figure 21. 17.03 Totalled Gun Characteristics.

1-6053

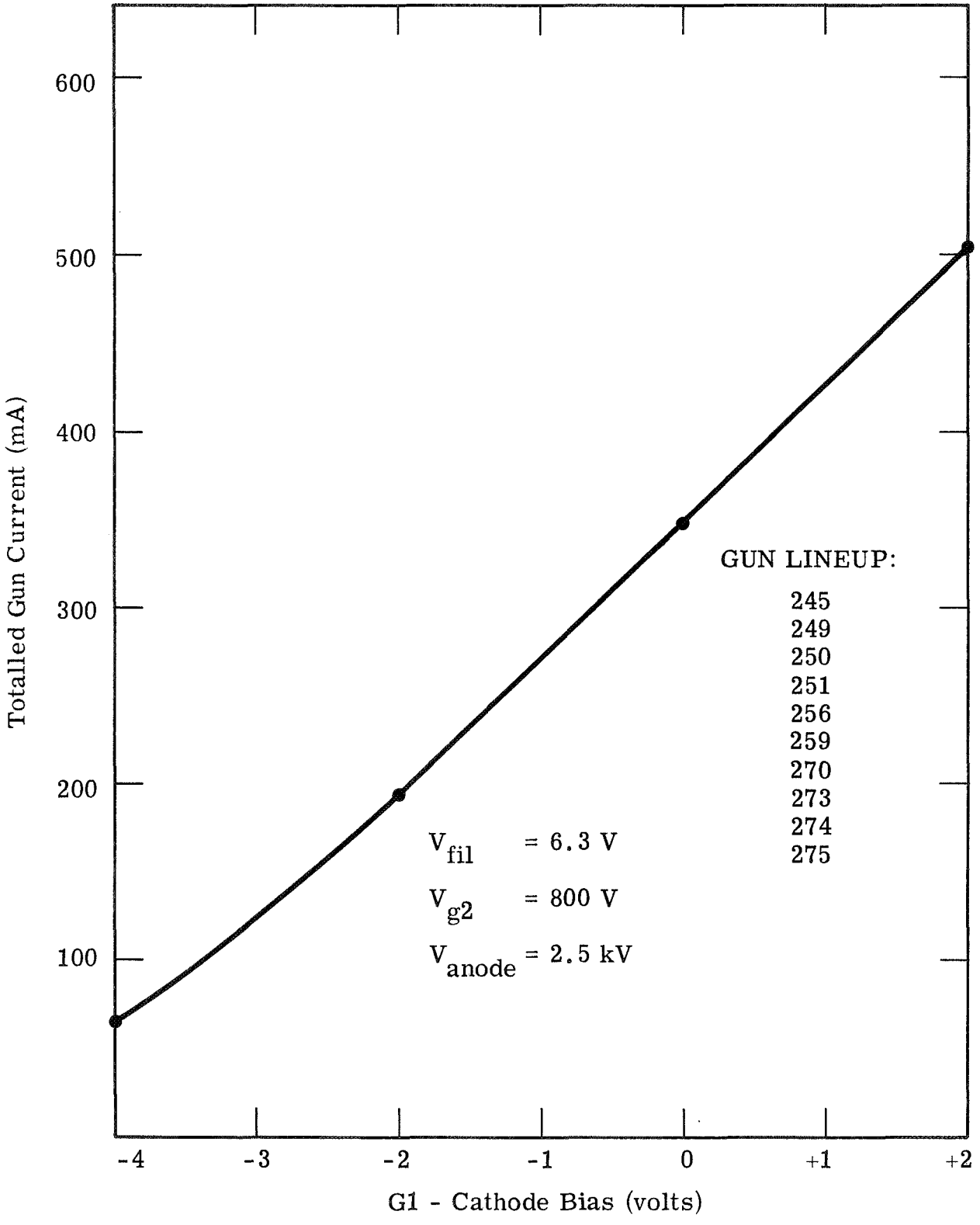

Figure 22. Totalled Gun Characteristics Unit 2.

1-6054

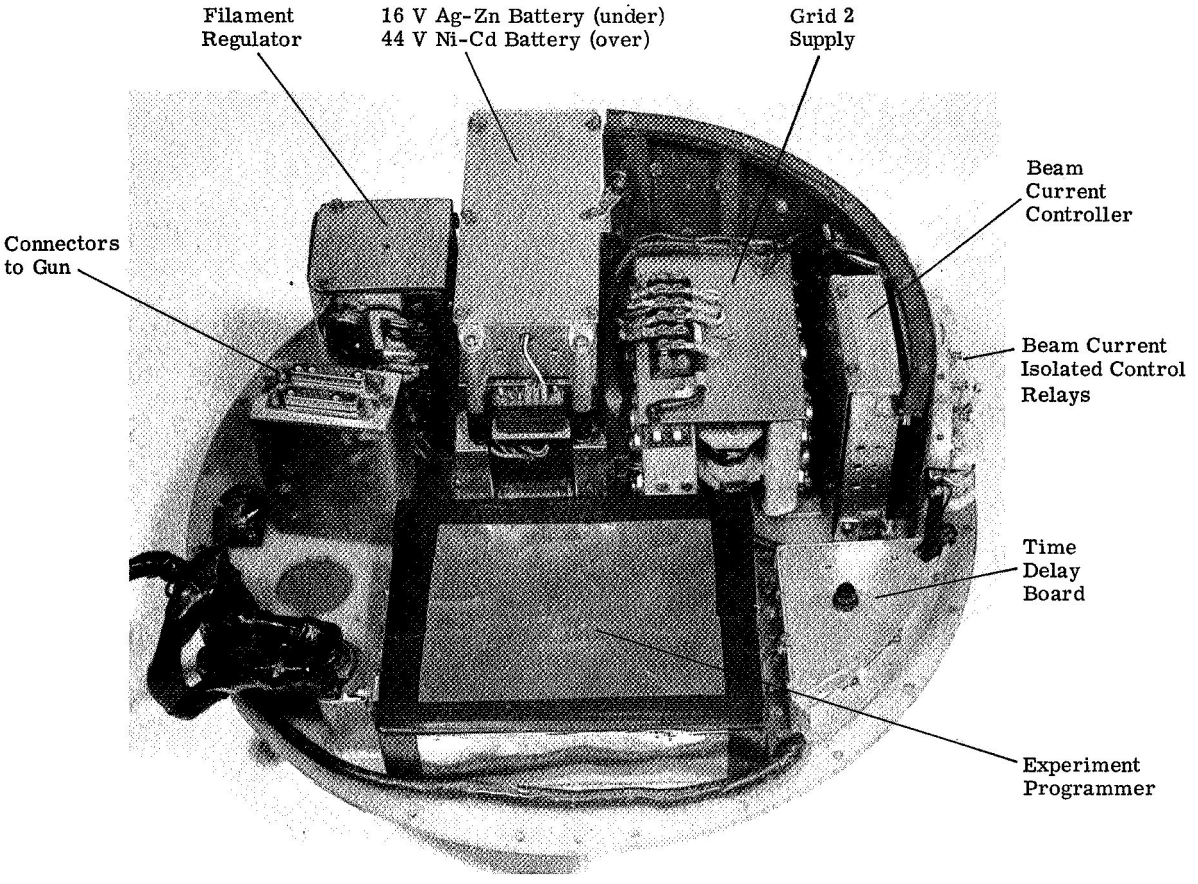

Figure 23. Insulated Plate Sub-Assembly - View 1.

2-1559

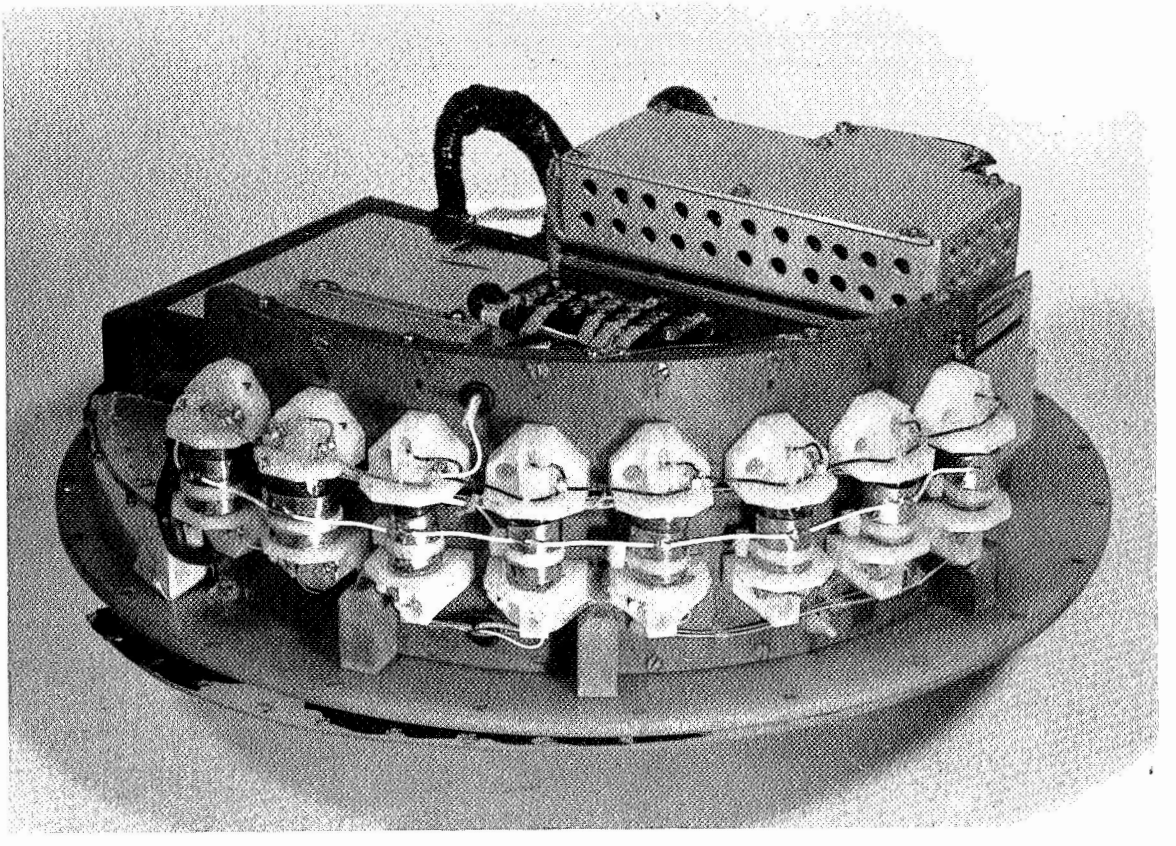

Figure 24. Insulated Plate Sub-Assembly - View 2.

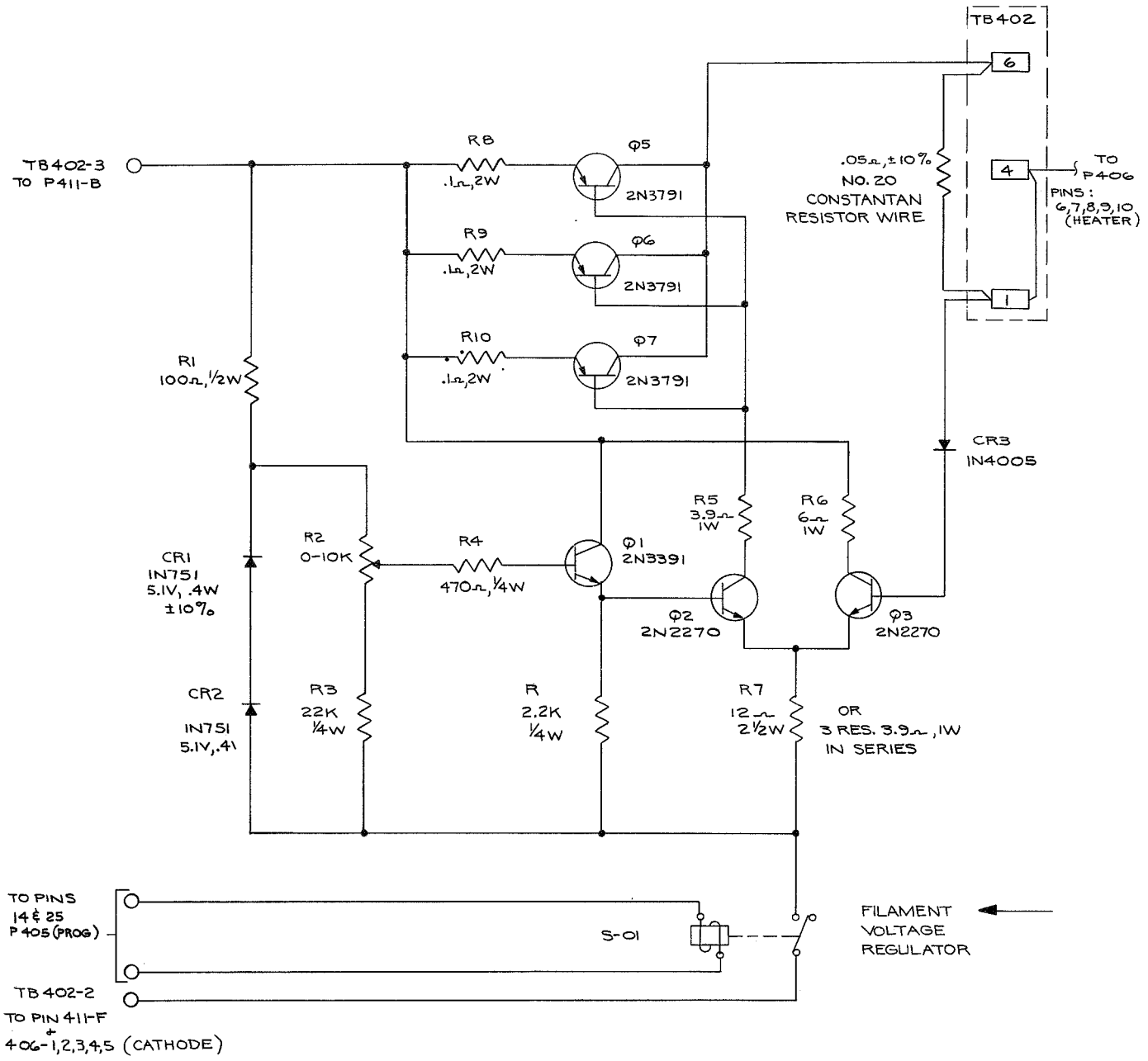

NOTES ~

1. ALL RESISTORS ARE ±10% TOL. UNLESS OTHERWISE SPECIFIED.

Figure 25. Filament Regulator Schematic.

1-6055

varied from about 6.0 to 8.5 volts. Output regulation for 12 to 15 volts input variation is 3%. With the input voltage set at 15 V, the output voltage varies 6% for a load change from 6 to 12 amp, (0.85 to 0.87 amp is correct for each gun). The aluminum chassis is sized to provide heat-sinking for at least 15 minutes of continuous operation.

1.3.2.2 Second Grid Supply

The second grid supply takes power from the 16V silver-zinc battery and converts it to 800V dc power which is applied through a h.v. diode to the second grids of the guns. A schematic of the circuit is given in Figure 26. The battery power passes through a series regulator consisting of Q_5, Q_6, and Q_7 regulator transistors, comparison amplifier Q_2 and Q_3, and zener voltage reference CR1 and CR2 in series.

A uni-junction pulser Q11, R20, R21, R33 and C2 provides pulses at an 8 kc rate to the IC-DT μL 931 which produces a square wave output to the driver stage of a driven bridge inverter. The inverter feeds torroidal transformer T_1.

It was determined during the development effort that high voltage breakdown in the gun structure occurred in the laboratory with closed guns, in the vacuum system with opened guns and would undoubtedly do so in space. The initial path of the breakdown would be from anode to second grid, the pulse passing down via the bleeder in the second grid supply, or through the supply itself. The high voltage diode was added and the bleeder changed to accommodate the total voltage drop across it during breakdowns. No further troubles were experienced by the supply during breakdowns after these additions. Figure 27 presents a view of the supply with cover removed - showing the h.v. bleeder and diode board. The isolated reed relay which turns the unit on and off can also be seen in the photographs.

Generally speaking the interception current on the 2nd grid does not rise above 5% of the beam current. At 50 mA/gun x ten guns = 500 mA total cathode current, 25 mA of this goes to the 2nd grid. The supply regulation over

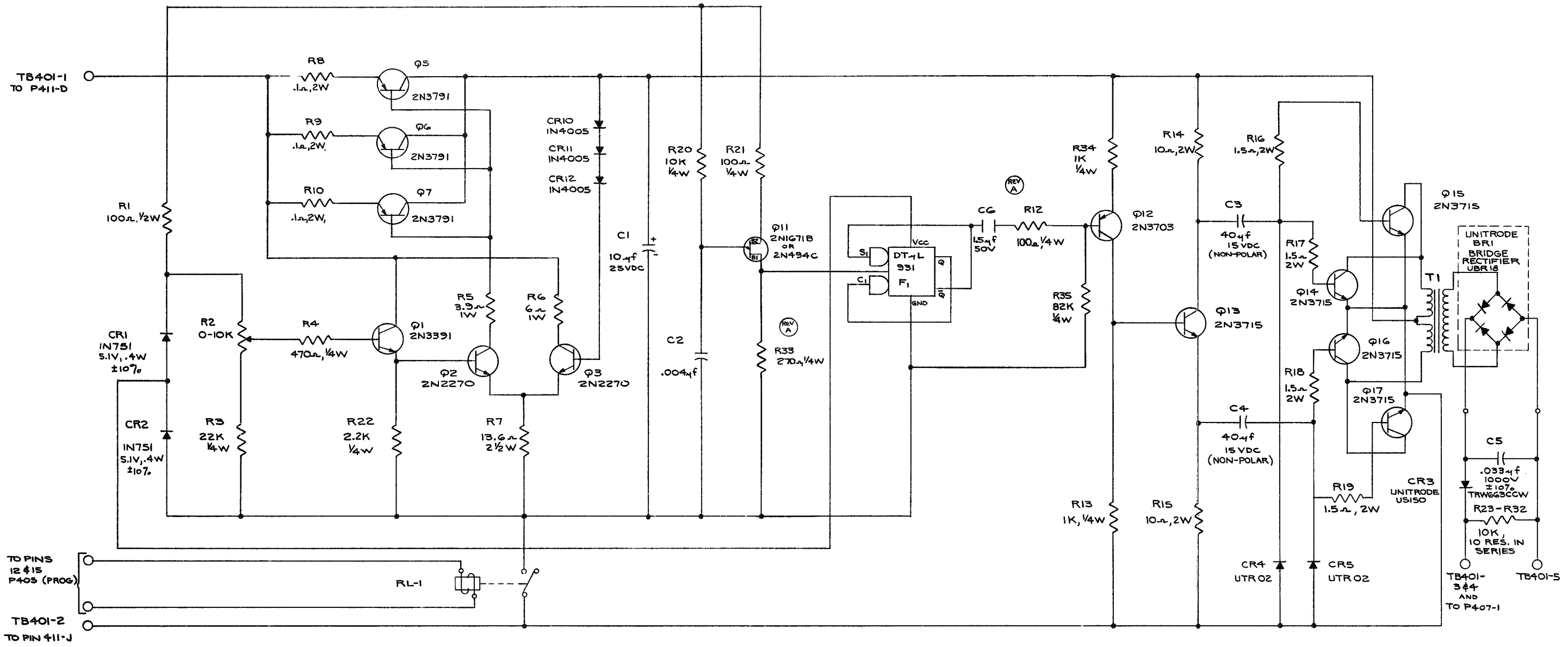

NOTES~

1. ALL RESISTORS ARE ±10% TOL. UNLESS OTHERWISE SPECIFIED

Figure 26. Pre-Accelerator 800 V Converter Schematic.

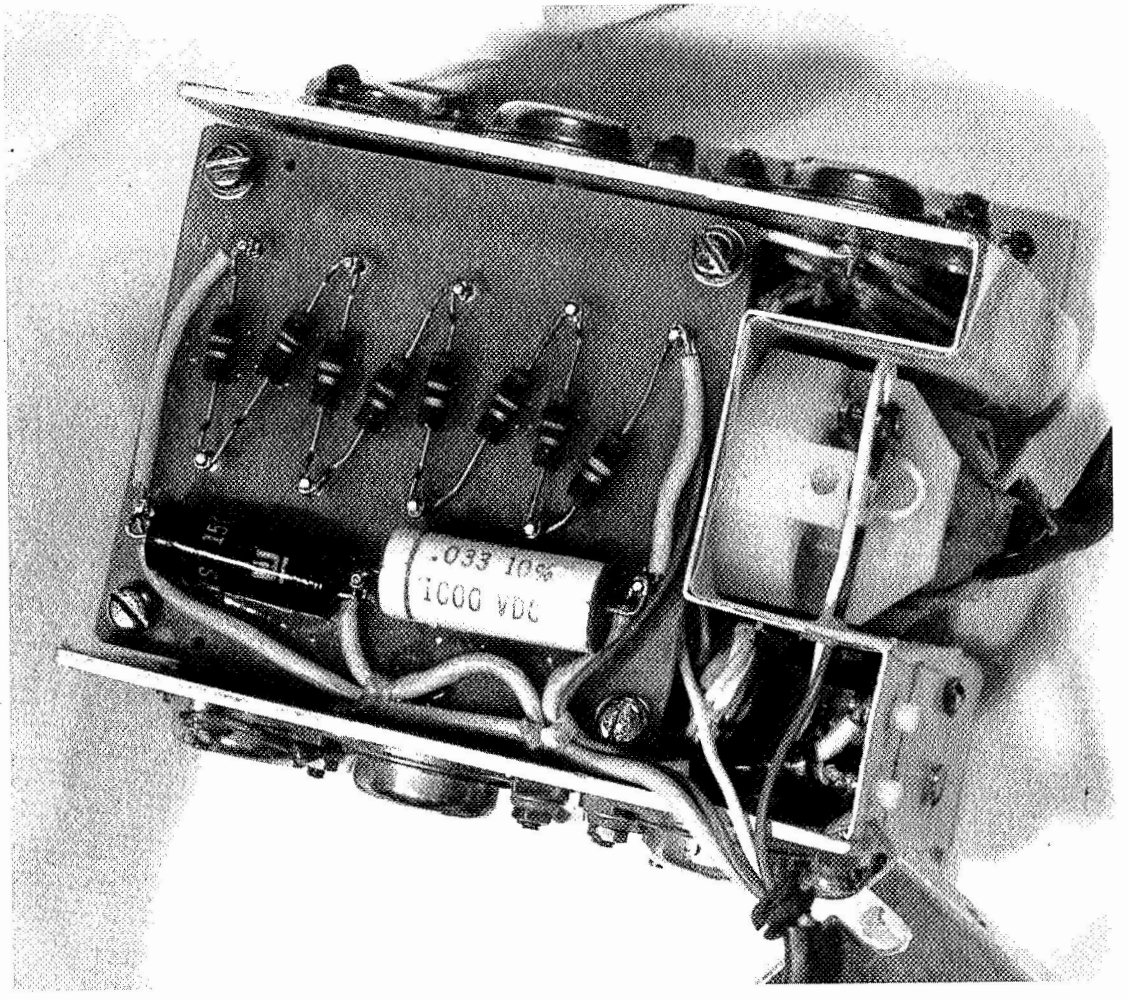

Figure 27. Pre-Accelerator Supply.

2-1561

an input voltage from 12 to 15V and load from zero to 50 mA is from 810 to 750 volts. This changes the required grid drive an insignificant amount.

1.3.2.3 Beam Current Controller

Beam current control is obtained by the use of a cathode follower arrangement. A sketch of the basic circuit is given in Figure 28. In the sequence of operation, the high voltage and 800V are turned on first by a signal from the experiment programmer. At this time only the 1.5 megohm resistor is in the cathode circuits, insuring that the guns remain effectively cut off. (Actually 35 micro-amperes of current can flow.) The current signals from the experiment programmer pass through delay circuitry derived from the 800 v converter turn-on signal, delaying signals to the several isolated reed relays for 100 msec. These relays, as seen by the full beam current controller sub-system schematic, Figure 29, control the insertion of resistors in parallel with the 1.5 meg cutoff resistor to bring the beam current to the desired current level. The resistors called out on the schematic are nominal. The exact resistors used are chosen to produce the correct current for the particular set of electron guns emplaced, making use of summed grid-bias curves such as in Figures 21 and 22. For the 500 mA currents three reed switches are required to remain safely inside their current rating; hence the three 225 Ω resistors in parallel.

During ground checkout of the system it is desirable to run at full current and power. With the guns closed this is possible but at only a very reduced duty cycle. The controller design incorporates circuitry to meet this criterion. At current settings under 500 mA, where all pulses are only 100 ms long, the power duty cycle is low enough on the gun caps so that no changes in duty cycle are required. At the 500 mA level, the circuits are set up so that only a short between ΔT10 and ΔT11 will produce the full flight duty cycle. With an open between these two lines the circuits allow the full 500 mA current to be produced for a time dependent upon the capacitance across these two points. With no added external capacitance (these lines are accessible to the GSFC Instrumentation section of the payload or via bipass hard lines to the IPC Checkout console) the full current pulse is about 8 ms long. After this time,

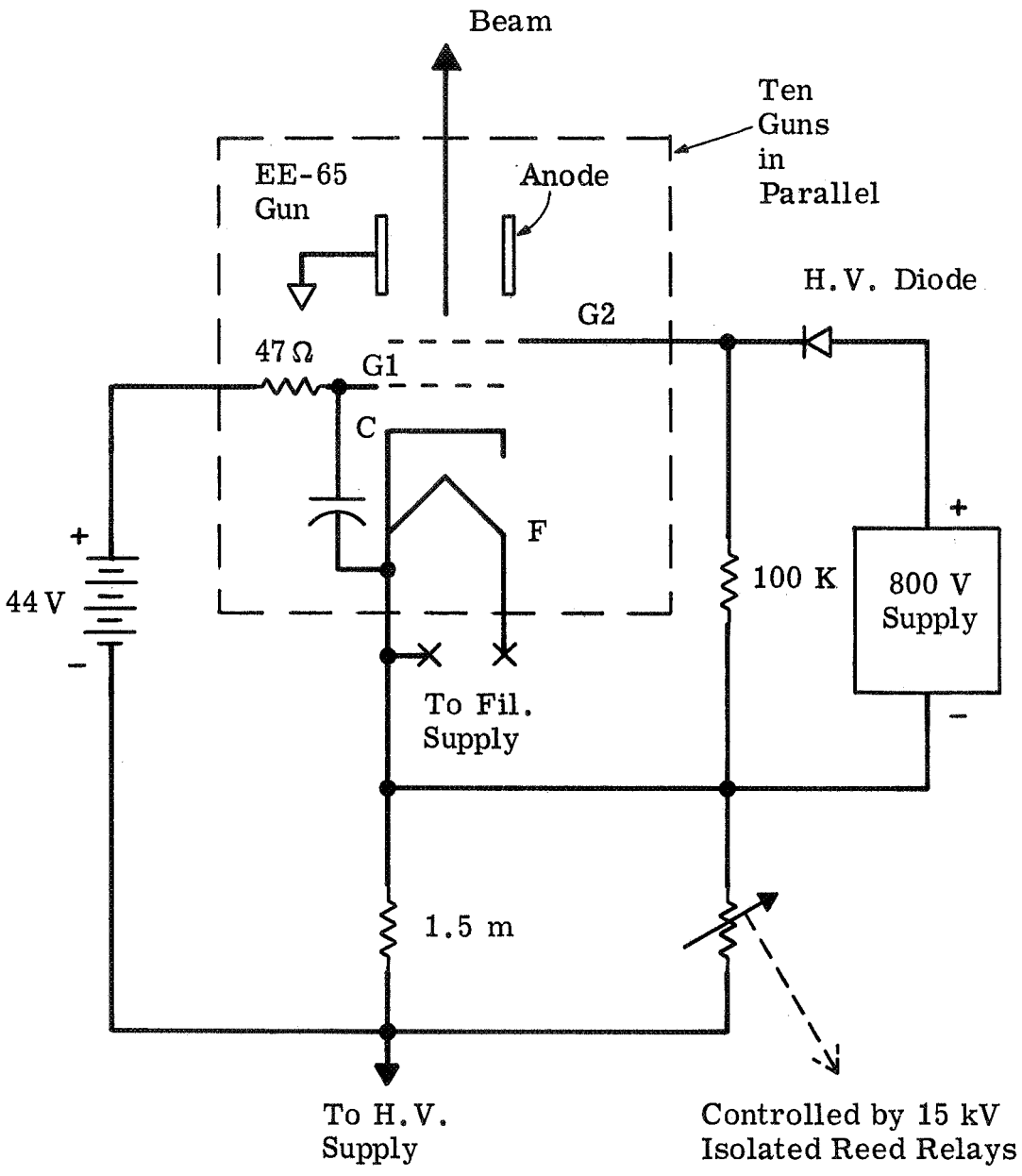

Figure 28. Basic at Volts Gun Circuit.

1-6057

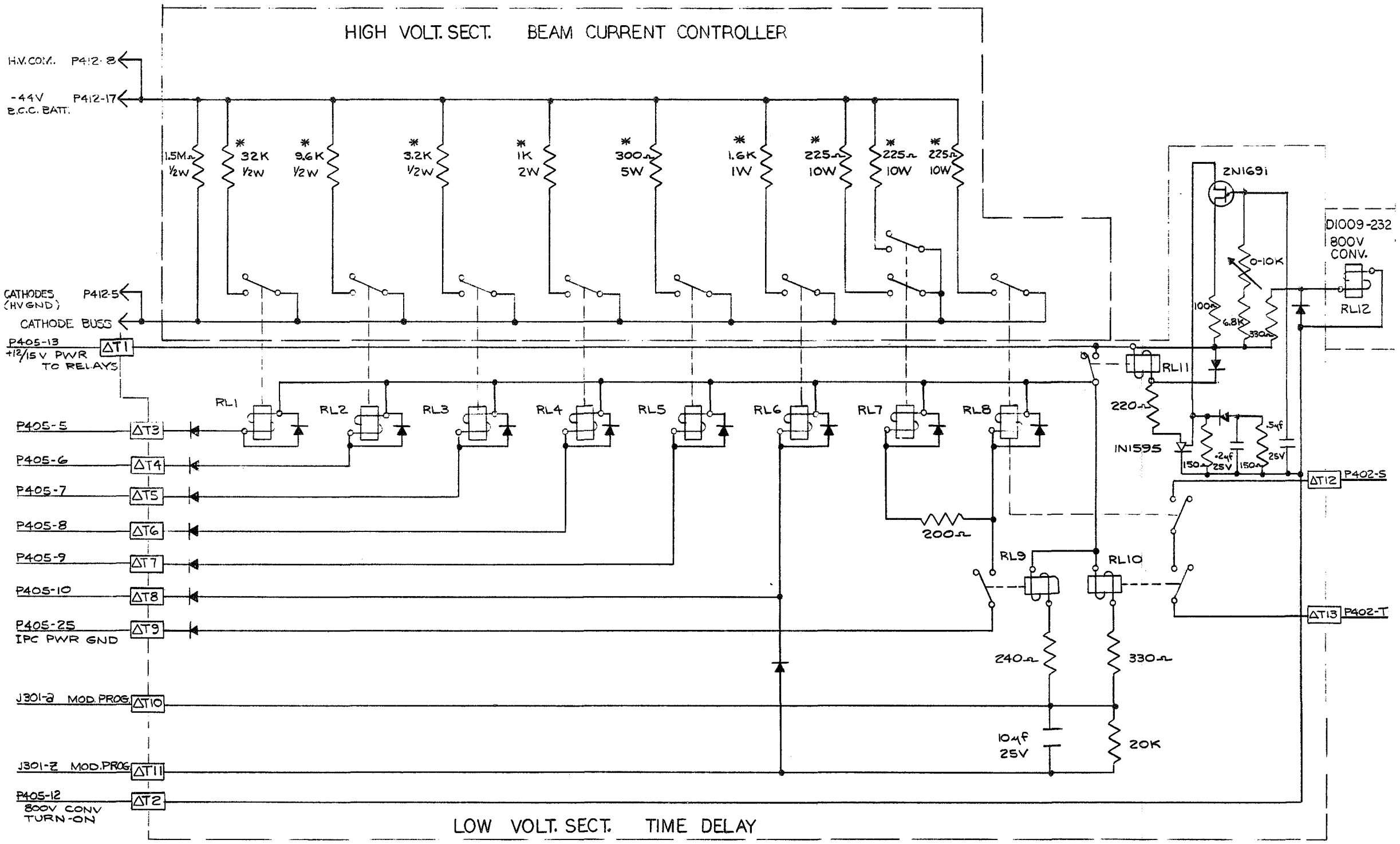

NOTES-

1. * SELECT RESISTORS FOR REQUIRED CURRENT
2. ALL DIODES (IN4001) UNLESS NOTED
3. RELAYS RL7 & RL8 ARE DOUBLE SW.
4. J301-a & J301-Z, SHORTED BY HAYDON TIMER FOR FLIGHT
5. RELAYS, RL9, RL10, ALLOW 8th MODULE TO TERN ON WHEN 500ma COMMAND IS GIVEN.

Figure 29. Beam Current Controller Schematic.

relay RL9 drops out, removing power from relays RL7 and RL8 which in turn remove the paralleled 225 ohm resistors from the cathode follower circuit leaving only relay RL6 and the 1.6 K resistor in the cathode circuit until the end of the 500 mA current pulse. This resistor is set up to produce a current of 38 mA, significantly different from the flight programmed currents as to not be confused with them, yet of sufficient current to easily observe and check the system operation, particularly pulse cut-off.

The controller circuitry low voltage section performs a third function related primarily to the operation of the high voltage converter. For the single pulse condition 10 kV, 500 mA, an 8th, 1.25 kV converter module must be switched in to improve the voltage regulation. The AND circuits feeding the 8th module are set up so that both of the switch elements in series between T12 and T13, as seen in the BCC schematic, must be closed in addition to the appropriate 10 kV turn-on gate signal from the experiment programmer to the converters, before the eighth module will turn on. It is imperative to preclude unnecessarily high gun voltages that this eighth module not be turned on during lower current operations. This of course includes the modified current utilized for ground checkout; hence, the rather complicated relay circuitry revolving around RL8, 9 and 10.

Upon voltage turn-on, the reed switch in RL8 inhibits eighth module turn-on until after 500 mA turn-on. In the flight position (short between T10 and T11) voltage cutoff occurs first, directly from programmer to converter circuitry prior to RL10 dropout.

In the modify current position (no short between T10 and T11), the resistances in series with RL9 and RL10 are adjusted so that RL10 drops out before RL9. The relay in the 8th module converter is a little faster than RL7 and RL8; consequently the eighth module drops out before the current reduction, insuring that the voltage does not rise.

Positioning of the major elements of the beam current controller can be seen in Figures 23 and 24. In Figure 24 the isolated reed relays RL1 to RL8 are shown mounted on a curved phenolic backing, starting with RL1 on the right of the illustration and proceeding to the left sequentially to RL8 at the left.

The low voltage section of the controller is exposed to view in Figure 30. Here also can be seen the cabling from time delay board to relays RL1 - 8 and RL12.

1.3.2.4 At-Volts Batteries

Two batteries are required at volts. The first is a 44 V positive bias battery in the grid one circuit; the second is a 16 volt battery for powering the filament regulator and the grid two supply. These batteries must be removed/replaced on occasion during test operations either by removal from the rear of the package by depressurizing, removal of the aft-most section of the package and then the insulated plate assembly; or secondly by removal of the Maier electron spectrum analyzer from the package front face. Positioning of the batteries can be seen in Figure 23; the 44 V battery essentially rests on top of the 16 volt battery. Removal of the battery is effected by removal of the two bolts passing thru posts in the 16 volt battery holder into the insulated plate. The rear of the battery box, visible in Figure 24, has a lip on it which fits snugly into a slot in the 16 volt battery hold down structure. The power connection must also be broken.

The battery consists of an aluminum box which houses two Gulton 17-VO-180-ssc nickel-cadmium batteries placed side by side in the box, connected in series. Each of these batteries contains seventeen button cells with welded interconnections. Each cell is sealed and has internally welded contacts to the (sintered) cell slug. Fully charged, the battery voltage under no load is 43.8 volts. Rated energy content is 180 mahr. Current drain on this battery is zero at negative bias so that only under 500 mA pulsing or high voltage breakdowns does the battery drain. As a consequence a fully charged battery holds its voltage over a long period of time with high reliability. During checkout the voltage on this battery is checked as the beam (cap) current is checked. If the cap current is within tolerance then the battery voltage is within tolerance.

The battery is many times rechargeable via constant current charging.

The second battery required is a 16 V nominal battery which must deliver 10 - 14 amperes to the filaments and to the 2nd grid supply. The filled battery box is shown in Figure 31. Nine special high capacity-high current cells

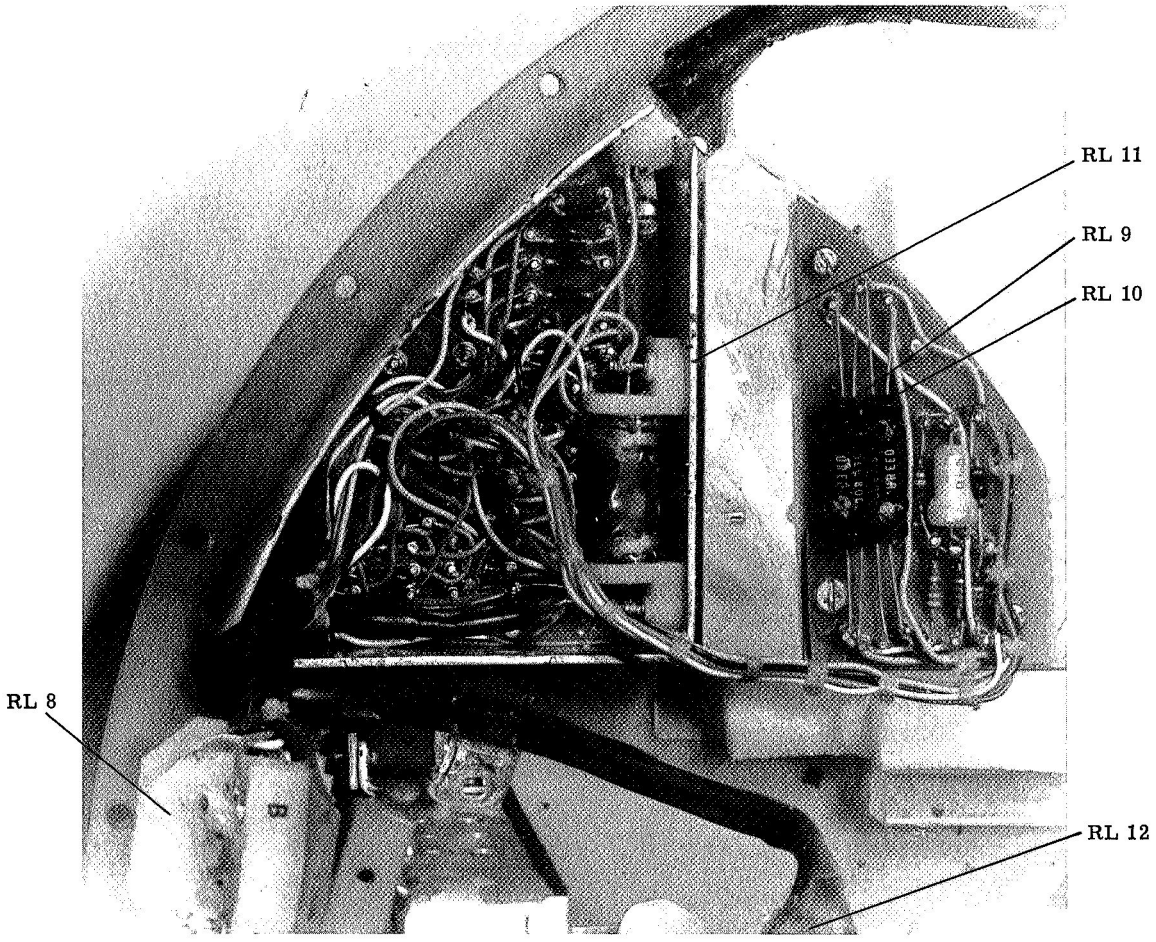

Figure 30. Low Voltage Section - Beam Current Controller Time Delay Board.

2-1562

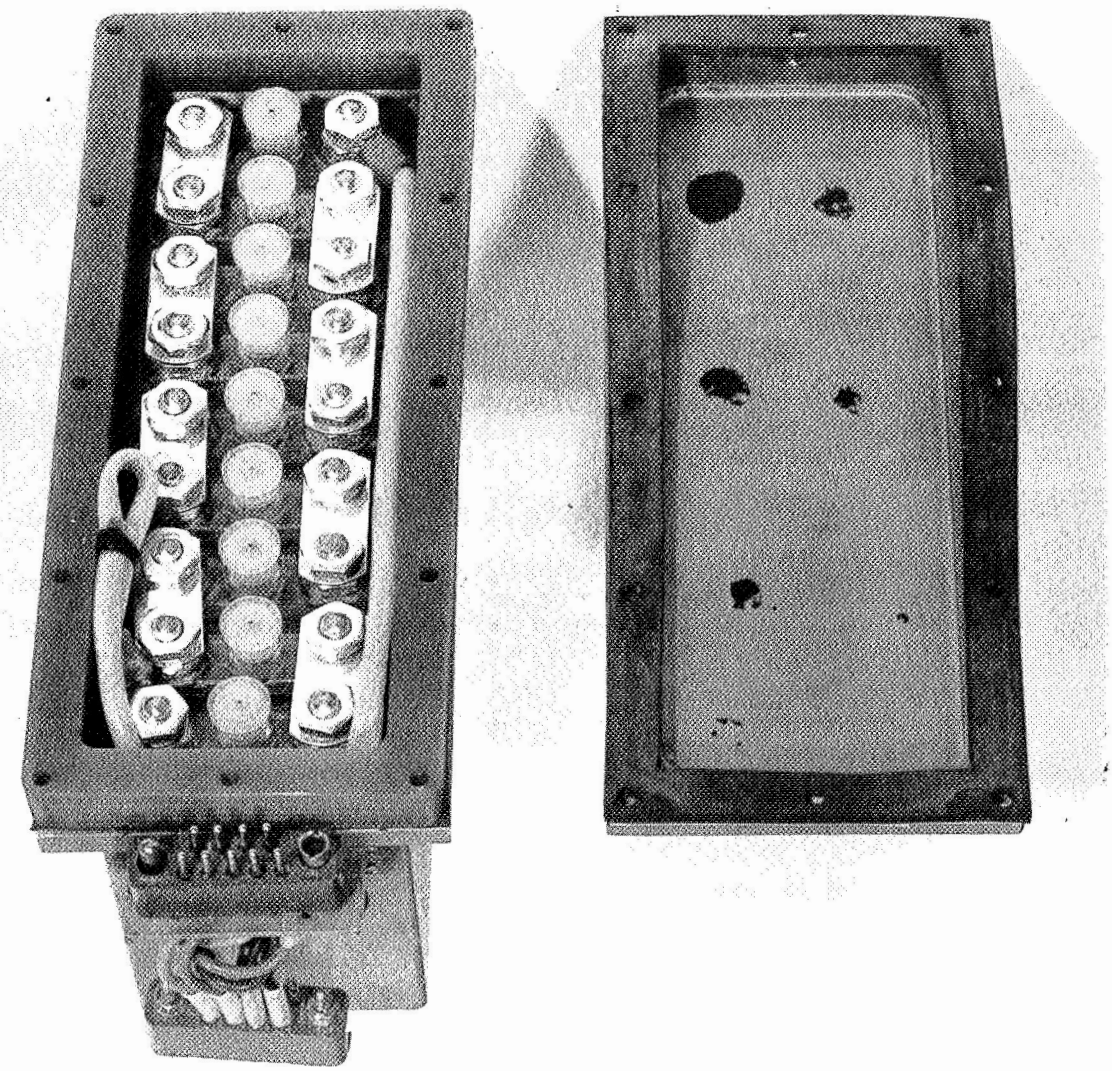

Figure 31. 16 Volt Battery.

are used to make up the battery. They are PMC-3-8 silver-zinc cells purchased from Yardney Electric Corporation. The box is made of non-magnetic stainless steel and is sealed by rubber gaskets and a fiberglass extender section visible in the figure. Power leads are passed through the wall with a number of small glass to metal feedthroughs. The battery can be removed and replaced after removal of the 44 V battery. The cells are provided initially in the dry charged condition with a filling kit. Upon filling and a 2 hour soaking period the battery is fully charged. Normal cell/battery capacity is 8 amphr.

Originally, PM-2 cells with a nominal 2 - 3 hour capacity were used in this battery during the development program but it was found that frequent replacements were necessary. The actual flight of 5 minutes nominal experiment duration should not take more than 1.5 amp. hr. of capacity; however, pre-flight checkouts, etc., plus the fact that a check on this battery voltage is not possible without battery removal dictated the change to the 8 amp-hr. capacity. The voltage load curve of this battery was determined during the development program over the operating experiment life. When fully charged after filling, the cells will have an open circuit voltage of 1.82 - 1.86 volts for a total of 16.4 - 16.7 volts.

During test operations it is possible to recharge the cells in this battery. For flight it is however advisable to use a fresh set of cells which have not been recharged. Charging is by the modified constant voltage method as recommended by the manufacturer except that a greater number of recharges can usually be obtained if charging currents are kept less than 1/2 amp.

1.3.3 Experiment Programmer

The experiment programmer is required via a 28 volt turn-on signal to activate the entire experiment except for the gun opening operation which is activated from a separate signal line. It must activate 11 relays, 4 of which turn on the high voltage converters, 6 determine the electron gun currents and 1 which turns on the screen grid voltage (800 V). The programmer has its own 10 cell nickel-cadmium battery which is switched on by a latching relay in the

programmer package and is also used to energize the Filament Current Regulator relay and the beam current control circuits as well as the programmer circuits.

The high voltage transients sometimes present in the system circuitry have required the programmer package to be heavily shielded against rfi/emi by the use of full spectrum shielding, rfi filters and bypass capacitors on all lines and massive copper grounding of the case to the package skin.

1.3.3.1 Mounting/Positioning

The programmer is mounted from below through a hole in the insulated plate. Position of the programmer can be seen in Figure 23. A single Cannon D connector connects all functions to the unit. Internally the programmer consists of two sections as can be seen in Figure 33. The first is a copper box containing the turn-on latching relay, rfi feedthroughs and bypass capacitors; the second contains the main programmer circuitry on three large boards and one small board.

The programmer battery, which contains two Gulton 5VO-180-ssc Ni-Cd button batteries in series is mounted in the top section of the pressure cannister as seen in Figure 32. Cabling from it passes into the T/M conditioning box where a charge and monitor for ground use is picked off. From there the lines pass into the programmer via the latching relay.

1.3.3.2 Sequencing

The programmer outputs are activated in a predetermined sequence at predetermined intervals in accordance with the flight experiment requirements following actuation of the latching relay via the rocket timer or transmitted command via on-board receiver. The programmer output sequence of 21 discrete configurations continues to repeat until power is removed.

The output sequence as designated by the experiment function is as follows:

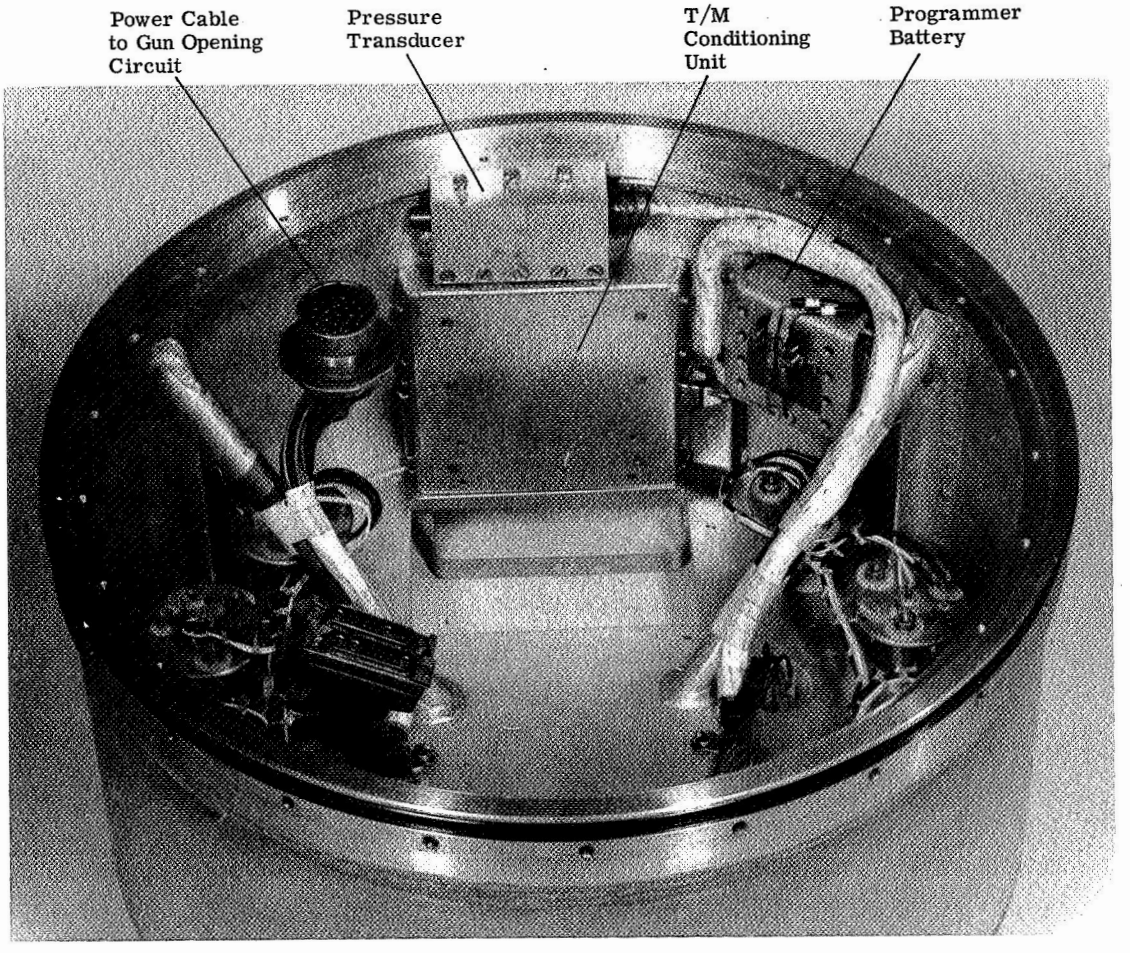

Figure 32. Top Section of Cannister.

2-1564

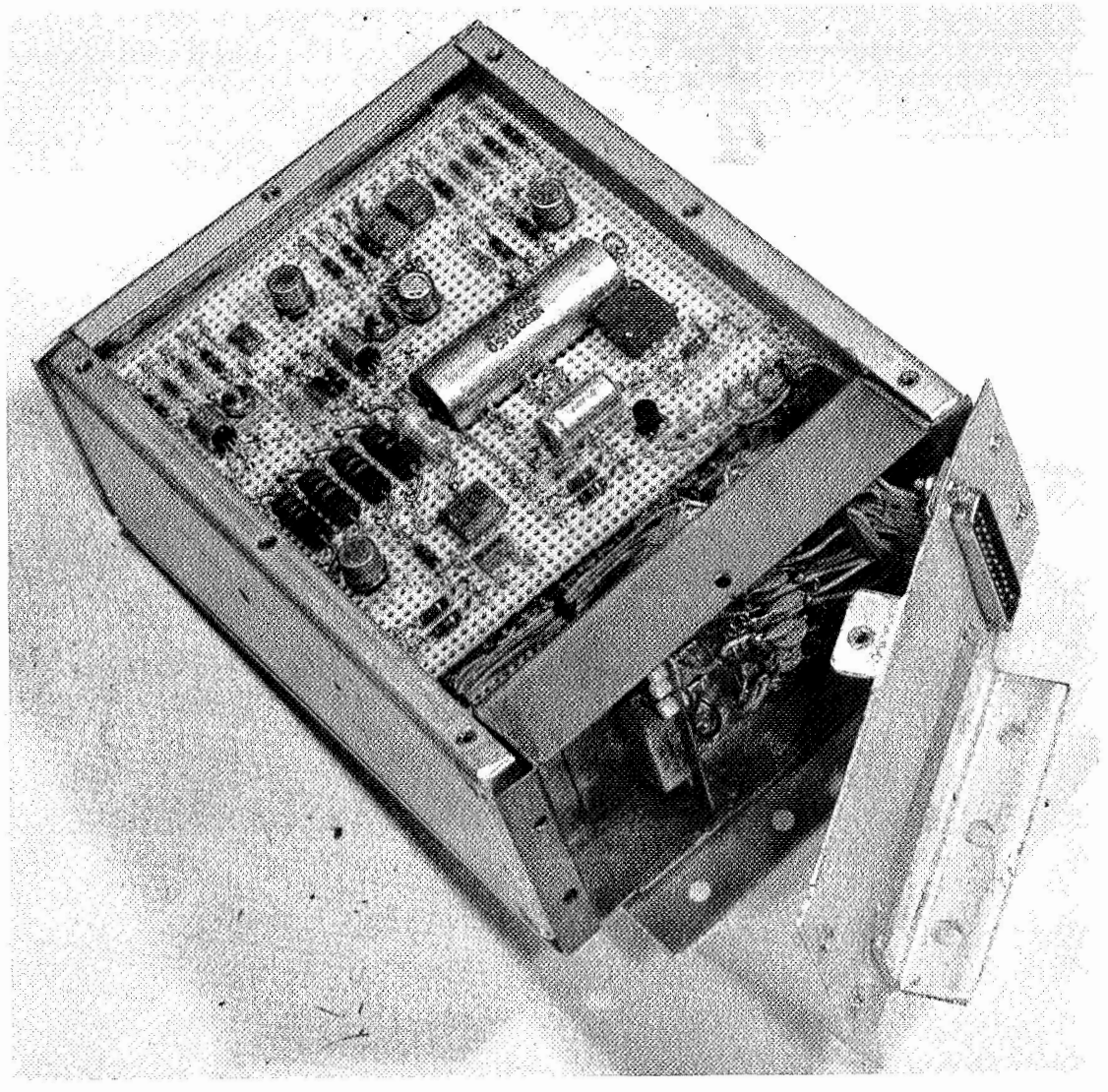

Figure 33. Experiment Programmer - Covers Removed.

2-1565

Pulse No.	Time	Event
	00 (seconds)	Latching relay "on" results in filament and gun bias activation.
	+12 seconds**	Programmer circuits energized
1	+15 seconds**	1.5 mA, 5 kV, +800 V outputs active
	+15.200 seconds**	All outputs inactive
2	+18 seconds	5 mA, 5 kV, +800 V outputs active
	+18.20 seconds	All outputs inactive
3	+21	15 mA, 5 kV, +800 V* active
	+21.2	All inactive
4	+24	50 mA, 5 kV, active
	+24.2	All active
5	+27	150 mA, 5 kV, active
	+27.2	All inactive
6	+30	500 mA, 5 kV, active
	+30.2	All inactive
7	+33	15 mA, 2.5 kV, active
	+33.2	All inactive
8	+36	50 mA, 2.5 kV, active
	+36.2	All inactive
9	+39	150 mA, 2.5 kV, active
	+39.2	All inactive
10	+42	500 mA, 2.5 kV, active
	+42.2	All inactive
11	+45	500 mA, 10 kV, active
	+46.1	All inactive
12	+48	15 mA, 1.25 kV, active
	+48.2	All inactive
13	+51	50 mA, 1.25 kV, active
	+51.2	All inactive

*800 v activated during each pulse
**adjustable

Pulse No.	Time	Event
14	+54	150 mA, 1.25 kV, active
	+54.2	All inactive
15	+57	500 mA, 1.25 kV
	+57.2	All inactive
16	+60	1.5 mA, 10 kV
	+60.2	All inactive
17	+63	5 mA, 10 kV
	+63.2	All inactive
18	+66	15 mA, 10 kV
	+66.2	All inactive
19	+69	50 mA, 10 kV
	+69.2	All inactive
20	+72	150 mA, 10 kV
	+72.2	All inactive
21	+75	500 mA, 10 kV
	+76.1	All inactive
22	+78***	1.5 mA, 5 kV
	+78.2	All inactive

***2nd cycle begins

1.3.3.3 Description of Operation of the Programmer Circuits

The programmer circuitry is given in Figure 34.

12 Second Delay to Power Supply Turn-On

Uni-junction Q9 runs at about 150 Hz putting a positive going pulse of a few hundred millivolts on the emitter of Q10. When the latching relay is closed, battery voltage is applied to Q9 which begins to oscillate and via a voltage regulator to Q10. C7 begins to charge thru R28. The emitter leakage current of Q10 is supplied by R29 until the voltage on C7 plus the pulse amplitude from Q9 is

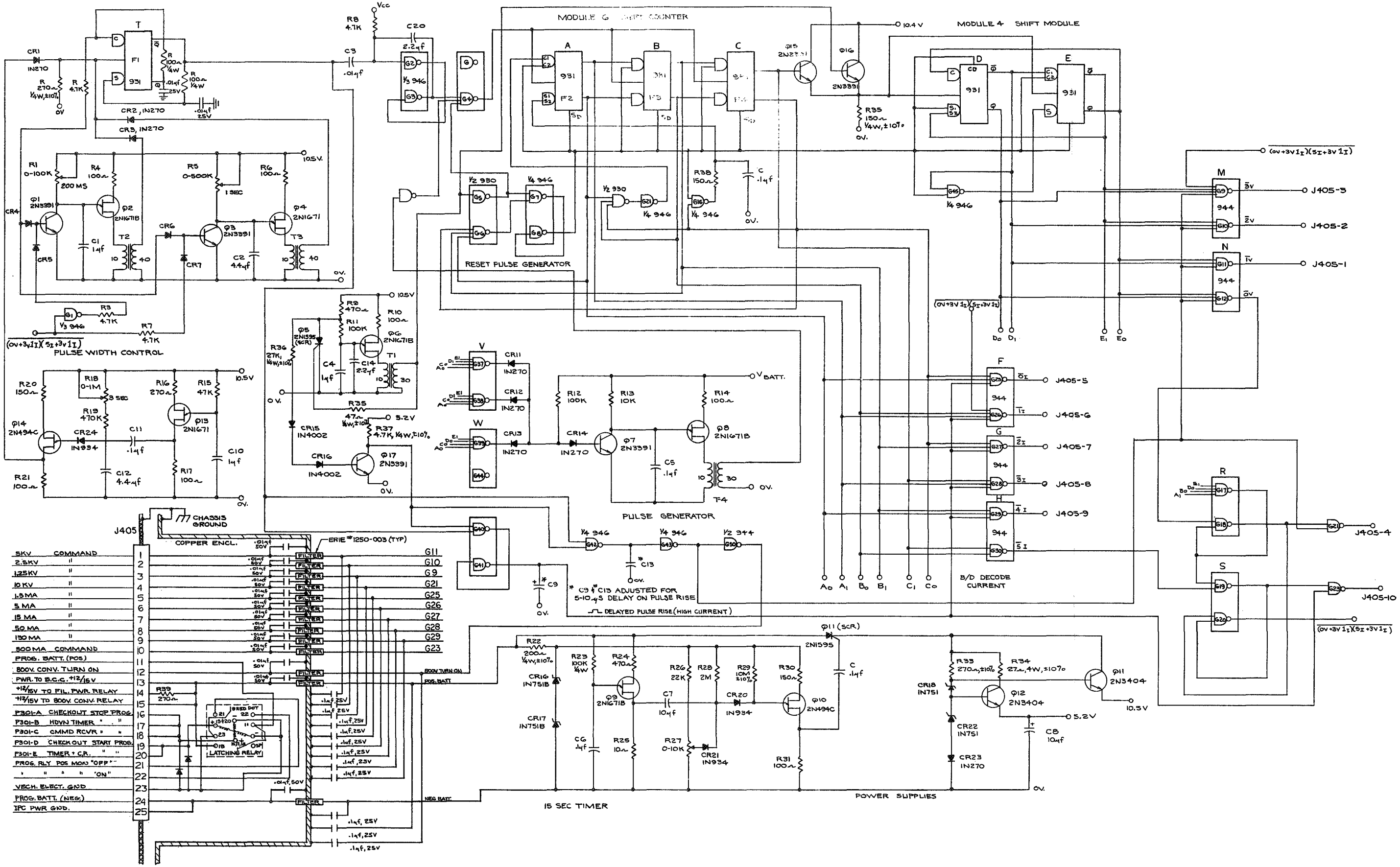

1-6059

Figure 34. Experiment Programmer Schematic.

sufficient to trigger Q10 which then puts a 3 or 4 volt pulse on Q11 which has been blocking up until this time. The time for Q10 to fire is varied with R27 which controls the initial voltage on C7, and therefore, the time to charge to the Q10 threshold level.

10.5 Volt and 5.2 Volt Power Supplies

The diodes CR18, CR22, and CR23 provide a voltage reference string for the base connections of Q11 and Q12 which provide approximately 10.5 volts and 5.2 volts respectively at a low impedance. R34 is provided to reduce the power dissipation of Q12. The 10.5 V power supply is used to energize the U.J.T. circuits since they do not operate well at voltages much less than 10.

3 - Second Timer

Following the initial 12 second delay, the 10.5 V power supply becomes active and Q14 begins to operate. This circuit (Q13/Q14) is similar to the 12 second timer and generates a positive going pulse after 3 seconds (or so) and every 3 seconds thereafter.

Integrated Circuit Logic

The integrated circuit logic used in the programmer is called diode-transistor logic or DTL. The input and output conditions are as follows:

Inputs

Low or "0" input - less than 100 ohms to ground or less than 1.2 volts to ground. High or "1" input - 2 volts or greater or more than 100 ohms to ground.

Outputs

Low or "0" output - corresponds to the saturation voltage of an NPN transistor, i.e., approximately 1/4 volt at up to 100 mA. High or "1" output -

load is connected to Vcc (= +5.2 volts) through 6 K ohms or in the case of the 944 is an open circuit.

The units used are:

931 - clocked	J - K	flip-flops with D.C. Set/Reset
930	2	4 input NAND gates
946	4	2 input NAND gates
944	2	4 input NAND gates (high power)

Pulse Width Timing

The integrated circuit T is a J - K flip (931 type) connected to "toggle", that is, each pulse applied to the clock input causes the outputs to change state. Each pulse from the 3 second timer causes the Q output to go "low", i.e., to about +0.3 volts. (The $\bar{Q}$ output simultaneously goes high.)

200 Millisecond Pulse Width

If the next pulse is to be a 200 ms. pulse, the output of G1 is low, so that when a Q goes low G1 is turned off and C1 begins to charge through R1. C1 charges until the threshold of Q2 is reached where upon it fires applying a positive pulse to the flip-flop, toggling it again and causing the Q output to go high. The Q output remains high until another pulse from the 3 second timer appears. When Q1 is on, C1 is essentially short-circuited and cannot charge to more than about +0.3 volts.

Second (signature) Pulse

When a signature pulse is to be produced, the output of G1 is high. Since the DTL gates are NAND gates, they invert the logic level, and the output of G1 is the complement of its input so that if the G1 output is high, its input is low and now Q3 is turned off when the Q line goes low. The R5-C2 combination determines the time to fire Q4 in the same manner as described for the 200 millisecond case. Thus, 200 millisecond or 1 second 'high' pulses are generated on

the $\bar{Q}$ output of flip-flop T every 3 seconds. These pulses 'clear' the ten output gates (G9, 10, 11, 25, 26, 27, 28, 29, 21, 23) so that when all the other inputs to any of these gates are high, those gate output levels will go low for the pulse duration, energizing the associated relay drivers. The gate G50 is also activated by this pulse to operate the 800 v converter power relay.

The clock pulse for the 'current' counter is derived by differentiation of the end of the timing pulse from flip-flop T so that the counter advances immediately at the end of a beam pulse. Additional clock pulses are provided from Q8 when it is desired to skip certain pulses.

A binary counter with 3 stages has 8 possible outputs, 2 of which are not used. These two are represented as follows:

		A	B	C	Cp. #
	$\bar{Q}$	0	1	0	
	Q	1	0	1	
and					
	$\bar{Q}$	1	0	1	
	Q	0	1	0	
1.5 mA	$\bar{Q}$	0	0	0	1
	Q	1	1	1	
5 mA		1	0	0	2
		0	1	1	
15 mA		1	1	0	3
		0	0	1	
50 mA		1	1	1	4
		0	0	0	
150 mA		0	1	1	5
		1	0	0	

	A	B	C	Cp. #
500 mA	0	0	1	6
	1	1 *	0	
1.5 mA	0	0	0	7
	1	1	1	

Module Six Counter Output States (Normal)

The possibility of a disturbance putting the counter into one of the unwanted states must be considered. It is evident that if this occurs, the counter will cycle between these 2 states. Gate G6 detects the first of these states and lowers the reset line so that when the next clock pulse appears, the counter is reset to the 1.5 mA state.

Referring to the table, the asterisk indicates the transition which produces the signal used to advance the module 4 counter sequencing the high voltage converters. In this manner the module for counter cycles once for each 4 cycles of the module 6 counter.

Signature Pulses

G19 and G18 detect the 500 mA, 10 kV counter states and G17 detects the 5 mA, 1.25 kV state. Either of these states activate G21 and G23 during a beam pulse. G20 is also activated during these states, and its output is used in conjunction with G1 to change the pulse width timers by blocking Q1 and freeing Q3 when the counters are in either of these states. Thus, for either of these counter conditions, the 500 mA, 10 kV drivers are activated, and the pulse width is one second in length.

Skipped States (1.5 mA, 2.5 kV; 5 mA, 2.5 kV; 1.5 mA, 1.25 kV)

When the 2 counters are in the states which code these output values G38, G37, or G39 are activated (when all gate inputs are high, the output of that gate goes low, otherwise it remains high). When the output of any one of these

gates goes low, Q7 is turned off and C5 charges causing Q8 to fire advancing the module 6 counter to its next state before the next beam pulse occurs.

Note that all counter state changes occur immediately following the beam pulses.

Power Turn-On

When power is first applied to the bi-stable counters, their resulting states are indeterminate so that the counters must be reset to the desired state. This applies to unit T as well, which means that the output gates may be active. The circuit comprising Q5, Q6 and Q17 prevents spurious operation in this instance.

When the 10.5 V and 5 volt power appears Q5 is blocking which turns on Q17 so that its collector voltage is low and G40 and G42 are inhibited (blocked) disconnecting unit T from the output gates and preventing any relay operation. The unit T will return to the quiescent state before Q6 fires, resetting the counters as follows.

An additional clock pulse is required (from Q6) when the counter is being reset after power turn-on. At this time, G8 output goes low bringing down the 'Set Direct' (SD) inputs to all the flip-flops. This action causes S_2 of A to go high and C_2 of A to go low which is also necessary to reset the counter to the 1.5 mA (starting) state.

The module - 4 counter is reset to the 5 kV condition similarly except that the reset line is applied to the 'Clear Direct' line and to S1 of D so that the initial state is:

	D	E
$\overline{Q}$	1	0
Q	0	1

to correspond to the decoding for the 5 kV output. (This reversed reset procedure results from a modification from the original 10 kV first pulse state.)

Module '6' Shift Counter

Flip-flops (type 931) A, B and C are connected for form a counter which cycles thru 6 discrete states in response to input pulses applied to the 'clock pulse' (CP) inputs of the 3 units. The flip-flops are master - slave devices. The complementary inputs applied to the 'Set' and 'clear' inputs are transferred to their corresponding outputs when the clock pulse goes positive. At the beginning of a cycle, the Q outputs are all high (the 1.5 mA condition), but the S and C inputs of A are opposite due to the feedback inversion provided by G, G21 and G16. Thus, the first clock pulse causes A to change state; the next two clock pulses transfer this condition to B and the C at which point the S and C inputs to A are reversed. Thus, the outputs of the 3 units are as described in the previously listed binary output table, column "CP".

1.3.4 High Voltage - Beam Current Supply

1.3.4.1 Subsystem General Characteristics

The basic subsystem power supply is designed to provide from 0 to 500 mA current at 1.4, 2.8, 5.6 and 10 kV nominal voltage, depending upon the logic signal from the experiment programmer. Short circuit protection is provided. The power producing elements are housed in a separate rfi-emi shielded section of the payload. Battery inputs, turn-on signals and certain T/M functions are passed through a massive aluminum bulkhead ground buss at the physical center of the payload using rfi feedthrough filters. The converter is partially mounted and partially built into the lower half of the pressurized cannister as can be seen in Figure 4, Figure 5 and Figure 35. Schematics, Figures 36, 37 and 38 describe the system electrically.

The basic electrical design consists of eight individual driven bridge converter modules, each capable of supplying 1.2 kV at 500 mA. Isolation on the high voltage sections of each converter for half of the modules is tested to 8 kV, the rest are tested to 15 kV. The outputs of all eight converters are connected in series. Turn-on of each module is controlled by a small reed relay in the drive oscillator stage of each module (see Figure 38).

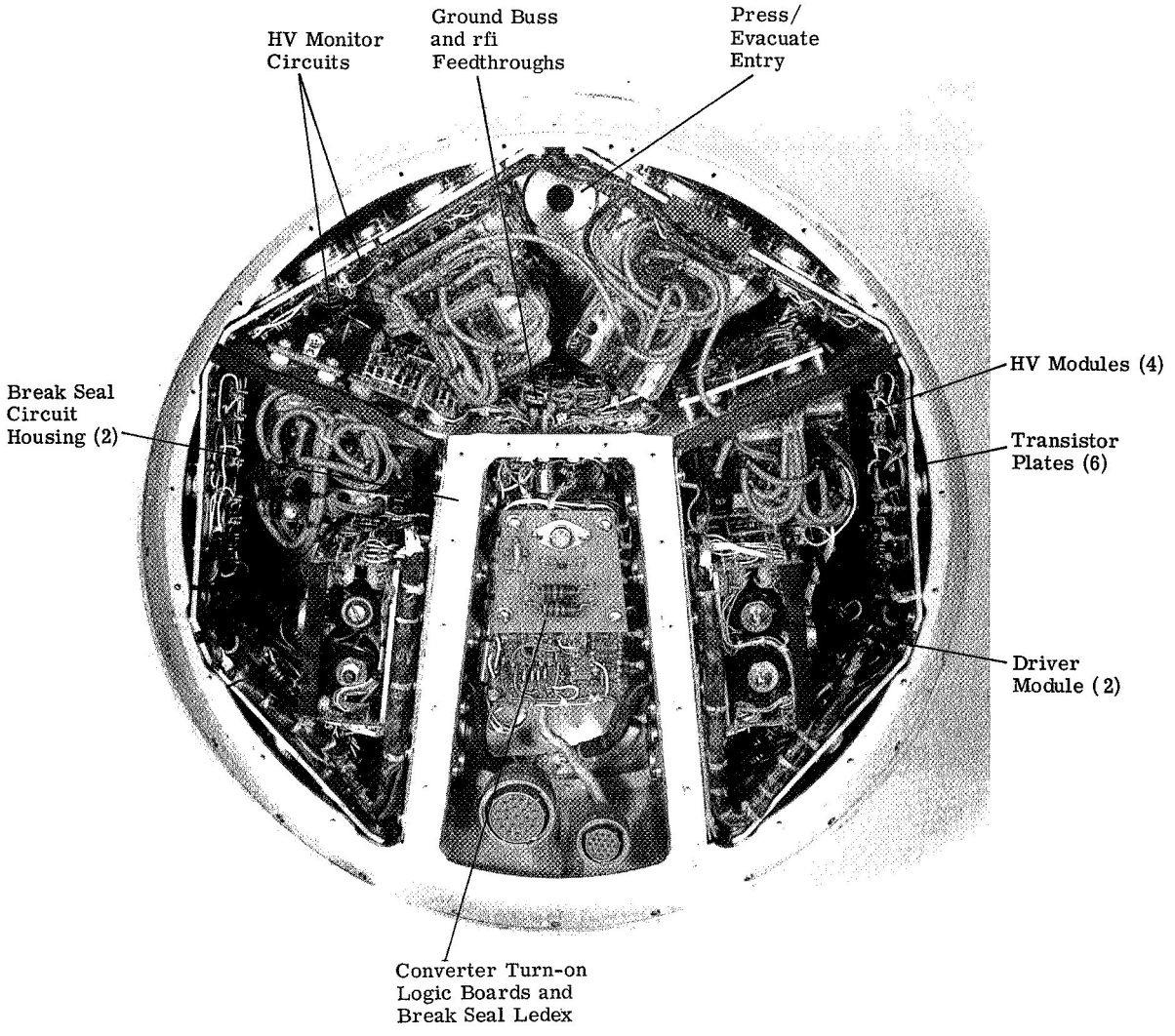

Figure 35. Lower Section of Pressure Cannister - Covers Removed.

2-1566

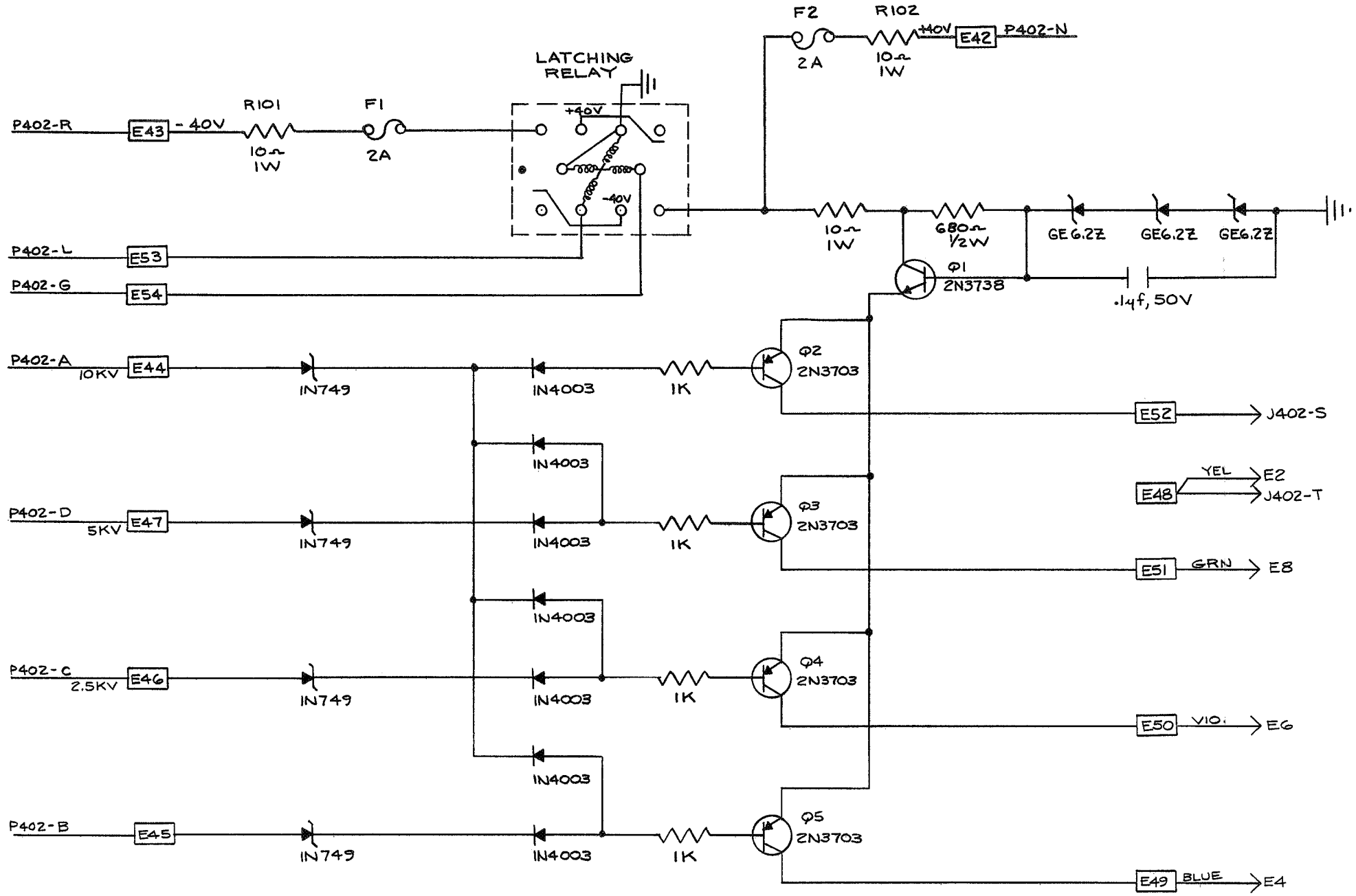

NOTES

1. DWG MADE FROM A-SK-89035-6

Figure 36. High Voltage Converter Control Logic/Amplifier Schematic

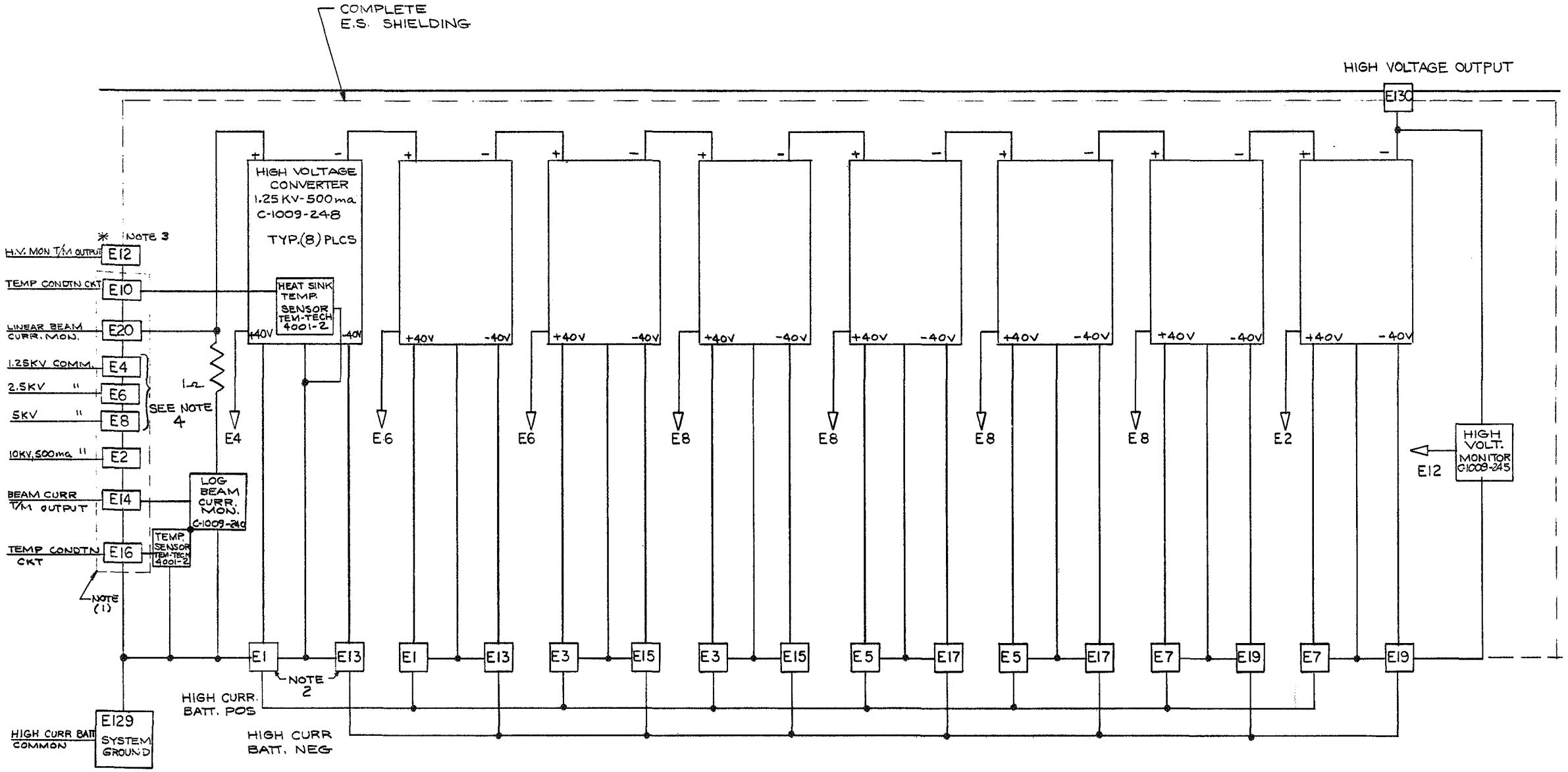

NOTES -

1. ERIE FILTER FEED-THRU # 052
2. " " " " 1202-052
3. " " " " 9004-000-1002
4. 7 CONVERTERS ARE TURNED ON AT 10KV COMMAND

*THE 8th CONV. IS ALSO TURNED ON AT 10KV, 500 ma

Figure 37. 10 kV - 500 mA High Voltage Converter Connection - Schematic.

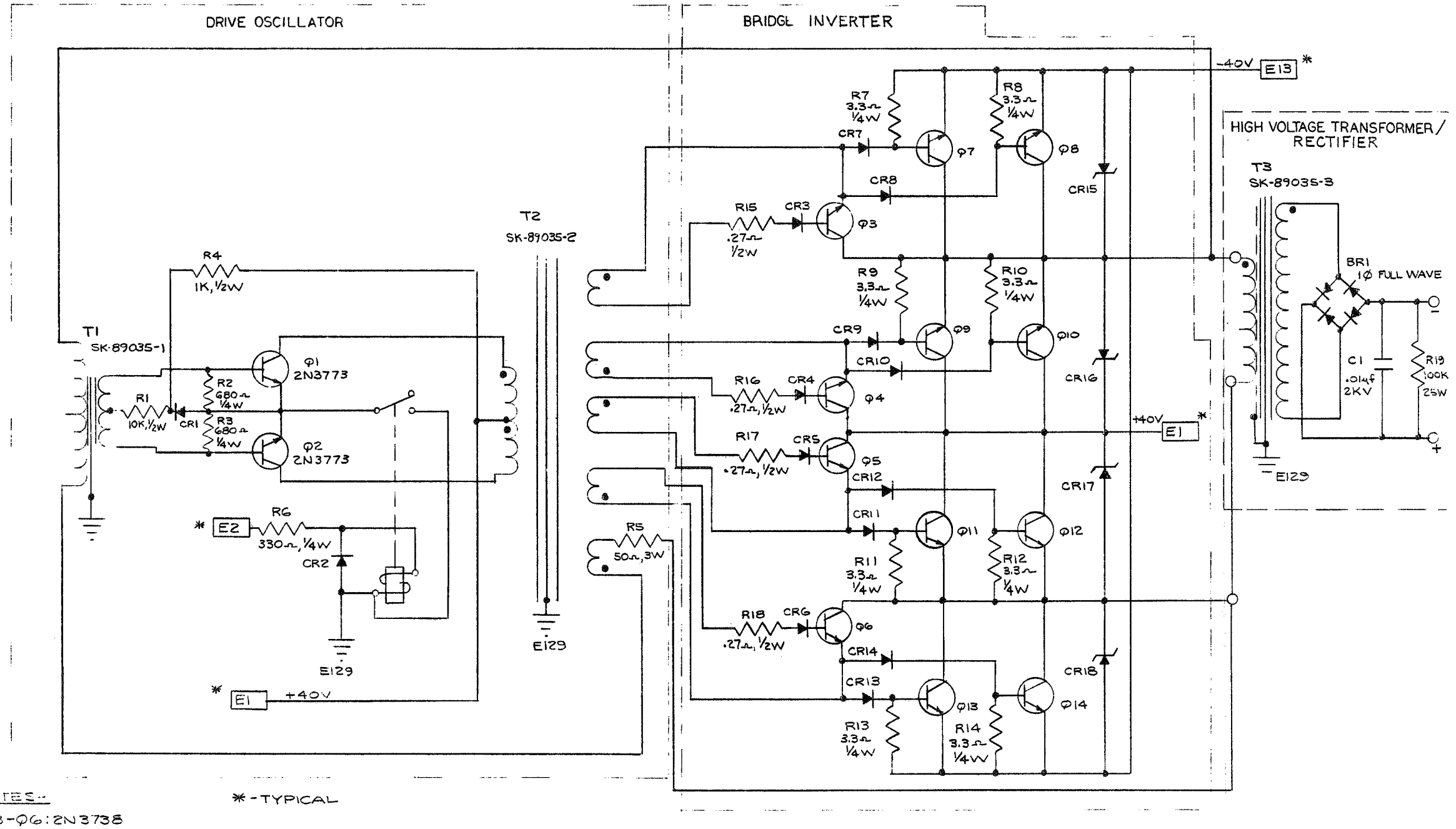

NOTES:-

1. Q3-Q6: 2N3738
   Q7-Q14: 2N3773
   CR1-CR14: 1N4003
   CR15-CR18: UZ-217
2. DOTS ON ALL TRANSFORMERS SHOW S PHASING

* - TYPICAL

Figure 38. 1.25 kV - 500 mA High Voltage Converter Module - Schematic.

1.3.4.2 Packaging Design

Referring again to Figure 35 and Figure 38 inside the converter section, there are three basic packages which make up the subsystem. The first is a package which contains two of the drive oscillator circuits including output and feedback transformers. Two of these packages are stacked and then mounted to the lower plate of the cannister.

The second basic package is a plate upon which the power transistors, diodes and resistors in the main converter bridge are mounted. These plates are mounted around the periphery of the cannister cylinder. In all there are six of these plates and one small auxiliary plate. The two largest plates each contain one complete bridge inverter and all but the driver transistors of a second. The four smaller plates each contain one complete bridge inverter. A seventh plate which contains the driver transistors belonging to the two large plate inverters, is mounted on one of the section braces.

The third basic package is the high voltage module which is made of a lucite box containing high voltage transformers, bridge rectifiers, filter capacitors, and bleeders for two of the 1.4 kV converters. These modules, four in number, are lagged down to the cannister bottom plate. The design is such that the elements at high voltage are mounted on the top of the module for easy connection in series with high voltage cabling to a high voltage feedthrough leading to the upper half of the cannister onto the insulated plate. This connector is not visible in Figure 35. It is mounted on the cover which has been removed to show the subsystem. Outside the rfi enclosure the logic circuitry and current amplifiers between programmer gates and turn-on relays are mounted on two circuit boards positioned as shown in Figure 35.

1.3.4.3 Circuit Operation

Circuit operation is quite straight forward. The IC gating signals come down from the experiment programmer and pass through IN749 zeners to a diode logic setup (see Figure 36) where they turn on via amplifying transistors Q2-Q5 the appropriate number of high voltage modules by means of the reed relays positioned in the oscillator modules. Connection between terminals E52

and E48 is made in the beam current controller on relay RL-8 as discussed in that section. When this connection is made and the gate signal is on the 10 kV line then and only then, the 8th high voltage module is turned on through feed-through E2.

A series regulator circuit from the positive main battery feeds power to the transistor amplifiers and reed relays (also shown in Figure 36). A latching relay, activated in parallel with the experiment programmer latching relays assures that no power is continuously leaked from the main batteries. It can be noted in the schematic that power to the T/M conditioning power supplies passes through this relay as well. Fuzes are placed in these lines to insure that shorts in the T/M conditioning do not terminate the experiment. Checkout light position sensing passes through this relay, in series with the position sensing of the programmer latching relay. In addition power to the rotary solenoid operating the break-seal circuit sequencer passes through this relay (not shown in the schematic).

Referring again to Figure 38, the reed relay completes the ground for the oscillator, turning it on, producing a 12 khz square wave on the input to T_2 the drive transformer, which has a 36 mm pot-core, Ferroxcube 3B7 ferrite. A feed back transformer T_1 a 26 mm pot-core of the same material is provided for short circuit protection along with a series winding on the driver transformer. The feed back signal is shown from the primary of the high voltage power transformer T_3.

The main power circuit is in the form of a driven bridge inverter feeding the h.v. transformer. Adequate drive power is provided to the bridge by Q_3 - Q_6. There are two transistors per arm of the bridge. To further protect against h.v. breakdowns and other transients, the h.v. transformer is carefully electrostatically shielded between primary and secondary. In addition zeners CR 15-18 directly protect bridge transistors against surges which pass the transformers. The power transformer is operated unsaturated.

Typical load regulation of a module is given in Figure 39. Line regulation is equal to battery regulation over the useable range of battery voltages and current loadings. It can be seen in Figure 39 that the short circuit protection

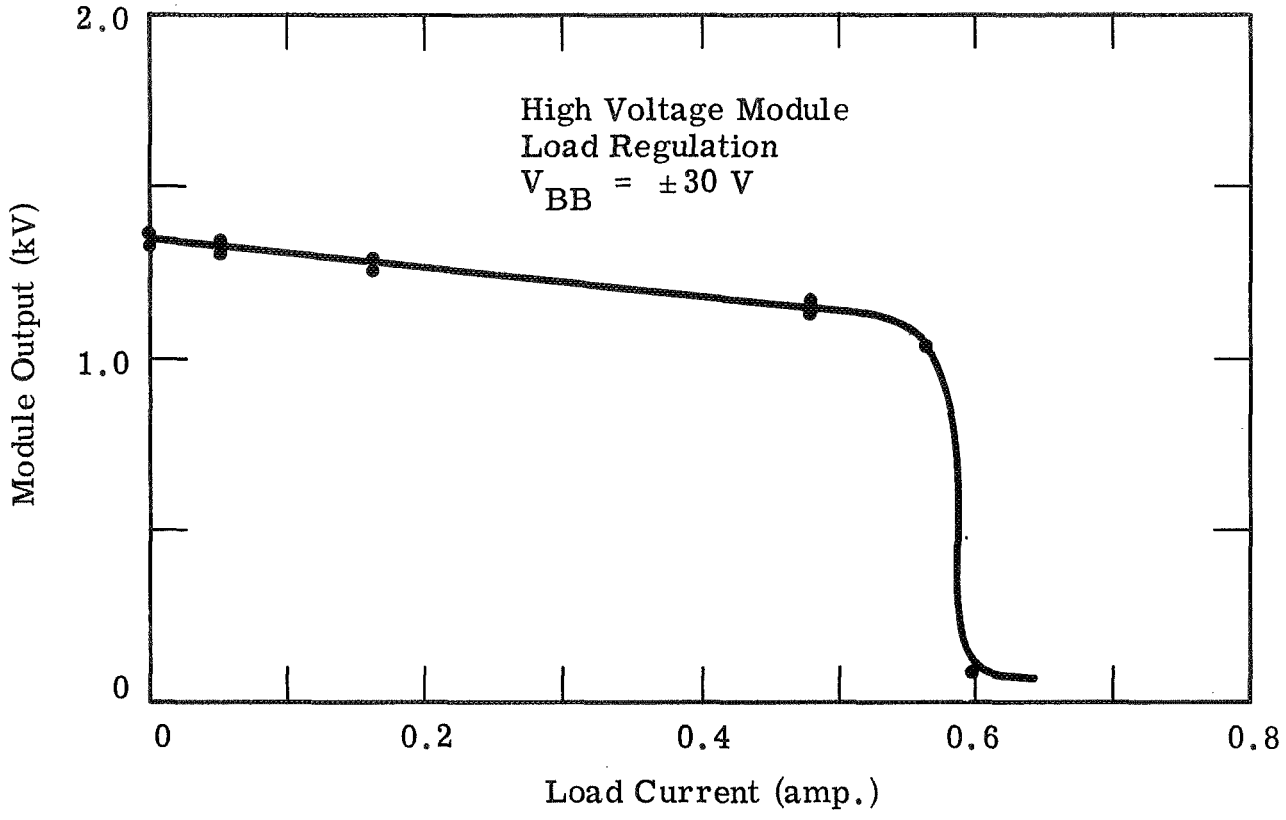

Figure 39. High Voltage Module Load Regulation.

1-6063

operates effectively above about 550 mA output, dropping the output voltage to a low value below 100 volts. This type of protection, however, does not turn the unit off.

At plus and minus 30 V input and no load the unit input draws about 0.5 amp. Fully loaded to 500 mA, the overall power efficiency including oscillator and driver stages is 71%.

1.3.5 Main Batteries

1.3.5.1 General Configuration

The main batteries are two in number: one which supplies positive 30 - 40 v to the system. A view of one of the batteries with cover removed is given in Figure 40. It is made up of 23 Yardney Electric Silver-Zinc primary cells type PMV-5-7-2 which are a special high current cell containing more plate area and inevitably thinner separators than the standard primary PM-5 silver-zinc cells. Cell terminals are heavier than normal, intercell torque down is higher, (20 in lb). The cells are encased in a vacuum-tight stainless steel box made so by hermetic connectors and an O-ring sealed cover. The box is penetrated by a pressurize-evacuate valve, a pressure relief valve, and a power connector for the center tap. Also in the box is a heater blanket and two thermostats in series.

The cells are shipped in the dry charge condition and must be filled with potassium hydroxide according to filling instructions supplied with a filling kit. Open circuit voltage per cell after filling and a 24 hour soak is 1.86 volts for a total O.C. battery voltage of 42.7 volts. Three of the lines to the power connector are connected to a tap on the battery such that the number of cells between tap and ground is 12 cells. This tap is used in the system to feed the break-seal (gun-opening) circuits to be described in the next sub-section. Since the battery has 23 cells, the negative battery is different from the positive battery. The power cable and mating connectors are color coded accordingly - black for the negative battery and red for the positive battery.

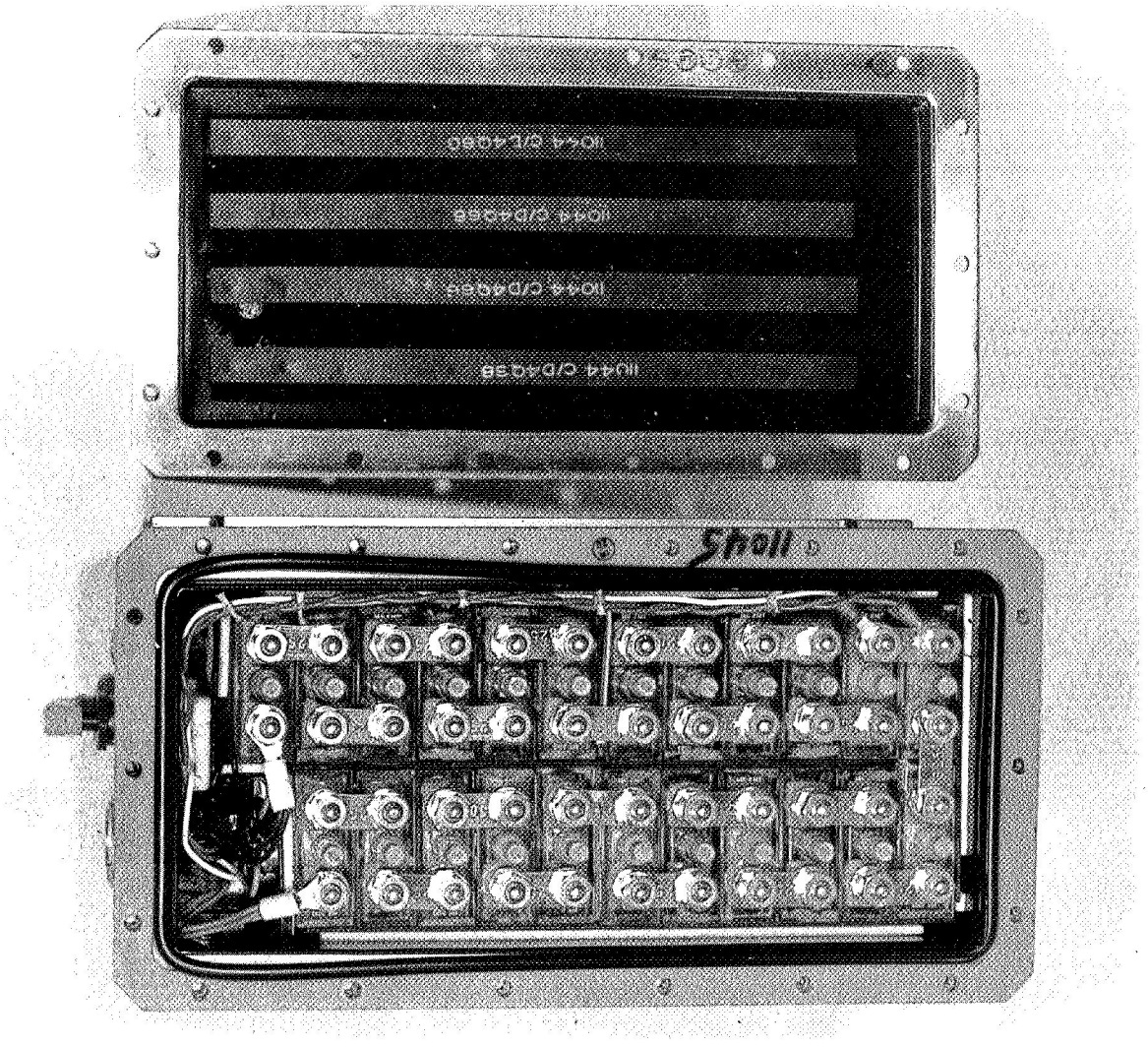

Figure 40. High Current Battery - Cover Removed.

2-1567

1.3.5.2 Mounting

The batteries are mounted with four bolts in the system package on the lower ring which is attached to the collector spool below (GSFC supplied). Positioning can be seen in Figures 1, 2, 3 and 4. To replace batteries, one of the removeable brackets must be unbolted and removed as well as the cables to the batteries.

1.3.5.3 Flight Preparations

In addition to a 24 hour soak period, each battery is pumped out to approximately one-half an atmosphere prior to use. This allows a considerable amount of gassing before the relief valve opens at 40 p.s.i. differential or the case vents at the cover at approximately 20 - 30 psi differential. Prior to launch the leakage currents in the package should be resupplied where possible and the heater blanket activated. (Requirements 40 V pulsed d.c. from the checkout console.)

1.3.5.4 Regulation

When properly heated by the blankets and torqued down according to instructions the batteries have the load characteristics given in Figure 41. These characteristics were established through a qualification test program at Yardney using a set of cells and through several tests at IPC. Tests in actual practice and during the 17.03 Aerobee flight tended to be closer to the lower edge of the range shown, e.g., under full loading conditions on the high voltage converters (10 kV, 500 mA), the batteries are approximately 28.5 V output at the converter input. This coupled with Figure 39 gives an output voltage of 8.7 kV, as observed during the 17.03 flight.

1.3.5.5 Lifetime - Rechargeability

The cells used have thin separators. In the dry condition under normal storage temperatures lifetime is up to two years. After filling, lifetime

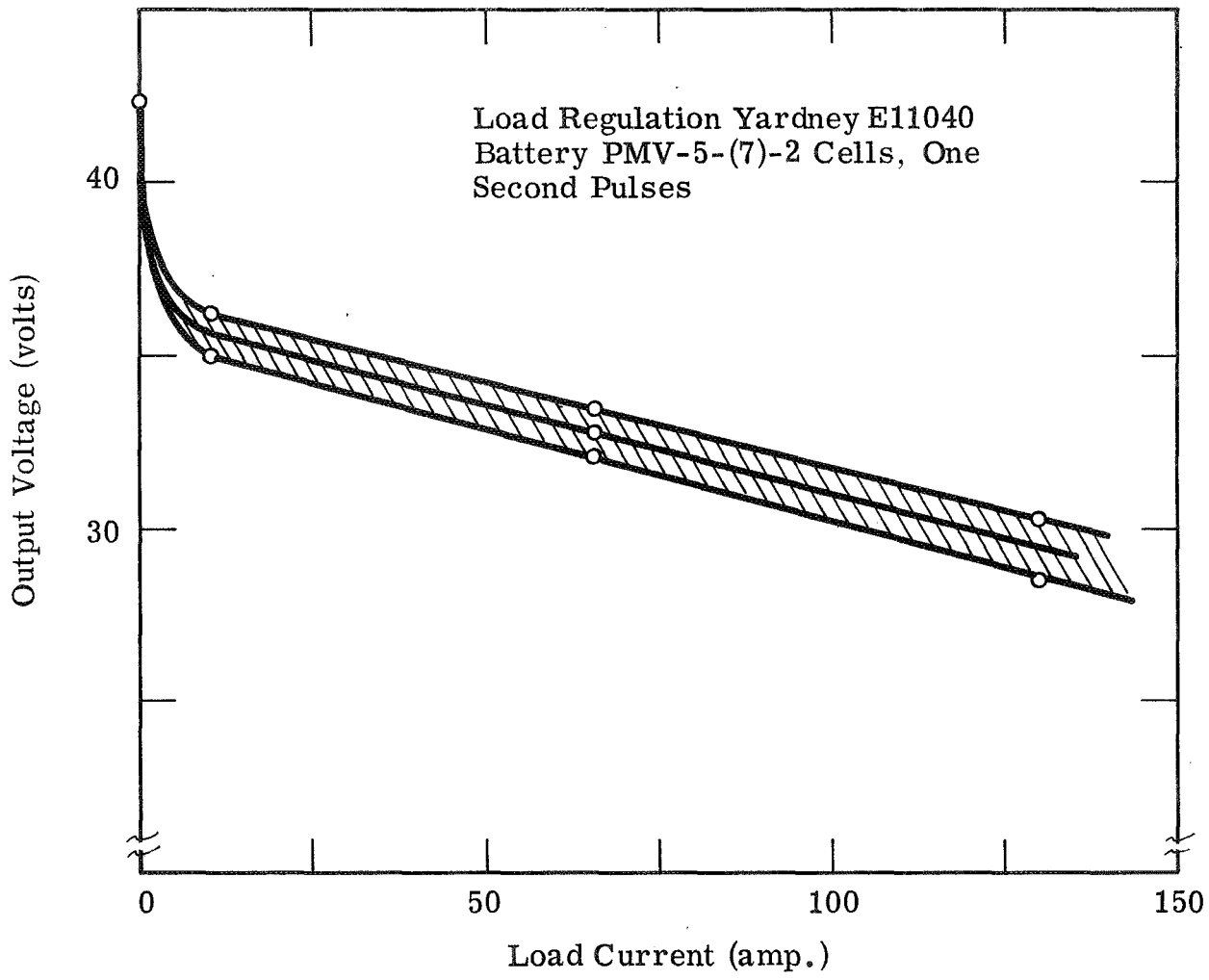

Figure 41. Load Regulation - Yardney XE71 Battery.

1-6064

is guaranteed for only two weeks. This guarantee is lengthened if the battery is refrigerated, just so long as it is warmed to room temperature before using.

The batteries can be recharged at a rate not to exceed 2 amperes according to the manufacturer; however to inhibit dendritic growth across the separator this rate should be reduced to 1/2 amperes. It has further been found that a battery which has been subjected to 100 ampere loadings (full converter loadings) for a significant portion of its energy content, never recovers its low impedance and energy content upon recharge, and is only good for test purposes thereafter. The dry charge energy content is given and has been qualification tested to 7 amp. hr. Upon recharge this is generally reduced to less than 5 amp. hr.

1.3.6 Gun-Opening (Break-Seal) Circuits

As has been pointed out in section 1.3.1.5 each gun opening band requires about 15V at 60 amperes for 2 - 3 seconds. In the system this power is supplied from a voltage tap on the main batteries. Switching is accomplished with transistor switches which are turned on in sequence by a Ledex rotary solenoid switch. The circuits are shown schematically in Figure 42. High power germanium transistors are used throughout. The circuit design is predicated on several major criteria, determined during the development phase of the program. The first is the necessity to keep voltages appearing in the vacuum environment (and on the bands consequently) as low as possible with respect to the skin voltage. The second is the requirement that the vacuum environment, particularly at the power feedthrough headers, not see at any time voltage differences greater than 15 volts. The third is that the batteries cannot individually handle any more than two bands at a time.

1.3.6.1 Mounting - Placement

Referring to Figure 35, the power transistor switches and interconnections are housed in two separate sections as shown. Transistors are mounted on the two main cross-braces separating the h.v. converter section from the rest

GUN OPENING ORDER		
0-3 SEC.	3-6 SEC.	6-9 SEC.
GUN 5	GUN 6	GUN 7
1	2	GUN 10
9	8	
GUN 3	GUN 4	

1-6065

Figure 42. Break Seal Circuit.

of the midsection circuitry. Wiring to the switches is accessible to the converter side of the bulkhead upon removal of rfi gasketed plates.

The timing circuits and Ledex rotary solenoid switch sequencer, are mounted on two boards hidden below the converter amplifier board visible in the pie-shaped section, Figure 35. The Ledex switch has been modified in the region of the ball detent by brazing the ball to half of the detent mechanism, precluding dropout during vibration.

1.3.6.2 Circuit Operation

Switches on the positive battery line are a simple Darlington circuit. On the negative battery the load is required to be in the emitter side of the switch transistor requiring slightly different circuit constants.

Turn-on occurs when lines 1J 302-H or G are energized with 28 V. This starts a uni-junction oscillator charging. When uni-junction Q1 discharges, a pulse is transmitted to SCR CR-3 gate turning it on and sending a pulse of current through the Ledex solenoid, providing that the latching relay in Figure 36 is turned on. (This latter connection is not shown in the schematic.) The SCR is turned off by the switch element as shown. At the same time the main switch shaft moves switches SIA-D and the input wafer to position 2, turning on the transistor switches to guns 5, 1, 9 and 3 and input power from the turn-on signal to a steady +28 V line. The second pulse from the uni-junction switches the Ledex to position 3 and so on until the Ledex returns to position 1, the homing position. It will be noted that position 2 and 3 turn-on circuits to 4 guns each while position 4 turns on only two guns. When in the homing position, a reapplication of 28 V on either of the turn-on lines would repeat the entire sequence. In the overall Aerobee 17.03 system one of these lines was passed to the output of one of the command receiver channel outputs through an altitude switch. By this means it was possible, if several or more of the guns did not open during the sequence to command the circuit to try to open these guns again from the ground.

One wafer on the Ledex is devoted to determining via pin 1J 302-F whether the sequence is in the homing position by the presence of a ground on this line.

1.3.7 T/M and Ground Monitoring Circuits

Monitoring circuits are provided for those outputs outlined in Section 1.2.2 of this report. Two of these outputs are to T/M clear channels, namely the beam voltage and the beam current. The rest of the T/M outputs are to commutated channels. All T/M subcarriers used in flight Aerobee 17.03 have an input impedance of approximately one megohm and have safe channel limits from -0.5 to +5.5 V. Accuracy is quoted at 2% of 5 V.

1.3.7.1 High Voltage Monitor

The high voltage monitor consists of a high voltage bleeder, an IC polarity inverter, a power supply for the IC and a zener resistor clamp output. The circuit is shown in Figure 43. The bleeder resistor is 10 MΩ and is attached to the h.v. end of the converter. Strictly speaking this is not the beam voltage which must be taken from gun cathode to anode; however, the gun cathode is always between 40 - 50 volts more positive than the h.v. converter output. To obtain true beam accelerating voltage subtract 40 volts from the monitor reading.

The power supply for the monitor is separate because of the prime nature of the voltage measurement. In the 17.03 payload pin J 302-K went to the T/M subcarrier IRIG FM/FM Channel 13 with a data frequency of 220 cps. Pin J 302-V went to the umbilical and thence to the checkout console where high voltage was one of the items monitored. These same provisions are available on the remaining payload. Calibration to 1% has been performed on the monitor. For Unit 1 on flight 17.03 the factor is as given in section 1.2.2 of this report (2.9 kV/volts). For the remaining unit 5-9326-3 ("2nd Unit") the calibration factor is 2.65 kV/volt.

Location of the monitor board is in the h.v. converter section mounted on one of the cross-braces (see Figure 35).

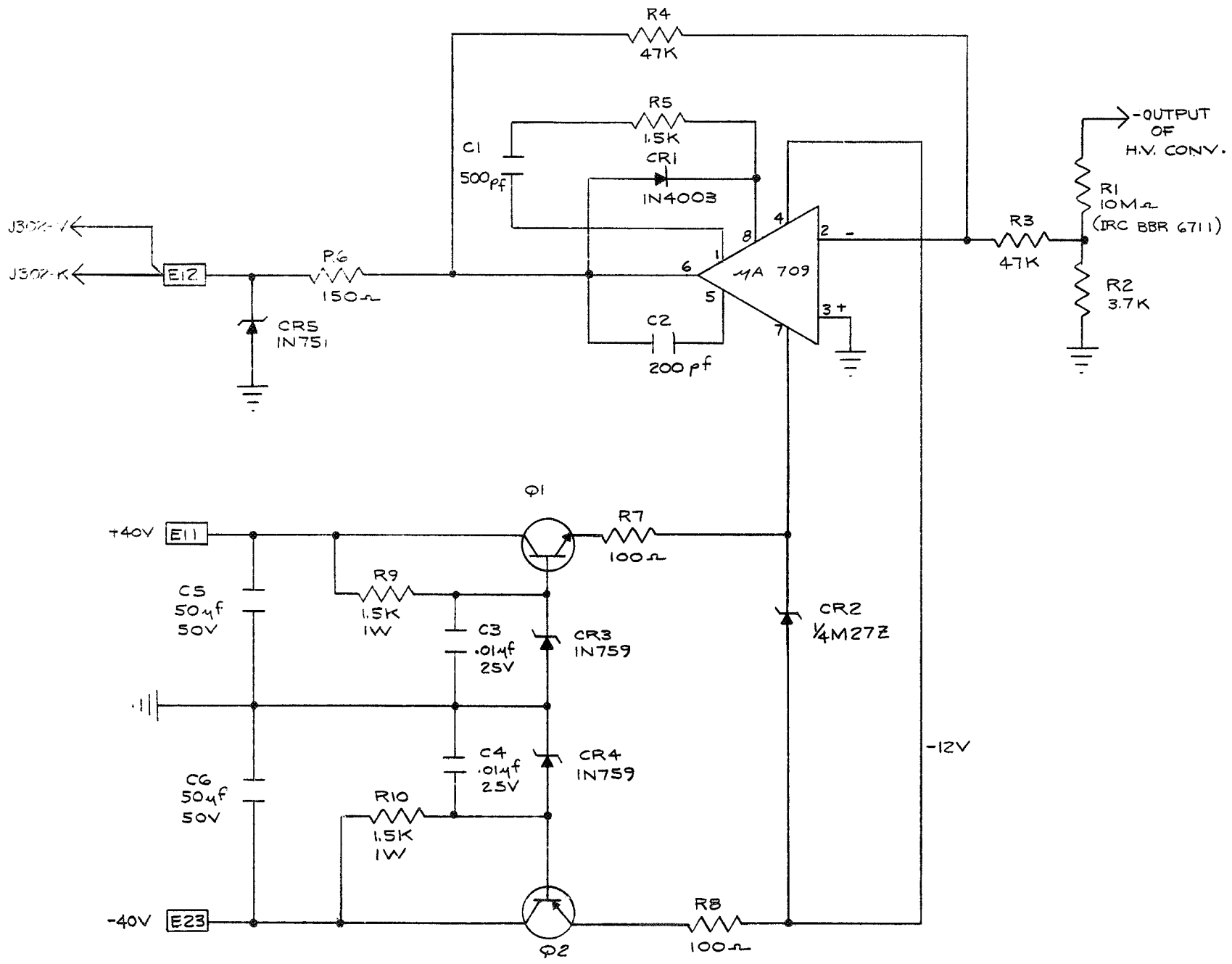

Figure 43. High Voltage Monitor Schematic.

1.3.7.2 Beam Current Monitor - Beam Current "Resistor"

Beam currents from 1.5 to 500 mA must be monitored, consequently a logarithmic monitor was called for. The resulting monitor is a passive one made up simply of diodes and resistors, so adjusted to utilize progressively the logarithmic portions of the diode characteristics. Electrically it is positioned between the bottom end of the lowest h.v. converter module and the vehicle skin. A one ohm precision resistor is actually interposed between converter and monitor to assist in situ calibrations of the monitor. The monitor schematic is given in Figure 44.

Since the diode knees are temperature sensitive the monitor calibration is temperature sensitive. The design takes care of this problem by potting the diodes and resistor directly to a "Tem Tech" flat resistive temperature sensor. This sensor passes through a circuit which conditions it for T/M commutation. The calibration curve for the unit 1 monitor, flown in 17.03 GE, is given in Figure 45. Figure 46 is the comparable calibration curve for Unit 2. Figure 47 presents the variation of output at 500 mA input as a function of the temperature sensor output to T/M for unit 1 at 500 mA. The sensitivity is roughly the same at lower currents and for the second unit monitor.

For the 2nd Unit, the resistor in series with the monitor has a calibration constant of 1.025 volts/amp.

Since the high voltage monitor is attached to ground the bleeder current will pass through the beam current monitor at all times that the voltage is on. As noted in Figure 45 it amounts to 100 μa/kV. When the beam voltage is turned on at the beginning of a pulse before the beam current, this bleeder current, which shows up on the beam current monitor, affords a crude redundant measurement of the high voltage.

1.3.7.3 Housekeeping Monitors

Monitoring sensors and circuits available to T/M (on a commutator for 17.03) are:

TM1 - Break Seal Monitor (nos. guns opened)

TM2 - Positive Main Battery Voltage

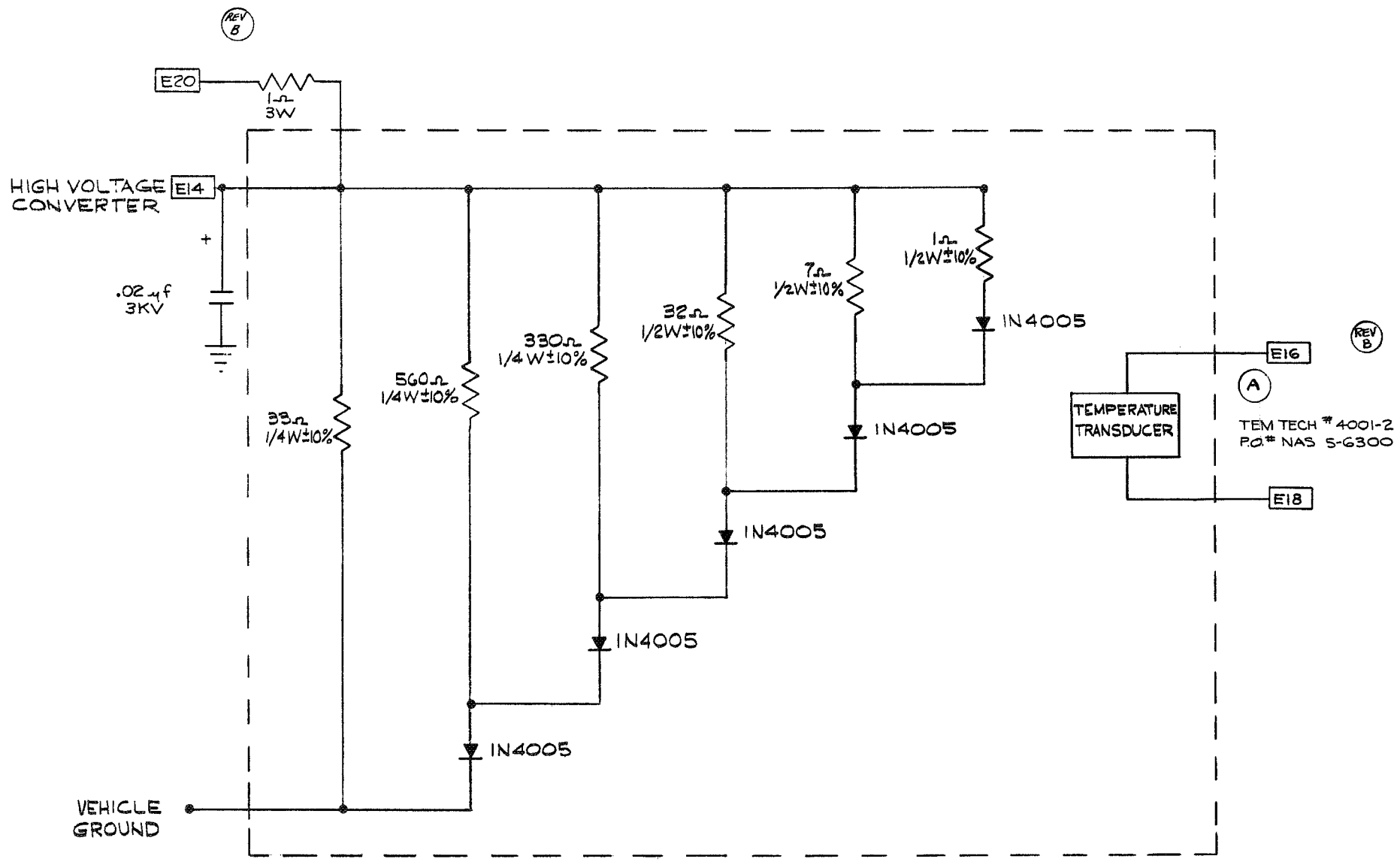

NOTE:

1. REQUIRES ACCURATE CALIBRATION CURRENT VS. VOLTAGE WITH TEMPERATURE 15°C TO 100°C.

Figure 44. Beam Current Monitor Schematic.

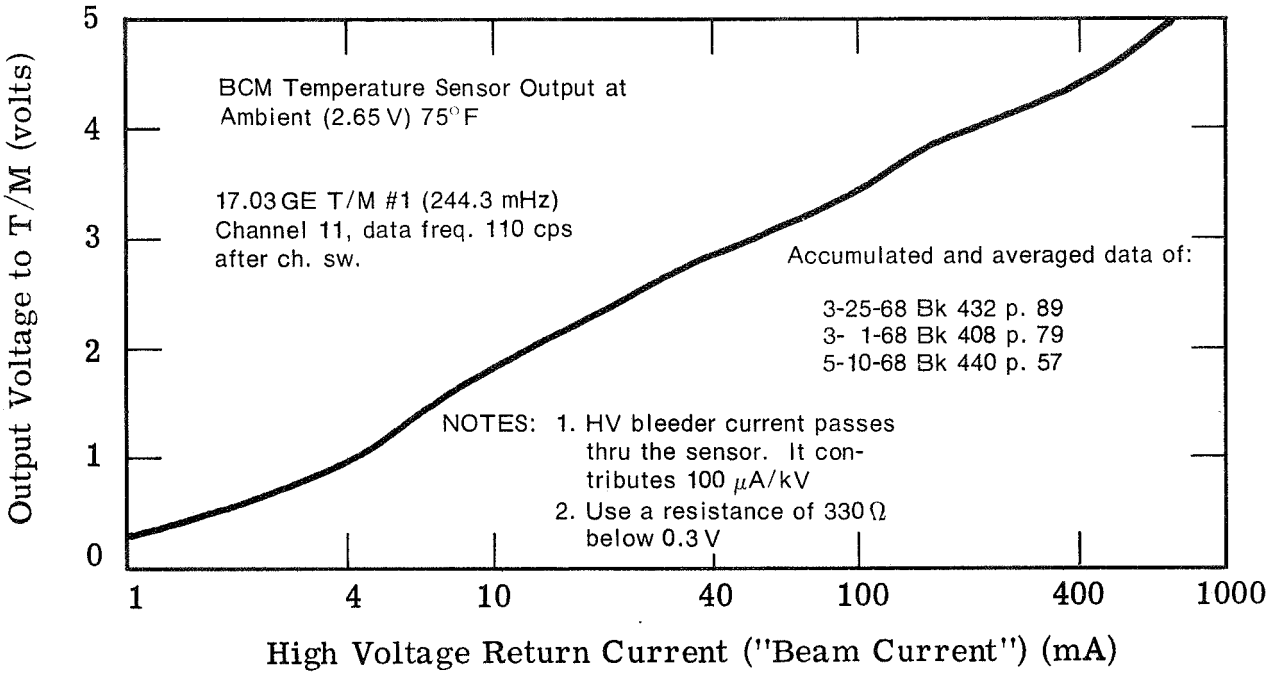

Figure 45. Beam Current Monitor Calibration Unit #1.

1-6068

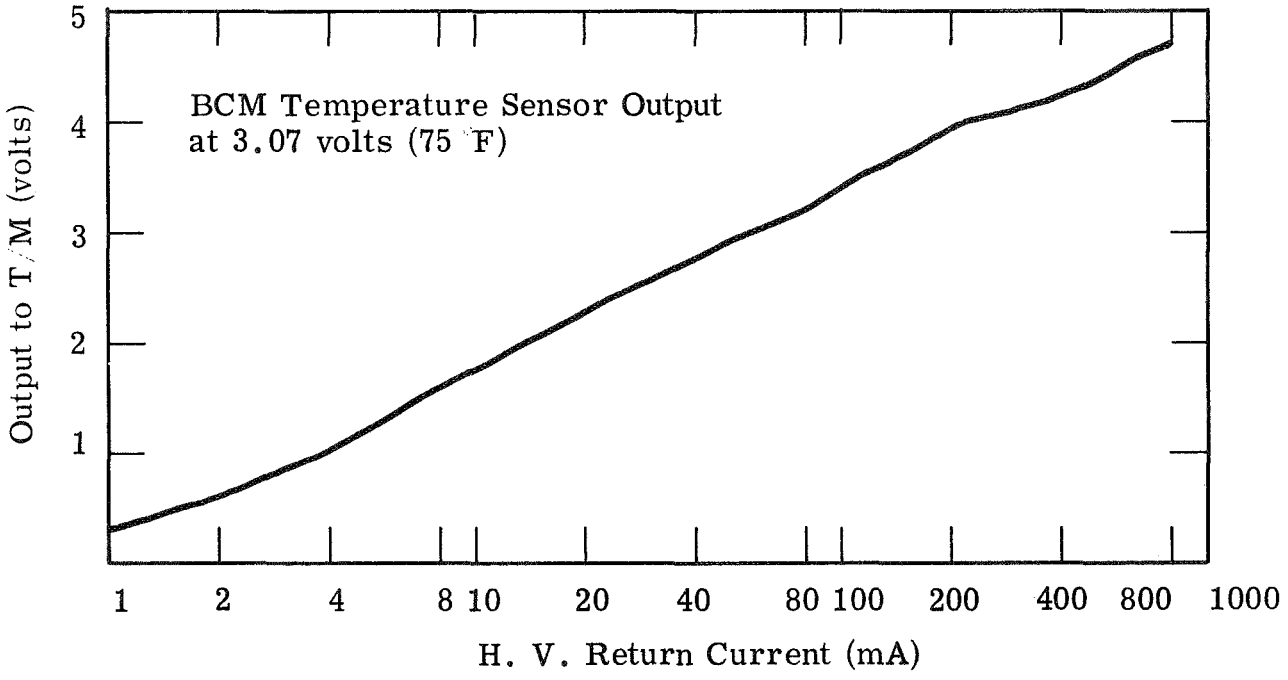

Figure 46. Beam Current Monitor Calibration Unit #2.

1-6069

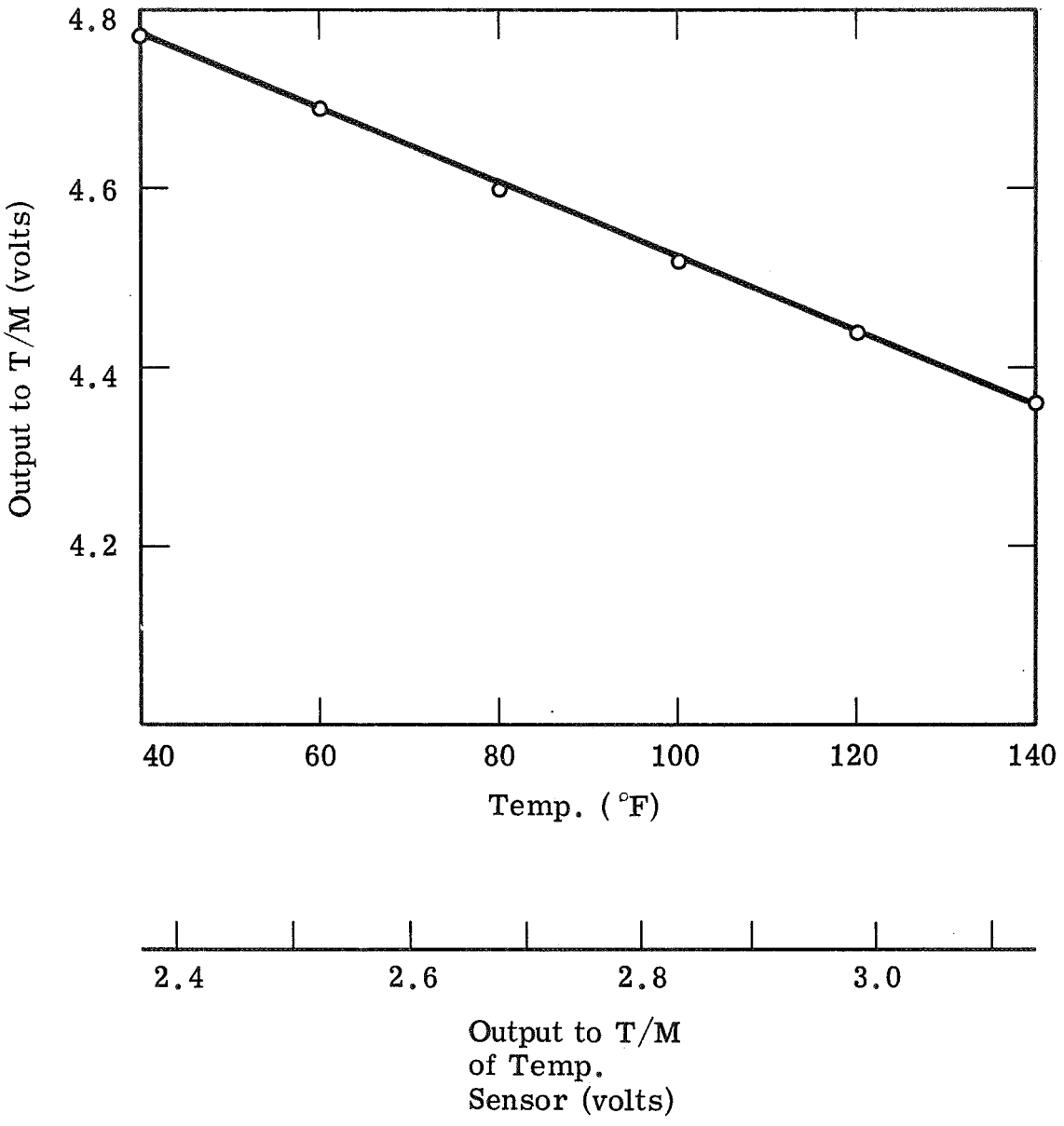

Figure 47. Beam Current Monitor Temperature Sensitivity at 500 mA Input - Unit #1.

1-6070

TM3 - Negative Main Battery Voltage

TM4 - Package Pressure

TM5 - Temperature - H.V. Converter Heat Sink Plate

TM6 - Temperature - Beam Current Monitor Block

Monitoring sensors and circuits available to ground checkout via the umbilical are:

C1 - H.V. Monitor output (via an r.f.i. filter)

C2 - Package pressure (via an r.f.i. filter)

C3 - Programmer battery charge and monitor (via an r.f.i. filter)

C4 - Main batteries charge and monitor (2)

C5 - Main batteries C/T charge and monitor (2)

C6 - Cap Current Monitor

C7 - One ohm resistor beam current monitor

The majority of these circuits are housed in a small box mounted into the side of the forward section of the pressure cannister. This box can be clearly seen in Figure 32. Also in this figure is the position of the pressure transducer. Figure 48 shows how the circuits are mounted in the box. Figure 49 gives a schematic of the contained circuitry. Included are TM1, 2, 3, 4 and C1, 2, 3, 6.

The main battery charge and monitors for the center taps (C5) are contained in the respective battery boxes, the monitoring lead passing out of the small three pin connector on each battery to the umbilical.

The rest of the circuits, TM5 and 6 and C4 (C7 is with the beam current monitor), are mounted on a board in the lower half of the pressure cannister and can be seen in Figure 35. C4 are simple diode resistor combinations; TM5 and 6 are relatively simple circuits as outlined in Figure 50.

Pressure Monitor:

The pressure transducer is a Transonics Model P106 bellows activated linear potentiometer output. It is set up for 0-25 psi absolute and is rated to 1% linearity over its range. It gets its power through a small 5 volt regulator from

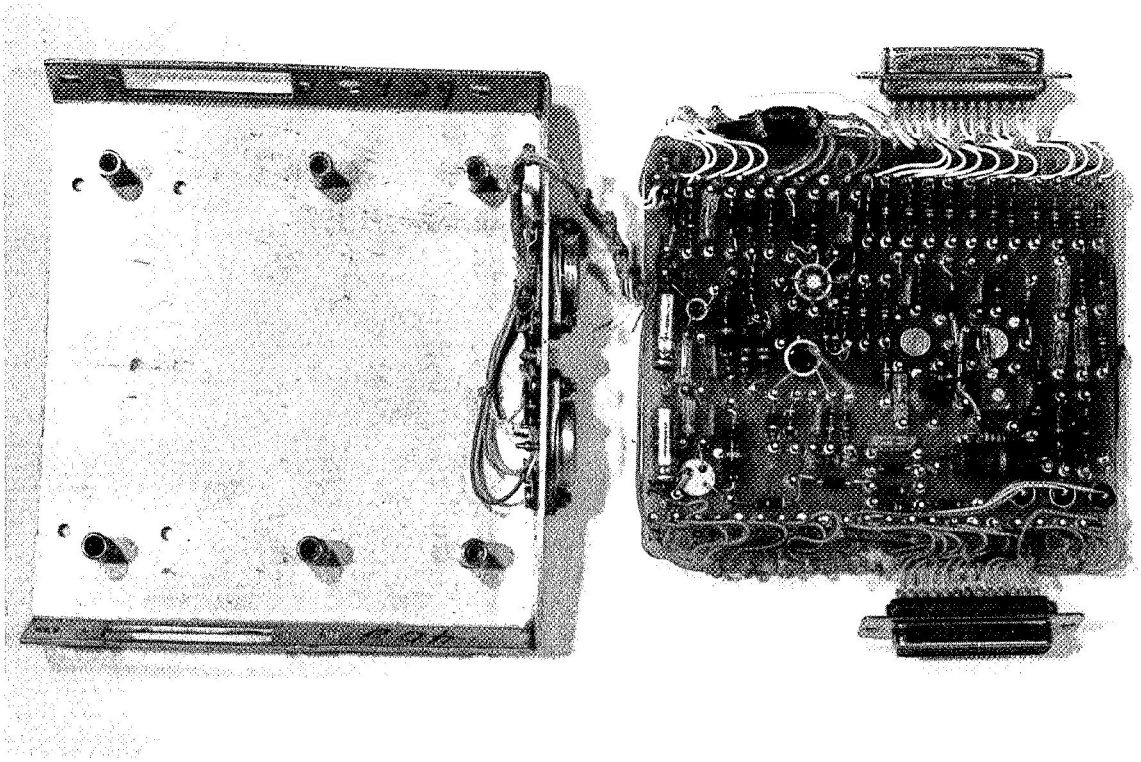

Figure 48. Upper Deck T/M Conditioning Box.

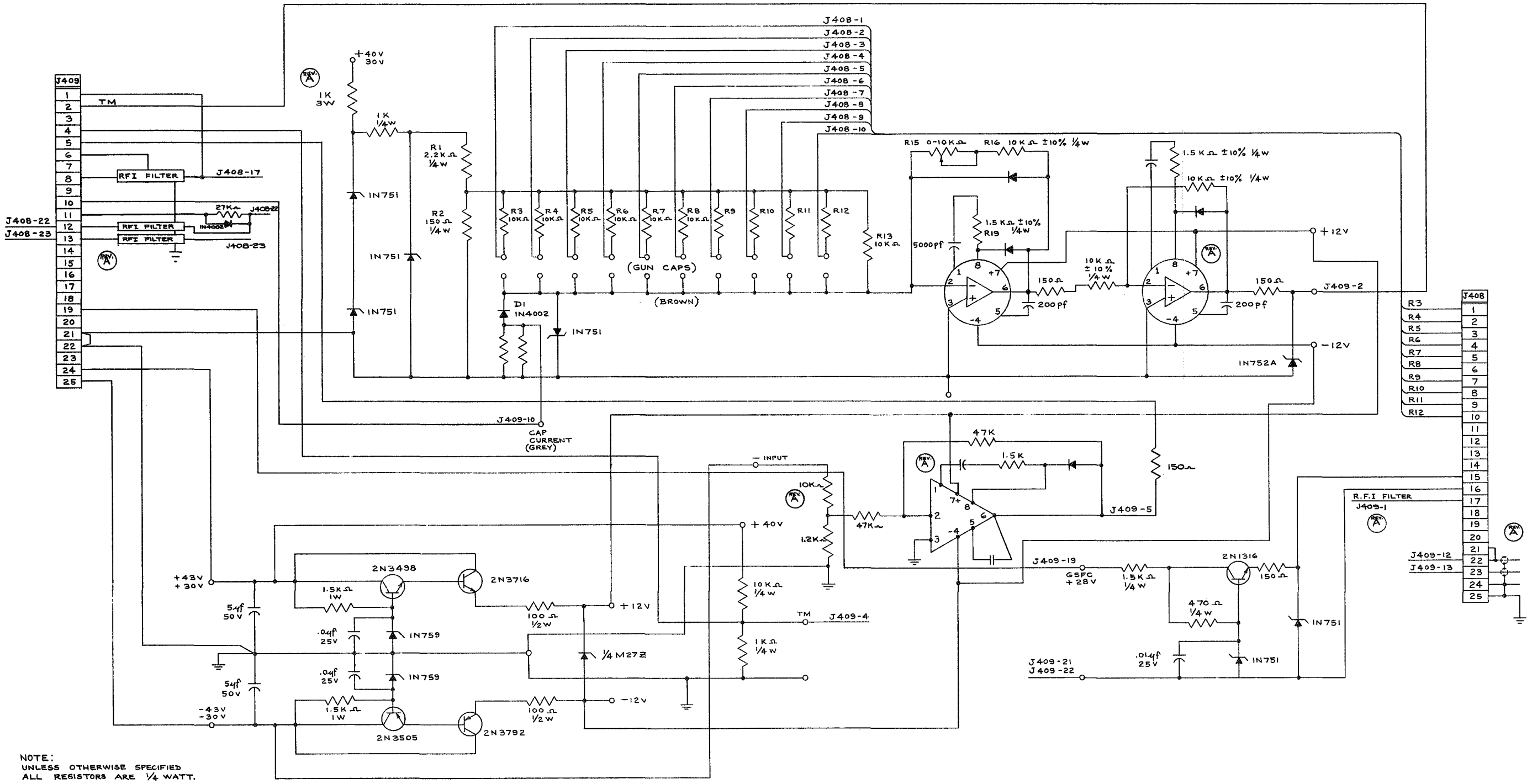

NOTE:
UNLESS OTHERWISE SPECIFIED
ALL RESISTORS ARE 1/4 WATT.

Figure 49. Upper Deck T/M Conditioning - Schematic.

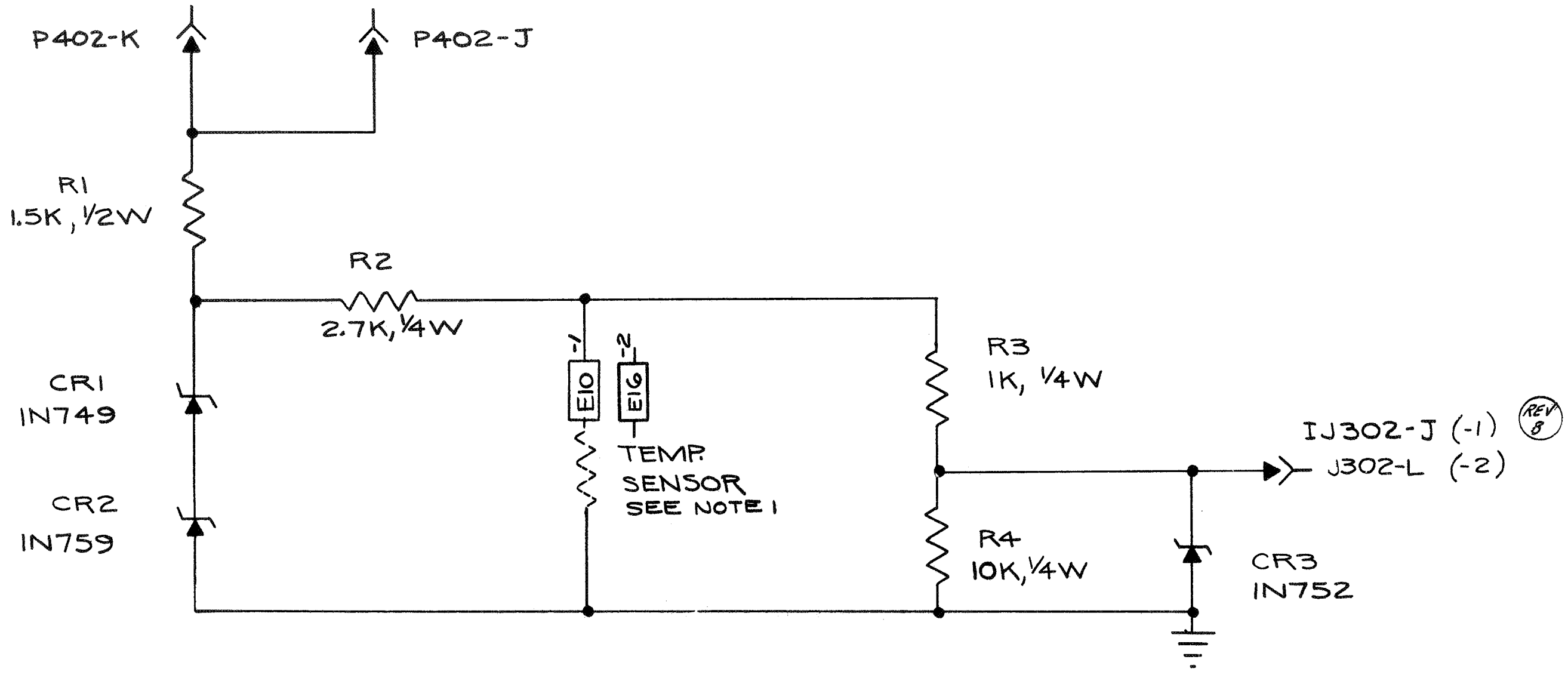

NOTE.

(A) 1. TEMTECH TRANSDUCER* 4001-2 P.O.* NAS 5-6300

(REV B) -1 HEAT SINK TEMP.
-2 BEAM CURRENT TEMP.

1-6072

Figure 50. Temperature Sensor Conditioning Circuit.

28 volts supplied from the T/M - Instrumentation section (GSFC). The calibration factor for Unit I is given in Section 1.2.2 of this report. Linearity to better than 1% was clearly established during calibrations as seen in Figure 51.

The calibration factor for the second unit is 5.77 psia/volt. The calibration curve is given in Figure 52.

Temperature Monitor - Converter Heat Sink

The sensor is a Tem Tech flat resistance element which is epoxied to one of the larger converter heat sink plates in the center, very near a transistor. Calibration-Curves are given in Figures 53 and 54 for Units 1 and 2 respectively.

Temperature Monitor - Beam Current Monitor Block

The circuit and sensor are identical to the above circuit. Calibrations give a curve identical to the Figure 53 for Unit 1. Unit 2 sensor and circuit has not been calibrated.

Main Battery Monitors to T/M

The positive battery monitor, as seen in Figure 49, is a simple resistive divider. Not shown in the schematic is zener clamping on the output.

The negative battery monitor feeds a divided signal into an inverting amplifier whence it goes to T/M through a clamp, not shown in the schematic. Positive and negative battery monitor calibrations are given in Figures 55 and 56 respectively for Unit 1 and Figures 57 and 58 respectively for Unit 2.

"Break Seal" Monitor

The "break-seal" monitor checks the number of guns that have been opened. It does this by passing a small current through the cap spring on each gun (see Figure 49) and into a current summing IC amplifier from whence it goes to T/M. By this means the voltage existing on the vacuum side of the gun deck

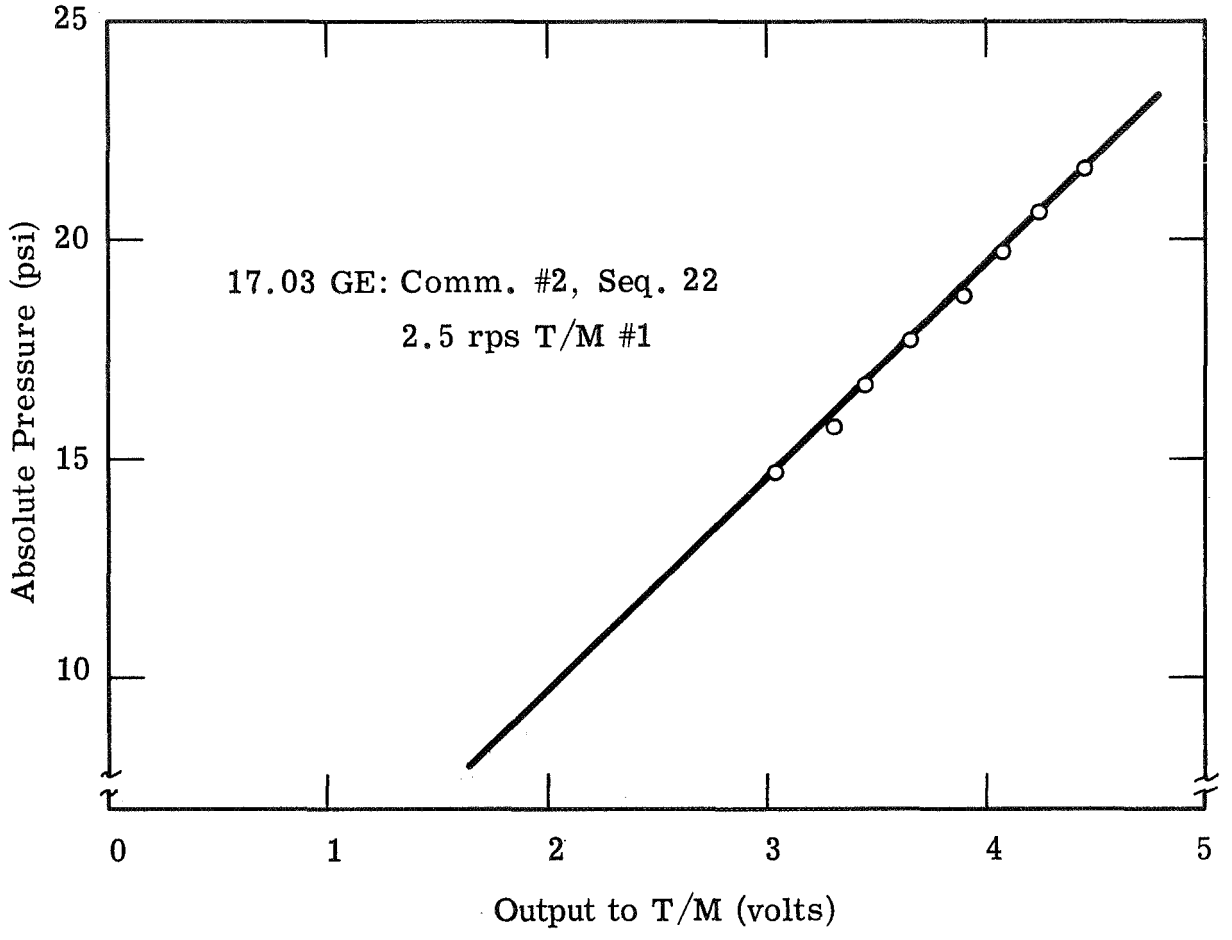

Figure 51. Package Pressure Monitor Unit #1.

1-6073

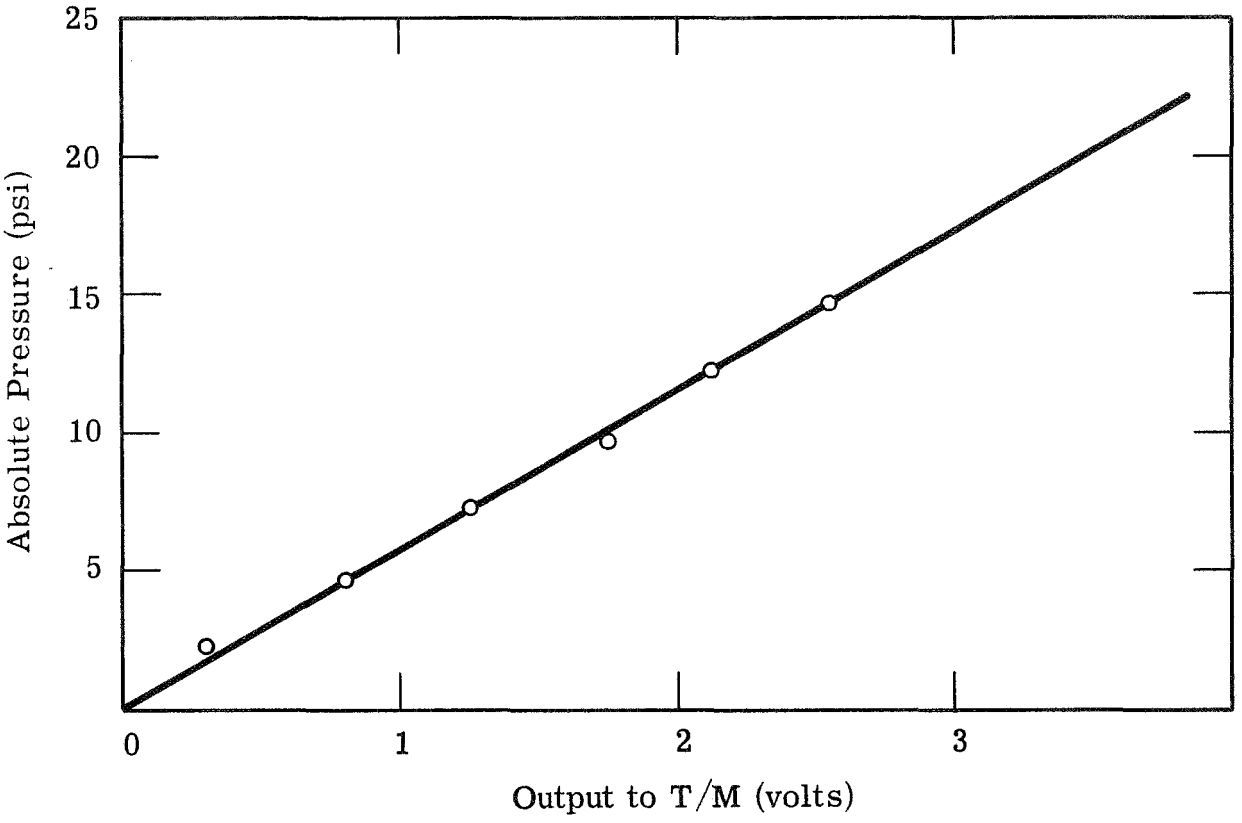

Figure 52. Package Pressure Monitor Calibration Unit #2.

1-6074

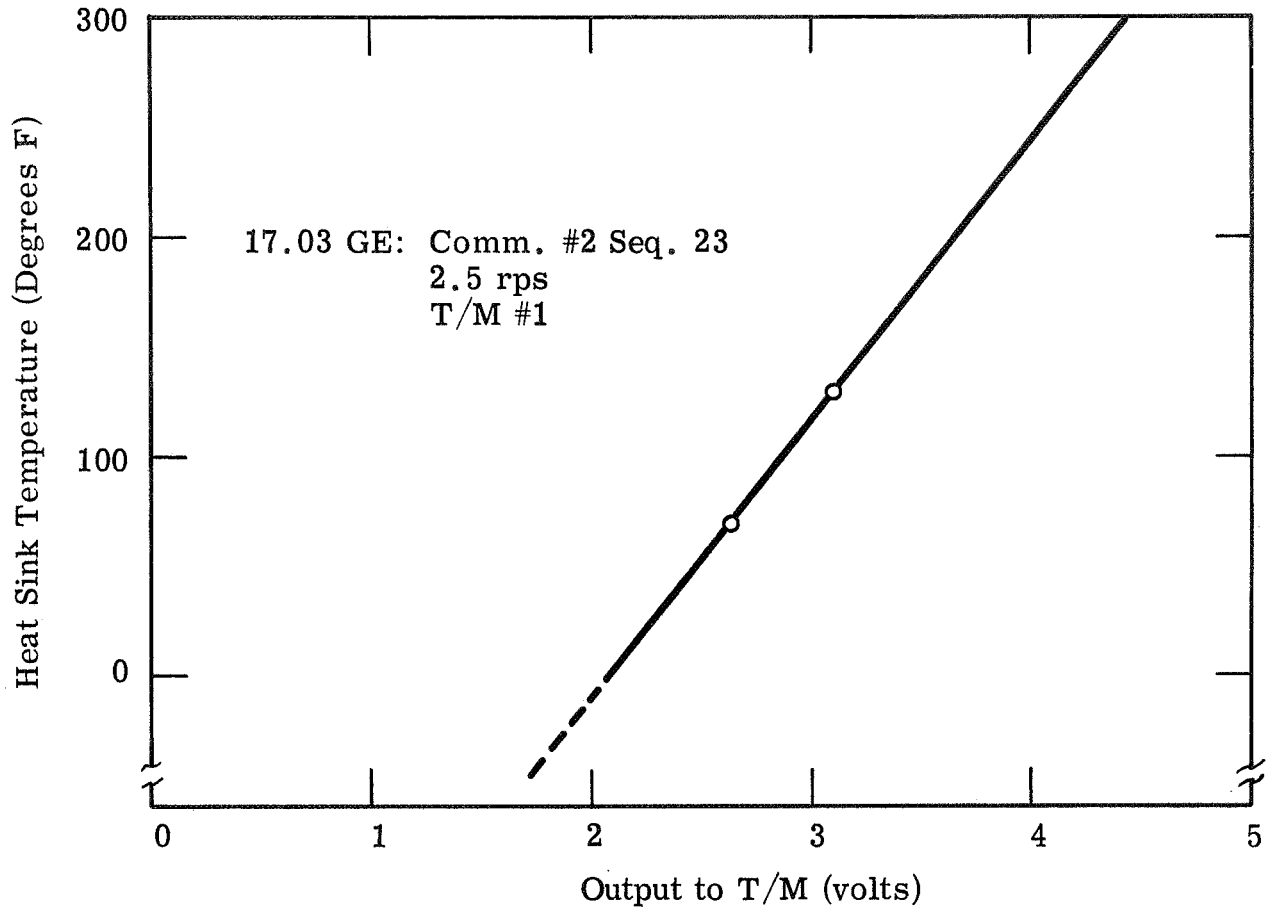

Figure 53. High Voltage Converter Heat Sink Monitor Unit #1.

1-6075

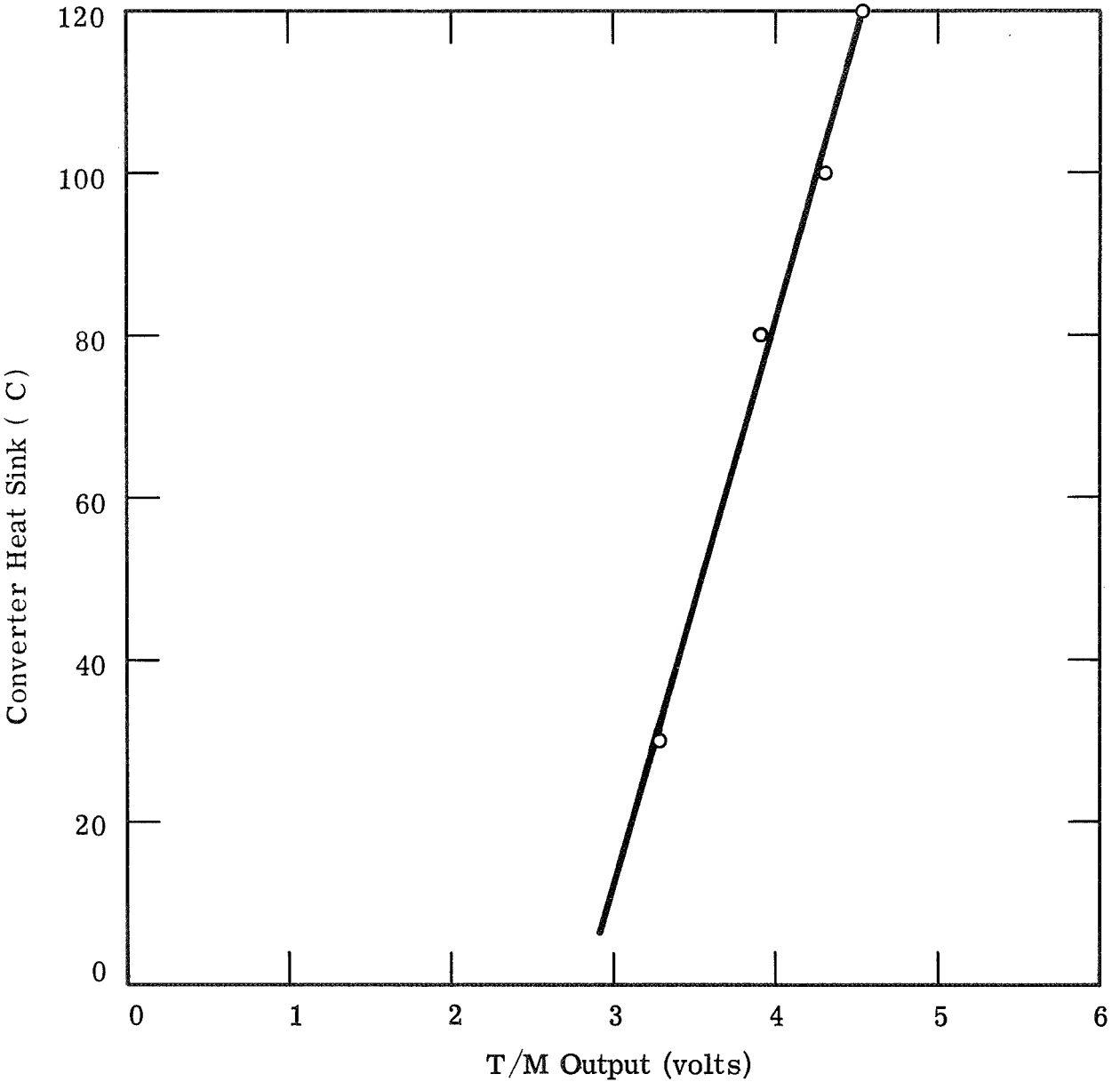

Figure 54. Converter Heat Sink Temperature T/M Calibration Unit #2.

1-6076

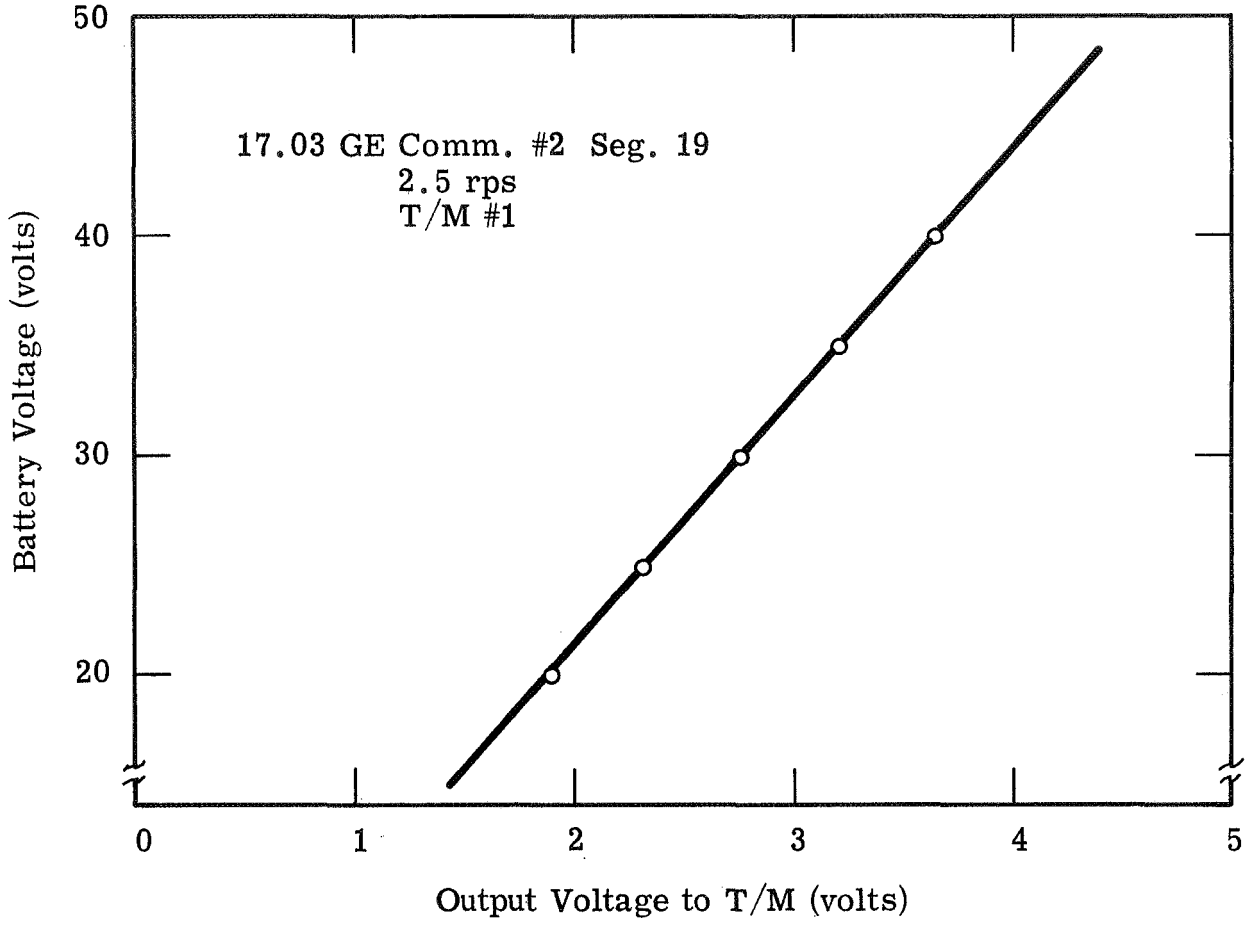

Figure 55. Positive Battery (#1) Monitor Calibration Unit #1.

1-6077

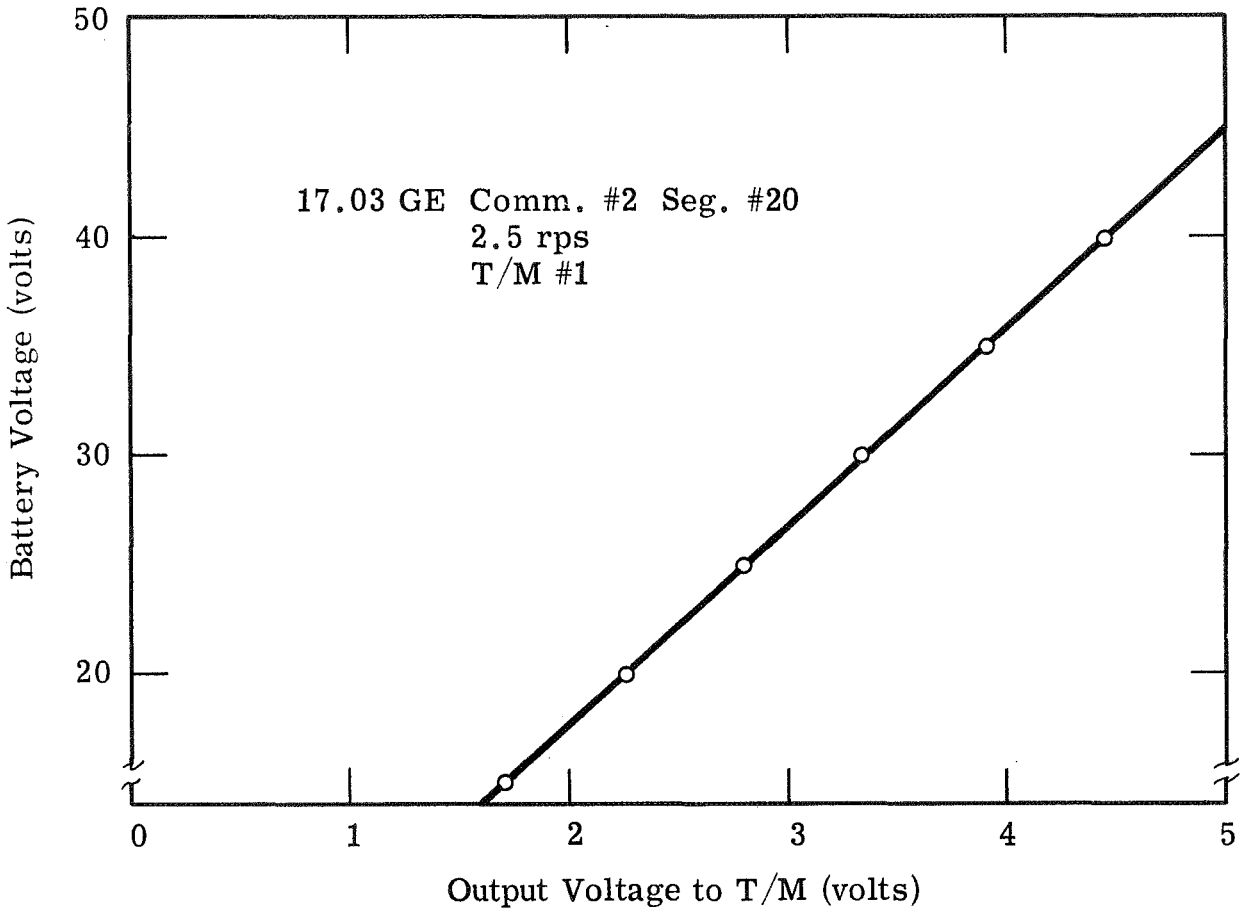

Figure 56. Negative Battery (#2) Monitor Calibration Unit #1.

1-6078

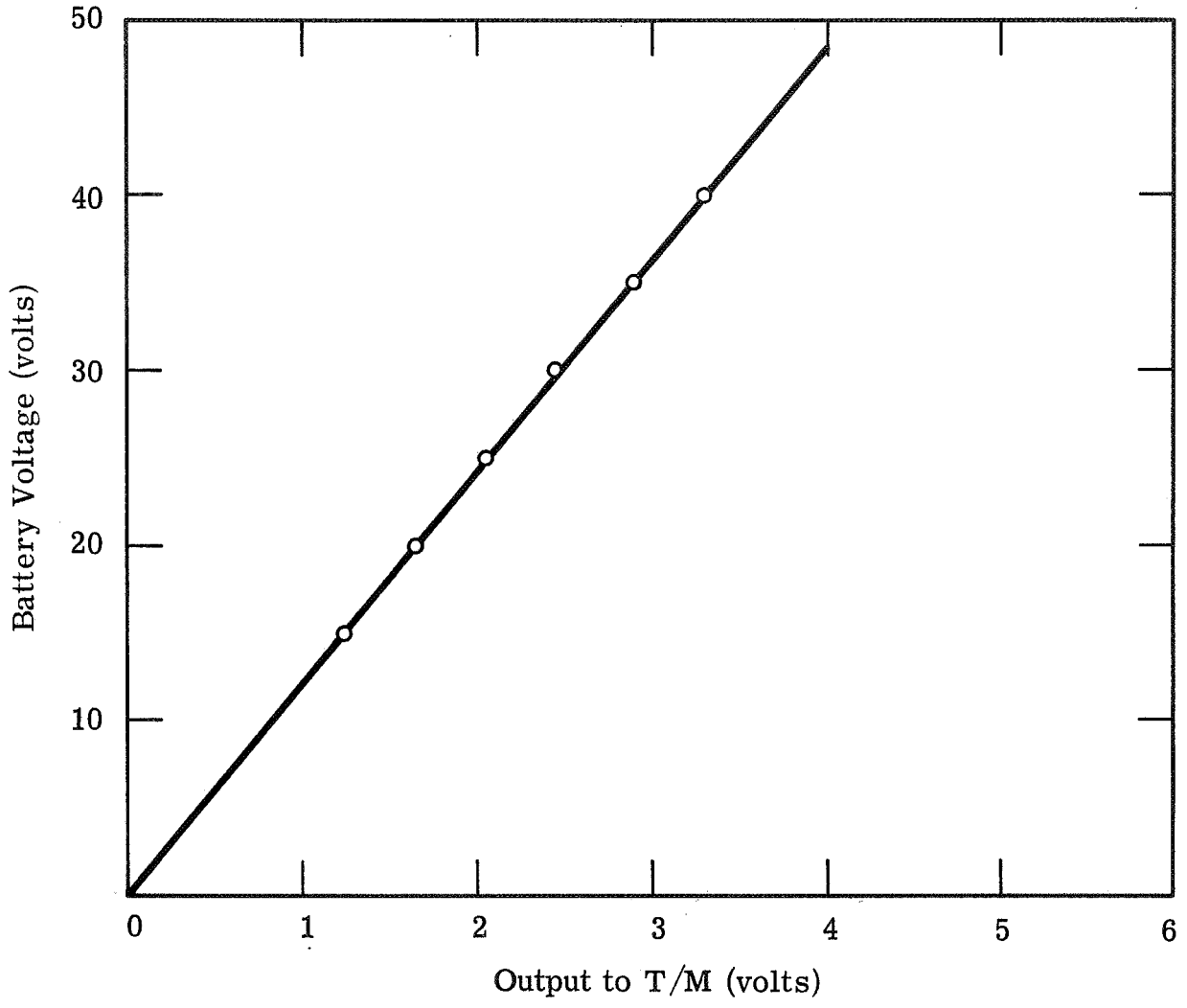

Figure 57. Positive Main Battery Monitor Calibration - Unit 2.

1-6079

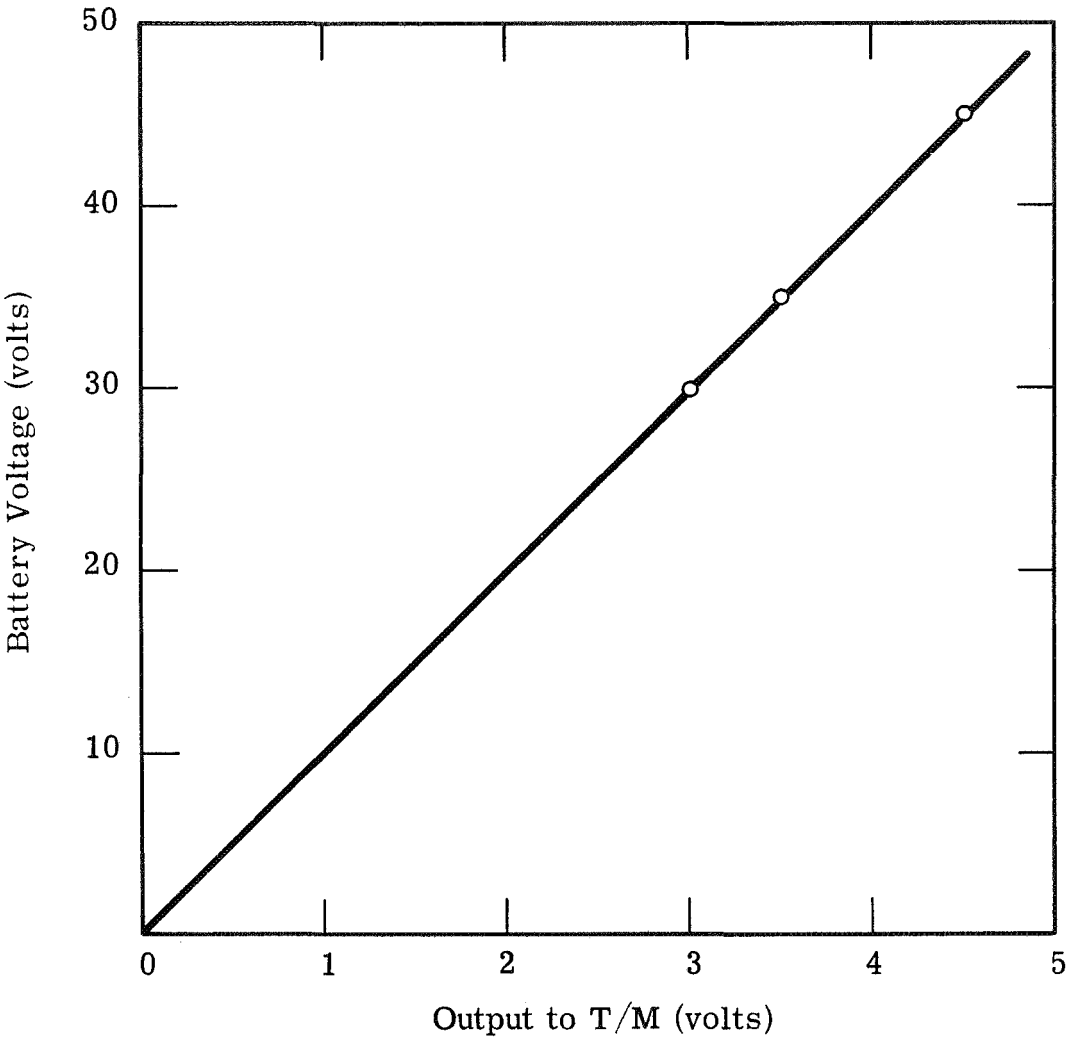

Figure 58. Negative Main Battery Monitor Calibration - Unit 2.

1-6080

is kept down to less than 250 mV, a requirement occasioned by the use of retarding potential analyzers in that area. The system is designed so that, for every gun opened, the output changes by about a half of a volt. When all are opened, one half of a volt remains. Figures 59 and 60 give the monitor calibrations for the Units 1 and 2 respectively. Output variations due to in tolerance temperature and power input variations are less than the data point radii.

Cap Current Monitor

Before the electron guns have been opened the beam current during operation impinges upon the gun caps which are shorted to the cap springs. To complete the circuit to ground and provide another measure of the beam current a resistor is inserted between caps and ground. As can be seen in Figure 49, a diode is also required in the line to block the break-seal monitor currents. A zener is also placed across the line to protect the IC's against transients. In Unit 1 this cap current resistance is 7.5Ω to 2% accuracy. In the second unit it has the same nominal value but since it has not been calibrated is known to be only within 5% of this value.

Interpretation of the apparent cap current as seen by the monitor is complicated by secondary electron emission from the copper and kovar end cap. With no biasing a goodly portion of those produced would reach the anode flange and cylinder, depending on the geometry. Secondary emission coefficients are large in the region of acceleration voltages. Figure 61 presents a curve for steel which is much the same as for copper; however, since the gun cathode is an oxide type operating at higher than rated temperature to inhibit poisoning effects during flight, it would be expected that some barium might find its way to the caps and modify the secondary emission coefficient. It might then be further expected that the cap current ratios might vary somewhat with gun history. This is illustrated by Figures 62 and 63. Both Figures show the same trends, i.e., a monatonic increase with beam energy corresponding to a drop in secondary emission characteristic. Also, in general, the slope of the curve is less at the higher currents. Other than this, the two sets of curves, the first taken with the original flight set and the second taken with the replacement and final flight

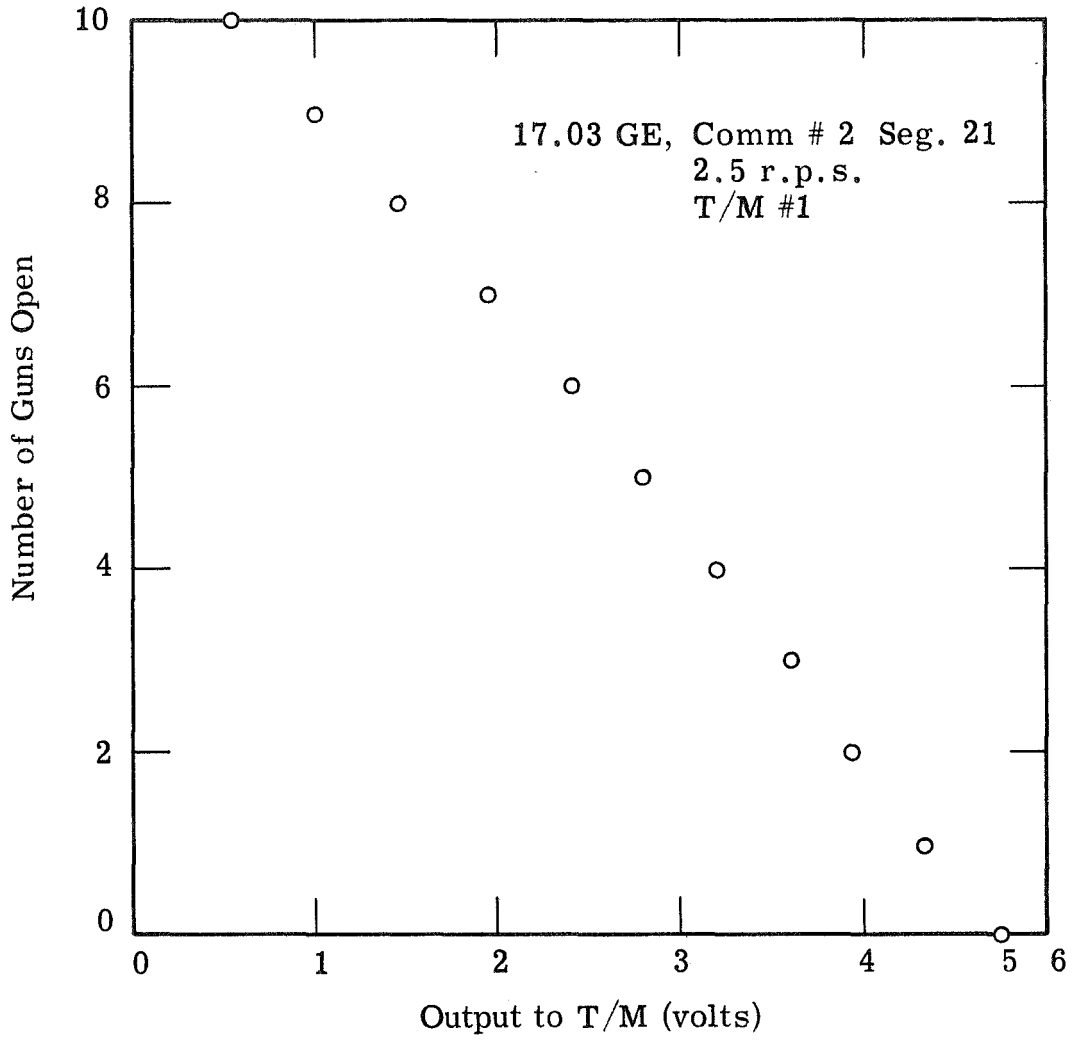

Figure 59. Break-Seal Monitor Calibration - Unit 1.

1-6081

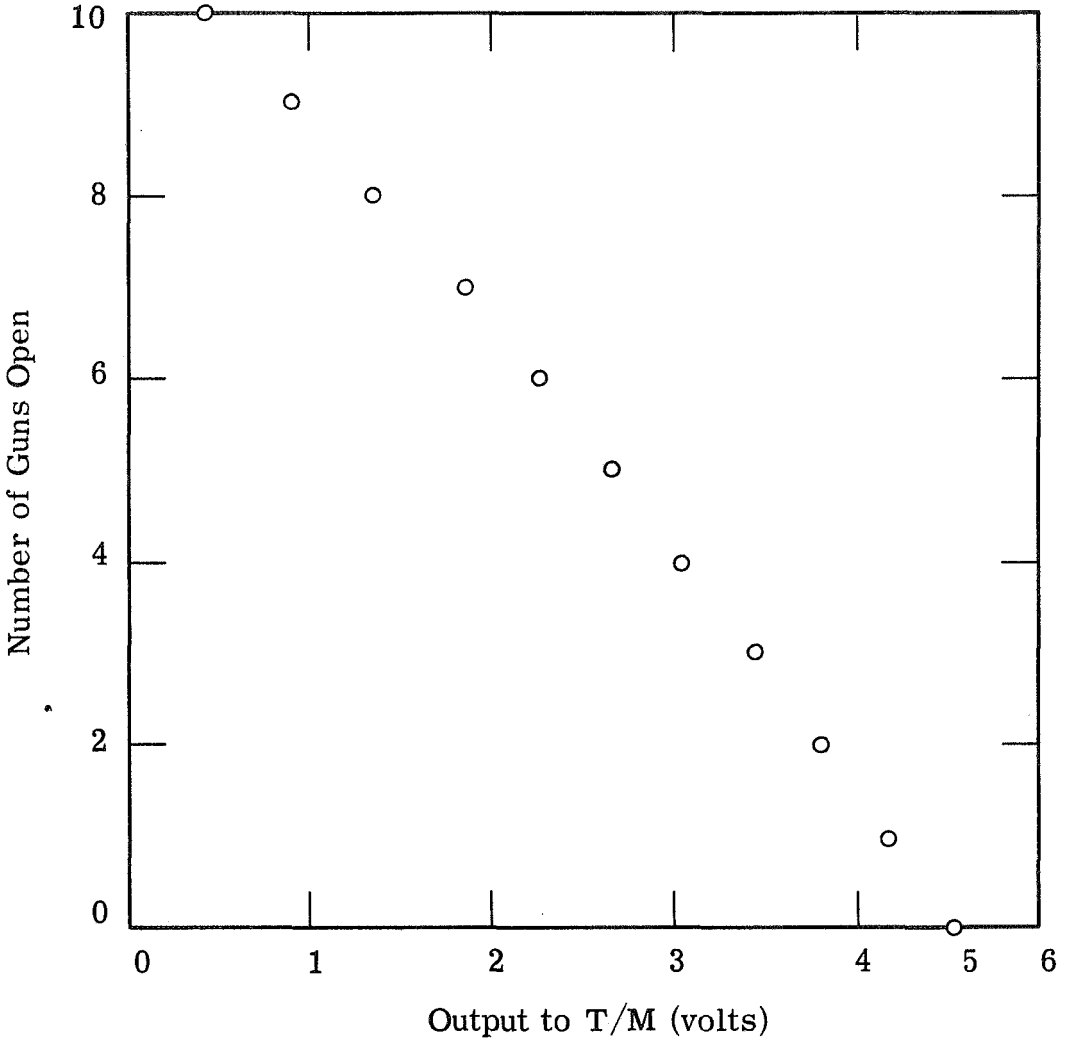

Figure 60. Break-Seal Monitor Calibration - Unit 2.

1-6082

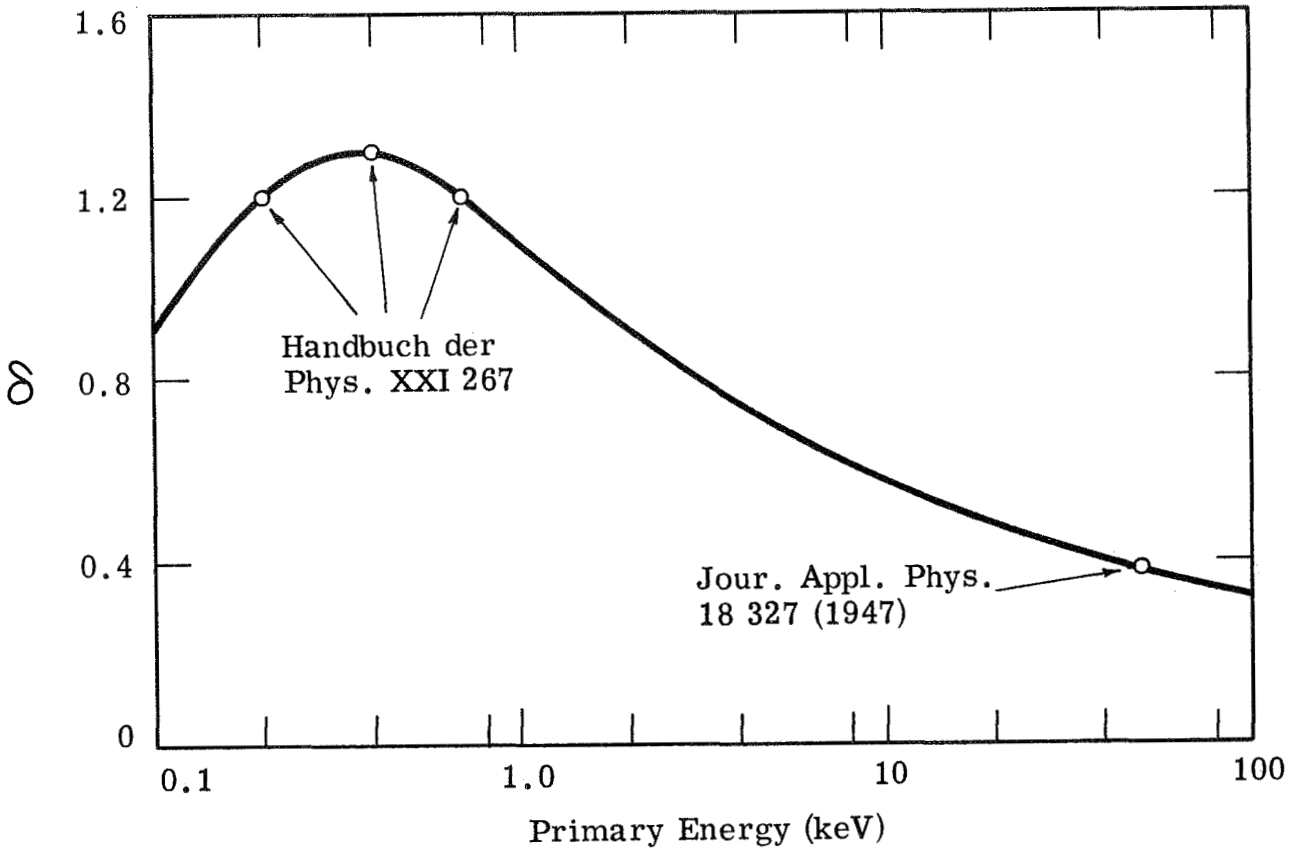

Figure 61. Secondary Electron Coefficient for Steel.

1-6083

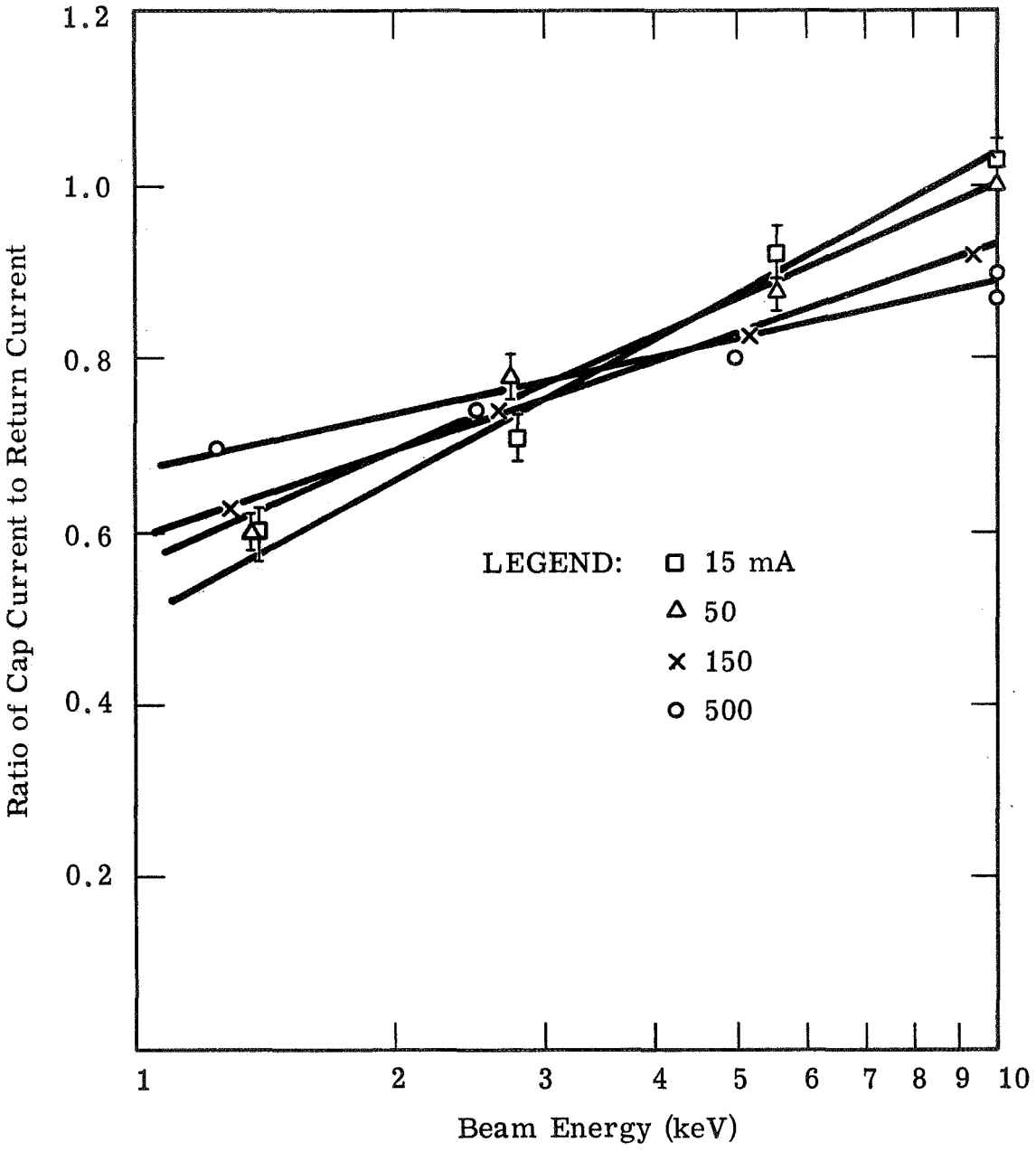

Figure 62. Cap Current to Return Current Ratio.

1-6084

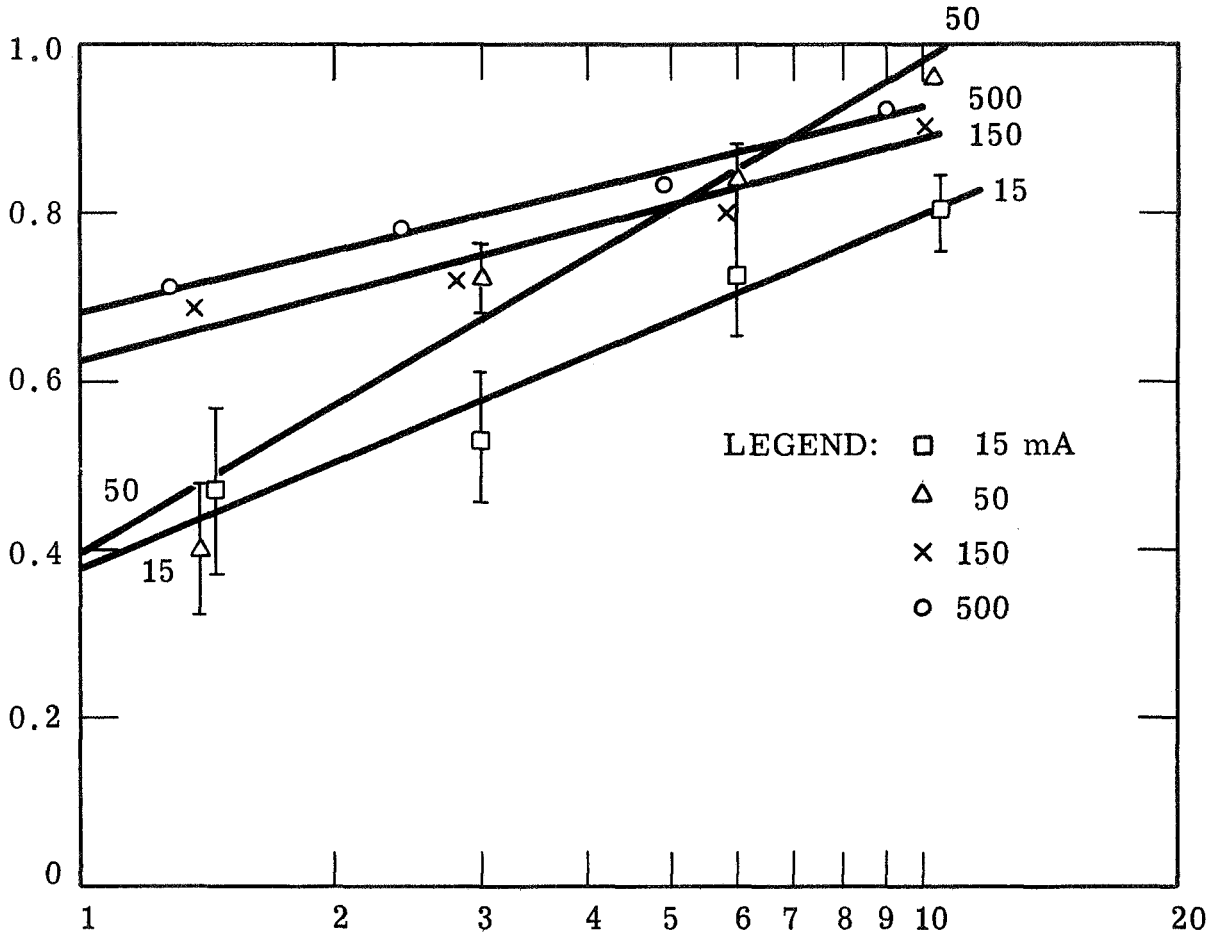

Figure 63. Cap Current to Return Current Ratio.

1-6085

set, are significantly different. As a consequence cap current data should only serve to uncover gross faults in the gun system while on the launcher. At other times the technique developed during test produces much better and consistent results. This technique involves removing the cap springs, replacing them with cylindrical aluminum heat sinks screwed onto the cap with electrical leads to a current sensing resistor in series with a biasing battery. When the battery potential is 20 V or more and of low enough impedance coupled with the correct sensor resistance range to keep at least 10 V bias during half-ampere pulsing, then all of the current is recovered.

1.4 Systems Test Console

The system test console has been designed to perform systems tests at IPC, at GSFC Beltsville, at GSFC Greenbelt and Wallops Station, Virginia up through the vehicle launch. As such it requires circuits during testing at IPC for simulating those normally supplied by the instrumentation section of the payload, supplied by GSFC-SRB. It contains circuits for checkout of the package after payload and vehicle integration. It also contains circuits for monitoring and maintaining the main batteries and the programmer battery. Figure 64 a & b is a schematic of the system wiring including IPC cabling between IPC payload and console or alternately between umbilical and console. A view of the console is given in Figure 65. A considerable amount of care has been taken with regard to the grounding system. The checkout system grounding includes a power ground and a separate instrument ground both which attach through the indicated cabling to the centralized ground in the IPC payload. Those functions which simulate functions in the instrumentation section of the overall payload relate to a completely separate ground bus.

This bus is located in a small junction box which contains as well as the bus, a 55 pin input connector which accepts cabling from the payload. An output connector which is the same as the umbilical connector in the skin of the vehicle, and a pair of rotary solenoid switches which simulate Ledex switches in the instrumentation section of the payload. The 55 pin connector and connections thereto are the same as is provided for entry to the instrumentation section

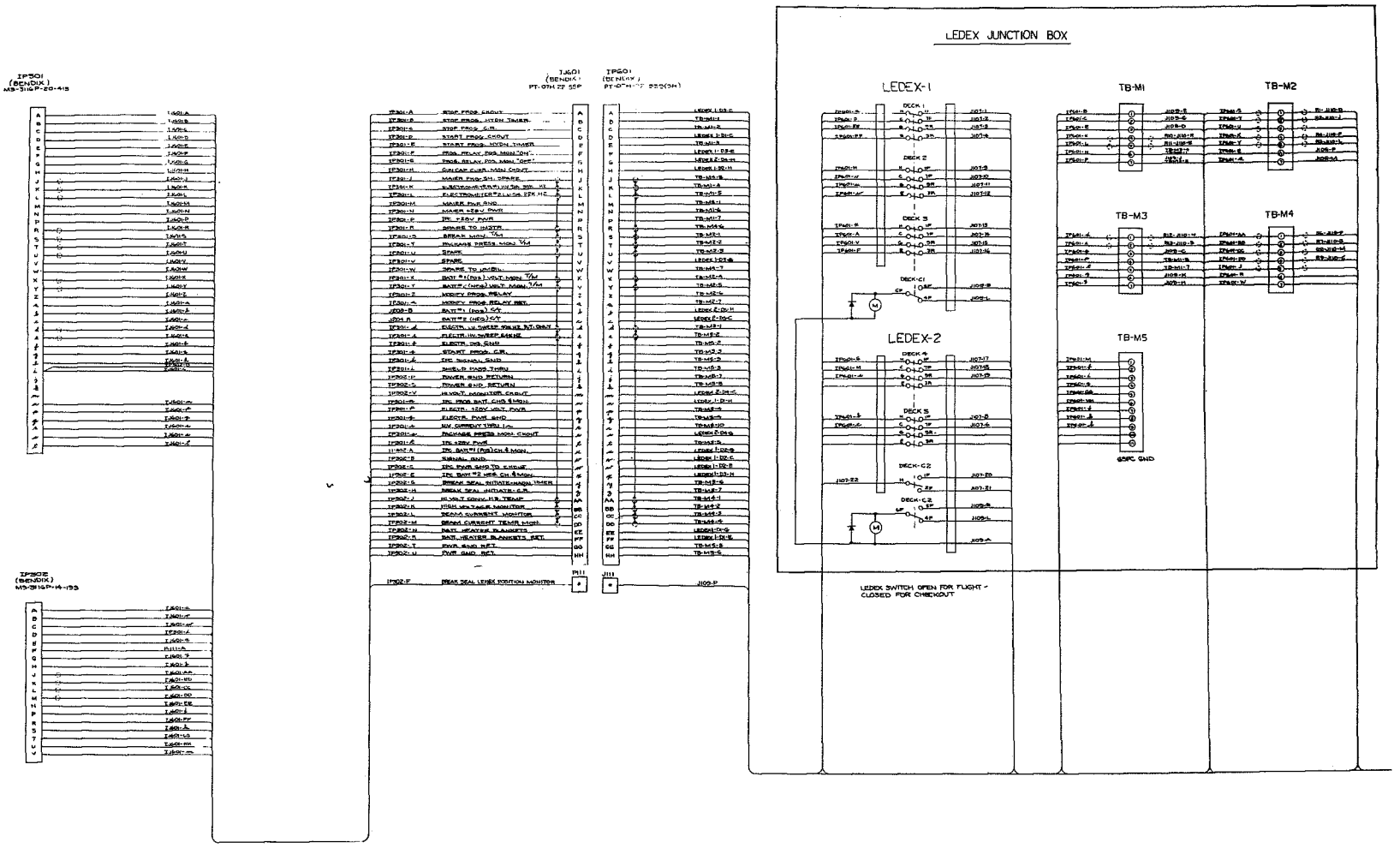

Figure 64a. Systems Checkout Console and Cable Interconnections.

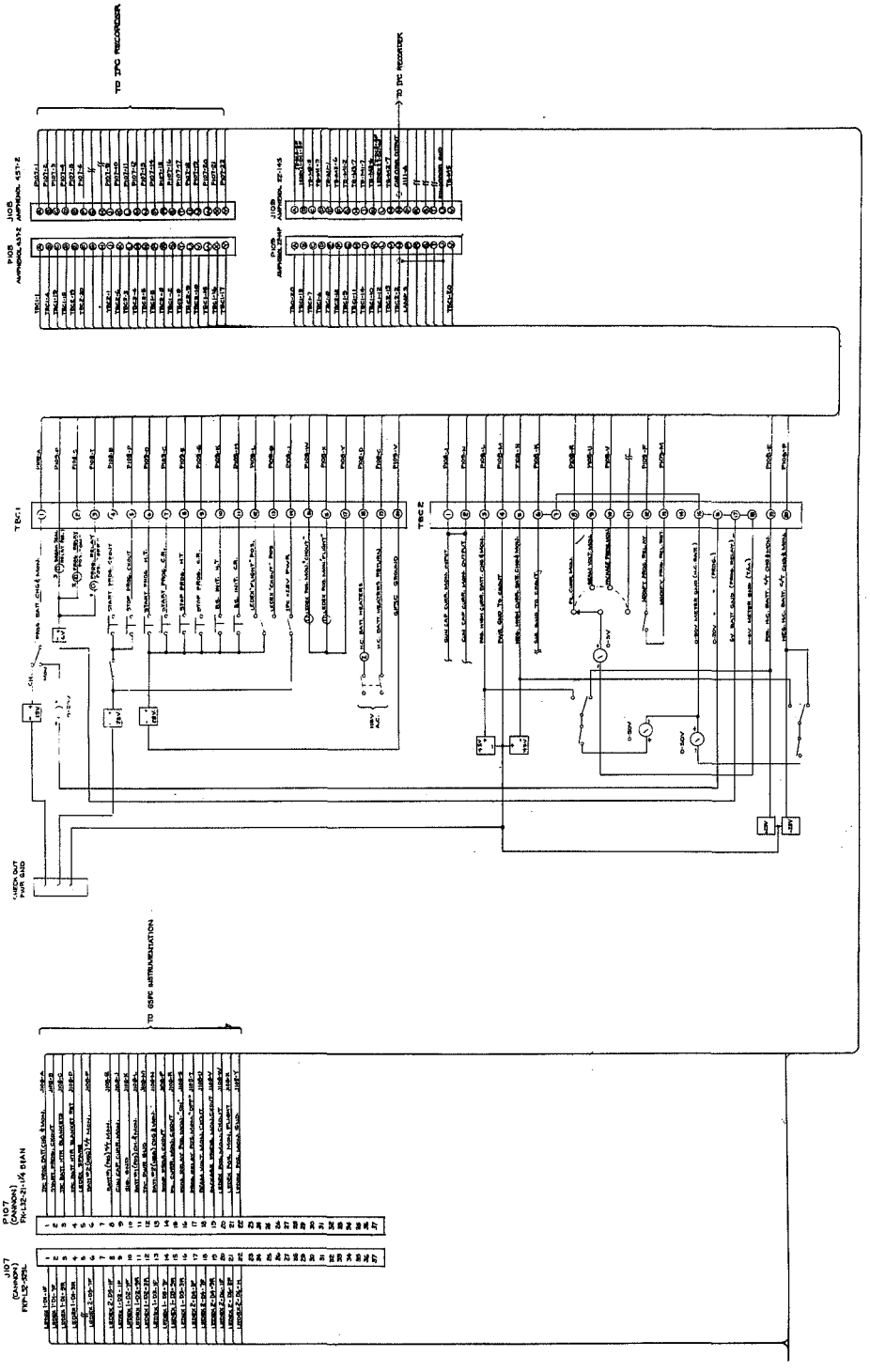

Figure 64b. Systems Checkout Console and Cable Interconnections.

1-6086b

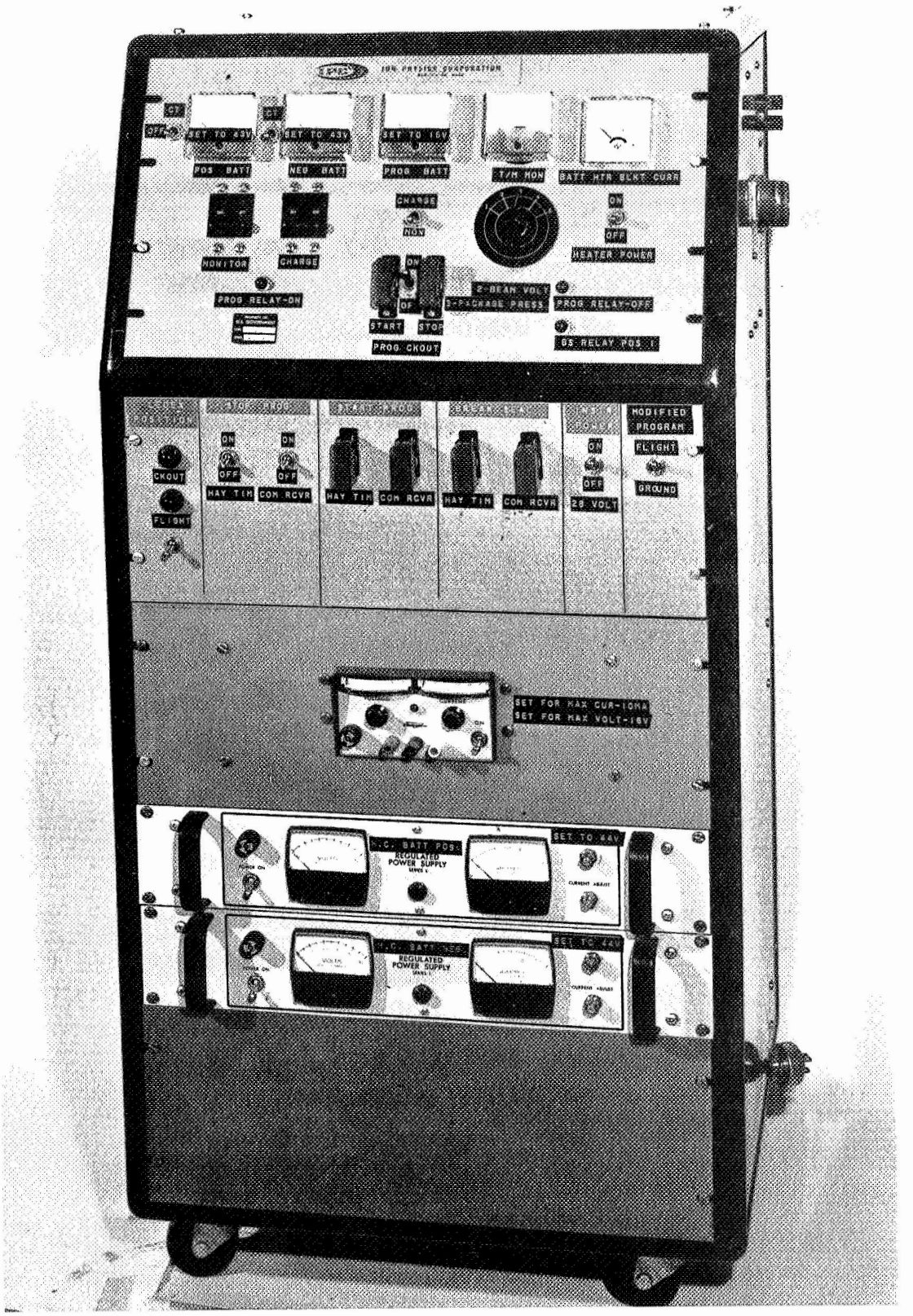

Figure 65. Systems Checkout Console.

2-1569

of the payload. The 55 pin connector and connections thereto are the same as is provided for entry to the instrumentation section of the payload.

In the field with payload integrated, the junction box is not used. The checkout cabling is plugged directly into the umbilical connector on the vehicle or a comparable connector provided by GSFC-SRB in the blockhouse. The 28 volt power required by the retarding potential analyzers is supplied by a separate external regulated supply. 28 volt power to manipulate the programmer relays and the breakseal relay are supplied by an internal 28 V supply. This supply also provides power to those monitors requiring 28 V from the instrumentation section of the payload, namely; the package pressure and temperature sensor monitors.

1.4.1 Top Panel Controls and Indicators

All functions on the top panel are related to the checkout system grounds and are activatable when plugged into the vehicle umbilical, excepting the "BS RELAY" position monitor which is functioning only if direct access is had to the payload, i.e., the lead carrying this function does not carry through the instrumentation section to the umbilical.

From the left, the two meters monitor the main battery voltages. The small switches when turned to "CT" position put center-tap to ground voltages on the meter. The dual switches on the left put the full battery voltages on the meters. The other dual switch places the output of the two power supplies positioned at the bottom of the console onto the battery lines.

The central meter on the console monitors the programmer battery voltage continuously when the switch below it is in the monitor position. In the neutral position the meter is disconnected. In the upper position the switch connects the small centrally located power supply visible above the larger supplies in Figure 65. Instructions on setting the supplies and monitors are taped on the controls as shown.

The T/M monitor meter is a 1% accuracy taut band suspension meter for measuring the beam voltage or package pressure depending upon the position of the switch below.

The meter on the right measures the pulsed DC current to the sum of the two main battery heater blankets. The circuit to the blankets consists simply of a small variac mounted inside the console, set to about 40 V output, in series with a diode to the heater leads to the package. This wiring is not shown in Figure 64. At this voltage level current to each blanket runs about 3 amp. As discussed before the blanket circuits are provided with thermostats which cut out when the battery is up to temperature.

Three switches are centrally located on the lower section of the panel. The center one turns 28 V power onto the other two switches acting as an arming switch. The guarded switch on the left is a momentary switch which turns on the Programmer. The switch on the left is also momentary and turns it off.

The lights on either side of these switches are connected to the latching relays in the package and indicate their position.

The solitary light marked BS Relay position is lit during checkout operation (Package separated) if and only if the break-seal relay is in the homing position. Controls on the lower panel all relate to the simulated instrumentation ground bus and simulation of instrumentation section functions. On the left a switch activates the Ledex switches, the lights indicating the Ledex position. The switch on the right labeled "MODIFIED PROGRAM" allows the modified program or the flight program to be run. Instrument power to the start, stop programmer and break-seal relays is provided by the INSTR. POWER switch. Each function is provided with two switches to completely exercise all input lines to the relays.

SECTION 2
DEVELOPMENT/TEST EFFORT

The development program leading to the packages described in Section 1 has been well documented from the beginning of the contract in March 1966 through August of 1968 in bimonthly reports numbers 1 thru 14. A very short summary will be given here of the principal problem areas encountered and their solution. This will be followed by a more explicit account of field operations involving Unit 1 up until launch on January 26, 1969 and the final test program with Unit 2 at IPC. The final section of the report, Section 3, will deal with the launch operations and post-data analysis.

2.1 Summary of the Development Effort

2.1.1 Gun Development

Development of the electron gun optics began at IPC almost immediately during the contract. Proprietary grid one-cathode-filament modules were obtained from Machlett Corporation and fitted to an experimental electrode structure rig positioned in an ultra-high vacuum chamber. The development effort proceeded reasonably smoothly and in three months time final electrode specifications were given to Machlett to incorporate into a production gun. At the same time as the above development effort Machlett was learning how to crack the break-seal bands. Initial thoughts of using pyrotechnically activated hammers on a stressed insulator very shortly gave way to learning how to girdle the insulator in exactly the same way that a band of red hot nichrome wire is used to cleanly crack large diameter glass tubing. As this development effort progressed it was feared that the very high current required would be too much for the batteries to be used. However, most of the attempts tried did not improve the situation. The shortness of schedule finally curtailed further activities in this direction. As called out in the sub-contract a large number of partial gun assemblies (less the gun-cathode end) were produced and shipped to IPC for an extensive reliability test program. Two kinds of nickel leads attached to the

metalized band were sent, perhaps 20 or so of them having markedly thinner leads than the majority which were doubled 1/8-inch leads. It was immediately established that the thin leads were unacceptable as 3 of the first 4 tested failed by a burnout of the lead before cracking. Tests were continued with only the thicker leads (which were used later in production guns). In all, 70 of the latter type were tested. Half of these were tested with the switching circuit to be used with the positive main battery and half were tested with the switching circuit to be used with the negative main battery. The tests were made at a number of input battery voltages ranging from 13.5 to 18 volts. (Prior testing of development models at Machlett had established the probably successful range of firing voltages.)

As reported in Section 1.3.1.5 of this report, the tests were highly successful. It was noted at the time that when the break occurred with a significant portion of the lot some of the metallized band would become incandescent, vaporize and spew off of the insulator, a portent of possible problems to come.

The gun production program continued smoothly through prototype to delivery of flight quality guns.

One significant concern resulting from the use of ten guns in parallel was the question of what might happen if one or more guns failed to be opened in flight. These guns would, like the opened guns, be turned on and for the full program. It would be expected that the closed guns would overheat, outgas and probably then sustain deleterious high voltage breakdowns, ending the useful experiment. To determine whether such events would occur, a production gun was mounted in a test fixture to a vacuum system to reproduce the thermal environment seen by guns in the package. This gun was then subjected, without opening, to a program of pulsing over the range of beam voltages in the experiment equivalent to the current duty cycle of the experiment. The test was continued for six minutes without incident. After shutdown the gun was retested for six minutes without incident. After shutdown the gun was retested for a change in characteristics. No significant changes were noted.

The results of this encouraging test together with the results of the break-seal test program gave to the system design a much increased confidence

level. To improve this level even further, the break-seal actuation was tied to a channel on the command receiver in the instrumentation section of the payload. The programmer turn off and on were also routed to command receiver channels. By this means if not enough guns opened during the automatic sequencing, as evidenced through the T/M break-seal monitor link to the ground, then the programmer would be turned off and restarted at the same time that the break-seal sequencer was reactivated in an attempt to open the remaining guns.

2.1.2 High Voltage Converter Development

Initial development of the converter system began about a month after contract start. Initially it was decided to build three converter types; a 5 kV, a 2.5 kV, and a 1.25 kV converter. Most of the development problems centered around the transformer designs and the choice of inverter transistors. These problems were complicated by a change in engineering personnel on the task five months into the contract. By the fifth month of the contract it had become obvious that:

(1) A driven bridge inverter would be the best to use.
(2) Ferrite cores should be used in the transformers.
(3) There was not enough time remaining to design three different converters, hence further designs concentrated upon development of a 1.25 kV converter.
(4) Very high current (100 amp.) transistors were too expensive and not adequately reliability demonstrated for use in the circuits; hence the change to 10 amp transistors of demonstrated reliability.
(5) Best frequency range would be limited to less than 10 kc.
(6) That the packaging of the system was going to be very tight.

With those criteria established development proceeded rather quickly. Ferrite pot cores were eventually used with the side cut out to take care of the high voltage isolation requirements. The tight packaging constraints forced the

design of a lucite encased transformer rectifier, bleeder, capacitor package which was successfully vibration tested and high potted to 15 kV.

2.2 First Vacuum Integration Test

Significant development problems were uncovered during the first vacuum integration test. In this test the prototype forward cannister was used and attached to a 6 ft. x 10 ft. vacuum system. The total system, including the test equipment console, was to be exercised for the full flight program. The guns were to be opened and the beam fired into the chamber to impinge on the cryoshrouds which for the purpose were metered to catch the beam.

When the program was initiated, several vacuum arcs occurred at the break-seal feedthroughs during the gun-opening sequence, burning out most of the break-seal switching circuitry and, from glass header melting, opening the package to the vacuum. Post examination showed that all of the circuits fed from the full battery taps (full battery to CT) had sustained arcs while none of those from CT to ground had (except one which was later identified as a pre-existing fault).

It was initially felt that material coming off of the break-seal bands during breaking had spanned the gap between pins on the headers and that breakdown had occurred between pins or between a pin and ground, causing high currents to be drawn through the leads. This eventually could cause the soft solder to melt and either evaporate or drip to another pin.

Some break-seal tests were run at -18 V to -36 V using lead-acid batteries and the operations visually observed. Of the four operations two were at -18 to ground and, because of the circuitry, the current was higher in these tests. In both cases, the seal broke mechanically but not electrically. In one of these the remainder of the band "cooked" for 2 sec. and spewed metal vapor out into the vacuum and partially onto the header. The second did not seem to spew out any metal into the system.

The literature was reviewed to determine the effect of various metal vapors on the voltage necessary to sustain an arc in vacuum. This was done with a view toward reducing the voltage on all header pins to 15 volts with respect to

ground. Table IV from Reference 1 indicates those metals which might be useful. It should be noted that tin, lead and antimony, the normal constituents of soft solder, are very low on the scale. In addition, cadmium and indium, constituents normally found in brazing alloys are also low on the scale. This suggested that the break-seal leads have to be connected to the header either by some fusion technique or by brazing with a Au - Cu or Ag - Cu alloy.

The final solution to the problem was obtained by (1) operating all of the circuits from CT to ground on the batteries, (2) insuring by proper routing that +15 and -15 V did not exist on the same feedthrough header at the same time, and (3) by switching to a gold-silver braze containing no constituents whose arc value voltages given in Table IV would fall below 15 volts. When these items were incorporated into the design no further problems of this nature occurred in subsequent test and launch.

Another major problem area uncovered during this test related to the unexpected existence of h.v. vacuum breakdowns in the electron guns which occurred occasionally during the test particularly at the 5 and 10 kV levels. These breakdowns did not appear very deleterious to the guns nor to the high-voltage converter system; however, the programmer exhibited extreme sensitivity to the transients, terminating pulses and shifting the registers to new pulse positions. The beam current controller failed on the transients, burning out output transistors and shorting several reed relays. Other circuits exhibited marked sensitivity to these transients, namely the filament current regulator and its readout circuitry, the 800 V converter, and the input pulse circuitry for the break-seal switches.

It should be noted that two of the units mentioned here do not appear in the final design. The original design beam current controller used a small resistor in the cathode line, fed this signal together with set in signals for each current desired to the summing junction of an operational amplifier. Output of the amplifier was fed into an additional two transistors amplifier to the control grid lines.

Also, originally, a rather complicated circuit was evolved to measure the total filament current to the guns. This circuit, operated via transformer coupling across the high voltage interface.

Table IV. Arc Voltage for Various Cathode Materials. (Taken from M. P. Reece, Proc. I.E.E., Vol. 110, No. 4, April 1963.)

Cathode Material	Arc Voltage
Hg	8
Bi	8.7
Pb	9.2
Brass	9.7
Sb	9.8
Cd	10
Zn	10.7
Na	11
Sn	11.3
Mg	12.5
Mo	24
Ni	15.5
non mag. s.s.	16.2
Al	16.7
Ag	17
W	26
C	20
Cu	21.5
*Steel	33

*Falls to 16 when raised above the curie point.

The solution of these problems occupied the attentions of the effort for almost a year through several further "vacuum integration tests until a successful test was performed in mid 1968.

The original input circuitry for the break-seal initiate utilized differentiation of the input 28 V signal into the SCR gate. This proved in the first test to be very sensitive to transients, not only from h.v. breakdowns but from relay closures as well. The requirement for a differentiated input was removed when the NASA Beltsville group succeeded in reducing the Haydon timer cam ON time to less than the total cycle time. It was possible then to remove the SCR gate from the input lines, the input now being used to charge up the uni-junction oscillator for its first Ledex pulse.

The second grid supply (800 V) required the addition of a high voltage blocking diode in series with its output in order to preclude the breakdown from passing through this supply. At the same time, the output bleeder was changed to sustain the full high voltage without breakdown. With these items incorporated this unit operated successfully for the rest of the program. Major problems were those associated with the beam current controller and the experiment programmer.

The beam current controller failed when the output transistor failed on an overcurrent from a breakdown. It became clear later in the program that the high current discharge path passed to the control grid when grid two was blocked. Further, with the circuitry used at that time, it was discovered after the test that several of the isolated reed relays had shorted permanently forcing a change from gold plated contacts on the switches throughout to indium plated.

Over the course of the next six months various attempts were made to improve the beam current controller operation by using higher current transistors, bypass diodes, improvements in summing junction circuitry, and finally operational amplifier changeover. All of these difficulties were removed when the decision to change over to a cathode follower form of controller was incorporated into the system design. Following this there were no further significant troubles with the controller. The circuit did initially exhibit instabilities consisting of oscillations of the beam system at a rate in excess of 100 kc. These

were simply suppressed by addition of small bypass capacitors from cathode to G1 along with the 47Ω parasitic suppressor in each grid line.

Malfunctioning of the programmer because of h.v. transients continued to plague the effort for the longest time. First solution was to improve the programmer battery situation by switching from the original Everready Ni-Cd button cells to Gulton Ni-Cd button cells with internally welded leads for much lower impedance operation. Also the reed relays to turn on the h.v. converters were removed from this battery drain to the main batteries through diodes and transistors.

To solve the problems, the programmer was eventually completely encased in full-spectrum rfi/emi shielding including a heavy copper bulkhead through which rfi feedthrough filters were passed for each lead entering the box. Additional by-pass capacitors were used internally on each line. The internal gating circuit for moving the shift registers was modified to slow it down so that more energy would be needed to flip it. Finally the ground bussing from the shielding and copper bus were attached via a large area copper plate directly to the side of the pressurized cannister. With these changes the programmer now would operate properly without terminating pulses nor shifting to new pulses when a h.v. transient was experienced.

2.3 Final Systems Testing Unit 1

As outlined in the preceding section the development of the system required a number of "vacuum integration" tests before the unit was considered acceptable for integration with the rest of the payload and the vehicle at Goddard Space Flight Center. The first of these tests has just been summarized. This test and results are well detailed in the progress reports. The second such test is notable in that the system was put together in its flight configuration, (i.e., not with the "prototype" top section of the cannister) run through a full series of vibration and acceleration tests, and after some minor repairs, placed completely in the vacuum system, including system batteries.

The vibration tests were performed at levels and rates called for in the SRB/GSFC S-320-SR-1 for Aerobee 350 payloads. They consisted of a

sinusoidal sweep along each of the three axis, a random test along each of the three axis and a centrifuge acceleration test along the thrust axis to 15 g: During all of the vibration tests the package was fully activated, and pressurized using main system batteries and hardline monitoring. The GSFC supplied Maier electron spectrum analyzers were mounted. To preclude catastrophes the main battery cables contained resistances in each line. By this means the voltages would be properly supplied to the package during normal operation. If faults were to develop during the test such as a converter input short, the battery voltage monitor would indicate a large drop in voltage, without allowing catastrophic high currents to flow. Throughout the tests no unusual behavior of the monitors was noted including loss of pressure as monitored by transducers. At the conclusion of the tests mechanical inspection revealed no system faults.

Fresh at-volt batteries were added, the programmer battery fully charged, fresh main batteries pressurized to one-half an atmosphere were added as in flight with the one exception that they were mounted with cells vertical. Then the entire system was placed in a vacuum system with hardline cabling through a connector in one of the chamber posts to outside recording equipment.

The vacuum system utilized was the 6 ft. diameter by 10 ft. long IPC facility shown in Figure 66 which has a permanent gas pumping capacity of 30,000 liters/sec, and a cryogenic three section liner. One end of the chamber is closed by a 36-inch square gate valve. A smaller chamber, as shown in the figure, 36 inches in diameter, can be attached to the gate valve end. The system was mounted in this chamber and the beam fired into the larger chamber as indicated schematically in Figure 67. The cryo liners in the chambers are insulated electrically from ground and each other allowing them to catch the beam and act roughly as a Faraday cage. For this purpose the circular cryo section on the end of the chamber was connected electrically to the furthest cylindrical section. For the tests the sections were biased to 22 V with lead acid batteries, for secondary electron suppression.

The large size of the chamber, the low energies of the beam and the earth's magnetic field which is oriented roughly perpendicularly to the chamber and emerging beam axis, serve to bend the beams significantly as indicated

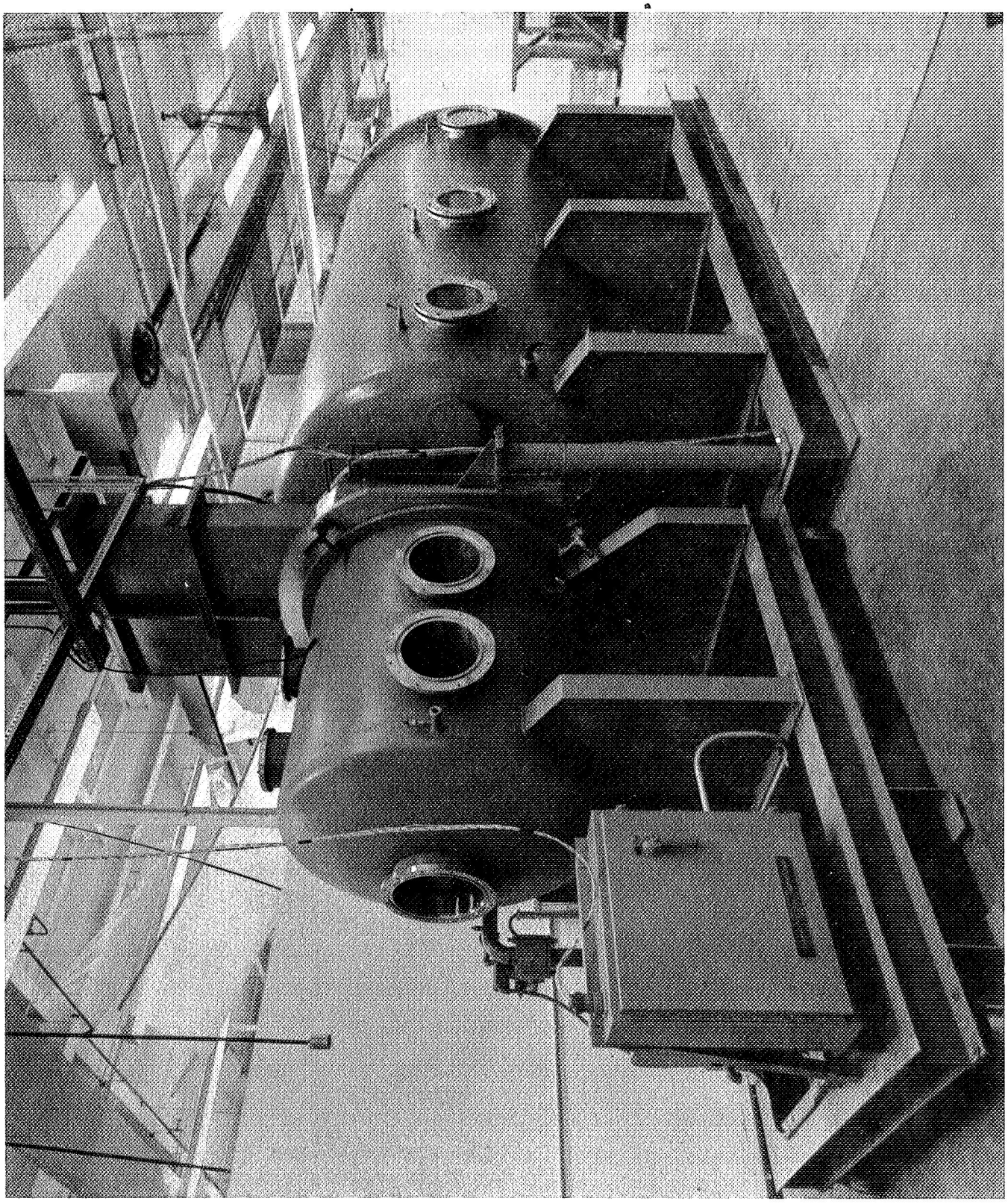

Figure 66. IPC Large Vacuum Facility.

2-1570

roughly in Figure 67. Beam divergence could, of course, alter the sketch significantly. Through the small opening in the end of the chamber, visual and movie camera observations of the breaking and subsequent gun operations were made.

The gun breaking operation was successfully performed after an initial delay due to a checkout equipment switching error. All ten guns broke open cleanly without initiating any deleterious breakdowns or arcs. The first position of the experiment program operated correctly but applications of the first signature pulse caused a high voltage transient turn-on immediately upon high-voltage turn-on. The transient caused the programmer to reset to the first pulse position. Pulsing continued correctly from thence to the signature pulse position. At this time the system experienced a transient current spike 53 ns after high voltage turn-on which shorted the output transistor in the beam current controller, causing all subsequent pulses to operate uncontrolled at approximately 550 mA. The test was terminated by command on the 24th pulse.

The faults evident in this test and their solution have already been discussed. Of significant interest in a positive way was that the system of sealed batteries, sealed pressure cannister with guns open to their external environment, did not poison the oxide cathodes of the guns, full emission being obtained after 25 minutes of being open to the vacuum and external package environment. This strongly indicates that the package(s) were adequately sealed and that steady outgassing rates of package externals was sufficiently low to insure specified gun and accelerator operation.

2.3.1 Final Vacuum Integration Test Unit 1

A complete flight sequence of 106 pulses was run on May 14, 1968 using the 1st unit, prototype top section, and flight batteries. The guns used had been used a month before for a previous test and had been re-activated several days before to almost their original emission. The flight batteries used were not freshly activated and had been recharged two times. Results of the run, (5-14C-68), were entirely satisfactory. The summation of beam current on the two collector segments is given in Table V. It can be noted in the table that the 500 mA pulses are slightly low due to incomplete activation of the cathodes.

Table V. Reduced Data - Vacuum Integration Test - Unit 1
Run 5-14C-68, Total Collected Current.

Nom. Beam Energy (keV)	Nom. Pulse Length (sec.)	Pulse Position	Total Beam Current (mA) for Sequence No:					
			1	2	3	4	5	6
5.6	0.1	1	~1	1	1	1	1	~1
		2	4	~4.5	~4.5	~6	~4.5	
		3	~15	~17	~14	~17	~15	
		4	51	51	52	52	52	
		5	148	150	152	149	151	
		6	452	463	470	477	480	
2.8	0.1	7	~16	~14	~14	~14	~15	
		8	51	50	50	50	49	
		9	146	144	151	154	150	
		10	456	464	478	480	484	
10	1.0	11 st.	438	464	474	480	473	
		11 end	472	488	492	496	496	
1.4	0.1	12	~17	~18	~16	~15	~17	
		13	51	52	50	51	50	
		14	152	150	153	153	155	
		15	476	478	478	500	481	
10	0.1	16	~1	~1	~1	~1	~1	
		17	~5	~5	~5	~5	~5	
		18	~16	~15.5	~14.5	~15.5	~14.5	
		19	47	46	49	49	49	
		20	150	150	150	152	152	
10	1.0	21 st.	442	468	475	482	483	
	1.0	21 end	481	492	498	495	496	

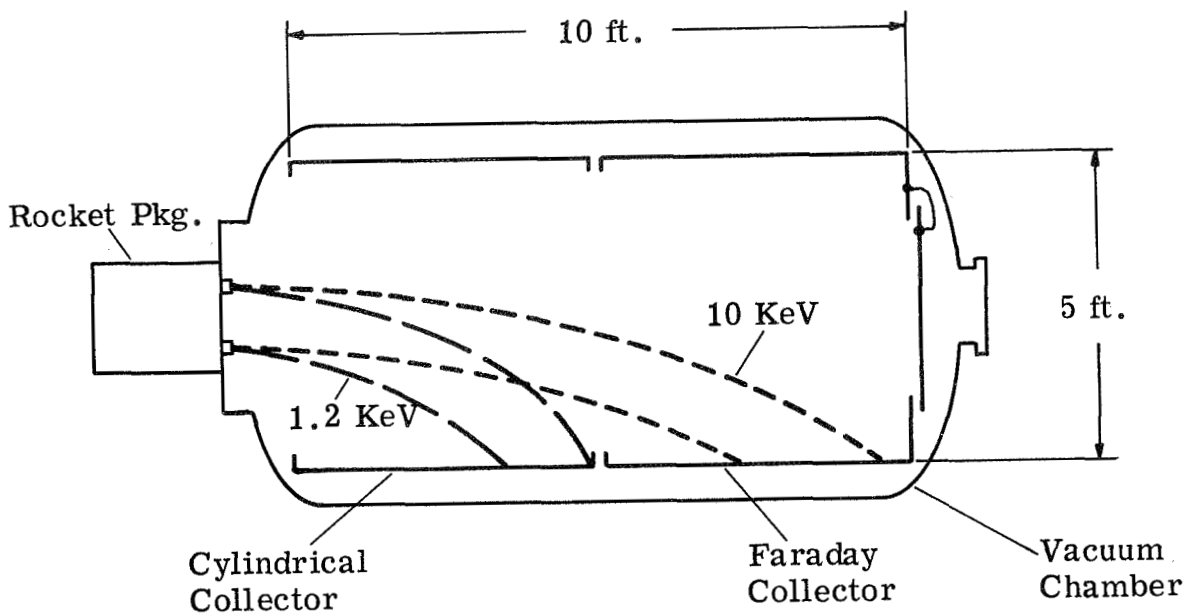

Figure 67. Test Setup - Large Vacuum Facility.

1-6087

This is further evidenced by the increase in current for the one second pulses (11 and 21) as the cathodes heat up. Table VI presents the beam voltage regulation over the experiment program. This was a bit disappointing but was traced to the poor performance of the recharged batteries. Temperature rises in heat sinks and as evidenced by pressure buildup in the package due to heating were insignificant.

One phenomenom, noted consistently in previous vacuum tests as well as this one was the transfer of beam current from the closest collector section to the farthest as a function of time. Typical data are presented in Figure 68 over a range of currents and voltages. This effect appears to be consistent with the buildup of a beam plasma during the pulse, which neutralizes or, perhaps more precisely, shields out the beam space-charge such that intially the beam blows up as a consequence of its own space-charge. As time progresses, ionizaation of the background gas and subsequent entrapment of the ions in the potential well of the beam center removes the radial forces due to space charge, leaving as the sole divergent effects, those produced in the beam optical system and those associated with collisions with the background gas.

A rough measure of the ionization rate can be obtained from the theory of Bethe. (See Bethe, 1953, pg. 253.) Here, the rate of energy lost by the electrons for the non-relativistic case is given by:

$$-\frac{dE}{dx} = \frac{2\pi q^4 NZ}{E} \log_e \frac{E}{E_i} (e/2)^{1/2} \qquad (1)$$

where

dE/dx - is the energy lost per unit of path length
q - is the charge on the electron
N - is the gas density in atoms per unit volume
Z - is the atomic number of the gas $\cong$ 7.3 for air

Table VI. Data Reduction - Vacuum Integration Test - Unit 1
Run 5-14C-68 - Beam Voltage Regulation.

Pulse No.	Nominal Beam Voltage (kV)	Measured Beam Voltage (kV)		% Deviation from Nom.	
		Seg. 1	Seg. 5	Seg. 1	Seg. 5
1	5.6	5.8	6.1	+ 3	+ 9
2	5.6	5.8	6.1	+ 3	+ 9
3	5.6	5.7	5.9	+ 2	+ 5
4	5.6	5.5	5.8	- 2	+ 3
5	5.6	5.4	5.5	- 4	- 4
6	5.6	4.7	4.8	-17	-14
7	2.8	2.8	3.0	+ 4	+ 7
8	2.8	2.7	2.9	+ 2	+ 4
9	2.8	2.7	2.8	+ 2	0
10	2.8	2.5	2.4	-11	-14
11	10.0	8.6	8.3	-14	-17
12	1.4	1.65	1.65	+18	+18
13	1.4	1.65	1.4	+18	0
14	1.4	1.4	1.4	0	0
15	1.4	1.26	1.4	-10	0
16	10.0	10.3	10.4	+ 3	+ 4.5
17	10	10.3	10.4	+ 3	+ 4.5
18	10	10.1	10.3	+ 1	+ 3
19	10	9.9	10.0	- 1	0
20	10	9.2	9.7	- 8	- 3
21	10	8.6	8.1	-14	-19

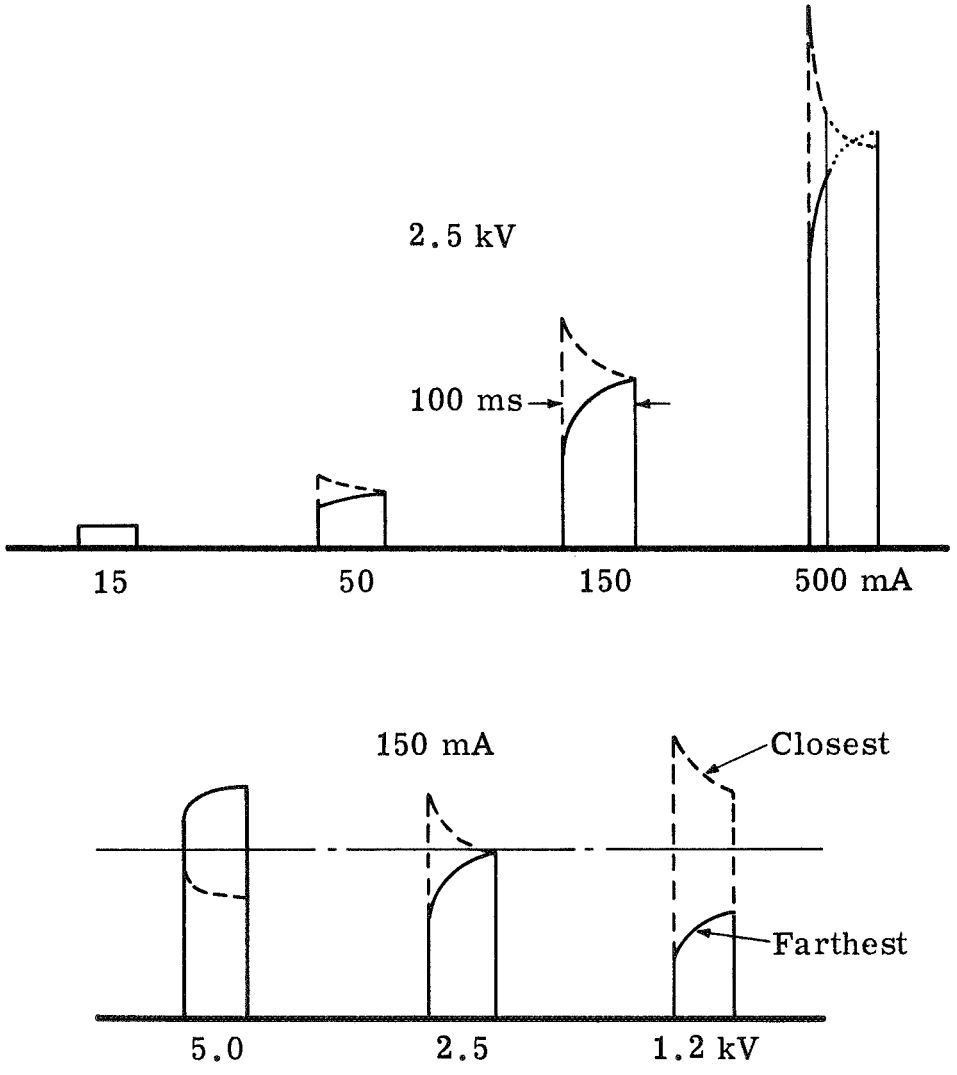

Figure 68. Typical Two Section Faraday Current Vacuum Integration Test.

1-6088

E - is the electron energy

E_i - is the "average excitation potential" of the gas (taken as 84 eV for air, see Bethe 53, pg. 203)

The ion pair or beam plasma production rate is related to the above expression through w, the energy loss per ion pair formed. This value has been shown by many, many workers to be remarkably independent of primary energy. For air its value is 34.7 eV per ion pair (see Bethe 53, pg. 233).

The rate of plasma buildup, $\dot{\rho}$ is given by:

$$\dot{\rho} = \frac{I}{qA} \cdot \frac{1}{w} \cdot \frac{dE}{dx} \tag{2}$$

where I is the beam current, and A the beam cross-sectional area.

The beam density is given by:

$$\rho_e = \frac{I}{qAv} = \frac{I}{qA\sqrt{2E/m}} \tag{3}$$

The time t_o to build up the background plasma to the beam density, which should be a good normalizing factor for the rate of neutralization, is given by:

$$t_o = \frac{\rho_e}{\dot{\rho}} = \left(\frac{V_o p_o}{2\pi q^4 n_o T_o (2/m)^{1/2}} \right) \cdot \frac{wT}{pZ} \cdot \frac{E^{1/2}}{\log_e (1.165\, E/E_I)} \tag{4}$$

where

V_o = 22.41 liters/mole

p_o = 760 torr

$n_o = 6.025 \times 10^{23}$ atoms/mole

$T_o = 273\ ^\circ K$

Evaluating the constants in the expression

$$t_o = 6.65 \times 10^3 \cdot \frac{wT}{pZ} \cdot \frac{E^{1/2}}{\log_e (1.165\ E/E_I)} \tag{4a}$$

where w is in ergs/ion pair, p is in torr and E is in ergs. For air, where Z = 7.3, w = 34.7 ev/ion pair, E_I = 84 eV:

$$\left(t_o\right)_{air} = 6.4 \times 10^{-14} \frac{T}{p} \frac{E^{1/2}}{\log_e (1.39 \times 10^{-2}\ E)} \tag{4b}$$

where

t_o - is in seconds

T - is in $^\circ K$

p - is in torr

E - is in eV

It is not expected that the background plasma produced will be effective when it has built up to just the beam density but rather we have the Debye shielding distance as a measure of the ability of the plasma to remove beam generated fields. We would expect effective neutralization to have occurred when the distance between beam electrons is on the average equal to the Debye distance, λ, or greater. This distance is given by the expression:

$$\lambda = \left(\frac{kT_\rho}{4\pi\ n\ q^2}\right)^{1/2} \tag{5}$$

About the highest density of electrons, on the average, which can exist is obtainable if the electrons are imagined to be in a crystalline lattice, again on the average, in a closed packed array, such as the close packed face-centered cubic array. The dimensions of the unit cell for a closest electron to electron spacing of λ are equal at $2\lambda/\sqrt{2}$.

The volume of the unit cell is then $4\lambda^3/\sqrt{2}$.

The number of electrons in the faced centered close packed cubic cell is four. It follows that the density ρ_e is given by

$$\rho_e = \frac{4}{4\lambda^3/\sqrt{2}} = \frac{\sqrt{2}}{\lambda^3} \tag{6}$$

where λ is as given in equation (5) and ρ_e is the same as in equation (3). Substituting equations (3) and (5) into (6) we obtain an expression for the plasma density required for complete neutralization.

$$\rho_p = n = \frac{k\,T_p}{4\pi\,q^2} \left(\frac{I}{2\,qA\,(E/m)^{1/2}} \right)^{2/3} \tag{7}$$

where

k - is the Boltzmann constant and

T_p - is the plasma electron temperature

Evaluating constants:

$$\rho_p = 2.91 \times 10^{-8} \cdot T_p \cdot (I/qA\sqrt{E})^{2/3}$$

In terms of the beam density ρ_e ,

$$\frac{\rho_p}{\rho_e} = \rho' = \frac{kT_p}{4\pi q^2} \left(\frac{2qA\sqrt{E/m}}{I} \right)^{1/3} \tag{8}$$

$$\rho' = 1.47 \times 10^4 \cdot T_\rho \cdot \left(\frac{qA}{I} \right)^{1/3} \cdot E^{1/6} \tag{8a}$$

where

ρ' - is in beam densities
T_p - in degrees Kelvin
A - in cm^2, and
E - in eV

One set of conditions displayed in Figure 68 is when:

I = 150 mA
E = 2.6 keV
p = 6×10^{-7} torr
T = 300 °Kelvin (ambient temperature)

Using these values in equation (4b) the time for the background plasma to reach one beam density is:

$$t_o = 4.45 \times 10^{-4} \text{ sec.}$$

In evaluating equation (8a) under these conditions there is a considerable uncertainty in the plasma electron temperature. As noted before the energy lost on the average to create an ion pair in air is 34.7 eV. But only about 14 eV, the ionization potential, goes into removing an electron from the atom. The

rest is eventually dissipated in heating ions, electrons, background neutrals, and in radiation to the chamber walls. The partition of this energy is most uncertain; however the time scales in question, milliseconds, are certainly long enough to allow electron equilibrium to exist at all times, and a considerable amount of ion and background gas heating. We might conclude that the electron temperature would then be something less than half of the available energy, i.e., somewhere between 1 and 10 eV.

The beam area is also not well known and is variable along the path length in the chamber. It is also obviously changing as shielding of the beam space charge is achieved. Each beamlet leaves the gun with an area of 1/2 cm^2 and appears, from gun tests to double in six inches. The beam path length in the chamber is perhaps 7 ft. A good average area would occur at 3.5 ft. with each beamlet having an area of 25 cm^2 for a total area:

$$A = 10 \times 25 = 250\ cm^2$$

Using a plasma temperature of 10^4 °K $\tilde{\equiv}$ 1 eV we obtain $\rho = 3.5 \times 10^3$ beam densities for complete shielding. The time it takes the beam plasma to reach this value would be:

$$t_n = \rho\ t_o = 1.60\ \text{sec} \qquad (9)$$

Looking back at equations (4b) and (8a) it can be seen that:

$$t_n \propto E^{2/3},\ I^{-1/3},\ p^{-1},\ \text{and}\ T_p$$

Referring to Figure 68 it can be seen that an equilibrium condition seems to be occurring perhaps a factor of ten sooner than calculated here for all 2.5 KeV pulses shown. The dependence on current seems to be occurring; however the dependence on energy appears to be quite different than expected, the time for shielding decreasing at the higher beam energies. This effect is

not understood. The complex geometry and uncertain beam shaping with energy have probably obscured the dependence. It is not certain that the equilibrium condition noted represents complete shielding or whether loss mechanisms are prominent in limiting the plasma buildup.

Further study of the effect under better conditions is certainly desirable; however it is quite certain that the time to shield out the beam is at least 2-1/2 orders of magnitude longer than that required to build up to beam density - much more in keeping with Debye shielding conditions.

This study has direct applicability to the beam ejection during the actual rocket experiment, the criterion being that phenomena associable with the existence of strong space charge generated fields should persist until the background plasma builds up to a level given in equation (8a) by ionization as given in equation (2) in combination with the existing background plasma taking into account the vastly different generation rates over the path length of the beam into the atmosphere.

2.4 Field Testing and Integration - Unit 1

Following the vacuum test just described the system was removed from the vacuum chamber, subsystems removed from the prototype top section and remounted in the flight forward half of the cannister. New guns were mounted and a final acceptance test given the unit on the bench, Run 5-31K-68, after taking care of several small problems associated mostly with change-over to the new guns.

The unit plus spares and field test equipment was shipped to Goddard Space Flight Center-Sounding Rocket Branch Beltsville, Maryland where it was integrated with the rest of the payload and vehicle over the course of the next six months.

Several significant events relating to the payload operation occurred during that time. The first involved an inadvertent turn-on of the IPC system by SRB personnel which allowed the system to operate until batteries went dead. The system, of course, was not designed for such a total energy input and might be expected to fail or be left in an overstressed condition. Tests were made on

all suspected subsystems. No apparent changes were noted except on the cap currents from the guns. This latter fact led to an eventual change-over to a new set of guns, requiring new testing, both electrical and environmental. It was determined during this time period that the original guns were probably quite acceptable for flight and that the cap current ratios appear for all guns to be somewhat a function of the operational logging time on each gun, probably as mentioned before, due to progressive barium deposition on the cap and anode interior surfaces.

As a result of a Flight Readiness Review Board meeting at GSFC it was determined that the leakage currents then existing in the main battery lines must be reduced to be acceptable to the Wallops Range Safety Officer. The second turn-on relay described in Section 1 was added at this time to cut all drains from the batteries prior to program turn-on other than those to the high voltage-high current converters and the gun-opening circuits. Of the remaining drains, which were accepted by range safety, about 90% are to the latter of the two subsystems. As finally configured the drains were measured to be as follows:

+40 V	22 mA	-40 V	28 mA
+C/T	24 mA	-C/T	41 mA
+Gnd	46 mA	-Gnd	69 mA

Net ground current to IPC pkg. gnd. is 23 mA.

The second item for action as a result of the board recommendations was that the change in guns required re-vibrating. The guns were replaced and several minor mechanical changes in the mounting sockets were made. A pre-vibration run was made in the modified current mode while monitoring all T/M outputs. It was decided at that time to vibrate the entire payload. Some repairs had been made in the Maier electron spectrum analyzer which had suffered grid damage during removal from the Dynamic Test Chamber Test at Greenbelt. The reworked package was remounted in the IPC package and the integrated system vibrated with dead unconnected main batteries at T&E, Greenbelt. Flight vibration test levels were used, as listed in S-320-8R-1 for three axis, both sinusoidal

sweep and random. Subsequent electrical tests, duplicating the pre-vibration test were made and compared to the pre-vibration test. Those comparisons are shown in Table VII and indicate no observable change in operational performance.

Shortly after these tests were completed the payload and vehicle were shipped to Wallops Island, Virginia where pre-launch operations began.

Table VIIa. Pre & Post Electrical Checkout Comparisons for Vibration Tests of 12-20-68, Unit 1.

Pulse/Event	BCM T/M Volts		Cap Current (mA)		High Voltage (kV)		% H.V. Pulse-down from No Load	
	Pre	Post	Pre	Post	Pre	Post	Pre	Post
1 Curr.	0.64	0.64	-	-	6.1	6.2	1.5	0
2	1.32	1.31	3	2	6.1	6.1	1.5	1.5
3	2.14	2.12	11	12	6.0	6.0	3	3
4	3.00	3.02	42	40	5.9	5.9	5	5
5	3.87	3.87	133	133	5.66	5.67	9	9
6	4.635	4.63	407	399	4.93	5.0	21	19
6 Mod.	2.735	2.73	27	27	5.90	5.9	5	5
7	2.10	2.11	8	10	2.96	3.0	1.0	0
8	3.01	3.01	35	37	2.90	2.9	3.5	3.5
9	3.87	3.87	119	119	2.88	2.86	4.0	4.7
10	4.62	4.62	380	372	2.40	2.4	20	20
10 Mod.	2.73	2.73	22	23	2.90	2.95	3	1.8
11	4.67	4.64	453	446	9.0	9.25	16	13.7
11 Mod.	2.77	2.76	32	29	10.23	10.3	4.5	3.8
12	2.11	2.11	7	9	1.45	1.5	3	0
13	3.02	3.02	20	31	1.42	1.45	5	3.5
14	3.88	3.88	111	106	1.39	1.4	7	6.5
15	4.65	4.62	350	344	1.27	1.28	15	14.5
15 Mod.	2.76	2.72	16	19	1.42	1.5	5	0
16	0.77	0.74	-	-	10.7	10.6	0	1.0
17	1.40	1.39	3	33	10.55	10.5	1.5	2
18	2.16	2.12	12	12	10.5	10.45	2	2.5
19	3.03	3.02	48	47	10.2	10.2	4.7	4.7
20	3.88	3.88	148	146	9.75	9.8	9	8.5
21	4.64	4.63	451	445	9.05	9.2	15.5	14
21 Mod.	2.77	2.74	32	31	10.3	10.2	4	5
22	0.65	0.64	-	-	6.05	6.1	2.5	0

Table VIIb. Pre & Post Vibration Timing Comparisons for Vibration Tests of 12-20-68, Unit 1.

From	To	Pre (sec.)	Post (sec.)
Prog Turn-On	start 1 pulse	16.382	16.543
start 1 pulse H.V.	start 2 pulse HV	2.936	2.90
2	3	2.92	2.91
3	4	2.900	2.89
4	5	2.918	2.91
5	6	2.912	2.90
6	7	2.940	2.93
7	8	2.90	2.89
8	9	2.921	2.91
9	10	2.914	2.90
10	11	2.92	2.94
start 11 pulse H.V.	end 11 pulse	1.097	1.102
start 11 pulse H.V.	start 12 pulse	2.96	2.96
12	13	2.90	2.89
13	14	2.93	2.91
14	15	2.92	2.91
15	16	2.93	2.95
16	17	2.93	2.91
17	18	2.93	2.91
18	19	2.91	2.90
19	20	2.94	2.93
20	21	2.97	2.92
start 21 pulse H.V.	end 21 pulse	1.104	1.102
start 21 pulse H.V.	start 22 pulse	3.024	3.12
Total Sequence Time (Start Pulse to Start Pulse 22)		61.525	61.39
Average Time From Start to Start Sub. Pulses		2.930	2.923

SECTION 3
17.03 ROCKET EXPERIMENT - OPERATION AND RESULTS

3.1 Launch Data - Payload Performance, Aerobee 17.03

Liftoff of Aerobee 17.03 occurred in the early morning hours of January 26, 1969, 0945 UT (4:45 EST) along an intended azimuth of 145 ° with effective launch elevation 87 °. One of the Aerobee motors malfunctioned and the actual flight was along 97 ° azimuth and effective launch elevation 89 °. All telemetering systems were fully operable and reception good during most of the flight. As programmed after burnout, the three axis attitude control system turned the vehicle over and pointed it down along the magnetic field. The nose cone was ejected as programmed and collector deployment began. A malfunction in the gas regulator used to inflate the collector did not pass the required gas, leaving the collector screen in a presumably flacid condition. During this early part of the flight program the collector probably was mostly deployed in its intended geometry. There is considerable evidence of movement of the screen during the flight; it is sometimes shorted to the vehicle. At certain times this screen appeared to shadow the command receiver antennae causing the receivers to lose lock a number of times. Table VIII presents most of the key performance events taking place during the flight.

3.1.1 Housekeeping Data Reduction

Figure 69 presents the gun opening sequence. Operation was somewhat different than on the ground, current being applied to the first four guns immediately upon turn-on rather than after a 3.65 sec wait. All guns opened and as in tests on the ground about half of the guns burned off the moly-manganese strip as indicated by the small r.f. injection across all T/M channels and indicated in the figure as "arcs". Figure 70 presents data on the main battery voltages during the operation together with the data of Figure 69. From this curve it is evident that the Ledex driving SCR was turned on by the break-seal turn-on signal or programmer turn-on signal, there being no initial 3.65 sec

Table VIII. 17.03 Key Events

Time - sec.	Event
9^h45^mOS UT	Liftoff
56.180	T/M Channel Switch - payload pressure and temperature readout
135.294	Nose Cone Eject Squib activated
135.57	Main r.p.a.s. operating
135.6	Electron Collector Shell Separation indication
139.22	Collector Inflation pressure up and oscillating
190.843	Experiment Programmer turned-on, ACS off
190.853	Gun Opening Circuits turned on
199.7	First indication that all guns are open
207.824	Start of First Pulse - H.V. on
207.937	First Pulse - beam on
208.035	First Pulse - ends
335.	ACS re-activated by Ground Command
335.2	First indications of pressure rising in r.p.a.s
346.9 - 347.2	Apparent T/M antenna partial shorting or shadowing
349.91	First indication of lower than programmed beam current in pulse 11C - probably due to partial gun poisoning
359.6	First breakdowns - in r.p.a.s
371.9	First breakdowns in guns - pulse 9C (10 kV)
377.3	Massive h.v. breakdowns in guns - pulse 21C (10 kV) - h.v. converter more or less continuously operating in short circuited mode.
380.3 - 381.2	Almost complete loss of T/M signal. Probable antenna shorting or shadowing by collector.
462.069	Start of beam current - last pulse (11E)
464.416	Programmer turned off - T/M transmitter switched to tape play back.

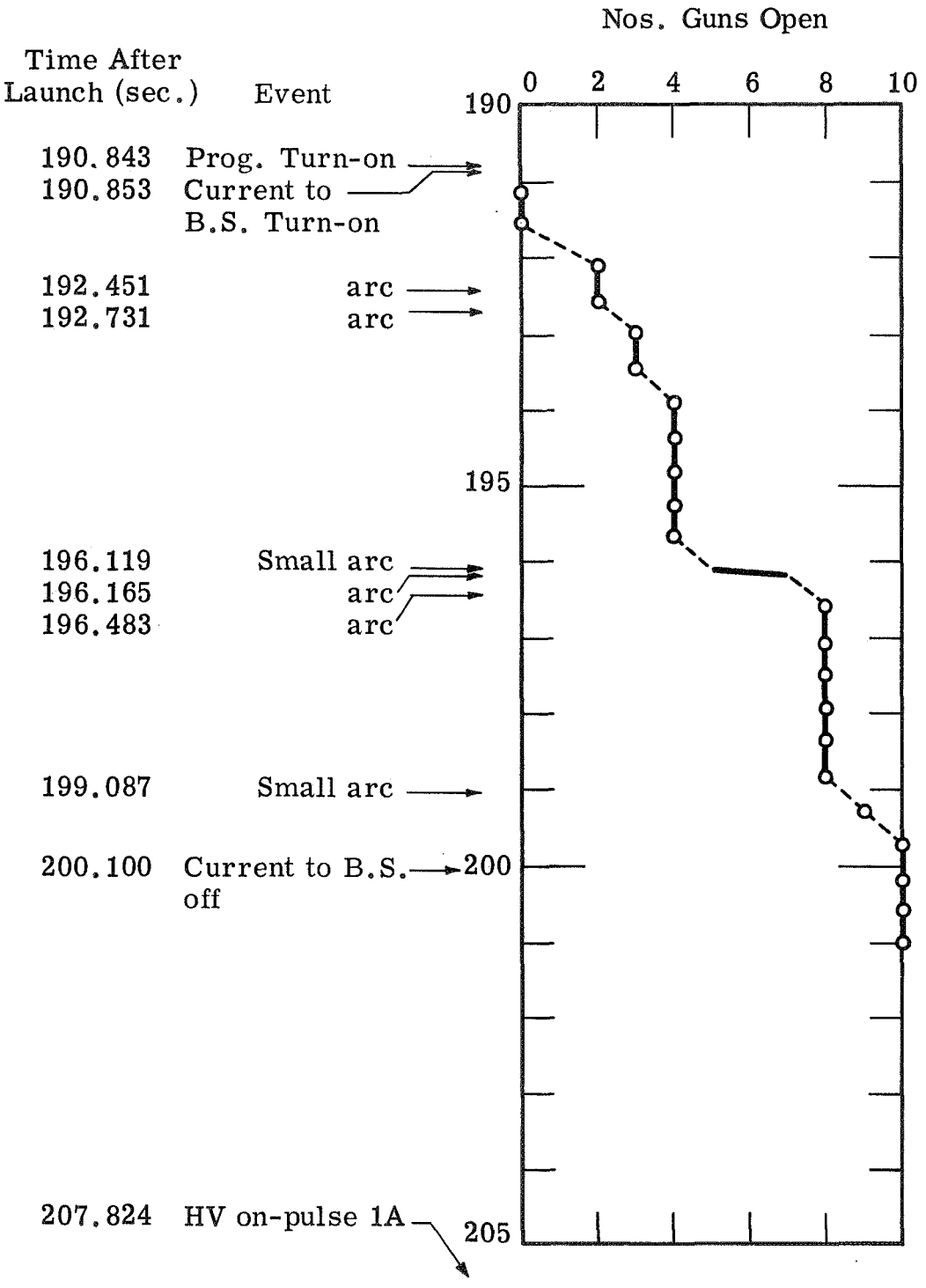

Figure 69. 17.03 Flight-Gun Opening Sequence

1-6089

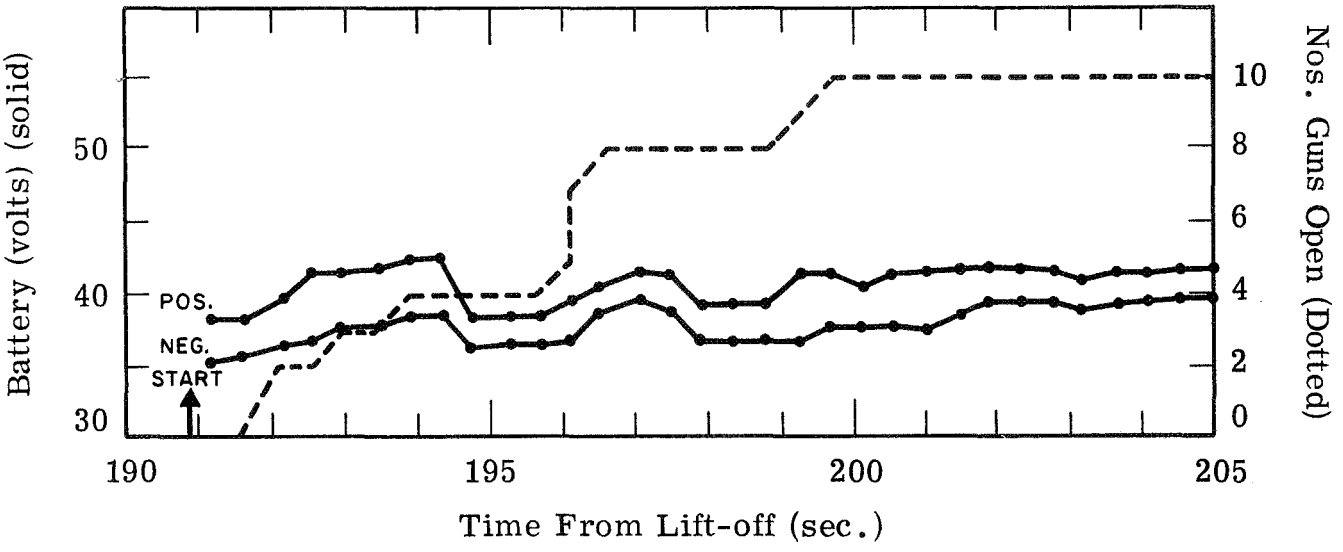

Figure 70. Battery Pulse-Down During Gun Opening.

1-6090

delay. The switching time to the second set is correct for initial turn-on, approximately 3.65 sec.

The negative battery voltage appears consistently low during the time period graphed. It appears that one cell in the negative battery may be shorted out right from the start of the program.

Table IX presents reduced housekeeping data on the package pressure, temperatures on the heat sink and beam current monitor, and the battery voltages. To the reading accuracy the package pressure stayed constant during the flight. Both temperature sensors seemed to record a slight increase in temperature over the flight program. This increase is not considered significant.

The negative battery voltage again appears consistently lower than for the positive battery. If the difference was due to a shorted cell and not a change in the monitor calibration then the cell did not adversely affect the experiment other than the loss in voltage.

The high voltage data, which is to be discussed, gives values consistent with a normal battery voltage, leading to the conclusion that the battery did not have a shorted cell and that the monitor probably was the culprit.

3.1.2 Pulse Program Data Reduction

The beam voltage, current and pertinent timing are given for all of the pulses in Table X along with the collector current discussed later. The nomenclature used to tag the pulses is taken from the pulse program Table I. Pulses are consecutively numbered in a sequence of 21 pulses. Each sequence is assigned a consecutive alphabetical letter. Timing information is obtained from the station tape utilizing the 36 bit fast time code. Reading accuracy for high voltage turn-on-times is ±3 ms. For current turn-on and off times it is better if it can be assumed that collector and rpa current monitors respond essentially instantaneously to the beam current which they appear to do. Reading accuracy for current turn-on-off is estimated at ±1.5 ms.

The beam current values given in the table require explanation. When in the package, the guns operate with their cathodes in a space charge limited region, there being plenty of reserve emission for each gun. The battery used

Table IX. Housekeeping During 17.03 Flight.

Time After Liftoff (sec.)	Pkg. Pressure psia	Heat Sink Temperature °F	B.C.M. Temperature °F	Positive Battery (Volts)	Negative Battery (Volts)
56.5	15.8	70	74	-	-
70.2	15.7	72	74	-	-
80.1	15.9	72	74	-	-
90.0	15.9	72	74	-	-
100.3	15.9	72	74	-	-
120.2	15.8	72	74	-	-
135.2	15.8	72	74	-	-
140.1	15.8	72	74	-	-
160.2	15.8	76	79	-	-
180.1	15.8	76	79	-	-
191.1	15.9	72	73	38.4	35.5
200.1	15.9	70	72	41.4	38.0
220.2	15.8	70	79	42.2	39.2
240.0	15.8	76	76	40.4	38.3
260.2	15.7	74	76	39.7	36.9
270.1	15.8	76	76	39.8	37.7
280.2	15.7	76	74	40.0	37.9
300.0	15.8	74	76	40.0	37.1
319.2	15.8	76	76	40.8	38.0
340.2	15.9	76	76	39.8	37.2
360.0	15.8	76	76	39.0	36.9
379.7	16.0	76	78	38.0	36.7
400.2	15.9	76	76	39.8	37.2
420.0	15.8	76	78	39.0	36.9
440.0	15.8	80	78	38.2	36.7
460.0	15.9	85	78	38.6	36.7
463.8	15.7	83	78	39.6	37.1

Table X. Electron Pulse Data Analysis

AEROBEE 17.03
LIFTOFF Jan. 26, 1969 9^h45^m UT
Electron Pulse Data Analysis 1st Sequence (A)

Pulse	Beam Voltage (kV)	Beam* Current (mA)	Collector Current (mA)	Time (sec. aft. 9^h45^m UT)	Event	Remarks
1A	5.9	-	-	207.824	hvs	
	5.9	1.6	no	.937	cs	
	5.9	1.6	no	208.035	end	
2A	5.9	-	-	210.586	hvs	
	5.8	5.2	6	.690	cs	
	5.8	5.2	6	.791	end	
3A	5.8	-	-	213.331	hvs	
	5.8	15	10	.435	cs	
	5.8	15	11	.538	end	
4A	6.0	-	-	216.067	hvs	
	5.8	51	42	.171	cs	
	5.8	51	52	.176		
	5.8	51	54	.184		
	5.8	51	54	.196		
	5.8	51	54	.221		
	5.8	51	54	.246		
	5.8	51	51	.272	end	
5A	5.9	-	-	218.793	hvs	
	5.4	156	0	.899	cs	
	5.4	156	80	.909		
	5.4	156	97	.919		
	5.4	156	100	.929		
	5.4	156	97	.939		
	5.4	156	97	.949		
	5.4	156	100	.969		
	5.4	156	101	.989		
	5.4	156	100	219.001	end	

hvs = High Voltage Start, cs = Current Start

*Nominal current values determined prior to launch are used where it is obvious that the package is functioning correctly. These values are more accurate under these circumstances than those obtained from the B.C. Monitor.

Table X. Electron Pulse Data Analysis - Sequence One (A) (Continued)

Pulse	Beam Voltage (kV)	Beam* Current (mA)	Collector Current (mA)	Time (sec. aft. 9^h45^m UT)	Event	Remarks
6A	5.8	-	-	221.516	hvs	
	4.4	490	102	.625	cs	
	4.4	490	87	.635		
	4.45	490	98	.645		
	4.5	490	83	.655		
	4.55	490	85	.665		
	4.6	490	98	.675		
	4.65	490	99	.685		
	4.7	490	110	.695		
	4.7	490	119	.705		
	4.75	490	102	.715		
	4.75	490	119	.722	end	
7A	3.1	-	-	224.239	hvs	
	3.0	15	10	.333	cs	
	3.0	15	10	.446	end	
8A	3.1	-	-	226.985	hvs	
	3.0	51	17	227.090	cs	
	3.0	51	35	.095		
	3.0	51	39	.100		
	3.0	51	41	.110		
	3.0	51	41	.120		
	3.0	51	41	.130		
	3.0	51	41	.140		
	3.0	51	41	.150		
	3.0	51	41	.160		
	3.0	51	41	.170		
	3.0	51	41	.180		
	3.0	51	41	.190	end	
9A	3.2	-	-	229.723	hvs	
	2.9	156	73	.827	cs	
	2.9	156	51	.837		
	2.9	156	51	.847		
	2.9	156	47	.857		
	2.9	156	50	.867		
	2.9	156	49	.877		
	2.9	156	47	.887		
	2.9	156	50	.897		
	2.9	156	53	.907		
	2.9	156	55	.917		
	2.9	156	60	.930	end	

hvs = High Voltage Start, cs = Current Start

Table X. Electron Pulse Data Analysis - Sequence One (A) (Continued)

Pulse	Beam Voltage (kV)	Beam* Current (mA)	Collector Current (mA)	Time (sec. aft. 9^h45^m UT)	Event	Remarks
10A	3.0	-	-	232.461	hvs	
	2.4	490	135	.564	cs	
	2.4	490	113	.566		
	2.4	490	135	.574		
	2.4	490	133	.584		
	2.4	490	135	.594		
	2.4	490	135	.604		
	2.4	490	135	.614		
	2.4	490	135	.624		
	2.4	490	135	.634		
	2.4	490	135	.644		
	2.4	490	135	.654		
	2.4	490	135	.664	end	
11A	10.1	-	-	235.200	hvs	
	7.7	490	180	.302	cs	
	8.1		160	.307		
	8.2		135	.312		
	8.3		154	.317		
	8.4		160	.322		
	8.4		156	.332		
	8.4		158	.342		
	8.5		167	.352		
	8.5		180	.362		
	8.6		190	.372		
	8.6		197	.382		
	8.7		201	.392		
	8.7		232	.402		
	8.7		256	.410		
	8.6		295	.431		
	8.6		320	.446	pk	
	8.6		282	.452	valley	
	8.6		335	.458	pk	
	8.6		275	.468	valley	
	8.6		355	.473	pk	
	8.7		367	.494		
	8.7		395	.515		
	8.7		415	.536		

hvs = High Voltage Start, cs = Current Start

Table X. Electron Pulse Data Analysis - Sequence One (A) (Continued)

Pulse	Beam Voltage (kV)	Beam* Current (mA)	Collector Current (mA)	Time (sec. aft. 9^h45^m UT)	Event	Remarks
11A Cont.	8.7	490	458	.557		
			458	.578		
			490	.599		
			465	.620		
			490	.641		
			465	.662		
			465	.683		
			490	.704		
			465	.725		
			465	.746		
			465	.767		
			490	.788		
			490	.800		
			490	.822		
			490	.844		
			490	.865		
			490	.886		
			490	.907		
			490	.928		
			465	.949		
			465	.970		
			490	.991		
			490	236.012		
			490	.033		
			465	.054		
			490	.075		
			490	.097		
			490	.118		
			465	.139		
			465	.160		
			465	.181		
			458	.202		
			465	.224		
			465	.245		
			465	.266		
			465	.275	end	
12A	1.45	-	-	237.932	hvs	
	1.45	15	10	238.036	cs	
	1.45	15	11	.086		
	1.45	15	13	.135	end	

hvs = High Voltage Start, cs = Current Start

Table X. Electron Pulse Data Analysis - Sequence One (A) (Continued)

Pulse	Beam Voltage (kV)	Beam* Current (mA)	Collector Current (mA)	Time (sec. aft. 9^h45^m UT)	Event	Remarks
13A	1.65	-	-	240.659	hvs	
	1.55	51	44	.766	cs	
	1.55	51	41	.776		
	1.55	51	40	.786		
	1.55	51	37	.796		
	1.55	51	35	.806		
	1.55	51	33	.816		
	1.55	51	33	.826		
	1.55	51	33	.836		
	1.55	51	33	.846		
	1.55	51	35	.856		
	1.55	51	36	.867	end	
14A	1.5	-	-	243.386	hvs	
	1.4	156	72	.491	cs	
			64	.496		
			54	.501		
			53	.511		
			54	.521		
			55	.531		
			55	.541		
			55	.551		
			56	.561		
			56	.571		
			53	.581		
	↓	↓	57	.593	end	
15A	1.6	-	-	246.113	hvs	
	1.2	490	150	.212	cs	
			220	.217		
			210	.222		
			215	.232		
			240	.242		
			210	.252		
			200	.262		
			210	.272		
			240	.282		
			185	.292		
	↓	↓	185	.316	end	

hvs = High Voltage Start, cs = Current Start

Table X. Electron Pulse Data Analysis - Sequence One (A) (Continued)

Pulse	Beam Voltage (kV)	Beam* Current (mA)	Collector Current (mA)	Time (sec. aft. 9^h45^m UT)	Event	Remarks
16A	10.6		-	248.837	hvs	
	10.6	1.6	~2	.943	cs	
	10.6	1.6	~2	249.042	end	
17A	10.5		-	251.563	hvs	
	10.4	5.1	~6	.667	cs	
	10.4	5.1	~6	.769	end	
18A	10.4	-	-	254.287	hvs	
	10.2	15	?	.391	cs -	(From here to the next reading a probable intermittent short.)
	10.2	15	15	.425		
	10.2	15	15	.492	end	(from .425 study at 15 mA)
19A	10.3	-	-	257.004	hvs	
	10.0	51	46	257.110	cs	
	10.0	51	46	.210	end	
20A	10.3	-	-	259.719	hvs	
	9.3	156	123	.823	cs	
	9.4	156	123	.833		
	9.5	156	132	.843		
	9.5	156	118	.853		
	9.5	156	121	.863		
	9.5	156	134	.873		
	9.6	156	140	.883		
	9.6	156	140	.893		
	9.6	156	140	.903		
	9.6	156	142	.913		
	9.6	156	141	.924	end	
21A	10.3	-	-	262.431	hvs	
	8.1	490	250	.537	cs	
	8.5	↓	260	.547		
	8.6		260	.557		
	8.8		270	.567		
	8.8		240	.577		

hvs = High Voltage Start, cs = Current Start

Table X. Electron Pulse Data Analysis - Sequence One (A) (Continued)

Pulse	Beam Voltage (kV)	Beam Current (mA)	Collector Current (mA)	Time (sec. aft. 9^h45^m UT)	Event	Remarks
21A	8.8	490	275	262.587		
Cont.	8.8		275	.597		
	8.9		290	.607		
	8.9		295	.617		
	8.9		315	.627		
	9.0		335	.637		
	9.1		390	.647		
	9.1		400	.657		
	9.0		420	.667		
	9.0		440	.677		
	9.0		470	.687		
	8.9		510	.697		
	8.9		460	.707		
	8.9		410	.717		
	8.8		470	.727		
			490	.737		
			490	.747		
			520	.757		
			540	.767		
			520	.787		
			520	.807		
			510	.827		
			540	.847		
			520	.867		
			?	.887	Collector Shorting	
			?	.907	Collector Shorting	
			?	.927	Collector Shorting	
			520	.947		
			520	.967		
			540	.987		
			540	263.007		
			540	.027		
			?	.047	More or less continuous collector shorting from here to the pulse end.	
				.510	end	

Table X. Electron Pulse Data Analysis - Sequence Two (B) (Continued)

Pulse	Beam Voltage (kV)	Beam* Current (mA)	Collector Current (mA)	Time (sec. aft. 9^h45^m UT)	Event	Remarks
1B	6.2	-	-	265.200	hvs	Probable Collector Shorting
	6.2	1.6	no	.305	cs	
	6.2	1.6	no	.407	end	
2B	6.1	-	-	267.916	hvs	
	6.0	5.1	no	268.022	cs	
	6.0	5.1	no	.120	end	
3B	6.0	-	-	270.629	hvs	
	5.8	15	no	.733	cs	
	5.8	15	no	.78		
	5.8	15	no	.833	end	
4B	6.0	-	-	273.365	hvs	
	5.8	51	no	.470	cs	
	5.7	51	no	.470	end	
5B	5.9	-	-	276.097	hvs	
	5.4	156	~8?	.203	cs	
	5.45	156	~8?	.25		
	5.5	156	~8?	.303	end	
6B	6.1	-	-	278.830	hvs	
	4.7	490	~8?	.935	cs	
	4.8	490	~8?	.96		
	4.9	490	~8?	279.01		
	4.9	490	~8?	.034	end	
7B	3.0	-	-	281.560	hvs	
	3.0	15	no	.666	cs	
	3.0	15	no	.771	end	
8B	3.0	-	-	284.295	hvs	
	2.9	51	~9?	.399	cs	Prob. Coll. Shorting
	2.9	51	~9?	.501	end	Prob. Coll. Shorting

hvs = High Voltage Start, cs = Current Start, no = not observable

Table X. Electron Pulse Data Analysis - Sequence Two (B) (Continued)

Pulse	Beam Voltage (kV)	Beam* Current (mA)	Collector Current (mA)	Time (sec. aft. 9^h45^m UT)	Event	Remarks
9B	3.0	-	-	287.026	hvs	
	2.8	156	34	.128	cs	Some oscillating and possible coll. partial shorting
	2.8		34	.133		
	2.8		41	.138		
	2.8		42	.143		
	2.8		44	.148		
	2.8		48	.153		
	2.8		48	.158		
	2.8		47	.163		
	2.8		46	.168		
	2.9		42	.173		
	2.9		46	.178		
	2.9		44	.183		
	2.9		42	.188		
	2.9		45	.193		
	2.9		47	.198		
	2.8		48	.201		
	2.8		42	.206		
	2.8		52	.211		
	2.8		50	.216		
	2.8		50	.221		
	2.8		46	.229	end	
10B	2.9	-	-	289.751	hvs	
	2.4	490	32	.855	cs	
	2.4	490	24	.90		
	2.4	490	27	.955	end	
11B	10.3	-	-	292.480	hvs	
	8.1	490	270	.586	cs	
	8.25		208	.590		
	8.5		235	.594		
	8.6		235	.598		
	8.7		250	.604		
	8.7		243	.608		
	8.7		240	.618		
	8.7		243	.629		

hvs = High Voltage Start, cs = Current Start

Table X. Electron Pulse Data Analysis - Sequence Two (B) (Continued)

Pulse	Beam Voltage (kV)	Beam Current (mA)	Collector Current (mA)	Time (sec. aft. 9^h45^m UT)	Event	Remarks
11B	8.8	490	243	292.650		
Cont.	8.8		275	.657	pk	
	8.8		263	.662	valley	
	8.9		293	.671		
	8.9		293	.681		
	8.9		240	.692	valley	
	8.9		355	.702		
	8.8		300	.712		
	8.8		320	.733		
	8.8		440	.754		
	8.8		430	.774		
	8.8		430	.793		
	8.8		430	.814		
	8.8		440	.835		
	8.8		470	.850		
	8.7		430	.871		
			470	.892		
			470	.913		
			470	.933		
			470	.954		
			470	.975		
			490	.996		
			510	293.037		
				.079		
				.100		
				.142		
				.183		
				.205		
				.246		
				.288		
				.309		
			490	.351		
			490	.392		
			490	.434		
			490	.475		
			490	.516		
			472	.560	end	

Table X. Electron Pulse Data Analysis - Sequence Two (B) (Continued)

Pulse	Beam Voltage (kV)	Beam* Current (mA)	Collector Current (mA)	Time (sec. aft. 9^h45^m UT)	Event	Remarks
12B	1.6	-	-	295.236	hvs	
	1.6	15	14	.340	cs	
	↓	↓	14	.350		
			13	.360		
			13	.370		
			13	.380		
			11	.390		
			14	.400		
			14	.410		
			14	.420		
			14	.430		
	↓	↓	14	.442	end	
13B	1.5	-	-	297.960	hvs	
	1.4	51	46	298.066	cs	
	1.4	51	46	.091		
	1.4	51	46	.116		
	1.4	51	46	.141		
	1.4	51	46	.166	end	
14B	1.5	-	-	300.682	hvs	
	1.4	156	70	.786	cs	
	↓	↓	65	.791		
			68	.796		
			78	.801		
			65	.806		
			58	.811		
			59	.816		
			65	.821		
			59	.826		
			65	.831		
			65	.836		
			59	.841		
			57	.846		
			67	.851		
			65	.856		
			61	.861		
			61	.866		
			57	.871		
			58	.876		
			70	.881		
	↓	↓	70	.887	end	

hvs = High Voltage Start, cs = Current Start

Table X. Electron Pulse Data Analysis - Sequence Two (B) (Continued)

Pulse	Beam Voltage (kV)	Beam* Current (mA)	Collector Current (mA)	Time (sec. aft. 9^h45^m UT)	Event	Remarks
15B	1.5	-	-	303.403	hvs	
	1.2	490	182	.508	cs	
	↓	↓	188	.513		
			200	.518		
			195	.523		
			182	.528		
			188	.533		
			175	.538		
			205	.543		
			195	.548		
			188	.553		
			188	.558		
			182	.563		
			182	.568		
			170	.573		
			175	.578		
			175	.583		
			182	.588		
			175	.593		
			182	.598		
	↓	↓	182	.607	end	
16B	10.3	-	-	306.129	hvs	
	10.3	1.6	no	.233	cs	
	10.3	1.6	no	.333	end	
17B	10.3	-	-	308.852	hvs	
	10.2	5.1	5	.959	cs	
	10.2	5.1	5	309.058	end	
18B	10.25	-	-	311.575	hvs	
	10.1	15	12	.682	cs	
	10.1	15	13	.73		
	10.0	15	15	.782	end	

hvs = High Voltage Start, cs = Current Start, no = not observable

Table X. Electron Pulse Data Analysis - Sequence Two (B) (Continued)

Pulse	Beam Voltage (kV)	Beam* Current (mA)	Collector Current (mA)	Time (sec. aft. 9^h45^m UT)	Event	Remarks
19B	10.2	-	-	314.292	hvs	
	9.8	51	47	.401	cs	
	9.8	↓	43	.410		
	9.8		43	.420		
	9.9		45	.430		
	9.9		45	.440		
	9.9		45	.450		
	9.9		42	.460		
	9.9		42	.470		
	9.9		42	.480		
	10.0		45	.490		
	10.0	↓	47	.500	end	
20B	10.3	-	-	317.012	hvs	
	9.2	156	110	.116	cs	
	9.2	↓	92	.126		
	9.2		88	.136		
	9.3		120	.146		
	9.3		100	.156		
	9.4		110	.166		
	9.4		110	.176		
	9.4		110	.186		
	9.4		130	.196		
	9.4		125	.206		
	9.4	↓	130	.219	end	
21B	?	-	-	319.72	hvs	Calib. during hvs
	?	490	220	.833	cs	↓
	?	↓	215	.846		
	?		260	.848		
	?		235	.849		
	?		235	.856		
	?		210	.857		
	?		235	.862		
	?		220	.873		
	?		215	.875		
	?		190	.878		
	8.9		215	.885		
	8.9		220	.893		
	8.9	↓	275	.899		

hvs = High Voltage Start, cs = Current Start

Table X. Electron Pulse Data Analysis - Sequence Two (B) (Continued)

Pulse	Beam Voltage (kV)	Beam* Current (mA)	Collector Current (mA)	Time (sec. aft. 9^h45^m UT)	Event	Remarks
21B	8.9	490	225	319.905		
Cont.	8.9		275	.921		
	9.0		255	.925		
	9.0		280	.933		
	9.0		295	.940		
	9.0		320	.950		
	9.0		360	.960		
	8.9		370	.970		
	8.9		360	.980		
	8.9		390	.990		
	8.9		390	320.000		
	8.9		400	.010		
	↓		450	.020		
			470	.030		
	↓		435	.040		
	8.8		450	.050		
	↓		400	.100		
			420	.150		
			435	.200		
	↓		490	.250		
	8.7		490	.300		
	↓		510	.350		
			530	.400		
			510	.450		
			490	.500		
			470	.550		
			450	.650		
			430	.700		
			430	.750		
			450	.800		
	↓	↓	435	.806	end	

Electron Pulse Data Analysis - Sequence Three (C)

1C	6.1	-	-	322.499	hvs	
	6.1	1.6	no	.605	cs	
	6.1	1.6	no	.705	end	

hvs = High Voltage Start, cs = Current Start, no = not observable

Table X. Electron Pulse Data Analysis - Sequence Three (C) (Continued)

Pulse	Beam Voltage (kV)	Beam* Current (mA)	Collector Current (mA)	Time (sec. aft. 9^h45^m UT)	Event	Remarks
2C	6.0	-	-	325.217	hvs	
	6.0	5.1	~3.5	.323	cs	
	6.0	5.1	~3	.37		
	6.0	5.1	~3.5	.423	end	
3C	6.0	-	-	327.937	hvs	
	5.9	15	11	328.042	cs	
	5.9	15	11	.09		
	5.9	15	11	.143	end	
4C	6.0	-	-	330.650	hvs	
	5.8	51	45	.756	cs	
	↓	↓	44	.776		
				.796		
				.816		
				.836		
	↓	↓	↓	.857	end	
5C	6.0	-	-	333.391	hvs	
	5.5	156	89	.497	cs	
	5.5	↓	102	.499		pk
	5.5		62	.506		valley
	5.5		86	.519		pk
	5.6		89	.527		valley
	↓		102	.529		pk
			98	.538		valley
			114	.543		pk
			98	.547		valley
			107	.557		pk
			107	.567		
			116	.577		
			128	.587		
	↓	↓	118	.598	end	
6C	5.9	-	-	336.131	hvs	
	4.9	490	380	.237	cs	
	↓	↓	510	.242		pk
			430	.247		valley
			490	.251		pk
	↓	↓	410	.256		valley

hvs = High Voltage Start, cs = Current Start

Table X. Electron Pulse Data Analysis - Sequence Three (C) (Continued)

Pulse	Beam Voltage (kV)	Beam* Current (mA)	Collector Current (mA)	Time (sec. aft. 9^h45^m UT)	Event	Remarks
6C Cont.	4.9	490	470	336.258		pk
			490	.269		pk
			410	.272		valley
			460	.276		pk
			380	.279		valley
			430	.282		pk
			380	.286		valley
			470	.293		pk
			380	.297		valley
			390	.300		pk
			410	.314		pk
			340	.316		valley
			420	.319		pk
			380	.324		valley
			430	.329		pk
			380	.337	end	
7C	3.0	-	-	338.876	hvs	
	2.9	15	11	.982	cs	coll. bkgnd is 34 mA
			14	.992		
			13	339.002		
			12	.022		
			12	.042		
			15	.062		
			14	.082	end	bkgnd still 34 mA
8C	3.0	-	-	341.586	hvs	
	2.8	51	34	.692	cs	coll. bkgnd is 26 mA
			34	.70		Hashy & Oscillating
			34	.710		
			34	.720		
			34	.730		
			33	.740		
			34	.750		
			35	.760		
			35	.770		
			34	.780		
			34	.790		
			33	.792	end	

hvs = High Voltage Start, cs = Current Start

Table X. Electron Pulse Data Analysis - Sequence Three (C) (Continued

Pulse	Beam Voltage (kV)	Beam* Current (mA)	Collector Current (mA)	Time (sec. aft. 9^h45^m UT)	Event	Remarks
9C	2.9	-	-	~344.326	hvs	Hashy & Oscillating
	2.9	156	150 pks, 80 val.	.431	cs	↓
	2.9		140 pks, 75 val.	.48		↓
	2.9		130 pks, 55 val.	.530	end	coll. bkgnd 13 mA
10C	2.9	-	-	~347.06	hvs	part. T/M signal loss
	2.4	156	~8	.168	cs	coll. bkgnd 20 mA
	2.4	156	~8	.22		
	2.4	156	~8	.267	end	
11C	10.2	-	-	349.806	hvs	coll. bkgnd 11 mA
	8.3	470	~5	.911	cs	coll. is shorted
	9.1	470	no	350.000		
	9.2	440	no	.100		
	9.1	440	no	.200		
	9.2	440	no	.300		
	9.6	390	no	.400		
	9.7	350	no	.500		
	9.9	320	no	.600		
	9.9	250	no	.700		
	10.1	250	no	.800		
	10.2	250	no	.883	end	bkgnd is now 15 mA
12C	1.5	-	-	352.542	hvs	coll. shorted, bkgnd 34 mA
	1.5	13	no	.647	cs	↓
	1.5	13	no	.749	end	↓
13C	1.5	-	-	355.279	hvs	coll. shorted, bkgnd 16 mA
	1.45	45	no	.383	cs	↓
	1.45	45	no	.43		↓
	1.45	45	no	.483	end	coll. shorted, bkgnd 28 mA

hvs = High Voltage Start, cs = Current Start, no = not observable

Table X. Electron Pulse Data Analysis - Sequence Three (C) (Continued)

Pulse	Beam Voltage (kV)	Beam* Current (mA)	Collector Current (mA)	Time (sec. aft. 9^h45^m UT)	Event	Remarks
14C	1.5	-	-	358.013	hvs	coll. shorted, bkgnd 20 mA
	1.45	96	no	.120	cs	
	1.45	130	no	.140	pk-bcm	
	1.45	86	no	.180		
	1.45	66	no	.222	end	
15C	1.5	-	-	360.750	hvs	coll. part. shorted bkgnd 20 mA
	1.4	105	no	.857	cs	
	1.4	160	no	.883	pk-bcm	
	1.4	145	?	.916		Hashy & Oscillating
	1.4	130	? (88 pk hash.)	.956	end	
16C	10.4	-	-	363.490	hvs	
	10.4	1.7	no	.592	cs	coll. prob. shorted
	10.4	1.7	no	.695	end	
17C	10.4	-	-	366.226	hvs	
	10.2	5	no	.333	cs	
	10.2	5	no	.433	end	
18C	10.3	-	-	368.964	hvs	
	10.1	14	no	369.071	cs	
	10.1	15	no	.172	end	
19C	10.4	-	-	371.700	hvs	
	10.1	50	no	371.805	cs	
	?	?	?	~371.9	end	h.v. breakdowns
20C	10.4	-	-	374.435	hvs	
	9.8	54	no	.537	cs	coll. prob. shorted
	10.1	25	no	.638	end	
21C	10.2	-	-	377.162	hvs	
	11.1	67	no	.270	cs	
	11.2	31	no	.334		h.v. breakdowns begin here and continue to the end of the pulse.
				378.245	end	

hvs = High Voltage Start, cs = Current Start, no = not observable

Table X. Electron Pulse Data Analysis - Sequence Four (D)

Pulse	Beam Voltage (kV)	Beam* Current (mA)	Collector Current (mA)	Time (sec. aft. 9^h45^m UT)	Event	Remarks
1D	5.9	-	-	379.923	hvs	
	5.9	1.3	no	380.030	cs	
	5.9	1.3	no	.130	end	
2D	6.0	-	-	382.662	hvs	
	5.9	3.7	no	.764	cs	
	5.9	3.7	no	.867	end	
3D	5.9	-	-	385.399	hvs	
	5.8	10	4.2	.501	cs	
	5.8	10	3.6	.601	end	
4D	5.9	-	-	388.127	hvs	
	5.7	30	42	.232	cs	
	5.7	38	23	.332	end	
5D	5.8	-	-	390.860	hvs	
	5.7	40	52	.962	cs	
	5.7	42	31	391.062	end	
6D	5.9	-	-	393.589	hvs	
	5.7	57	61	.691	cs	
	5.7	40	52	.791	end	
7D	2.9	-	-	396.322	hvs	
	2.9	9	17	.426	cs	
	2.9	10	17	.525	end	
8D	2.9	-	-	399.052	hvs	
	2.9	26	23	.157	cs	
	2.9	25	24	.256	end	
9D	2.9	-	-	401.782	hvs	
	2.85	44	39	.884	cs	
	2.85	37	32	.985	end	
10D	2.95	-	-	404.512	hvs	
	2.9	54	no	.612	cs	
	2.9	40	no	.713	end	

hvs = High Voltage Start, cs = Current Start, no = not observable

Table X. Electron Pulse Data Analysis - Sequence Four (D) (Continued)

Pulse	Beam Voltage (kV)	Beam* Current (mA)	Collector Current (mA)	Time (sec. aft. 9^h45^m UT)	Event	Remarks
11D	10.2	-	-	407.242	hvs	
	10.5	160	no	.348	cs	
	10.8	130	no	.850		Abrupt Curr. Change
	10.9	112	no	.850		Abrupt Curr. Change
	10.8	130	no	408.323	end	
12D	1.45	-	-	410.001	hvs	
	1.45	10.4	-	.106	cs	
	1.45	10.4	-	.206	end	
13D	1.45	31	-	412.727	hvs	
	1.45	31	44	.831	cs	
	1.45	31	42	.890		Abrupt Curr. Change
	1.45	21	34	.890		Abrupt Curr. Change
	1.45	21	34	.932	end	
14D	1.5	-	-	415.457	hvs	
	1.4	80	38	.559		coll. curr. very hashy
	1.4	68	52	.660		coll. curr. very hashy
15D	1.45	-	-	418.182	hvs	
	1.4	127	110	.286	cs	
	1.4	105	98	.385	end	
16D	10.4	-	-	420.912	hvs	
	10.3	1.3	no	421.020	cs	
	10.2	1.3	no	.119	end	
17D	10.3	-	-	423.645	hvs	
	10.3	4	3	.752	cs	
	10.3	4	3	.851	end	
18D	10.2	-	-	426.379	hvs	
	10.1	12	4	.483	cs	
	10.2	12	8	.582	end	
19D	10.3	-	-	429.106	hvs	
	10.1	12	29	.209	cs	
	10.1	12	27	.308	end	

hvs = High Voltage Start, cs = Current Start, no = not observable

Table X. Electron Pulse Data Analysis - Sequence Four (D) (Continued)

Pulse	Beam Voltage (kV)	Beam* Current (mA)	Collector Current (mA)	Time (sec. aft. 9^h45^m UT)	Event	Remarks
20D	10.3	-	-	431.830	hvs	
	9.7	96	62	.934	cs	oscillating
	9.7	86	62	432.035	end	oscillating
21D	10.2	-	-	434.560	hvs	
	10.2	190	170	.661	cs	
	10.6	200	170	.920		Abrupt Current change - before
	10.6	170	150	.920		Abrupt Current change - after
	10.6	170	150	435.636	end	

Electron Pulse Data Analysis - Sequence Five (E)

1E	6.0	-	-	437.337	hvs	
	5.9	1.2	1	.445	cs	
	5.8	1.2	1	.542	end	
2E	5.9	-	-	440.070	hvs	
	5.8	3.8	1	.172	cs	
	5.8	3.8	1	.272	end	
3E	6.0	-	-	442.800	hvs	
	5.8	10.5	2	.904	cs	
	5.9	12	2	443.004	end	
4E	6.1	-	-	445.526	hvs	
	5.8	33	20	.630	cs	
	5.8	33	20	.730	end	
5E	6.5	-	-	448.251	hvs	
	5.8	58	76	.353	cs	
	5.8	67	62	.455	end	
6E	5.9	-	-	451.003	hvs	
	5.6	90	97	.109	cs	
	5.6	58	120	.207	end	

hvs = High Voltage Start, cs = Current Start

Table X. Electron Pulse Data Analysis - Sequence Five (E) (Concluded)

Pulse	Beam Voltage (kV)	Beam* Current (mA)	Collector Current (mA)	Time (sec. aft. 9^h45^m UT)	Event	Remarks
7E	2.9	-	-	453.734	hvs	
	2.9	9.4	28	.837	cs	
	2.9	9.4	32	.939	end	
8E	2.95	-	-	456.460	hvs	
	2.9	25	30	.565	cs	
	2.9	20	26	.662	end	
9E	3.0	-	-	459.213	hvs	
	2.9	11	13	.316	cs	
	2.9	10	13	.416	end	
10E	2.9	-	-	461.965	hvs	
	2.9	3.7	no	462.069	cs	
	2.9	3.5	no	.168	end	
End of pulse program at				464.416	programmer OFF	

hvs = High Voltage Start, cs = Current Start, no = not observable

in the grid bias circuit is a nickel-cadmium battery which is called upon in normal operation of the system to draw very little of its current capacity, insuring plenty of reserve capacity for normal operation and a constant voltage. These two considerations coupled to the passive nature of the cathode follower design and the demonstrated stability of the 2nd grid supply have led to confidence in the stability of the current values obtained during operation.

The beam current monitor is also a passive device but one which is temperature sensitive. Its basic accuracy is no better than can be obtained by a 2-1/2 decade logarithmic monitor and the available T/M subcarrier accuracy and linearity. From these the basic accuracy of the monitor measurement exclusive of temperature sensitivity is no better than ±4% using the greatest of care data from paper readouts. The ground determined current values which have been measured to better than 2% accuracy have been entered as the correct beam current values where it is obvious that operation is normal. Where there is some doubt that it is not, the monitor values, which have been determined for all pulses, are used.

Beam voltage measurements listed are estimated to be accurate to ±150 eV over the entire range. Cathode resistor drops have not been subtracted from any of the listed values. This amounts to 44 V at the highest currents and around 50 volts at the lowest.

Operation of the program was excellent over the entire experiment period. All pulses were handled as designed without shifting or pulse shortening. Pulse spacings varied over the program from 2.70 to 2.76 sec. Beam pulse lengths were in all cases within 5% of the nominal 0.100 and 1.0 sec lengths. No high voltage breakdowns occurred during normal operation. It is obvious, however, that the effects from reactivating the attitude control system at 335 sec into the flight were extremely deleterious to the remainder of the experiment. As suspected, the gases from the jets caused loss of emission in the electron gun cathodes as evidenced by subsequent inability to reach programmed currents. The gas caused high voltage breakdowns to occur in both the r.p.a. and the electron gun systems. Both recovered without apparent permanent damage even though the gun system sustained rather complete arcing at the 600 mA level over a full one second pulse.

It can be concluded, that other than the loss in gun emission, the entire IPC payload operated without fault throughout the experiment.

3.2 Collector Current Monitor-Data Reduction and Associated Experiment Analysis

Incorporation of a current monitor in the experiment between the 85 ft. collector and the vehicle skin was recommended originally by W. C. Beggs of IPC and E. J. R. Maier of NASA/GSFC. Fairchild-Hiller was charged with developing and calibrating the unit. There was, until very recently when NASA TM-X-63664 was published, no complete calibrations of the unit, which had been designed as a "pseudo" logarithmic sensor. R. Groves of GSFC/SRB had calibrated the unit against input voltage across the one ohm input resistor from 50 mV to 2 V input. Just prior to launch the unit was calibrated versus current on site by Beggs and M. Trichel of NASA/MSC through the T/M loop. This attempt was singularly unsuccessful upon post-examination because of the high background noise encountered.

After the flight, Serial No. 2 monitor with identical circuitry was calibrated accurately versus current at IPC in Burlington, Mass. by C. Salisbury and these data compared to the data of Groves. This comparison is given in Figure 71 and shows excellent agreement within the known accuracy of the one ohm input resistor. There was still the uncertainty in the correspondence of the two units at the very low currents since that end of the monitor would be more dependent upon the individual input characteristics of the F. E. Transistor amplifier used. Subsequent publication of TM-X-63664 gave a calibration of the "Collector Log Amplifier" which extended to the 1 mA level. The data for that calibration in the 50 - 1000 mA region was sparse and did not agree very well with the confirmed shape of the previous calibrations. As a consequence it was decided that the best calibration curve for the unit would be obtained if the two calibrations were combined using the Log Amp. calibration below 50 mA and the Current Amplifier calibration of Groves above this value. Figure 72 is the result of this choice and has been used in obtaining the current values from the T/M tapes. These current values are listed in Table X along with the beam current

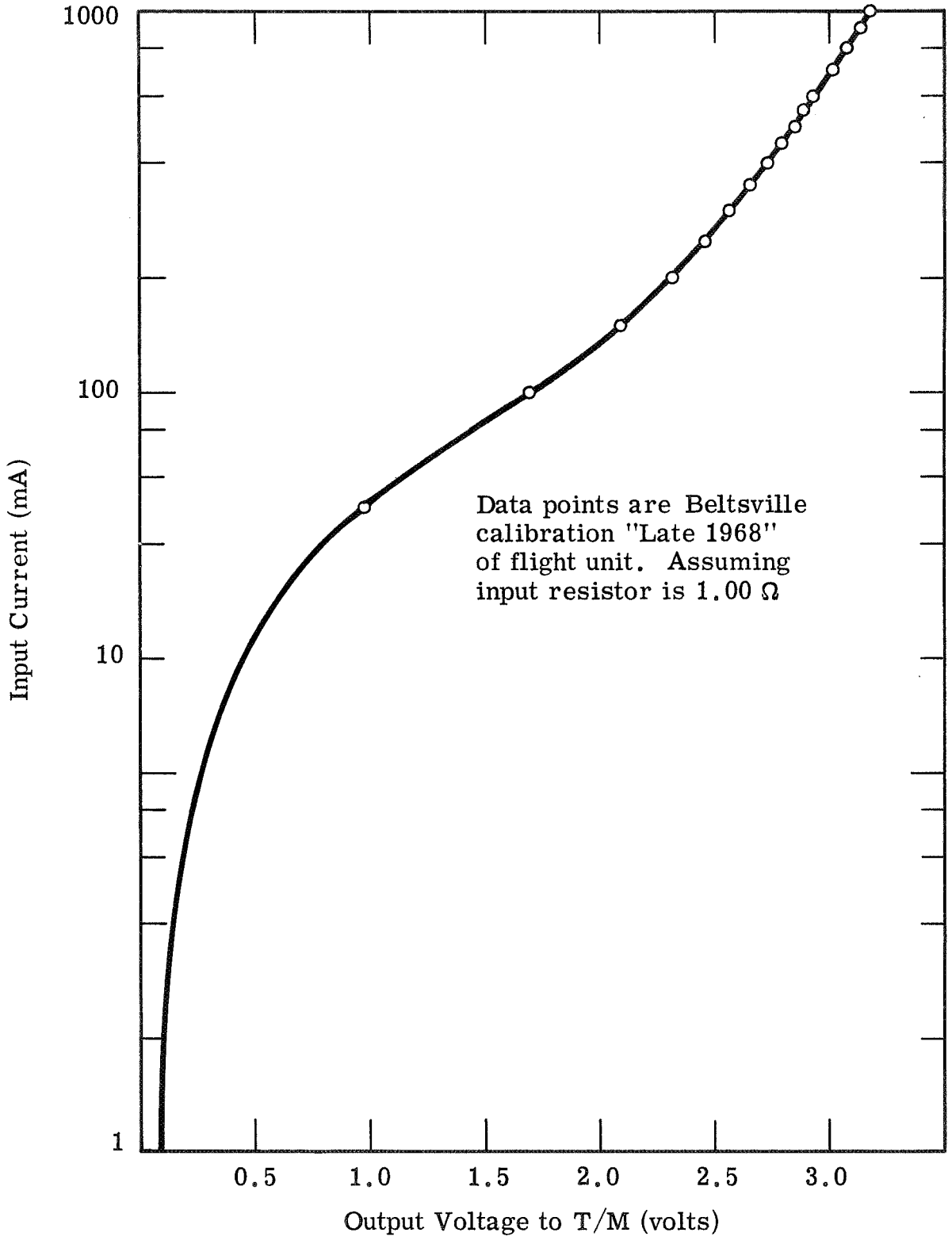

Figure 71. 17.03 Collector Current Monitor Calibration Comparison of Flight and Back-up Units.

1-6091

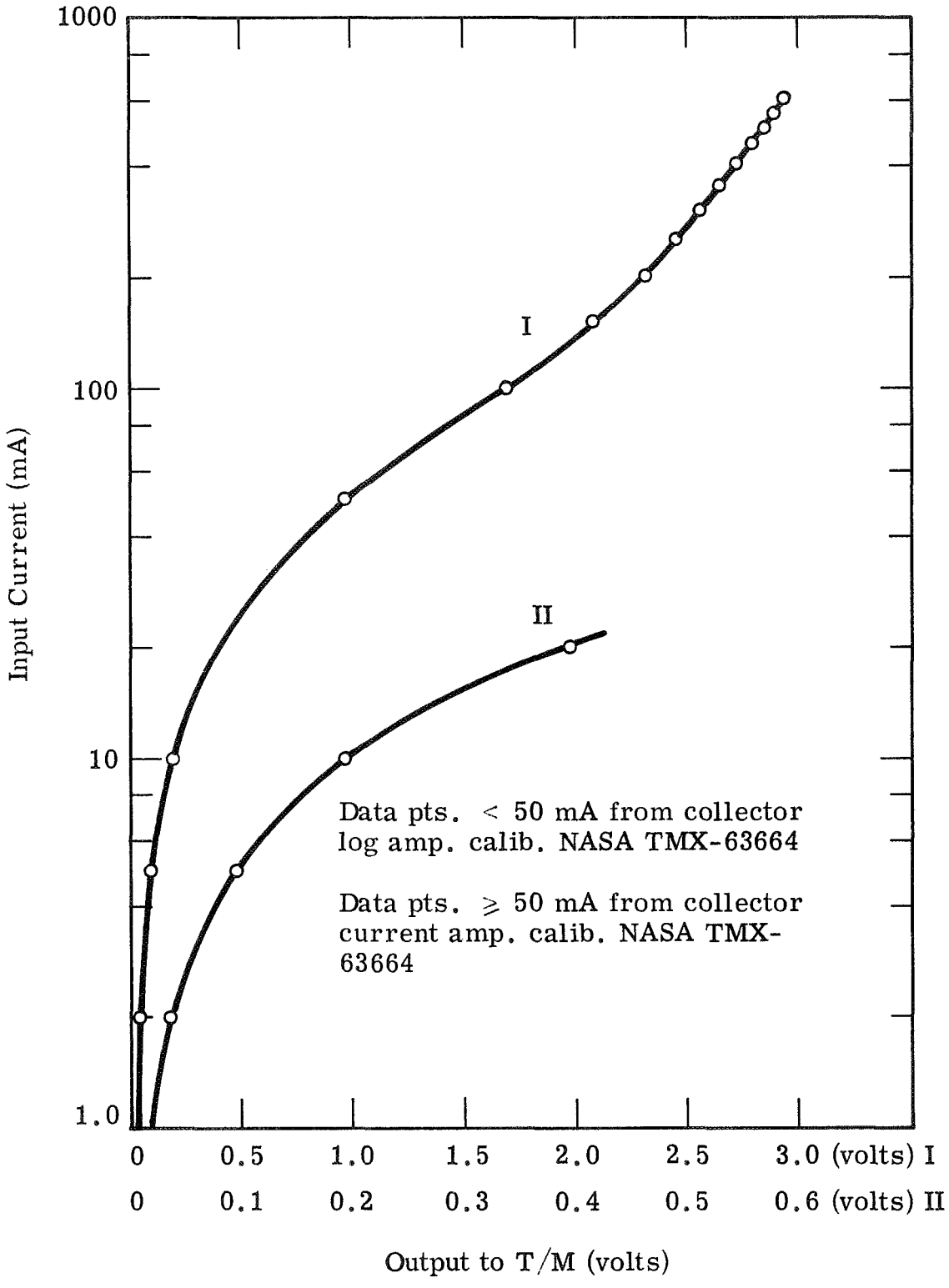

Figure 72. Collector Current Monitor S/N 1 17.03 Flight "BEST" Calibration Curve.

1-6092

and voltage. The accuracy of the collector current measurements for the higher currents is probably no better than ±10%. At the lower currents where the background is significant, the accuracy is probably no better than ±30%. For these currents, the background level which was as much as 30 mA, was subtracted from the gross current obtained. No attempt has been taken, at this time, to measure the background in an organized fashion, nor explain its presence. It would be, perhaps, very interesting if this could be pursued when time permits. It might be possible to relate this current or perhaps better voltage difference to the electric fields which can be sustained across the magnetic field.

In general, the returning current appeared to be very hashy on occasion or to vary periodically at observable rates. For those pulses considered to be significant, a large number of data points have been taken to extract as much of this information as possible. The interpretation of these effects is strongly affected by the low band width of the T/M subcarrier. Experiments in the future might obtain very significant information if instrumented to observe frequencies more typical to the background plasma.

Performance-wise there is considerable evidence of the collector itself shorting to the vehicle during many of the pulses, particularly during the early pulses in the second sequence and during the ACS manuevers during the third sequence. During this latter period there is additional evidence of loss of T/M signal due either to shorting or shadowing. All of these data together with the low inflation pressure and high bottle pressure on the collector strongly support the picture of a flacid, floppy collector of somewhat indeterminate orientation and cross-sectional area perpendicular to the magnetic field lines.

Of perhaps the greatest and most unexpected significance to the collector current data is the lack of correspondence on short pulses at higher current levels between collector and beam currents and the slow rise from lower currents to equal the beam current for the one second signature pulses. This is demonstrated in Figure 73 for pulse 11A (here the beam current values shown are those taken from the T/M returns directly. Figures 74, 75, and 76 present the comparable data on the collector current monitor for signature pulses 21A, 11B, and 21B. During pulse 21A there appears to be collector - vehicle skin shorting during most of the pulse. The causes of this phenomena have been

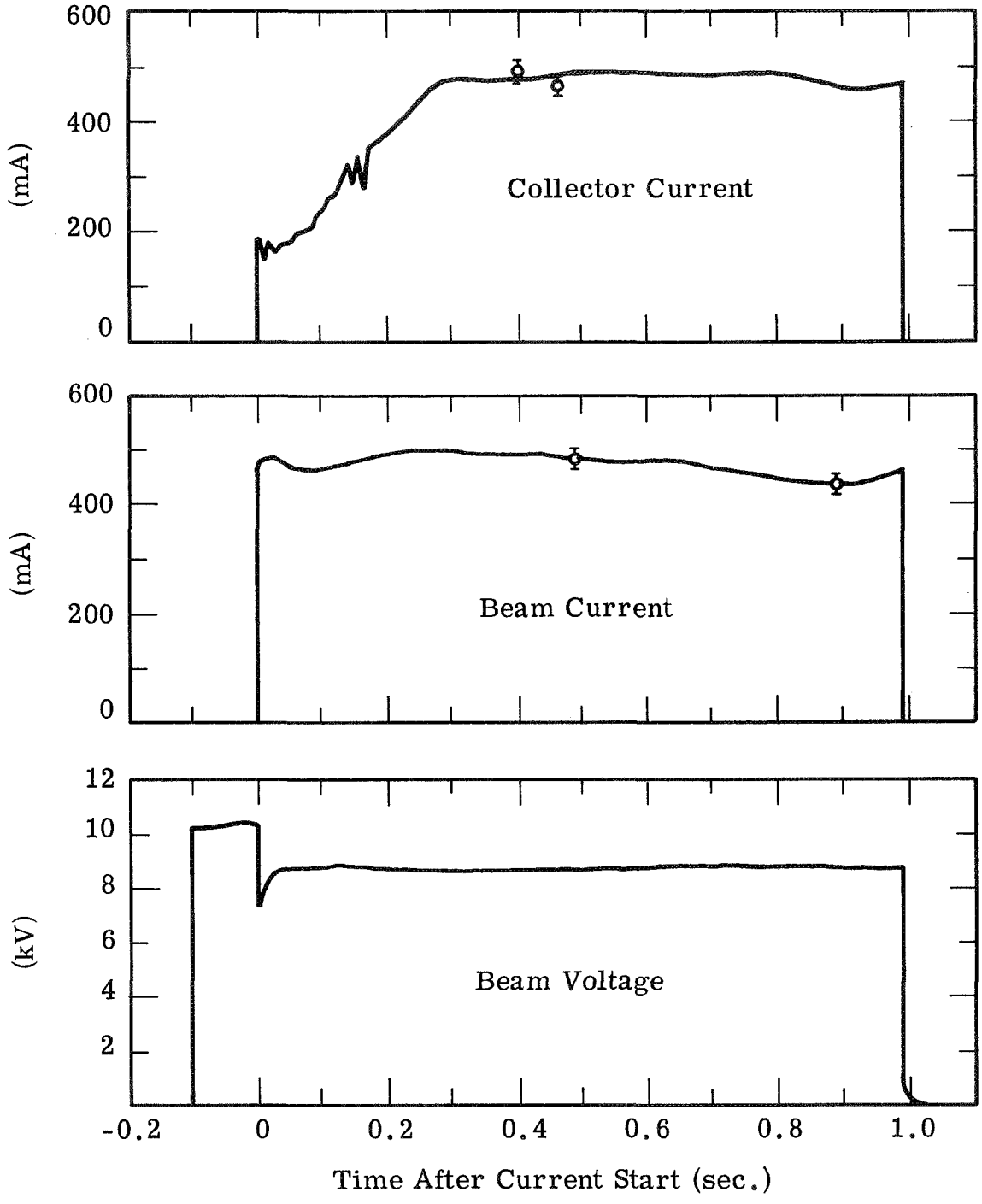

Figure 73. 1st Signature Pulse $9^h48^m55^s.306$ UT.

1-6093

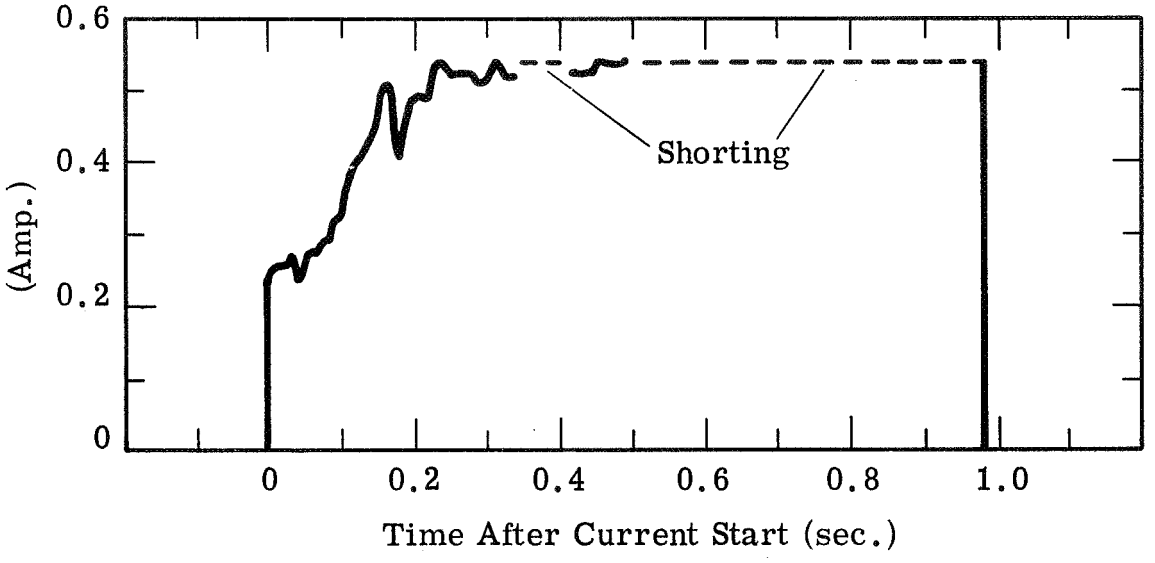

Figure 74. 2nd Signature Pulse-Collector Current $9^h49^m22^s.537$ UT.

1-6094

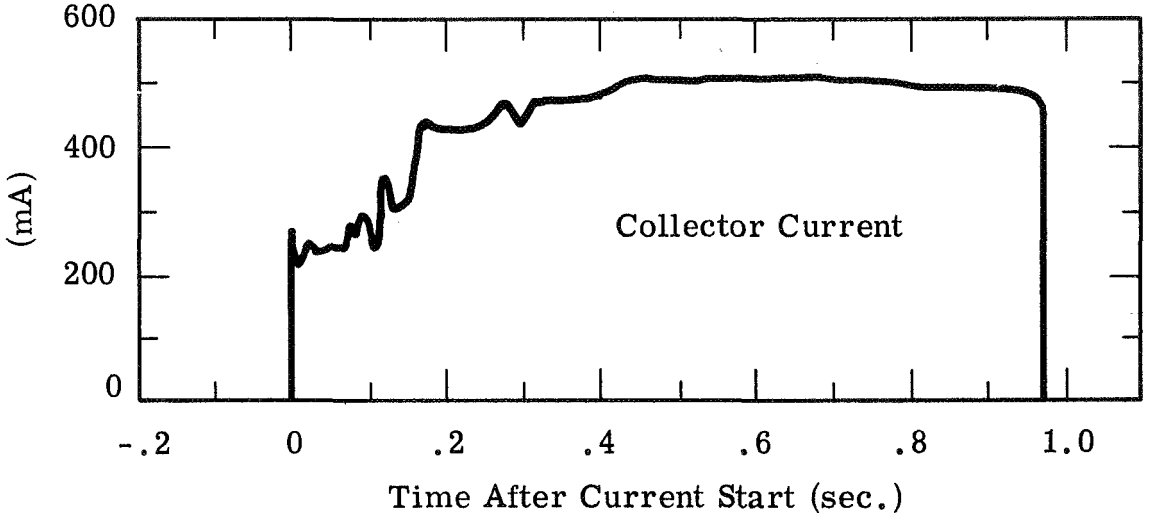

Figure 75. 3rd Signature Pulse 8.8 kV, 500 mA $9^h49^m52^s.586$ UT.

1-6095

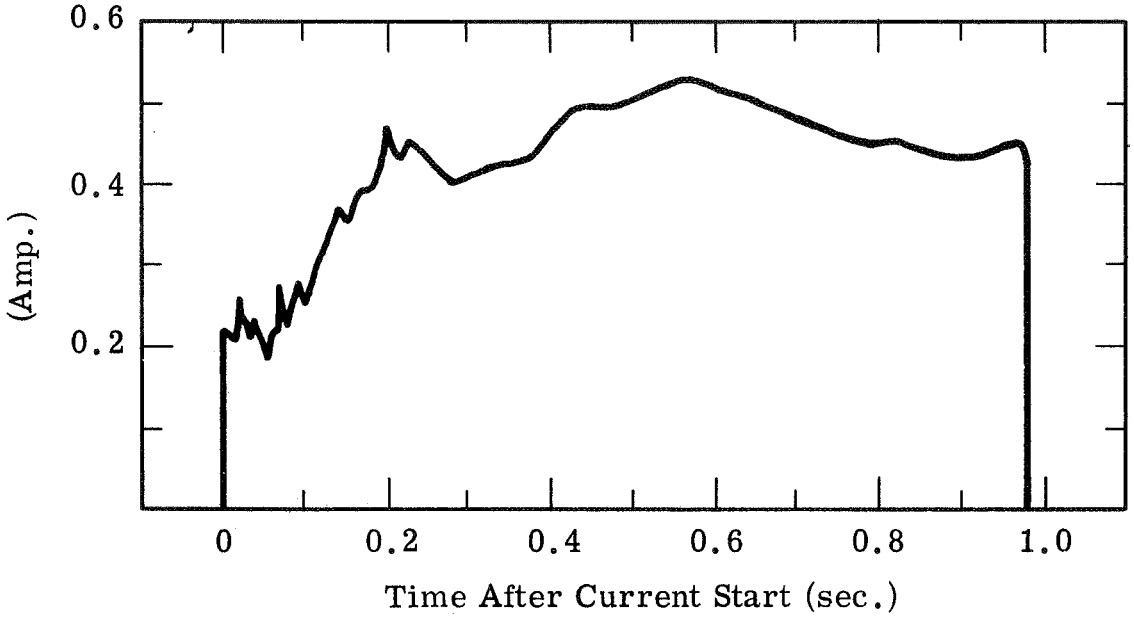

Figure 76. 4th Signature Pulse $9^h49^m22^s.537$ UT Collector Current.

1-6096

discussed in papers presented at the annual AGU meeting in 1968 (Hess 68) and 1969 (Beggs 69) and in an article to be published in the JGR (Trichel 1970).

REFERENCES

Beggs 69 — "Artificial Aurora Experiment - Electron Beam Launching and Propagation", Paper SPM63, Presented at the Annual AGU Meeting, Washington, D.C., April 20 - 24, 1970.

Bethe 53 — Experimental Nuclear Physics - Edit. by E. Segre, Vol. 1, Part II "Passage of Radiations Through Matter", H. A. Bethe and J. Ashkin, J. Wiley & Sons, N.Y. 1953.

Groves 69 — Aerobee 350, Flight 17.03 GE Instrumentation Information and Calibration Data, J. R. Groves & T. E. Thompson, Jr., NASA-TM-X-63664 (N69-37693), August, 1969.

Hess 68 — "Generation of an Artificial Aurora by a Rocket-Borne Accelerator", W. Hess, M. Trichel, E. Maier and W. Beggs, Paper STM99 Presented at the Annual AGU Meeting, Washington, D.C., April 22 - 24, 1969.

Trichel 70 — "Artificial Aurora Experiment - Electron Spectrum and Return Current Measurements", M. Trichel, E. Maier and W. Beggs in Prep. for Submission to JGR, Fall - 1970.

APPENDIX

Electron Gun Characteristics as Measured at Machlett Corporation

Test No.	Ef A	1_f A	$-E_{c1}$ Vdc	e_{c1} v	Prr pps	$+_p$ ms	$-E_{c2}$ Vdc	i_{c2} mA	i_{c1} mA	E_{bb} kVdc	i_b mA	i_b mA	Δi_k	HV Test	Remarks
44	6.3	.83	10	8.5	8	5	700			10	2.5	100			Prototype
55	6.3	.85	10	10	8	5	700			10	2.0	100			Prototype
88	6.3	.84	10	9.5	-	-	700			10	2.4	100			Prototype
96	6.3	.83	7.7				700			10	.005	-			Structurally sound
107	6.3	.85	8.5	4.0	8	5	800	-	10	10	3.4	75			Production gun
108	6.3	.83	8.5	4.5	8	5	800	-	10	10	3.4	75			Production gun
109	6.3	.85	9.8	3.8	8	5	800		10	10	3.3	75			Production gun
110	6.3	.83	9.8	2.0	8	5	800	2	5	10	3.4	75			Production gun
123	6.3	.83	9.6	4.5	8	5	800	2	10	10	3.5	75			Production gun
126	6.3	.85	7.2	6.0	8	10	800	0	12	10	3.8	75			Production gun
127	6.3	.85	7.1	6.5	8	10	800	-	12	10	3.5	75			Production gun
130	6.3	.82	6.5	8.0	8	5	800		10	10	2.8	75			Production gun
152	6.3	.82	7.9	4.6	8	5	800		8	10	3.4	75			Production gun
153	6.3	.84	7.2	6.4	8	5	800		8	10	3.5	75			Production gun
156	6.3	.83	9.6	8.0	8	5	800		8	10	3.2	150			Production gun
159	6.3	.82	8.5	3.7	8	5	800		8	10	3.6	75			Production gun
160	6.3	.83	9.3	2.2	8	5	800		5	10	3.4	75			Production gun
187	6.3	.84	8.9	3.5	8	5	800		8	10	3.5	75			Production gun
188	6.3	.85	7.5	4.5	8	5	800		10	10	3.6	75			Production gun
189	6.3	.84	7.5	3.6	8	5	800		4	10	3.4	75			Production gun

Tube No.	Ef A	1_f A	$-E_{c1}$ Vdc	e_{c1} v	Prr pps	$+_p$ ms	$-E_{c2}$ Vdc	i_{c2} mA	i_{c1} mA	E_{bb} kVdc	i_b mA	i_b mA	Δi_k	HV Test	Remarks
190	6.3	.85	6.8	5.0	8	5	800	-	-	10	3.4	75			Production gun
192	6.3	.85	6.8	8.0	8	5	800	-	-	10	4.0	75			Production gun
193	6.3	.85	8.8	4.5	8	5	800	-	-	10	4.8	75			Production gun
194	6.3	.84	8.0	4.5	8	5	800			10	3.8	75			Production gun
196	6.3	.85	7.5	6.7	8	5	800	-	-	10	4.1	75			Production gun
197	6.3	.80	8.9	7.2	8	5	800	-	-	10	4.2	75			Production gun
199	6.3	.80	6.9	7.5	8	5	800	-	-	10	4.2	75			Production gun
200	6.3	.84	7.0	7.7	8	5	800			10	4.1	75			Production gun
203	6.3	.83	8.2	5.5	8	5	800			10	4.0	75			Production gun
204	6.3	.85	7.2	6.3	8	5	800			10	4.0	75			Production gun
205	6.3	.84	9.7	4.2	8	5	800			10	4.1	75			Production gun
206	6.3	.85	8.5	4.2	8	5	800			10	4.1	75			Production gun
208	6.3	.85	9.9	3.3	8	5	800			10	4.0	75			Production gun
209	6.3	.84	7.5	4.3	8	5	800			10	3.9	75			Production gun
210	6.3	.84	8.7	4.0	8	5	800			10	3.8	75			Production gun
211	6.3	.83	7.1	5.3	8	5	800			10	4.0	75			Production gun
213	6.3	.85	6.7	7.1	8	5	800			10	4.1	75			Production gun
215	6.3	.82	6.6	6.7	8	5	800			10	4.0	75			Production gun
216	6.3	.84	7.0	5.3	8	5	800			10	3.7	75			Production gun
217	6.3	.83	8.7	3.5	8	5	800			10	3.9	75			Production gun

Test No.	Ef A	1_f A	$-E_{c1}$ Vdc	e_{c1} v	Prr pps	$+_p$ ms	$-E_{c2}$ Vdc	i_{c2} mA	i_{c1} mA	E_{bb} kVdc	i_b mA	i_b mA	Δi_k	HV Test	Remarks
218	6.3	.83	7.6	5.6	8	5	800			10	3.8	75			Production gun
219	6.3	.84	7.8	5.5	8	5	800			10	3.8	75			Production gun
221	6.3	.82	7.5	5.7	8	5	800			10	4.0	75			Production gun
222	6.3	.84	7.0	6.0	8	5	800			10	3.6	75			Production gun
223	6.3	.82	8.3	5.2	8	5	800			10	3.8	75			Production gun
224	6.3	.82	7.0	5.7	8	5	800			10	3.5	75			Production gun
225	6.3	.82	6.7	7.5	8	5	800			10	3.8	75			Production gun
226	6.3	.82	6.3	6.8	8	5	800			10	3.8	75			Production gun
227	6.3	.80	7.3	6.2	8	5	800			10	3.8	75			Production gun
229	6.3	.80	11.0	4.2	8	5	800			10	3.8	75			Production gun
230	6.3	.82	7.1	7.7	8	5	800			10	4.0	75			Production gun
231	6.3	.79	7.0	6.0	8	5	800			10	4.0	75			Production gun
232	6.3	.81	6.3	8.5	8	5	800			10	3.8	75			Production gun
233	6.3	.80	5.0	6.7	8	5	800			10	4.0	75			Production gun
234	6.3	.80	4.7	9.5	8	5	800			10	3.9	75			Production gun
235	6.3	.80	4.7	9.0	8	5	800			10	3.9	75			Production gun

Test No.	Ef A	I_f A	$-E_{c1}$ Vdc	e_{c1} v	Prr pps	^{+}p ms	$-E_{c2}$ Vdc	i_{c2} mA	i_{c1} mA	E_{bb} kVdc	i_b mA	i_b mA	Δi_k	HV Test	Remarks
															Heater Current
															Ins. Test
				No #2 Grid per Request of I. P.C.											Cut-Off Test
															Pulse Test
															Heater Current
															Ins. Test
							800			10		.005			Cut-Off Test
					8	5	800			10	4.2	75			Pulse Test
237	6.3	.82													Heater Current
	6.3		500												Ins. Test
	6.3	.82	6.9				800			10		.005			Cut-Off Test
	6.3	.82	10	3.6	8	5	800			10	3.9	75			Pulse Test
238	6.3	.82													Heater Current
	6.3		500												Ins. Test
	6.3	.82	10.5				800			10		.005			Cut-Off Test
	6.3	.82	10	3.2	8	5	800			10	4.0	75			Pulse Test

Tube No.	Ef A	1_f A	$-E_{c1}$ Vdc	e_{c1} v	Prr pps	$+_p$ ms	$-E_{c2}$ Vdc	i_{c2} mA	i_{c1} mA	E_{bb} kVdc	i_b mA	i_b mA	Δi_k	HV Test	Remarks
239	6.3	.83													Heater Current
	6.3		500												Ins. Test
	6.3	.83	7.5				800			10		.005			Cut-Off Test
	6.3	.83	10	3.3	8	5	800			10	3.5	75			Pulse Test
240	6.3	.82													Heater Current
	6.3		500												Ins. Test
	6.3	.82	6.7				800			10		.005			Cut-Off Test
	6.3	.82	10	3.7	8	5	800			10	3.8	75			Pulse Test
242	6.3	.83													Heater Current
	6.3		500												Ins. Test
	6.3	.83	7.2				800			10		.005			Cut-Off Test
	6.3	.83	10	3.4	8	5	800			10	3.7	75			Pulse Test
245	6.3	.84													Heater Current
	6.3		500												Ins. Test
	6.3	.84	7.7	-	-	-	800	-	-	10	-	.005	-	-	Cut-Off Test
	6.3	.84	10	5.6	8	5	800	0	18	10	4.0	75	-	-	Pulse Test

Tube No.	Ef A	I_f A	$-E_{c1}$ Vdc	e_{c1} v	Prr pps	^{+}p ms	$-E_{c2}$ Vdc	i_{c2} mA	i_{c1} mA	E_{bb} kVdc	i_b mA	i_b mA	Δi_k	HV Test	Remarks
247	6.3	.84													Heater Current
	6.3		500												Insulation Test
	6.3	.84	9.5	-	-	-	800	-	-	10	-	.005	-	-	Cut-Off Test
	6.3	.84	10	3.5	8	5	800	0	15	10	4.0	75	-	-	Pulse Test
249	6.3	.84													Heater Current
	6.3		500												Insulation Test
	6.3	.84	8.2	-	-	-	800	-	-	10	-	.005	-	-	Cut-Off Test
	6.3	.84	10	6.2	8	5	800	0	18	10	4.0	75	-	-	Pulse Test
250	6.3	.85													Heater Current
	6.3		500												Insulation Test
	6.3	.85	8.0	-	-	-	800	-	-	10	-	.005	-	-	Cut-Off Test
	6.3	.85	10	4.2	8	5	800	0	17	10	4.0	75	-	-	Pulse Test
251	6.3	.85													Heater Current
	6.3		500												Insulation Test
	6.3	.85	7.5	-	-	-	800	-	-	10	-	.005	-	-	Cut-Off Test
	6.3	.85	10	5.8	8	5	800	0	17	10	4.2	75	-	-	Pulse Test

Tube No.	Ef A	I_f A	$-E_{c1}$ Vdc	e_{c1} v	Prr pps	$+_p$ ms	$-E_{c2}$ Vdc	i_{c2} mA	i_{c1} mA	E_{bb} kVdc	i_b mA	i_b mA	Δi_k	HV Test	Remarks
252	6.3	.85													Heater Current
	6.3		500												Insulation Test
	6.3	.85	8.8	-	-	-	800	-	-	10	-	.005	-	-	Cut-Off Test
	6.3	.85	10	3.2	8	5	800	0	15	10	4.0	75	-	-	Pulse Test
253	6.3	.85													Heater Current
	6.3		500												Insulation Test
	6.3	.85	7.7	-	-	-	800	-	-	10	-	.005	-	-	Cut-Off Test
	6.3	.85	10	5.1	8	5	800	0	17	10	4.0	75	-	-	Pulse Test
254	6.3	.84													Heater Current
	6.3		500												Insulation Test
	6.3	.84	9.7	-	-	-	800	-	-	10	-	.005	-	-	Cut-Off Test
	6.3	.84	10	2.8	8	5	800	0	14	10	4.0	75	-	-	Pulse Test
256	6.3	.84													Heater Current
	6.3		500												Insulation Test
	6.3	.84	6.8	-	-	-	800	-	-	10	-	.005	-	-	Cut-Off Test
	6.3	.84	10	6.7	8	5	800	0	18	10	4.2	75	-	-	Pulse Test

Tube No.	Ef A	I_f A	$-E_{c1}$ Vdc	e_{c1} v	Prr pps	^{+}p ms	$-E_{c2}$ Vdc	i_{c2} mA	i_{c1} mA	E_{bb} kVdc	i_b mA	i_b mA	Δi_k	HV Test	Remarks
257	6.3	.85													Heater Current
	6.3		500												Insulation Test
	6.3	.85	8.8	-	-	-	800	-	-	10	-	.005	-	-	Cut-Off Test
	6.3	.85	10	3.6	8	5	800	0	15	10	3.7	75	-	-	Pulse Test
258	6.3	.85													Heater Current
	6.3		500												Insulation Test
	6.3	.85	8.3	-	-	-	800	-	-	10	-	.005	-	-	Cut-Off Test
	6.3	.85	10	5.2	8	5	800	0	10	10	4.4	75	-	-	Pulse Test
259	6.3	.85													Heater Current
	6.3		500												Insulation Test
	6.3	.85	8.5	-	-	-	800	-	-	10	-	.005	-	-	Cut-Off Test
	6.3	.85	10	6.2	8	5	800	0	18	10	3.7	75	-	-	Pulse Test
261	6.3	.81													Heater Current
	6.3		500												Insulation Test
	6.3	.81	8.5				800			10		.005			Cut-Off Test
	6.3	.81	10	5.2	8	5	800	0	17	10	4.0	75			Pulse Test

Tube No.	Ef A	1_f A	$-E_{c1}$ Vdc	e_{c1} v	Prr pps	$+_p$ ms	$-E_{c2}$ Vdc	i_{c2} mA	i_{c1} mA	E_{bb} kVdc	i_b mA	i_b mA	Δi_k	HV Test	Remarks
262	6.3	.81													Heater Current
	6.3		500												Insulation Test
	6.3	.81	9.2				800			10		.005			Cut-Off Test
	6.3	.81	10	3.8	8	5	800	0	16	10	3.6	75			Pulse Test
263	6.3	.85													Heater Current
	6.3		500												Insulation Test
	6.3	.85	10.2	-	-	-	800	-	-	10	-	.005	-	-	Cut-Off Test
	6.3	.85	10	2.5	8	5	800	0	14	10	3.6	75	-	-	Pulse Test
264	6.3	.85													Heater Current
	6.3		500												Insulation Test
	6.3	.85	9.7	-	-	-	800	-	-	10	-	.005	-	-	Cut-Off Test
	6.3	.85	10	4.5	8	5	800	0	16	10	4.2	75	-	-	Pulse Test
269	6.3	.81													Heater Current
	6.3		500												Insulation Test
	6.3	.81	8.4				800			10		.005			Cut-Off Test
	6.3	.81	10	4.8	8	5	800	0	16	10	3.9	75			Pulse Test

Tube No.	Ef A	I_f A	$-E_{c1}$ Vdc	e_{c1} v	Prr pps	$+_p$ ms	$-E_{c2}$ Vdc	i_{c2} mA	i_{c1} mA	E_{bb} kVdc	i_b mA	i_b mA	Δi_k	HV Test	Remarks
270	6.3	.80													Heater Current
	6.3		500												Insulation Test
	6.3	.80	10.7				800			10		.005			Cut-Off Test
	6.3	.80	10	2.5	8	5	800	0	14	10	3.8	75			Pulse Test
271	6.3	.82													Heater Current
	6.3		500												Insulation Test
	6.3	.82	9.0				800			10		.005			Cut-Off Test
	6.3	.82	10	4.7	8	5	800	0	16	10	4.0	75			Pulse Test
273	6.3	.81													Heater Current
	6.3		500												Insulation Test
	6.3	.81	8.0				800			10		.005			Cut-Off Test
	6.3	.81	10	5.7	8	5	800	0	18	10	3.8	75			Pulse Test
274	6.3	.80													Heater Current
	6.3		500												Insulation Test
	6.3	.80	8.0				800			10		.005			Cut-Off Test
	6.3	.80	10	5.2	8	5	800	0	17	10	3.7	75			Pulse Test

Tube No.	Ef A	1_f A	$-E_{c1}$ Vdc	e_{c1} v	Prr pps	^+p ms	$-E_{c2}$ Vdc	i_{c2} mA	i_{c1} mA	E_{bb} kVdc	i_b mA	i_b mA	Δi_k	HV Test	Remarks
275	6.3	.80													Heater Current
	6.3		500												Insulation Test
	6.3	.80	7.5				800			10		.005			Cut-Off Test
	6.3	.80	10	5.7	8	5	800	0	17	10	3.9	75			Pulse Test
276	6.3	.83													Heater Current
	6.3		500												Insulation Test
	6.3	.83	8.5				800			10		.005			Cut-Off Test
	6.3	.83	10	4.1	8	5	800	0	16	10	3.7	75			Pulse Test
277	6.3	.81													Heater Current
	6.3		500												Insulation Test
	6.3	.81	9.2				800			10		.005			Cut-Off Test
	6.3	.81	10	3.7	8	5	800	0	16	10	3.6	75			Pulse Test